International Journal of computational Engineering Research (IJCER)

ISSN: 2250-3005

VOLUME 2 July-August 2012 ISSUE 4

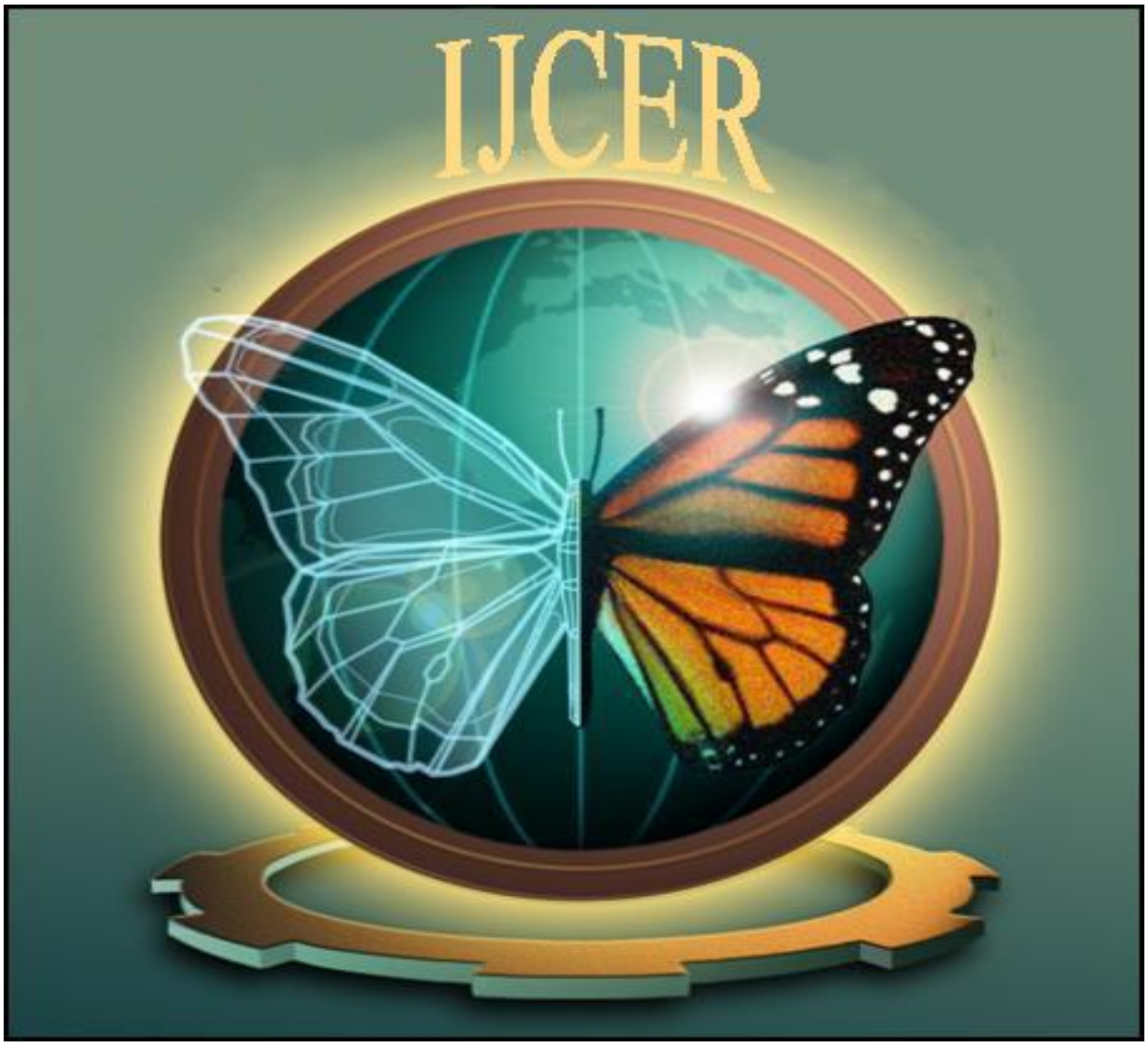

Email: ijceronline@gmail.com **Url : www.ijceronline.com**

International Journal of computational Engineering Research (IJCER)

Editorial Board

Editor-In-Chief

Editorial Committees

CONTENTS :

Performance Evaluation and Model Using DSDV and DSR routing in Ad-hoc network

Chetan adhikary[1], Dr. HB Bhuvaneswari[2], Prof K. Jayaraman[3]

[1] M.Tech Scholar, Department of Electronics and Communications Engineering, AMC Engineering College, Bangalore-560010

[2] Professor, Department of Electronics and Communications Engineering, AMC Engineering College, Bangalore-560010

[3] Research Scholar, Mentor & Competancy Developer

Abstract:
A mobile ad hoc network (MANET) is a collection of wireless mobile nodes communicating with each other using multi-hop wireless links without any existing network infrastructure or centralized administration. Previously, a variety of routing protocols targeting specifically at this environment was developed and some performance simulations were made. However, the related works took the simulation model with a constant network size. On the contrary, this paper considers the problem from a different perspective, using the simulation model with dynamic network size. Furthermore, based on Quality Of Service QoS (delay, jitter) and routing load, this paper systematically discusses the performance evaluation and comparison of two typical routing protocols of ad hoc networks with different simulation model and metrics.

Keywords*:* Ad hoc networks, Performance evaluation, QoS, Routing protocols, Network simulation.

1. Introduction

In an Ad hoc network, mobile nodes communicate with each other using multi-hop wireless links. Such networks find applicability in disaster management environment, crowd control, military applications and conferences. Each of these applications has specific QoS to be met. There is no stationary infrastructure such as base stations in ad hoc networks. Each node in the network is also acts a router, forwarding data packets for other nodes. Moreover bandwidth, energy and physical security are limited. These constraints in combination with network topology make routing protocols in ad hoc networks challenging.

In this paper a systematic performance study of two routing protocols of ad hoc networks, which is distance vector routing protocol DSDV [2] and Dynamic Source Routing DSR [3] is done. Destination Sequenced Distance-Vector (DSDV) routing protocol is one of the first protocols proposed for ad hoc wireless network. It is an enhanced version of the distributed Bellman-Ford algorithm. DSDV is a table driven protocol. Every mobile node in the network maintains a routing table in which all of the possible destinations within the network and the number of hops to each destination are recorded. DSR has an on-demand behavior, in which they initiate routing activity only in the presence of date packet in need of a route.

This paper discusses the performance evaluation of DSDV and DSR routing protocol which takes the QoS (delay, jitter) and routing load as evaluation metrics.

2. Simulation Model and Evaluation Metrics

The simulator for evaluating routing protocol is implemented with the Network Simulator version 2 (ns2) [4]. Simulation model varies the network size from 10 to 50 nodes placed within 1000m×1000m area. The mobile nodes are stationary. Time required for each simulation 50s.

A. Channel and radio model

Generally there are three propagation models in ns2, the free space model, two-ray ground reflection model and the shadowing model. The free space propagation model assumes the ideal propagation condition where there is only one clear line-of-sight path between the transmitter and receiver. H.T Friss[5] presents the following equation to calculate the received signal power in free space at distance *d* from the transmitter.

$$P_r(d) = \frac{P_t G_t G_r \lambda^2}{(4\pi)^2 d^2 L} \quad (1)$$

where P_t is the transmitted signal power, G_t and G_r are the antenna gains of the transmitter and receiver respectively, $L(L>=1)$ is the system loss and λ is the wavelength. Generally, $G_t = G_r = 1$ and $L=1$ in ns2 simulations. The free space model basically represents the communication range as a circle around the transmitter. If the receiver is within the circle, it receives all the packets. A single line-of-sight path between two mobile nodes is seldom the only means of propagation.

The two-ray ground reflection model considers both the direct path and a ground reflection path. S. Corson and J. Macker [6] showed that this model gives more accurate prediction at long distance than the free space model. The received power at distance d is predicted by

$$P_r(d) = \frac{P_t G_t G_r h_t^2 h_r^2}{d^4 L} \qquad (2)$$

where h_t and h_r are the heights of the transmitting and receiving antennas respectively.

The above equation shows a faster power loss than Eq.(1) when the distance increases. However, the two-ray model does not give a good result for a short distance due to oscillation caused by the constructive and destructive combination of the two rays. Instead, the free space model is still used when d is small. Therefore, a cross-over distance d_c is calculated in this model. When $d<d_c$ Eq. (1) is used. When $d>d_c$, Eq.(2) is used . At cross-over distance, Eqs.(1) and (2) give the same result. So d_c can be calculated as

$$d_c = \frac{(4\pi h_t h_r)}{\lambda} \qquad (3)$$

The free space model and the two-ray model predict the received power as a deterministic function of distance. They both represent the communication range as an ideal circle. In reality, the received power at certain distance is a random variable due to multipath propagation effects, which is also known as fading effects. In fact, the above two models predicts the mean received power at distance d.

B. MAC protocol and traffic pattern

The IEEE 802.11 MAC protocol with Distributed Coordination Function (DCF) [7] is used as the MAC layer in our scenarios. DCF is the basic access method used by the mobile nodes to share the wireless channel under independent ad hoc configuration. It uses a RTS/CTS/DATA/ACK pattern for all unicast packets and simply sends out DATA for all broadcast packets. The access scheme is Carrier Sense Multiple Access/collision avoidance (CSMA/CA) with acknowledgements.

A traffic generator named cbrgen was developed to simulate constant bit rate sources in ns2. We use it to generate 6 pair/12 pair/24 pair/30 pair/60 pair of udp stream stochastically. Each CBR package size is 512 bytes and one package is transmitted in 1second.

C. Performance metrics

The following metrics are applied for comparing the protocol performance. Some of these metrics are suggested by the MANET working group for routing protocol evaluation [6].

- Average end-to-end data delay: This includes all possible delays caused by buffering during routing discovery latency, queuing at the interface queue and retransmission delays at the MAC, propagation and transfer times.
- Jitter: the delay variation between each received data packets
- Normalized routing load: the sum of the routing control messages such as HELLO,RREQ etc., counted by k bit/s.

3. Simulation Results and Performance Analysis

A. End to End delay analysis

DSDV protocol exhibits a shorter delay because it is a kind of table-driven routing protocol, each node maintains a routing table in which all the possible destination are recorded, only packets belonging to valid routes at the ending instant get through. A lot of packets are lost until new (valid) route table entries have been propagated through the network by the route update messages in DSDV.

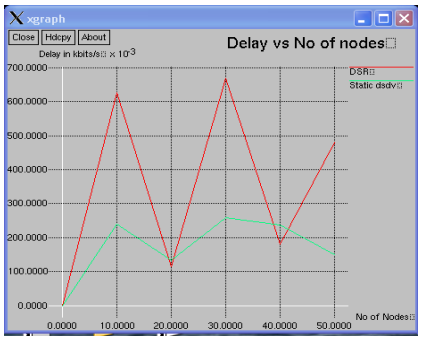

Fig 1. End to end delay versus number of nodes.

When requesting a new route, DSR first searches the route cache storing routes information it has learned over the past routing discovery stage and has not used the timer threshold to restrict the stale information which may lead to a routing failure. Moreover DSR needs to put the routes information not only in the route reply message but also in the data packets which relatively makes the data packets longer than before. Both of the two mechanism make DSR to have a long delay than DSDV.

B. Jitter Analysis

DSDV is continuous to present the trend of ascending with the size larger than 20. This is depicted in Fig 2.

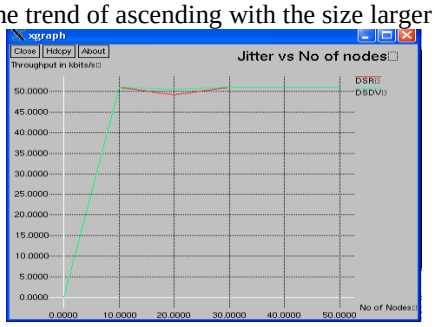

Fig 2. Average jitter versus no of nodes

C. Routing Load Analysis

The routing load of a protocol has influenced node efficiency of battery energy and decided its scalability especially under an environment of narrower bandwidth and easier congestion.

For DSDV the routing load naturally increases at a faster rate along with the number of nodes increasing as shown in Fig.3.

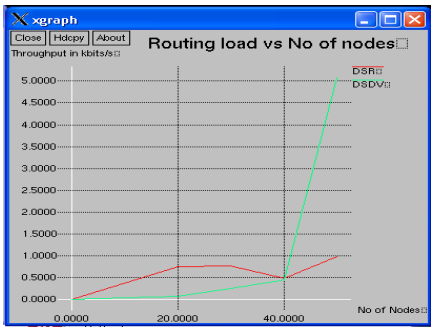

Fig 3. Routing Load versus no of nodes.

Nearly an order of magnitude separates DSR, which has the heavier overhead with the number of nodes smaller than 50.

D. Performance summary

When DSDV must maintain the entire situation information, when topology changes frequently and network size increases, the increment of routing load is very quick, and it is not fit for large scale and high speed moving wireless environment.

DSR routing load is moderate and a long delay which is suitable to a medium scale network environment without higher delay demand.

4. Conclusion

DSDV can be employed in scenario wherein the network topology is known and not dynamically changing. An existing wired network protocol can be applied to ad hoc wireless network with many fewer modifications.

This paper discusses the simulation model for variable network size. This paper contributes in area of impact of different simulation model on routing protocol.

References

[1] Li Layuan, Li Chunlin and Yaun Peiyan, "Performance evaluation and simulations of routing protocols in Adhoc network", Computer communication 30 (2007) 1890-1898.

[2] Charles E. Perkins and Pravin Bhagwat "Highly dynamic Destination Sequenced Distance Vector routing (DSDV) for mobile computers", in: Proceedings of SIFCOMM' 94 Conference on Communication Architectures, Protocols and Applications, August1994, pp.234-244.

[3] David B. Johnson, David A. Maltz and Yih-Chun Hu, "The Dynamic Source Routing Protocol for Mobile Ad Hoc Networks", draft-ietf-manet-dsr-10.txt, July 2004.

[4] The Network Simulator –ns2. Available from http://www.isi.edu/nsnam/ns/index.html/

[5] H.T Friss, "A note on a simple transmission formula", in: Proc: IRE, 34, 1946.

[6] S. Corson and J. Macker, "Mobile Ad hoc Networking (MANET) Routing Protocol Performance Issues and Evaluation[S]", RFC2501, 1999.

[7] T.S Rappaport, Wireless Communication: Principles and Practice, Oct, Prentice Hall, Upper Saddle River, NJ, 1995.

[8] IEEE Computer Society LAN MAN Standards Committee,"Wireless LAN Medium Access Protocol (MAC) and Physical Layer (PHY) Specification", IEEE Std 802.11-1997, The Institute of Electrical and Electronics Engineers, New York, 1997.

Determine the Fatigue behavior of engine damper caps screw bolt

R. K. Misra
School of Mechanical Engineering, Gautam Buddha University,
Greater Noida, Uttar Pradesh-201308

Abstract
In this paper, fatigue strength of the engine damper cap screw bolt is determined. Engine damper cap screw is critical fastener. Critical fastener is a term used to describe a cap screw that, upon failure, causes immediate engine shutdown or possible harm to person. So, determination of fatigue strength is important. S-N method is used for cap screw fatigue strength determination by testing number of samples at different alternating load keeping mean load constant. Alternating load is increased until cap screws begin to fail. But for measurement of axial load in fasteners, ultrasonic bolt gauging method is used. It has been observed that fatigue failure takes place on the thread of cap screw bolt due to high stress concentration on the thread.

Keywords: Caps screw bolt, Fatigue strength, Ultrasonic elongation, Preload.

1. Introduction

Generally pure static loading is rarely observed in engineering components or structures. The majority of structures are subjected to fluctuating or cyclic loads. There is difficulty to detect fatigue failure of bolts in complex system until a catastrophic fracture occurs, without warning [1]. In complex structure, it is difficult to determine the response analytically. Therefore, experimental, numerical or a combination of both methods are used for fatigue life evaluations. Nut and bolts are very important elements in automobiles and aerospace industries. They are used in large scale in modern car and aircraft and potential source of fatigue crack initiation. There are various parameters which are responsible for failure of bolts are thread root radius, low tightening force, material [2-6]. Bolts and nut are usually manufactured in either coarse or fine threads. Various researchers have studied experimentally the effect of thread pitch on fatigue life of bolts [7].

An ultrasonic method is used to measure tensile stress in high tension bolts after developing longitudinal and shear wave velocities. But main problem is the precision, how much tightening force is required in bolts. Insufficient or excessive tightening force is also the cause of bolted joint failure. There are various procedures to measure the bolt tension. The ultrasonic method is considered as a best method to measure elongation of bolts based on time of flight because it is easy to measure bolt tension with accuracy. However, before fastening ultrasonic method requires original length of the bolts and material constants such as young's modulus to determine the actual tensile load from ultrasonic elongation of the bolts [8]. However, it is difficult to determine the fatigue behavior of a nut-loaded bolt due to complexity of the stress distribution. This complexity is present in the system. There are three causes for this: distribution of non-uniform load between the teeth of bolt and nut [9, 10], teeth generates the stress concentration [11] and due to presence of residual stresses (manufacturing process), stress field distorted [12, 13].

The effects of internal stresses were studied experimentally and numerically. Experimental evaluation is complex therefore scientist did more theoretical work [14, 15]. Experimental data are very limited [16]. But James–Anderson approach is very popular. It is used mostly [17, 18].

Earlier study was limited to stress analysis of the thread connectors [19-21].Later on using the finite element analysis; stress analysis of the thread root was studied. It gave the distribution laws of the stress concentration factors. The photo elastic stress-frozen technique was applied to determine the stress distributions both at the thread roots and on the screw flanks [22-23].Distribution of non-uniform load direct influence stress analysis of the connectors, especially in higher stress zone. Zhao [24] studied the behaviour of load distribution in a bolt-nut connector using the Virtual Contact Loading (VCL) method. Results obtained from VLC method was near to analytical and numerical solutions [25-26]. This method is based on mixed finite element and stress influence function methods. It has higher computational accuracy and efficiency [27]. In this paper fatigue strength of the cap screw bolt using S-N curve and failure location of bolt under fatigue testing has been studied.

2. Experimental Studies

- **Damper**

A damper is designed to reduce torsional vibrations by converting vibration energy into heat. For engine generally two types of engine damper is used. These are following

- ❖ Tuned, rubber (or elastomer) dampers
- ❖ Viscous fluid dampers

Engine dampers are normally effective at natural frequency of crank vibration and do not affect attached system vibrations. Sometimes damper are installed in other parts of driveline to add inertia and de-tune components.

- **Critical fastener**

Critical fastener is a term used to describe a cap screw that, upon failure, causes immediate engine shut down, mission disabling malfunction, or possible harm to person such as operators or bystanders. The critical fasteners are defined as cylinder head, main bearing cap, connecting rod, vibration damper and flywheel cap screws.

- **Damper cap screws**

The purpose of bolt is to clamp two or more parts together. The clamping load stretches or elongates the bolt, the load is obtained by twisting the nut until the bolt has elongated to the elastic limit. If the bolt does not loosen, this bolt tension remains as the preload or clamping force. This clamping force is called the pre-tension or bolt preload. It exists in the connection after the nut has been properly tightened no matter whether the external load P is exerted or not. When tightening, the mechanic should hold the bolt head stationary and twist the nut in this way the bolt shank should not bear the thread friction torque. During clamping, the clamping force which produces tension in the bolt induces compression in the members [28]. Damper cap screws are used to secure a vibration damper to crankshaft. Cap screws are subjected to vibration, fatigue and corrosive environment. Damper cap screw bolts mounting on engine has been shown in Figure 1.
Design of cap screw is an iterative process. The designer must balance preload requirement with acceptable alternating loads by adjusting grade selection and thread diameter. All cap screws must verify the preload, fatigue strength, torque requirement behavior and other attributes.

Technical specifications of the Damper cap screw bolt

Damper cap screws are used to secure a damper to the crankshaft. Details of the cap screw are given below [29]:

Type	: 12 point cap screw bolt
No. of cap screw	: 06 Nos.
Assembly torque	: 410 lb-ft
Nut factor	: 0.16 to 0.2
Mean dia	: 0.71
Length	: 4”
Grade	: 8
Thread	: ¾- 16 fine thread series UNF
Stress Area	: 0.373 inch^2
Thread per inch	: 16
Pitch	: 1/16 = 0.0625 inch
Proof Load	: 44800 lb
Tensile Strength (Min)	: 5600 lb

3. Evaluation of Mechanical Properties

Figure 2 shows the approach to determine the fatigue strength of cap screw bolt.

- **Material property evaluation requirements**

a. Surface hardness, Ultimate tensile strength was obtained prior to the fatigue test. Cap screws which were used in the evaluation. Those cap screws were not used as a fatigue test specimens.
b. Hardness of the shank is obtained through hardness tester.
c. Cap screws were tested to failure in tension, using the grip length or gage length and thread engagement of the intended fastener application.
d. Chemical analysis results obtained at the center of head after clean- up the surface

- **UTS (Ultimate tensile strength)**

Tension tests provide information on the strength and ductility of materials under uniaxial tensile stresses. To perform tensile test, SAE [29, 30] and ASTM [31] procedure has been adopted. Figure 3 shows the ultimate tensile machine (UTM) and cap screw with adopter. Details of the test procedure have been given below:

❖ The cap screw was inserted in the UTS machine with the test washer placed under the cap screw head.
❖ The test nut was assembled onto the cap screw by turning the cap screw head until the cap screw is seated against the hardened washer.
❖ Precaution was taken that a minimum of two threads protrude through the nut. Wedge grips were used for holding the specimen.

❖ Then the cap screw were continuously and uniformly tightened at a speed not to exceed 30 rpm with a torque-measuring device or equivalent means, until either the torque or the tension value, as required, was developed and both torque and tension readings were recorded.
❖ Axial loading was applied until failure.
❖ It was ensured that the cap screw shall not fracture before having withstood the minimum tensile load specified for the applicable size, thread series, grade and the failure location.
Table 1 shows the ultimate test results. Stress area, mean tensile strength and mean tensile stress is 0.373 inch^2, 71361 pound and 191315 pound/inch^2 respectively.

- **Chemical Analysis**

Chemical analysis was performed using spectrometer [32] and spectrometer has been shown in figure 4. Procedure for chemical analysis has been given below:
❖ Specimen was prepared for chemical analysis at the center of cap screw head by cleaning upper surface.
❖ A capacitor discharge was produced between the flat, ground surface of the disk specimen and a conically shaped electrode by spectrometer. The discharge was terminated at a predetermined intensity time integral of a selected iron line, or at a predetermined time, and the relative radiant energies of the analytical lines were recorded. The most sensitive lines of arsenic, boron, carbon, nitrogen, phosphorus, sulfur, and tin lie in the vacuum ultraviolet region. The absorption of the radiation by air in this region was overcome by evacuating the spectrometer and flushing the spark chamber with argon.
❖ Chemical composition for each element (C, Si, Mn, P, S, Cr, Mo, Ni) in percentage was noted. Chemical analysis results have been shown in table 2.

- **Hardness and Microstructure**

The Rockwell hardness test is an empirical indentation hardness test that can provide useful information about metallic materials. This information may correlate to tensile strength, wear resistance, ductility and other physical characteristics of metallic materials, and may be useful in quality control and selection of materials. Figure 5 shows the hardness tester and microscope for analysis of hardness and microstructure of cap screw respectively.
Test procedure has been described below:
❖ Placed the cap screw on hardness tester as per attached figure.
❖ Moved the indenter into contact with the test surface in a direction perpendicular to the surface.
❖ Measured the hardness of cap screw.
❖ Observed the microstructure of specimen at microscope.
Table 3 shows the hardness & microstructure test results of the cap screw.

- **Coating**

Cap screw bolts were coated with the zinc phosphate and oil coatings to provide a corrosion protection and a low & consistent friction coefficient. The most consistent preload is achieved with an as-received zinc phosphate and oil coating.

- **Minimum grade requirement**

Critical cap screws were used for dampers shall be grade 8 or above [29] for inch products or property class 10.9 or above [33] for metric products. Property class 12.9 fasteners are susceptible to stress corrosion cracking and are not recommended.

4. Determination of bolt pre-load

The purpose of the bolt was to clamp two or more parts together. The clamping load stretches or elongates the bolts; the load was obtained by twisting the nut until the bolt elongated to the elastic limit. When the bolt did not loosen, this bolt tension remains as the preload or clamping force. This clamping force is called the pre-tension or bolt preload. It exists in the connection after the nut has been properly tightened no matter whether the external load P is exerted or not. The preload is the force required to hold the joint together correctly. The preload cannot be calculated directly, but it can be estimated using available empirical data and then confirmed by measurements for the particular cap screw and joint.

- **Theoretical calculation of preload**

The relationship between the torque applied to a fastener and tension created from the resulting bolt elongation has been described below

T= F. K.D
Where T, K, D & F are torque, friction factor, bolt diameter and preload respectively. The K value can be thought of as summarization of anything and everything that affect the relationship between torque and preload. Table 4 gives brief list of

some estimated K factors [34]. A K factor for zinc phosphate coated cap screws was assumed between 0.16 and 0.20 for approximate calculations of preload. Preload value of the damper cap screw has been shown in table 5.

- **Experimental measurement of preload**

In this work, axial load is measured by ultrasonic method using ultrasonic bolt gauge. Figure 6 shows the ultrasonic bolt gauge. The purpose of ultrasonic bolt gauging is to estimation of axial load in fasteners. The ultrasonic method of measuring the elongation of bolts based on time of flight to measure bolt tension with better accuracy. However, the ultrasonic method requires the original length of bolts and Young's modulus before fastening to determine the actual tensile load from ultrasonic elongation of the bolts [8].

The purpose of using ultrasonic bolt gage is to use ultrasonically measured elongation to determine cap screw preload. The cap screws are calibrated in a load frame to relate cap screw stretch (the ultrasonic elongation) to applied load. The cap screw stretches as torque is applied to joint. Using the ultrasonic length measurement, the stretch is related to preload through the cap screw calibration**.**

Before calibration, bolt gage were ground on top and bottom. Grinding improves connection between ultrasonic transducer to bolt. Preparation of the bolt surface has been shown in figure 7. After preparation of the cap screw bolt surface, cap screw bolt gage has been calibrated. Figure 8 shows the calibration set up. Length of the calibration bar is measured in this process. It is very necessary to makes sure that the bolt system is working properly. Initially ultrasonic length is measured before loading the bolt. Later on load is applied on bolt to measure ultrasonic elongation. Load and elongation were used to determine a calibration curve and load factor. Calibration of the damper capscrew bolt has been shown in Table 6 and Figure 9. After that, cap screw was installed on engine to mount damper with crankshaft. The cap screws were tightened in sequence. Torque all cap screw as per specification. Load (tension) was calculated for all stretch by multiplying the load factor, determined through calibration curve. Table 7 shows the value of preload using ultrasonic bolt gauge. 40651 lbf, average pre-load on cap screw bolts has been determined. Therefore 40,000 lbf, mean load has considered for fatigue test.

5. Fatigue testing

The purpose of the fatigue test is to make sure that a cap screw has adequate fatigue strength to survive in an engine environment under engine loading. Engine conditions are measured and duplicated in a tension-tension axial fatigue test.

- **Fatigue test procedure**

i. Mounted the screw bolt test fixture on closed loop servo hydraulic fatigue test system.
ii. Set gage length 64 mm.
iii. Set the load on the servo hydraulic fatigue test system.
iv. Cycle of the machine was set at approximately 15 Hz.
v. Maintained mean load 40000 lbs during testing & alternating load varying from 2000 lbs to 7500 lbs (Fatigue testing of samples should be at 2 to 4 times engine alternating load).
vi. Recorded the load and cycles to failure.
vii. Repeated above steps for all samples.

- **Fatigue test cycle**

In the conventional fatigue design, the fatigue limit was obtained at 10^7 number of stress cycle to determine the allowable stress level for design against high cycle fatigue.

Post test processing of the raw test data was used to obtain the estimate of the cap screw's mean fatigue strength, standard deviation, coefficient of variation of strength. These post test results can be used for comparison with a minimum fatigue test requirement .Table 8 shows the fatigue test results. Raw data can be effectively presented in an S-N plot and Goodman plot.

- **S-N Curve**

S-N curve for cap screw was determined using the alternating load. The load was increased until cap screw begin to fail.16 sample were tested to determine the shape of fatigue curve. The Data from this sample were analyzed using software and M.S. Excel. After drawn S-N curve, Endurance limit was determined. Figure 10 and 11 shows the S-N curve made using M.S. Excel and fatigue software respectively.

- **Goodman diagram**

Goodman diagram is a tool for estimating infinite fatigue life of a component undergoing mean and alternating load.

6. Results and discussion

Following observation is observed after analyzing the table 1, 2 & 3:

- Damper cap screw bolt can bear maximum tensile stress 191315 pound square inch before failure.
- It contains maximum amount of manganese. After that, chromium, nickel and carbon come in the row. Due to presence of high manganese hardenability, machinability and strength improves.
- Chromium and nickel improves toughness. Therefore bolt bears maximum distortion energy before fracture.
- The role of carbon is also very significant. Carbon increases the damping property. When fatigue load is applied, bolt dissipates more amount of energy to atmosphere. So life of the bolt increases.
- Bolt is very hard. Its hardness varies between 39-42 HRC.
- Tempered martensite structure is observed after seeing the bolt from microscope and thread rolling is done after heat treatment. Laps/cracks are absent at root or flanks of the threads.

Table 5 shows the pre-load calculations theoretically of the damper cap screw bolt. Preload is applied to hold the joint together correctly. The preload cannot be calculated directly, but it can be estimated using available empirical data and then confirmed by measurements for the particular cap screw and joint. Theoretical average value of the preload is 38737.8 pound. To measure the value of preload experimentally, ultrasonic method is used. Table 7 shows the value of preload using ultrasonic bolt gauge**.** 40651 pound average pre-load has been determined from ultrasonic bolt gauge. After calculating preload from both procedures, fatigue experiment has been performed. At the time of performing fatigue test, maximum and minimum load were changing but mean load was fixed. That was 40,000 pound. It was very near to average preload. Fatigue test results have been shown in table 8. When minimum and maximum load was 35,500 pound and 44,500 pound respectively, bolt was safe after passing 10000000 cycles. As soon as the value of maximum load reaches up to 45,000. Bolt fails at 7608380 cycles. Number of cycles decreases drastically after addition of 500 pound load in maximum load. S-N curve has been drawn using table 8 data in MS Excel sheet. Figure 10 shows the S-N curve. To validate table 8 data and S-N curve, fatigue software was used. Figure 11 shows the S-N curve by fatigue software. It is observed that bolt is safe, when alternating load is below 5000 pound.

Goodman line has been shown in figure 12.The Goodman line is used as criteria of failure when the component is subjected to mean stress as well as stress amplitude.

Conclusion

The fatigue strength of damper cap screw bolt is determined by S-N curve method. Data for S-N curve was generated on servo hydraulic fatigue test system by axial force controlled method. Fatigue strength of cap screw bolt is 4582 pound at mean load of 40000 pound.

The purpose of fatigue test is to make sure that a cap screw has adequate fatigue strength to survive in an engine environment under engine loading. Engine conditions are measured and duplicated in a tension-tension axial fatigue test.

Alternating load due to engine operation for particular damper cap screw bolt should be less than 4582 pound. For better design the alternating load should be half of fatigue strength. Goodman diagram plotted based on fatigue strength, mean load and ultimate tensile strength to find the Goodman diagram can be used for finding the design margin at different mean load & alternating load.

References:

1. Nishida, S, Failure analysis in engineering applications. Great Britain: Butterworth-Heinemann; 1992.
2. Milan MT, Spinelli D, Bose Filho WW, Montezuma MFV, Tita V. Failure analysis of a SAE 4340 steel locking bolt. Eng Fail Anal 2004; 11:915–24.
3. Baggerly RG. Hydrogen-assisted stress cracking of high-strength wheel bolts. Eng Fail Anal 1996; 3(4):231–40.
4. Yu Z, Xu X. Failure analysis of connecting bolts and location pins assembled on the plate of main-shaft used in a locomotive turbocharger. Eng Fail Anal 2008; 15: 471–9.
5. Chen Hsing-Sung, Tseng Pi-Tang, Hwang Shun-Fa. Failure analysis of bolts on an end flange of a steam pipe. Eng Fail Anal 2006; 13:656–68.
6. Rabb R. Fatigue failure of a connecting rod. Eng Fail Anal 1996; 3(1):13–28.
7. Majzoobi, G.H., Farrahi, G.H, Habibi, N. Experimental evaluation of the effect of thread pitch on fatigue life of bolts. International Journal of fatigue 2005; 27:189-196.
8. Nohyu, Kim and Minsung, Hong. Measurement of axial stress using mode-converted ultrasound. NDT&E International 2009; 42:164-169.
9. Goodier J. The distribution of load in threads of screws. J Appl Mech Trans ASME 62; 1940, p. A10–A16.
10. D'Eramo M, Cappa P. An experimental validation of load distribution in screw threads. Exp Mech 1991; 31:70–5.
11. Pilkey W. Peterson's stress concentration factors. 2nd Ed. New York: Wiley; 1997. [ISBN: 978-0-471-53849-3].
12. Fetullazade E et al. Effects of the machining conditions on the strain hardening and the residual stresses at the roots of screw threads. Mater Des 2009; 31(4):2025–31.

13. Bradley N. Influence of cold rolling threads before or after heat treatment on the fatigue resistance of high strength fine thread bolts for multiple preload conditions. In: Toor P, editor. ASTM STP 1487 structural integrity of fastener. West Conshohocken, PA: ASTM International; 2007, p. 98–112.
14. Olsen K. Fatigue crack growth analyses of aerospace threaded fasteners – Part I: State-of-practice bolt crack growth analyses method. In: Toor P, editor. ASTM STP 1487 structural integrity of fastener. West Conshohocken, PA: ASTM International; 2007, p. 125–40.
15. Toribio J et al. Stress intensity factor solutions for a cracked bolt under tension, bending and residual stress loading. Eng Fract Mech 1991; 39(2):359–71.
16. Mettu S, et al. Stress intensity factor solutions for fasteners in NASGRO 3.0. In: Toor P, editor. ASTM STP 1391 structural integrity of fasteners, vol. 2. West Conshohocken, PA: ASTM International; 2000, p. 133–9.
17. James L, Anderson W. A simple procedure for stress intensity calibration. Eng Fract Mech 1969; 1:565–8.
18. Shen H, Guo W. Modified James–Anderson method for stress intensity factors of three-dimensional cracked bodies. Int J Fatigue 2005; 27:624–8.
19. Fukuoka, T., Yamasaki, N., Kitagawa, H. and Hamada, M., Stress in bolt and nut. Bull. JSME, 1986, 29, 3275–3279.
20. Tanaka, M., Miyazawa, H., Asaba, E. and Hongo, K., Application of the finite element method to bolt-nut joints. Bull. JSME, 1981, 24, 1064–1071.
21. Tafreshi, A. and Dover, W. D., Stress analysis of drillstring threaded connections using the finite element method. Int. J. Fatigue, 1993, 15, 429–438.
22. Kenny, B. and Patterson, E. A., Load and stress distribution in screw threads. Exp. Mech, 1985, **25**, 208–213.
23. Fessler, H. and Jobson, P. K., Stress in a bottoming stud assembly with chamfers at the ends of the threads. J. Strain Anal, 1983, 18, 15–22.
24. Zhao, H., Analysis of the load distribution in a bolt-nut connector. Comput. Struct, 1994, 53, 1465–1472.
25. Sopwith, D. G., The distribution of load in screw threads. Proc. Inst. Mech. Engrs, 1948, 159, 319–398.
26. Bretl, J. L. and Cook, R. D., Modeling the load transfer in threaded connections by the finite element method. Int. J. Numer. Meth. Engng, 1979, 14, 1359–1377.
27. Zhao, H., The virtual contact loading method for contact problems considering material and geometric nonlinearities. Comput. Struct, 1996, 58, 621–632.
28. Shigley, J.E and Mischake, C.R., Mechanical engineering design. McGraw Hill Publications, 1989.
29. SAE J429, Mechanical and material requirements for externally threaded fasteners, 1999.
30. SAE J174, Torque-Tension test procedure for steel threaded fasteners – inches & metric series, 1998.
31. ASTM standard E8/E8M, Standard test methods for tension testing of metallic materials, 2008.
32. ASTM standards E415, "Standard test method for atomic emission vacuum spectrometric analysis of carbon and low-alloy steel", 2008.
33. ASTM standard F568M, "Standard specification for carbon and alloy steel externally threaded metric fasteners", 2007.
34. FS7028, "Fastenal Technical reference guide", 2005.

Figure

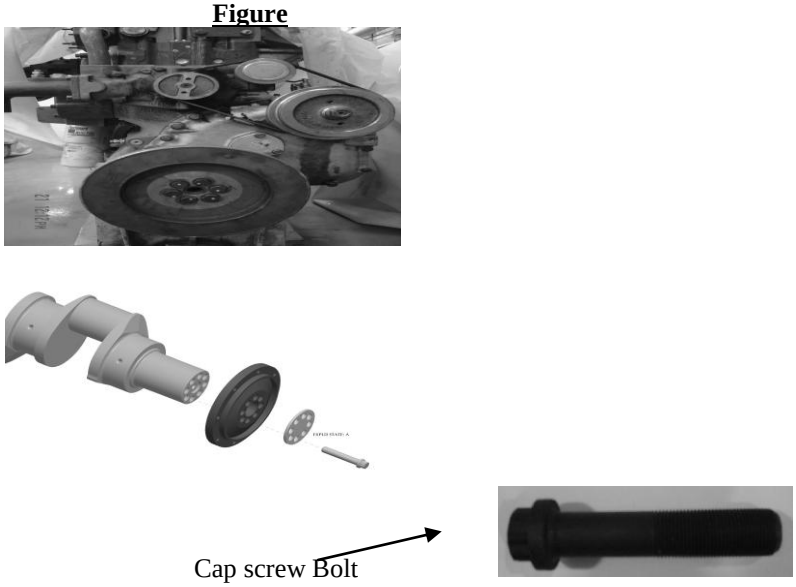

Figure 1: Cap Screw Bolt Mounting on Engine

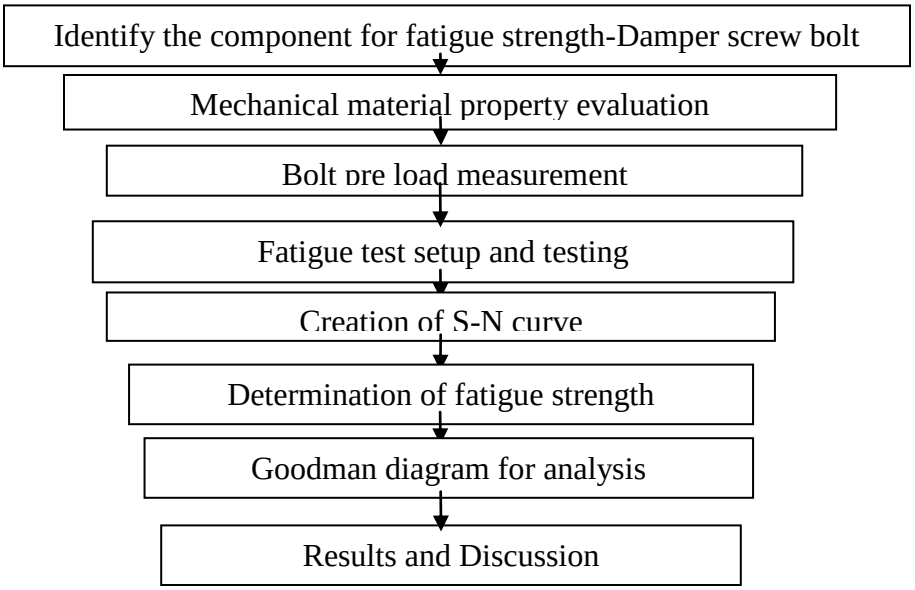

Figure 2: Flow diagram to determine fatigue strength

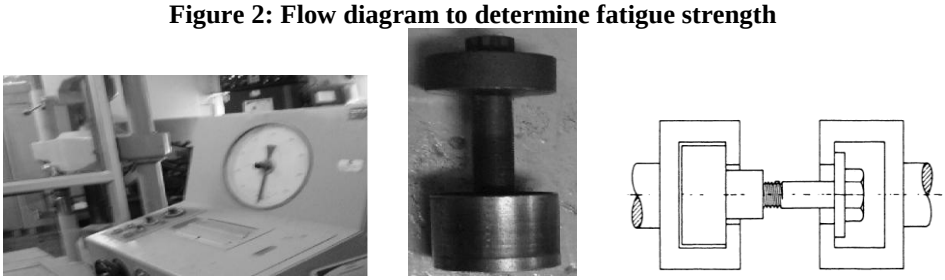

UTM Cap screw Cap screw with adopter

Figure 3: **Ultimate tensile testing machine and cap screw with adopter**

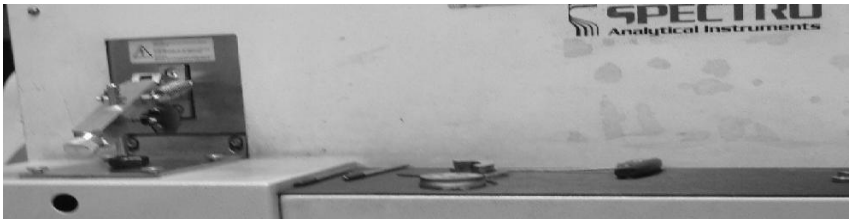

Figure 4: Spectrometer for chemical analysis

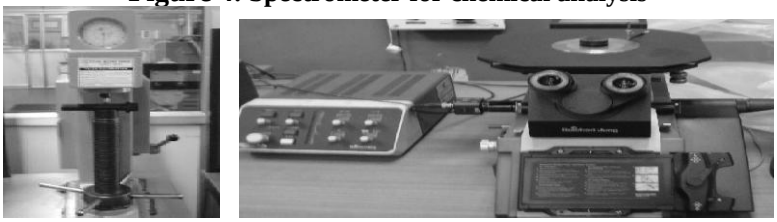

Hardness Tester Microscope

Figure 5: Hardness & Microstructure of cap screw

Figure 6: Ultrasonic bolt gage

Figure 7: Bolt Surface Preparation

Figure 8: Bolt Calibration setup

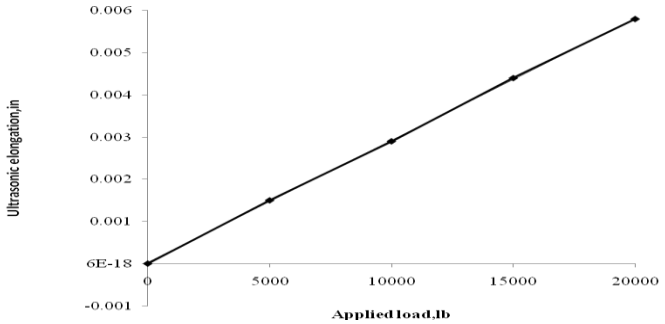

Load factor (slope) 3447784 Y-intercept 67.5 R^2 0.999857

Figure 9: Cap screw bolt calibration

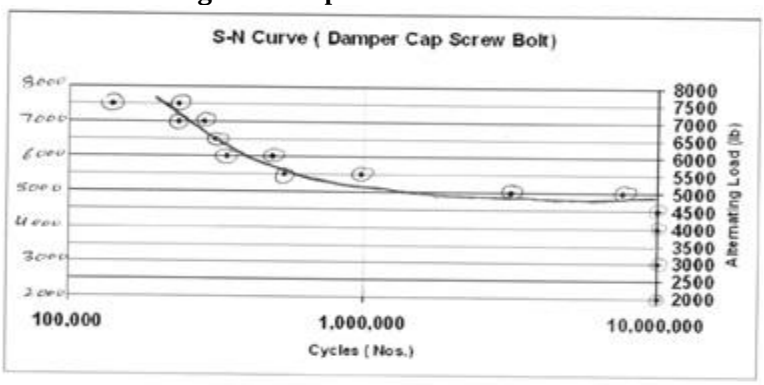

Figure 10: S-N Curve by MS Excel

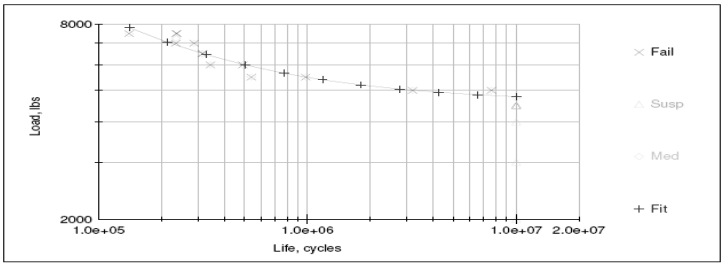

Figure 11: S-N Curve by fatigue software

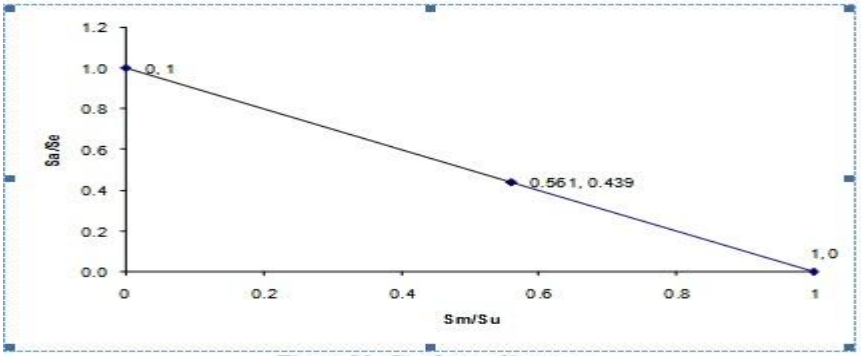

Figure 12: Goodman diagram

Table

Table 1: Ultimate tensile test results

Sr. No.	Sample	Failure Load (KN)	Failure Load (lb)	Failure Stress (Psi)
1	1	320	71939	192865
2	2	324	72838	195276
3	3	330	74187	198892
4	4	322	72388	194069
5	5	314	70590	189249
6	6	310	69691	186839
7	7	302	67892	182016
Average(UTS)		**318**	**71361**	**191315**

Table 2: Chemical Analysis results

Sr. No.	Element %	C	Si	Mn	P	S	Cr	Mo	Ni
1	Lot1	0.41	0.25	0.88	0.014	0.006	0.51	0.15	0.51
2	Lot1	0.4	0.26	0.85	0.02	-----	0.54	0.16	0.5
3	Lot1	0.38	0.15	0.73	0.017	0.01	0.58	0.19	-------
Standard	ASTM E415	0.37/ 0.44	0.15/ 0.35	0.70/ 1.05	0.035 max	0.04 max	0.35/ 0.65	0.15/ 0.25	0.35/ 0.75
Standard	SAE 8640	0.38/ 0.43	0.15/ 0.35	0.75/ 1.00	0.035 max	0.04 max	0.40/ 0.60	0.15/ 0.25	0.40/ 0.60

Table 3: Hardness & Microstructure test results

Sr. No.	Sample	Hardness	Microstructure
1	1	39-42 HRC	Fine tempered martensite. Cracks/laps are not observed at root/flanks of the threads. Decarburization
2	2	38-39 HRC	Tempered martensite. Thread rolling is done after heat treatment. Laps/cracks are absent at root or flanks of the threads.
3	3	38-40 HRC	Tempered martensite. Thread rolling is done after heat treatment. Laps/cracks are absent at root or flanks of the threads.

Table 4: K factors

Bolt Condition	K
Non-plated, black finish	0.20 ------ 0.30
Zinc-plated	0.17 ------ 0.22
Lubricated	0.12 ------ 0.16
Cadmium-plated	0.11 ------ 0.15

Table 5: Preload calculation –Damper cap screw

Assembly torque (T) lb.ft	410	410	410	410	410
Capscrew diameter (D_{in}) inch	0.71	0.71	0.71	0.71	0.71
Capscrew diameter (D),ft = D_{in}/12	0.0592	0.0592	0.0592	0.0592	0.0592
Nut factor (K), assume	0.16	0.17	0.18	0.19	0.20
Preload (P), lb = T/(D*K)	43309.9	40762.2	38497.7	36471.5	34647.9
Average Torque (lb.ft)	**38737.8**				

Table 6: Damper Capscrew bolt calibration

Sr. No.	Applied load, lb	Measured ultrasonic elongation, in
1	0	0.0000
2	5000	0.0015
3	10000	0.0029
4	15000	0.0044
5	20000	0.0058

Table 7: Torque tension test results

Torque = 400 lb.ft & Load factor = 3447784		
Cap Screw No.	**Stretch**	**Load**
1	0.0110	37960
2	0.0117	40339
3	0.0129	44476
4	0.0121	41718
5	0.0131	45166
6	0.0112	38615
7	0.0118	40684
8	0.0127	43787
9	0.0114	39305
10	0.0116	39994
11	0.0120	41373
12	0.0101	34823
13	0.0120	41373
14	0.0111	38270
15	0.0116	39994
16	0.0126	43442
17	0.0114	39305
18	0.0119	41029
19	0.0112	38615
20	0.0124	42753
Sample size	**Average stretch**	**Average load**
20	**0.0118**	**40651**
Std Dev = 2504, Min load = 34823 &Max load = 45166		

Table 8: Fatigue test results

Sample No.	**Mean load, (lbs)**	**Alternating load, (lbs)**	**Min load, (lbs)**	**Max load, (lbs)**	**Cycles to failure**	**status**
1	40000	2000	38000	42000	10000000	**Pass**
2	40000	3000	37000	43000	10000000	**Pass**
3	40000	4000	36000	44000	10000000	**Pass**
4	40000	4500	35500	44500	10000000	**Pass**
5	40000	5000	35000	45000	7608380	**Fail**
6	40000	5000	35000	45000	3190347	**Fail**
7	40000	5500	34500	45500	539646	**Fail**
8	40000	5500	34500	45500	982412	**Fail**
9	40000	6000	34000	46000	342895	**Fail**
10	40000	6000	34000	46000	490985	**Fail**
11	40000	6500	33500	46500	314736	**Fail**
12	40000	6500	33500	46500	314780	**Fail**
13	40000	7000	33000	47000	235024	**Fail**
14	40000	7000	33000	47000	286642	**Fail**
15	40000	7500	32500	47500	236327	**Fail**
16	40000	7500	32500	47500	140086	**Fail**

Removal of Impulse Noise Using Eodt with Pipelined ADC

[1]Prof.Manju Devi,[2] Prof.Muralidhara, [3]Prasanna R Hegde

[1] Associate Prof, ECE, BTLIT Research scholar,[2] HOD, Dept. Of ECE, PES MANDYA.[3] VIII- SEM ECE, BTLIT,

Abstract

Corrupted Image and video signals due to impulse noise during the process of signal acquisition and transmission can be corrected. In this paper the effective removal of impulse noise using EODT with pipelined architecture and its VLSI implementation is presented. Proposed technique uses the denoising techniques such as Edge oriented Denoising technique (EODT) which uses 7 stage pipelined ADC for scheduling. This design requires only low computational complexity and two line memory buffers. It's hardware cost is quite low. Compared with previous VLSI implementations, our design achieves better image quality with less hardware cost. The Verilog code is successfully implemented by using FPGA Spatron-3 family.

Index Terms—Image denoising, impulse noise, pipeline architecture, VLSI.

1. Introduction

Most of the video and image signals are affected by noise. Noise can be random or white noise with no coherence, or coherent noise introduced by the capturing device's mechanism or processing algorithms. The major type of noise by which most of the signals are corrupted is salt and pepper noise. You might have observed the dark white and black spots in old photos, these kind of noise presented in images are nothing but the pepper and salt noise. Pepper and salt noise together considered as Impulse noise.

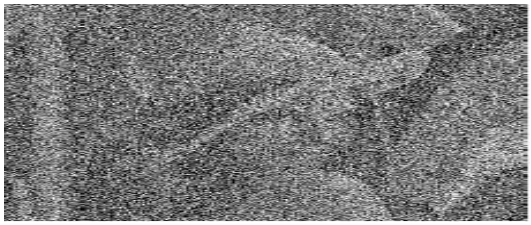

Fig1. Example of pepper and salt noise

The above pictures give us the insight of impulse noise. Number of dots in the pictures will bring down the clarity and quality of the image. In other applications such as printing skills, scanning, medical imaging and face recognition images are often corrupted by noise in the process of signal acquisition and transmission. It's more sophisticated in medical imaging when the edges of the object in image are affected by noise, which may lead to the misdetection of the problem. So efficient denoising technique is important in the field of image processing. many image denoising methods have[1]-[8] been proposed to carry out the impulse noise suppression some of them employ the standard median filter or its modifications to implement denoising process. However, these approaches might blur the image since both noisy and noise-free pixels are modified. The switching median filter consists of two steps:

1) Impulse Detection and
2) Noise filtering.

New Impulse Detector (NID) for switching median filter. NID used the minimum absolute Value of four convolutions which are obtained by using 1-D Laplacian operators to detect noisy pixels. A method named as differential rank impulse detector (DRID) is presented in. The impulse detector of DRID is based on a comparison of signal samples within a narrow rank window by both rank and absolute value. Another technique named efficient removal of impulse noise (ERIN)[8] based on simple fuzzy impulse detection technique.

2. Proposed Technique

All previous techniques involve high computational complexity and require large memory which affects the cost and performance of the system. So less memory consumption and reduced computational complexity are become main design aspects. To achieve these requirements Edge Oriented Denoising Technique (EODT) is presented. This requires only two line memory buffers and simple arithmetic operations like addition, subtraction.

EODT is composed of three components: extreme data detector, edge-oriented noise filter and impulse arbiter. The extreme data detector detects the minimum and maximum luminance values in W, and determines whether the luminance values of P(i,j) and its five neighboring pixels are equal to the extreme data. By observing the spatial correlation, the edge-oriented noise filter pinpoints a directional edge and uses it to generate the estimated value of current pixel. Finally, the impulse arbiter brings out the Result.

3. Vlsi Implementation Of Eodt

EODT has low computational complexity and requires only two line buffers, so its cost of VLSI implementation is low. For better timing performance, we adopt the pipelined architecture which can produce an output at every clock cycle. In our implementation, the SRAM used to store the image luminance values is generated with the 0.18μm TSMC/Artisan memory compiler. According to the simulation, we found that the access time for SRAM is about 6 ns. Since the operation of SRAM access belongs to the first pipeline stage of our design, we divide the remaining denoising steps into 6 pipeline stages evenly to keep the propagation delay of each pipeline stage around 6 ns. The pseudo code and the RTL schematic (Fig2) we obtained is given below

Pseudo code

```
for(i=0; i<row; i=i+1)  /* input image size: row(height) × col(width) */

{
   for(j=0; j<col; j=j+1)
    {

 / * Extreme Data Detector * /
          Get W, the 3×3 mask centered on (i, j);
        Find MINinW and MAXinW in W;
/ * the minimum and maximum values from the first W to current W * /
φ=0;                                                    / * initial values * /
if ((f_{i,j} = MINinW) or (f_{i,j} = MAXinW))
φ=1;                                                    / * P_{i,j}  is suspected to be a noisy pixel * /
if(φ=0)
{
f̄_{i,j} = f_{i,j};
break;                                          / * P_{i,j} is a noise-free pixel * /
}
B = b1b2b3b4b5 = "00000";                       / * initial values * /
if ((f_{i,j-1} = MINinW) or (f_{i,j-1} = MAXinW))
b1=1;                                           / * P_{i,j-1} is suspected to be a noisy pixel * /
if ((f_{i,j+1} = MINinW) or (f_{i,j+1} = MAXinW))
b2=1;                                           / * P_{i,j+1} is suspected to be a noisy pixel * /
if ((f_{i+1,j-1} = MINinW) or (f_{i+1,j-1} = MAXinW))
b3=1;                                           / * P_{i+1,j-1} is suspected to be a noisy pixel * /
if ((f_{i+1,j} = MINinW) or (f_{i+1,j} = MAXinW))
b4=1;                                           / * P_{i+1,j} is suspected to be a noisy pixel * /
if ((f_{i+1,j+1} = MINinW) or (f_{i+1,j+1} = MAXinW))
b5=1;                                           / * P_{i+1,j+1} is suspected to be a noisy pixel * /

/ * Edge-Oriented Noise Filter * /
Use B to determine the chosen directions across P_{i,j} according to figure 4.;
if(B="11111")
f̂_{i,j} = (f̄_{i-1,j-1} + 2 × f̄_{i-1,j} + f̄_{i-1,j+1})/4;    / * no edge is considered * /
else
{
Find D_min (the smallest directional difference among the chosen directions);
f̂_{i,j} = the mean of luminance values of the two pixels which own D_min
```

```
}
/ * Impulse Arbiter * /
if(|f_{i,j} - f̂_{i,j}| > T_s)
        f̄_{i,j} = f̂_{i,j} ;                    / * P_{i,j}  is judged as a noisy pixel * /
else
f̄_{i,j} = f_{i,j} ;                  / * P_{i,j} is judged as a noise-free pixel *
   }
}
```

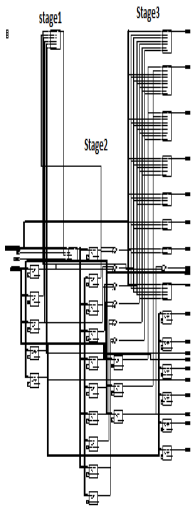

Fig2. RTL Schematic of EODT

3.1 Extreme data Detector

The extreme data detector detects the minimum and maximum luminance values (MIN in W and MAX in W) in those processed masks from the first one to the current one in the image. If a pixel is corrupted by the fixed value impulse noise, its luminance value will jump to be the minimum or maximum value in gray scale. If ($f_{i,j}$) is not equal to (MIN in W and MAX in W) , we conclude that ($P_{i,j}$)is a noise-free pixel and the following steps for de-noising ($P_{i,j}$) are skipped.
If $f_{i,j}$ is equal to MINinW or MAXinW, we set φ=1, check whether its five neighboring pixels are equal to the extreme data and store the binary compared results into B.

3.2 Edge-oriented noise filter

To locate the edge existed in the current W, a simple edge catching technique which can be realized easily with VLSI circuit is adopted. To decide the edge, we consider 12 directional differences, from D1toD2, as shown in fig 3. Only those composed of noise free pixels are taken into account to avoid possible misdetection. If a bit in B is equal to 1, it means that the pixel related to the binary flag is suspected to be a noisy pixel. Directions passing through the suspected pixels are discarded to reduce misdetection. In each condition, at most four directions are chosen for low-cost hardware implementation. If there appear over four directions, only four of them are chose according to the variation in angle.

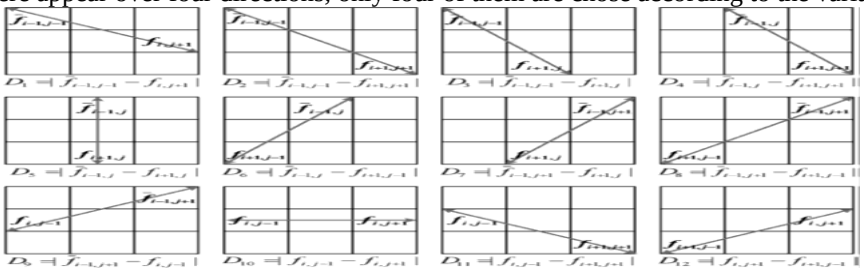

Fig3. 12 Directional difference of EODT

B	The Chosen Directions	B	The Chosen Directions
00000	D_2,D_5,D_8,D_{10}	10000	D_2,D_5,D_8,D_{12}
00001	D_3,D_5,D_8,D_{10}	10001	D_1,D_5,D_8,D_{12}
00010	D_2,D_8,D_{10},D_{12}	10010	D_2,D_4,D_8,D_{12}
00011	D_1,D_6,D_8,D_{10}	10011	D_1,D_6,D_8,D_{12}
00100	D_2,D_5,D_7,D_{10}	10100	D_1,D_2,D_5,D_7
00101	D_3,D_5,D_7,D_{10}	10101	D_1,D_5,D_7
00110	D_2,D_4,D_9,D_{10}	10110	D_1,D_2,D_4
00111	D_1,D_9,D_{10}	10111	D_1
01000	D_2,D_5,D_8,D_{11}	11000	D_2,D_5,D_6,D_8
01001	D_3,D_5,D_7,D_9	11001	D_3,D_5,D_6,D_8
01010	D_2,D_6,D_8,D_{11}	11010	D_2,D_4,D_6,D_8
01011	D_6,D_8,D_9	11011	D_6,D_8
01100	D_2,D_5,D_9,D_{11}	11100	D_2,D_4,D_5,D_7
01101	D_3,D_5,D_9	11101	D_3,D_5,D_7
01110	D_2,D_4,D_9,D_{11}	11110	D_2,D_4
01111	D_9	11111	N/A

N/A – Not Available

Table1. Thirty two possible values of B and their corressponding directions.

Table 1 shows the mapping table between and the chosen directions adopted in the design. If $P_{i,j-1}$, $P_{i,j+1}$, $P_{i+1,j-1}$, $P_{i+1,j}$ and $P_{i+1,j+1}$ are all suspected to be noisy pixels (B = "11111") , no edge can be processed, so $\hat{f}_{i,j}$ (the estimated value of $P_{i,j}$) is equal to the weighted average of luminance values of three previously denoised pixels and calculated as $\hat{f}_{i,j} = (\bar{f}_{i-1,j-1} + 2 \times \bar{f}_{i-1,j} + \bar{f}_{i-1,j+1})/4$.

The smallest directional difference implies that it has the strongest spatial relation with, and probably there exists an edge in its direction. Hence, the mean of luminance values of the two pixels which possess the smallest directional difference is treated as $\hat{f}_{i,j}$.

3.3 Impulse arbiter

Since the value of a pixel corrupted by the fixed-value impulse noise will jump to be the minimum/maximum value in gray scale, we can conclude that if $P_{i,j}$ is corrupted, $f_{i,j}$ is equal MINinW or MAXinW. However, the conversion is not true. If $f_{i,j}$ is equal to MINinW or MAXinW, $P_{i,j}$ may be corrupted or just in the region with the highest or lowest luminance.

In other words, a pixel whose value is MINinW or MAXinW might be identified as noisy pixel even if it is not corrupted. To overcome this drawback, we add another condition to reduce the possibility of misdetection. If $P_{i,j}$ is a noise free pixel and the current mask has high spatial correlation, $f_{i,j}$ should be close to $\hat{f}_{i,j}$ and $|f_{i,j} - \hat{f}_{i,j}|$ is small. That is to say, $P_{i,j}$ might be a noise-free pixel value is MINinW or MAXinW if $|f_{i,j} - \hat{f}_{i,j}|$ is small.

We measure $|f_{i,j} - \hat{f}_{i,j}|$ and compare it with a threshold to determine whether $P_{i,j}$ is corrupted or not. The threshold, denoted as T_s, is a predefined value. Obviously, the threshold affects the performance of proposed method.

A more appropriate threshold can achieve a better detection result. However, it is not easy to derive an optimal threshold through analttic formulation. According to our experimental result, we set the threshold T_s as 20. If $P_{i,j}$ is judged as a corrupted pixel, the reconstructed luminance value $f_{i,j} = \hat{f}_{i,j}$. The part of the scheduling of EODT is shown in Table 2.

Cycle	Image In	Reg4	output of detector	output of noise filter	output of arbiter
1	$f_{i+1,j+2}$	$f_{i,j}$	Φ_{j-3}	$\tilde{f}_{i,j-4}$	$\tilde{f}_{i,j-6}$
2	$f_{i+1,j+3}$	$f_{i,j+1}$	Φ_{j-2}	$\tilde{f}_{i,j-4}$	$\tilde{f}_{i,j-5}$
3	$f_{i+1,j+4}$	$f_{i,j+2}$	Φ_{j-1}	$\tilde{f}_{i,j-3}$	$\tilde{f}_{i,j-4}$
4	$f_{i+1,j+5}$	$f_{i,j+3}$	$\Phi_{i,j}$	$\tilde{f}_{i,j-2}$	$\tilde{f}_{i,j-3}$
5	$f_{i+1,j+6}$	$f_{i,j+4}$	Φ_{j+1}	$\tilde{f}_{i,j-1}$	$\tilde{f}_{i,j-2}$
6	$f_{i+1,j+7}$	$f_{i,j+5}$	Φ_{j+2}	$\hat{f}_{i,j}$	$\tilde{f}_{i,j-1}$
7	$f_{i+1,j+8}$	$f_{i,j+6}$	Φ_{j+3}	$\tilde{f}_{i,j+1}$	$\hat{f}_{i,j}$

Table 2: Part of the scheduling of EODT

From Table 2 it is clear that one clock cycle is required to fetch the pixel from register bank, and three clock cycles are required for extreme data detector and 2 clock cycles needed for edge oriented noise filter and finally impulse arbiter needs one clock cycle to provide the result.

4. Simulation Results:

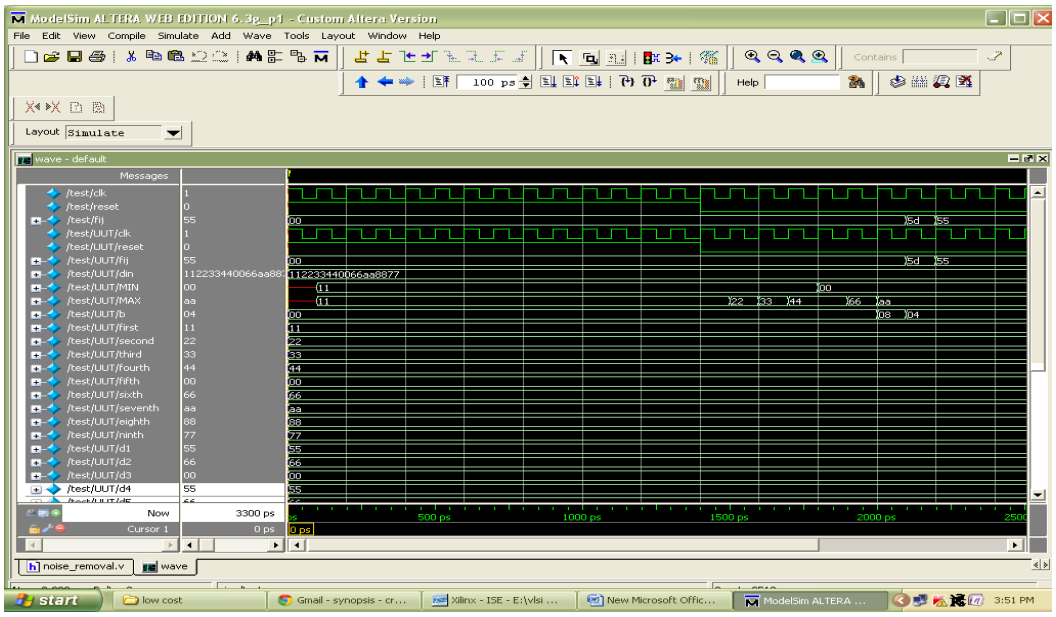

Fig4: simulation results

If the current part of the image is corrupted by fixed value of impulse noise then the value will jump either to the minimum or to the maximum in gray scale. So in our approach we are considering the minimum value pixel is a noisy pixel. For example if the values of nine pixels of corrupted part of the image are 11_22_33_44_00_66_AA_88_77 then we assume 5th pixel is noisy as shown in Fig 4. So now we will take the average values of its neighboring pixels. Here neighboring pixels are having the values 44 and 66 (in hexadecimal) first these two pixels are added and then divided by 2. That is 66+44=AA, when AA divided by 2 will get 55. This new value will be restored in the place of corrupted pixel.

5. FUTURE WORK

In EODT we are using 12 directional differences and it's quite difficult to understand and more time consuming. This problem can be solved out by introducing new technology called Reduced EODT. This technique uses only 3 directional differences and only 5 clock cycles are needed to complete the process. But due to only three directional differences the image quality may not be as good as EODT

6. CONCLUSION

In this paper, an efficient removal of impulse noise using pipelined ADC is presented. The extensive experimental results demonstrate that our design achieves excellent performance in terms of quantitative evaluation and visual quality, even the noise ratio is as high as 90%. For real-time applications, a7-stage pipeline architecture for EODT is developed and implemented. As the outcome demonstrated, EODT outperforms other chips with the lowest hardware cost. The architectures work with monochromatic images, but they can be extended for working with RGB colour images and videos.

REFERENCES

[1] W. K. Pratt, *Digital Image Processing*. New York: Wiley-Interscience,1991.

[2] T. Nodes and N. Gallagher, "Median filters: Some modifications and their properties," *IEEE Trans. Acoust., Speech, Signal Process.*, vol. ASSP-30, no. 5, pp. 739–746, Oct. 1982.

[3] S.-J. Ko and Y.-H. Lee, "Center weighted median filters and their applications to image enhancement," *IEEE Trans. Circuits Syst.*, vol. 38,no. 9, pp. 984–993, Sep. 1991.

[4] H. Hwang and R. Haddad, "Adaptive median filters: New algorithms and results," *IEEE Trans. Image Process.*, vol. 4, no. 4, pp. 499–502, Apr. 1995.

[5] T. Sun and Y. Neuvo, "Detail-preserving median based filters in image processing," *Pattern Recog. Lett.*, vol. 15, no. 4, pp. 341–347, April 1994.

[6] S. Zhang and M. A. Karim, "A new impulse detector for switching median filter," *IEEE Signal Process. Lett.*, vol. 9, no. 11, pp. 360–363, Nov. 2002.

[7] I. Aizenberg and C. Butakoff, "Effective impulse detector based on rank-order criteria," *IEEE Signal Process. Lett.*, vol. 11, no. 3, pp.363–366, Mar. 2004.

[8] W. Luo, "Efficient removal of impulse noise from digital images,"*IEEE Trans. Consum. Electron.*, vol. 52, no. 2, pp. 523–527, May 2006.

[9] W. Luo, "An efficient detail-preserving approach for removing impulse noise in images," *IEEE Signal Process. Lett.*, vol. 13, no. 7, pp. 413–416, Jul. 2006.

[10] K. S. Srinivasan and D. Ebenezer, "A new fast and efficient decisionbased algorithm for removal of high-density impulse noises," *IEEE Signal Process. Lett.*, vol. 14, no. 3, pp. 189–192, Mar. 2007.

[11] C.-T. Chen, L.-G. Chen, and J.-H. Hsiao, "VLSI implementation of a selective median filter," *IEEE Trans. Consum. Electron.*, vol. 42, no. 1, pp. 33–42, Feb. 1996.

[12] Pei-Yin Chen, Chih-Yuan Lien, and Hsu-Ming Chuang, "A Low-Cost VLSI Implementation for Efficient Removal of Impulse Noise" IEEE 2009.

Prof. Manju Devi

Working as an Associate Professor in the department of ECE at BTLIT,B'lore. Almost sixteen years of teaching experience in engineering colleges. Completed B.E in Electronics and Communication Engg. ,M.Tech in Applied Electronics and pursuing Ph.D from VTU in the field of analog and mixed mode VLSI.

Dr K.N.Muralidhara:

Obtained his B.E. In E&C engg from PES college of Engg , Mandya during 1981, ME during 1987from and Ph.D during 2002 from University of Roorkee. His field of interest is on semiconductor devices and presently working as professor and Head at the Dept. He is guiding 5 candidates for Ph.D programme and actively participated in all the developmental activities of the college. He has about 25 publications to his credit.

Prasanna R Hegde

Obtained B.E in Electronics and Communication Engineering from BTLIT in 2012. His field of interest is on Digital electronics and VLSI. Actively participated in National and International level conferences. Student member of IETE.

Analysis of Handover in Wimax for Ubiquitous connectivity

Pooja bhat[1], Bijender mehandia[2]
[1,2]Gurgaon Institute of Technology and Management, Bilaspur, Gurgaon

Abstract
WIMAX is Wireless Interoperability for Microwave Access. It is a telecommunication technology that provides wireless data over long distances in several ways, from point-to-point links to full mobile cellular type access. The main consideration of Mobile Wimax is to achieve seamless handover such that there is no loss of data. In Wimax both mobile station (MS) and base station (BS) scans the neighbouring base stations for selecting the best base station for a potential handover. Two types of handovers in wimax are: Hard handover (break before make) and Soft handover (make before break). To avoid data loss during handover we have considered soft handovers this research topic. We have proposed a technique to select a base station for potential soft handover in wimax. We have developed a base station selection procedure that will optimize the soft handover such that there is no data loss; handover decision is taken quickly and thus improving overall handover performance. We will compare the quality of service with hard handover and soft handover. We have analysed the proposed technique with an existing scheme for soft handover in wimax with simulation results.

Keywords: Wimax, Topology, handover, QOS, ubiquitous connectivity.

I. Introduction
IEEE 802.16 standard defines the air interface for fixed Broadband Wireless Access (BWA) systems to be used in WMANs (Wireless Metropolitan Area Networks), commonly referred to as Wimax

(Worldwide Interoperability for Microwave Access). The original standard IEEE 802.16 does not support mobility and for this purpose IEEE 802.16e-2005 was introduced. It is also known as Mobile Wimax .It is the new mobile version of the older Wimax specification known as IEEE 802.16e-2004 which is wireless but fixed, it lacks the ability for user to move during data transmission. The main purpose of Wimax is to provide users in rural areas with high speed communications as an alternative to expensive wired connections (e.g. cable or DSL). That is Wimax is capable to provide high speed internet to last mile connections. But this is not the only purpose of Wimax systems. Mobile Wimax allows the user to move freely during data transmission. The main consideration of mobile Wimax is that there should be no data loss when the moving user switches from one base station to another i.e. during handover. Handover is procedure when a mobile station changes the serving base station. The reason for handover could be relatively low signal strength or work load of base station.

Wimax is a state-of-the-art wireless technology which utilizes adaptive modulation and coding, supports single carrier (SC) and orthogonal frequency division multiplexing techniques (OFDM) and several frequency bands for different operation environments.

II. Materials and methods

1.1 Handovers in Wimax
A special requirement of a mobile device is the ability to change its serving base station if there exists another base station with better signal strength in the reach of mobile station (MS). Handover is a procedure that provides continuous connection when a MS migrates from the air-interface of one BS to another air-interface provided by another BS without disturbing the existing connections. Handovers are needed to support mobility.
For a handover to occur, one needs to have at least two base stations : serving base station(SBS) and target base station(TBS). The handover is generally considered as change in serving base station but it does not necessarily mean that the base station must be changed. In some cases there may be different reasons why a handover might be conducted:

- When the MS is moving away from the area covered by one cell and enters the area covered by another cell the connection is transferred to the second cell in order to avoid data loss when the MS gets outside the range of the first cell;
- When the capacity for connections of a given cell is used up, the new connection which is located in an area overlapped by another cell, is transferred to that cell in order to free-up some capacity in the first cell for other users, who can only be connected to that cell;
- When the channel used by the MS becomes interfered with by another MS using the same channel in a different cell, the call is transferred to a different channel in the same cell or to a different channel in another cell in order to avoid the interference;
- Signal strength is not enough for maintaining proper connection.

Behaviour of MS changes, for example in case of fast moving MS suddenly stopping; the large cell size can be adjusted by a small size cell with better capacity.
In CDMA networks a soft handover may be induced in order to reduce the interference to a smaller neighbouring cell due to the "near-far" effect even when the phone still has an excellent connection to its current cell;

1.1.1 Stages of Handover procedure:

- Call restriction
- Handover decision/initiation
- Synchronization
- Termination of service

Types of handovers

There are two types of handovers used in cellular network systems: hard handover and soft handover

Hard handover

The hard handover is used when the communication channel is released first and the new channel is acquired later from the neighbouring cell. For real-time users it means a short disconnection of communication. Thus, there is a service interruption when the handover occurs reducing the quality of service.

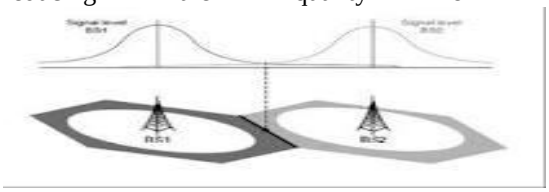

1.2.1 Methods of Soft Handovers in Wimax

I. Macro Diversity Handover (MDHO)

The MDHO supported by MS and by BS, the "Diversity Set" is maintained by MS and BS. The Diversity Set is a list of the BSs, which are involved in the handover procedure. The Diversity Set is maintained by the MS and BS and it is updated via MAC (Medium Access Control) management messages. A sending of these messages is usually based on the long-term CINR (Carrier to Noise plus Interface Ratio) of BSs and depends on two thresholds: Add Threshold and Delete Threshold. Threshold values are broadcasted in the DCD (Downlink Channel Descriptor) message. The Diversity Set is defined for each MS in the network. The MS continuously monitors the BSs in the Diversity Set and defines an "Anchor BS". The Anchor BS is one of the BSs from Diversity Set in MDHO. The MS is synchronized and registered to the Anchor BS, further performs ranging and monitors the downlink channel for control information. The MS communicates (including user traffic) with Anchor BS and Active BSs in the Diversity Set[1]

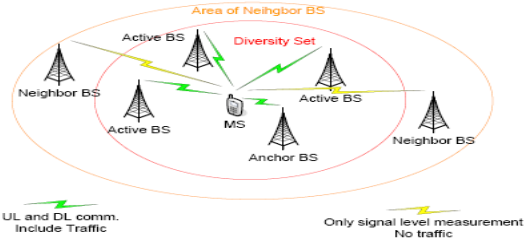

II. Fast Base Station Switching (FBSS)

We are considering fast base station switching technique. In this method a diversity set is maintained for each mobile station. The serving base station and mobile station monitors the neighbouring base stations that can be added in diversity set. Diversity set is maintained by both mobile station and serving base station. Diversity set is collection of base stations that can chosen as target base station for a handover. Handover decision can be taken by mobile station, base station or base station controller depending upon the implementation.

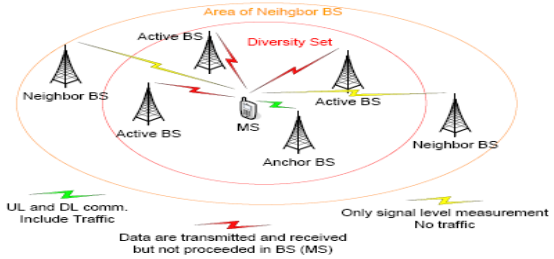

Modification in Efficient FBSS technique

In the proposed technique, we are trying to modify the FBSS procedure to optimize target base station selection for soft handovers in wimax. We have introduced monitor base station which is selected from diversity set of mobile station. The function of monitor base station (MBS) is to communicate with mobile station and maintain the database of potential target base stations for a handover for mobile station. Another advantage of MBS is that whenever ABS fails, mobile station can start data communication with MBS without any loss of data by sending register message.
The mobile station sends its current location to MBS and according to history of mobile station movement and its current location, MBS sorts the TBS's having maximum div parameter.
Div= s/w- d
S= received signal strength
w= work load
d= distance between mobile station and base station
$d=\sqrt{(x_s - x_i)^2 + (y_s-y_i)^2}$
where (xs , ys) are coordinates of mobile station and (xi , yi) are coordinates of i'th base station where i=1,2,3…. N
N = total number of base station in diversity set
s= (k* st)/d
Where st= transmitted signal strength
k= other factors affecting signal (interference)

The MBS scans the neighbouring base stations and calculates div parameter for each base station. Then MBS sorts the BS's in diversity set using sorting algorithm in descending order such that the BS having maximum value of div is on the top of diversity set.

Selection of MBS

When a mobile station gets registered to a Serving Base Station (SBS), it sends scan_req message to SBS, it responds to this message by sending the data of its neighboring base stations through scan_rsp message. With this data the mobile station will choose the MBS having maximum value of div parameter. That is mobile station will communicate with best suited target base station so at any point if SBS goes down, the mobile station can easily switch to MBS. As the mobile station is moving continuously the diversity set is required to updated according to current location of mobile station.

If the div value of MBS goes below the threshold value. It will send the stored information to SBS and SBS will select new MBS the mobile station. The Serving Base Station (SBS) periodically broadcasts Neighbor Advertisement (NBR_ADV) message that contains network topology information or channel information of available neighbouring base stations. The mobile station sends

(SCN_REQ) message to the serving base station to scan the neighbouring base station according to the current location (div) of mobile station. The serving base station responds to SCN_REQ message by sending the information of neighboring base station as per the calculation, the base station with maximum value of div parameter is selected as monitor base station.

Whenever mobile station requires a handover, it sends HO_INIT

(Handover Initiation) message to monitor base station that sends the information of target base station to mobile station. The mobile station synchronizes the downlink and uplink frequencies with target base station. The mobile station can now start the data communication with target base station

III. Simulation and Result

The proposed technique is implemented in NS-2.34 Simulator in Linux environment. We have modified ns-2.34 by adding mac802.16-e layer to it for supporting Wimax. The wimax.tcl file is coded on c++, when executed it generates a .nam file which can be viewed in Network Animator tool of ns2 simulator.

Parameters Used

Packet size : 1500 bytes

Time interval of data sent : 6 ms

Total Number of nodes : 3

Number of Base Station : 2

Physical layer : 802.11

Data link layer : 802.16-e

Step 1

Fig. shows 3 nodes used in simulation of base station selection procedure for soft handover. Here node 1 is mobile station and all the other nodes are base stations. The simulation shows the handover procedure as mobile station changes its position

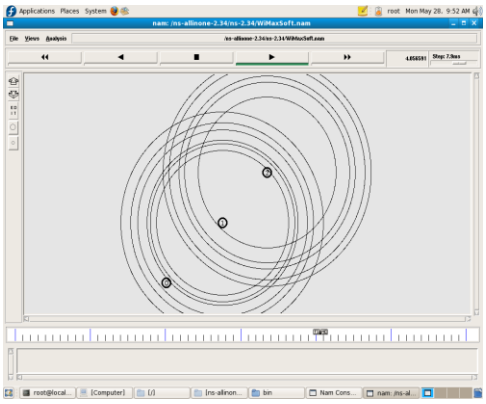

Fig Nam file for soft handover

Step 2

Above figure shows the ranging between node 0 and node 1. The node 0 acts as serving base station for mobile station (node 1). The node 1 starts data communication with node 0. As the mobile station moves, its distance from serving base station increases and the mobile station looks for another base station for soft handover ie. Target Base Station. The below figure shows handover when the mobile station connects with target base station. Node 2 is target base station.

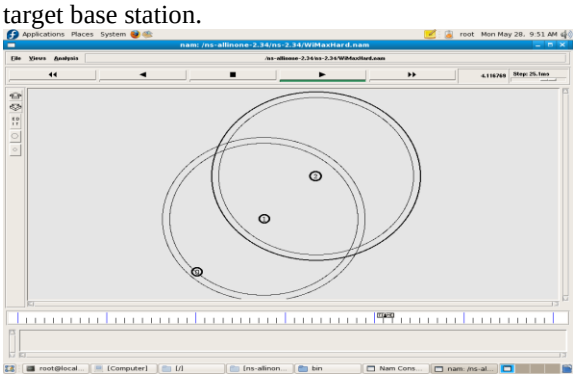

Fig Signaling with serving base station

Step 3

First result is comparison between the fast base station switching handover and our proposed technique. It shows that using the proposed technique the performance of soft handover is improved.

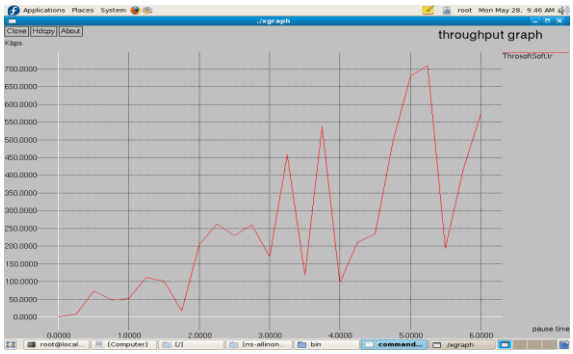

Fig Graph of soft handover with modified FBBS technique

Step 4

The x axis denotes the time and y-axis denotes the packet received

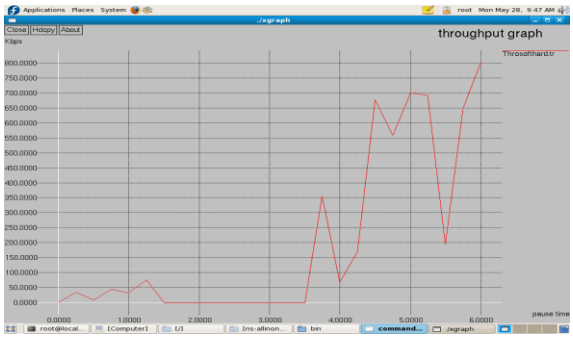

Fig Graph for hard hand over

IV. Conclusion:

We simulated the more realistic handover in the mobile WiMAX using NS-2 with WiMAX and mobility modules. The goal of this simulation is to find out the relationship between the handover latency and the velocity of mobile station. It can be seen that the current handover mechanics used in the NS-2 module meets the requirement of seamless handover in mobile WiMAX when the mobile station travel at the speed of 20 m/s. Although, using link-going down mechanism will dramatically reduce the handover latency, it is still a challenge to achieve the full mobility: up to 120 km/h, handover latency of less than 50 ms with an associated packet loss that is less than 1 percent.

V. Future scope:

As extension to this research work, two topics for future research investigations are suggested. Since there is a trade off between handover threshold and margin, an adaptive threshold window could be used to balance the load of base station and the QoS of the mobile.Also, the current work is restricted to hard handover only. Possibilities of extending this work to macro diversity and fast base station switching can be worthy of an investigation. Although these are soft handover techniques and currently optional in the WiMAX standard, the BS selection procedure based on location predication algorithms and current load factors of the target BSs give an alternative way of deciding the target BS. Further, reducing the number of handovers is highly desirable from a system perspective.

References:

[1] Andrews, J. G., A. Ghosh, Fundamentals of WiMAX Understanding broadband wireless networking, Prentice Hall ,et al. (2007).

[2] Zdenek Becvar, Jan Zelenka ,Handovers in the Mobile WiMAX.

[3] N. P. Singh, Brahmjit Singh, Performance Enhancement of Cellular Network Using Adaptive Soft Handover Algorithm.

[4] Zdenek BECVAR, Pavel MACH, Robert BESTAK, Initialization of Handover Procedure in WiMAX Networks.

[5] Kumar Mrinal , Chetan Aneja, Vikram Gupta, Swati Sharma , Mobility Improvement In IEEE 802.16.

[6] Rajat Prakash and Venugopal V. Veeravalli, Locally Optimal Soft Handoff Algorithms.

[7] IEEE Std: "Soft Handover and Fast BS Switching Procedure," IEEE 802.16 Broadband Wireless Access Working Group, June 2004.

Dampening Flow Induced Vibration Due To Branching Of Duct at Elbow

M.Periasamy[1], D.B.Sivakumar[2], Dr. T. Senthil Kumar[3]

[1, 2, 3,] Post Graduate Student, Department of Mechanical Engineering, Anna University Of Technology, Trichy

Abstract

Ducts are closed path used for conveying air, Flue gas, Material, ash and etc from one system to another, in the power plant and in the industries. Ducts are routed to long distances, having abrupt change in direction and cross section which requires proper design for preventing the energy losses. Elbows are used for changing the direction of flow to 90^0.Due to this abrupt change, eddies, Recirculation zones are formed. These Eddies having energy gradients, which produces thrust and in turn Vibration to the duct wall. Eddies Should be broken by stream lining the flow before taking any branching from the main duct. But in some ducting system either in power plant or Industrial, due to constraints Elbow duct itself is to be branched out. This paper presents dampening flow induced vibration, by analyzing the various arrangements using computational Fluid dynamic software Gambit-Fluent.

Keywords- Flow Induced Vibration, Flow Recirculation, Eddy, Sharp Elbow Branching

1. Introduction

Elbow ducts are used pre dominantly in the ducting system for diverting the flow to 90^0. Guidelines is to be followed for avoiding pressure drop, recirculation etc in the design of elbow. Three Dimensional Model of a typical ducting is shown in Fig 1. This ducting having sharp elbow, but as per design guidelines, guide vanes are to be used to streamline the flow at the elbow. Since branching is done at sharp elbow, Guide vanes could not be used. So the duct system becomes sharp 90^0 Elbow with branching at the elbow itself. The flow inside this ducting system is quite complicated and its difficult to predict the flow in this system by analytical methods. The flow pattern inside this arrangement can be visualised by using computational fluid dynamic software Gambit- Fluent.

Grid is formed representing Flow field by using elements connected at the nodes using elements in the Gambit. The grid is then exported to Fluent , where the Boundary condition is applied and Solved. The Fluent have inviscid, Laminat, Spalart Almaras(1 equation), K-epsilon(2 equation), K omega(2 Equation), Reynolds stress(7 Equation),Detached Eddy simulation and Large eddy simulation for modeling the Viscous flow

The K-epsilon model is one of the most common turbulence models, although it just doesn't perform well in cases of large adverse pressure gradients. It is a two equation model that means, it includes two extra transport equations to represent the turbulent properties of the flow. This allows a two equation model to account for history effects like convection and diffusion of turbulent energy. The first transported variable is turbulent kinetic energy, K. The second transported variable in this case is the turbulent dissipation,€ . It is the variable that determines the scale of the turbulence, whereas the first variable, K, determines the energy in the turbulence.

There are two major formulations of K-epsilon models that of Launder and Sharma is typically called the "Standard" K-epsilon Model. The original impetus for the K-epsilon model was to improve the mixing-length model, as well as to find an alternative to algebraically prescribing turbulent length scales in moderate to high complexity flows.K-epsilon model has been shown to be useful for free-shear layer flows with relatively small pressure gradients. Similarly, for wall-bounded and internal flows, the model gives good results only in cases where mean pressure gradients are small; accuracy has been shown experimentally to be reduced for flows containing large adverse pressure gradients. The equation for the K-epsilon model is in built in fluent software itself.

2. Modified System

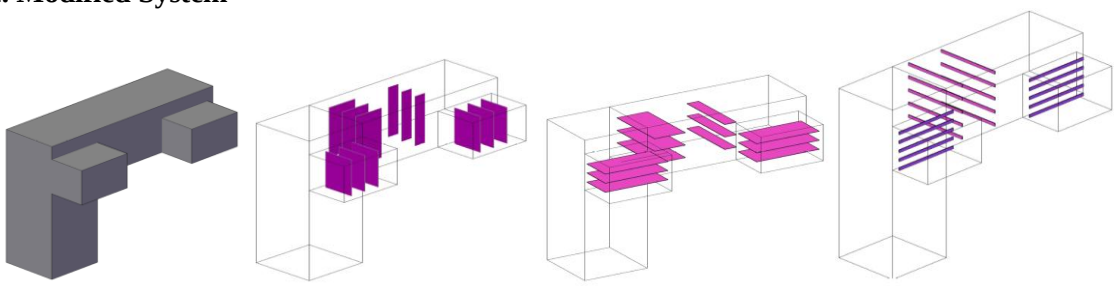

Fig.1 Three Dimensional Model (Base Duct, With Vertical Divider, With Horizontal Divider, With Distributor)

Guide Vanes are used for streamlining the flow at sharp 90^0 elbows. Since there is a branch in elbow itself, Guide vanes cannot be provided. Hence for streamlining the flow three options Vertical Divider, Horizontal Divider, Distributor are considered.

Vertical divider is placed parallel to the vertical axis, spaced equally by dividing the flow volume by fourth. Vertical divider is located 200 mm minimum away from the cavity. Horizontal divider is placed parallel to the Horizontal axis, spaced equally by dividing the flow volume by fourth. Horizontal divider is located 200 mm minimum away from the cavity. Both horizontal and vertical divider does not affect flow volume much since thickness face only opposes the flow. Distributor is located and staggered to vertical axis as in Figure. Distributor obstructs flow volume unlike in horizontal and vertical divider. Distributor also placed by maintaining 200 mm gap minimum from the cavity.

3. Results and Discussion

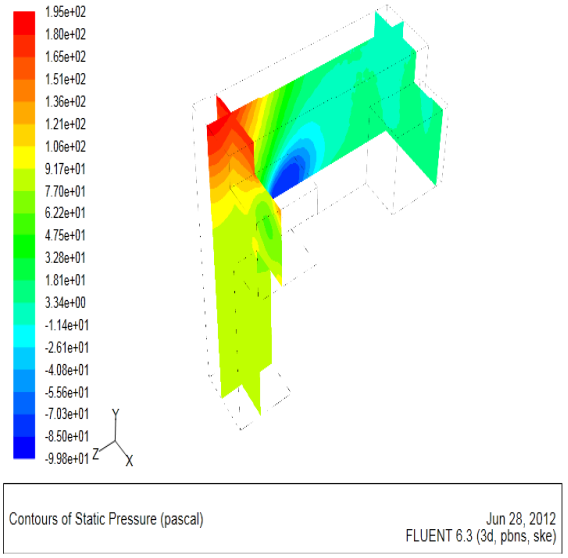

Base Model Static Pressure

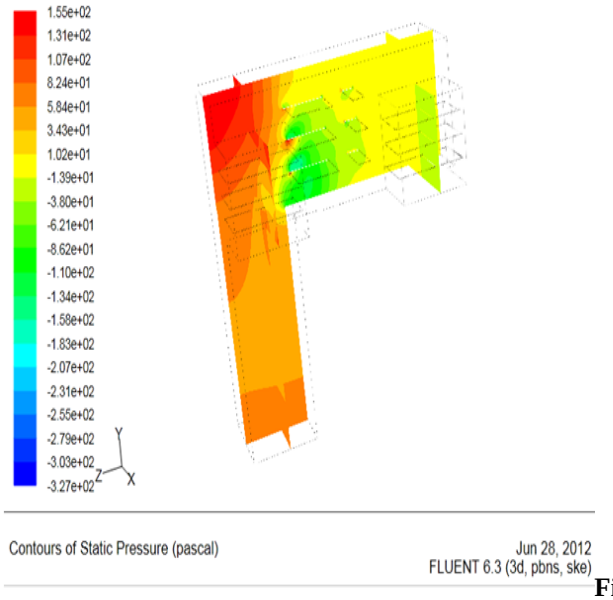

Fig.3 Horizontal Divider Static Pressure

Fig.2

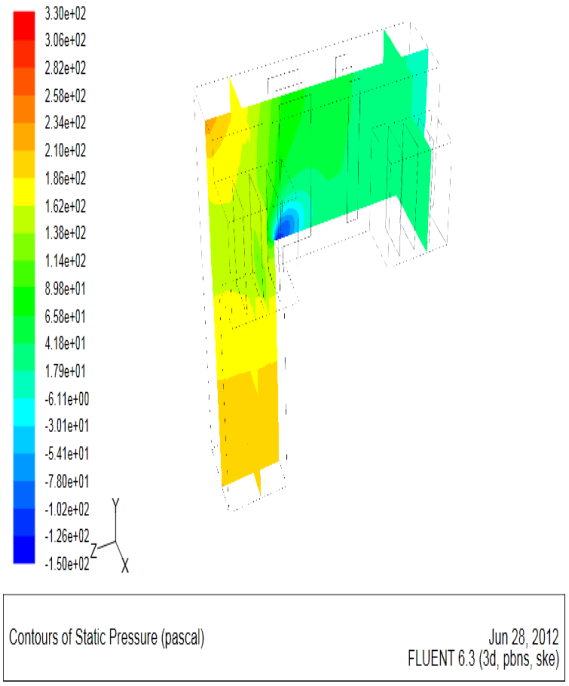

Fig.4 Vertical Divider Static Pressure

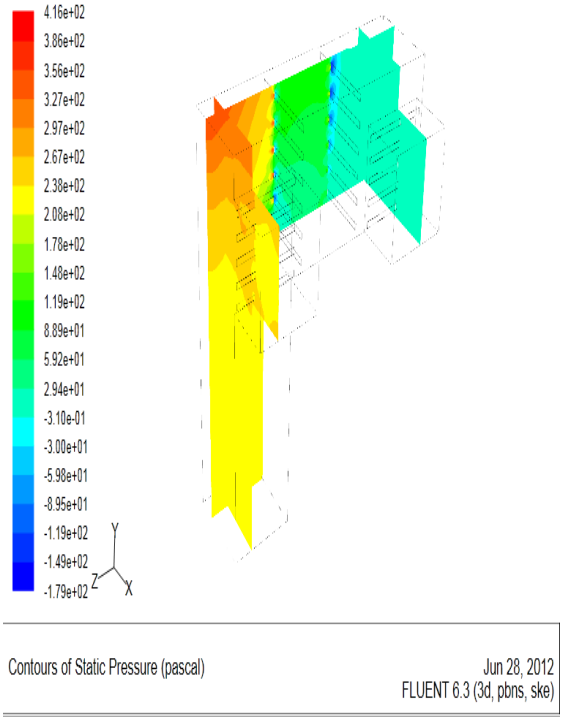

Fig.5 Distributor Static Pressure

Pressure gradients as in Fig.2 creates eddies. The energy in eddies creates vibration on the duct wall. Horizontal Divider breaks the eddies to some extend as the velocity gradient decreases. Even Though vertical divider breaks the eddies to 90 percent as in Fig 5, there exist some low pressure zone. But in Distributor model the pressure distribution is uniform at the vibrating Zone as in Fig.5

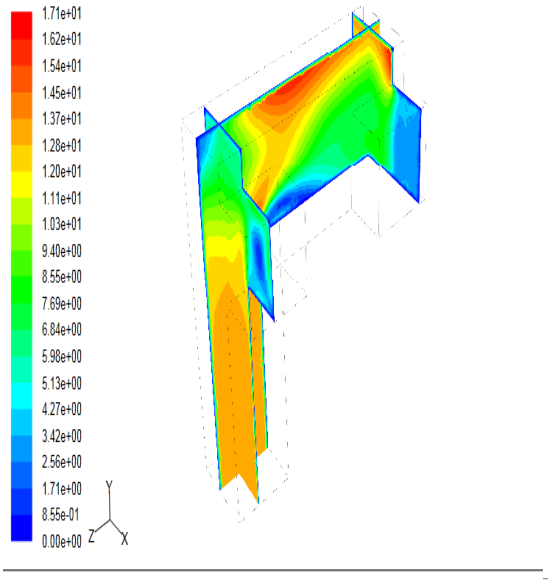

Fig.6 Base Model Velocity

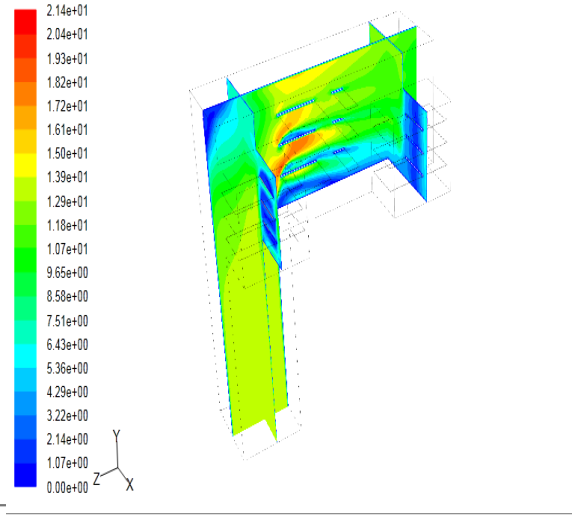

Fig.7 Horizontal Divider Velocity

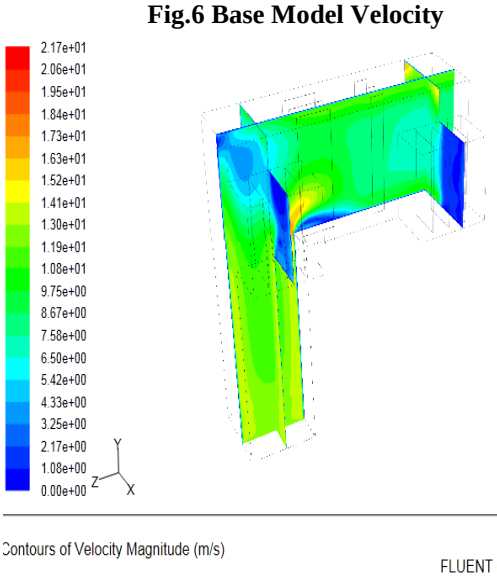

Fig.8 Vertical Model Velocity

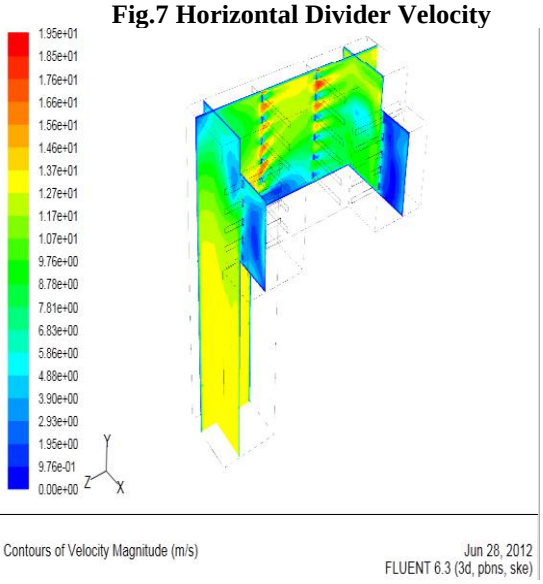

Fig.9 Distributor Velocity

The Velocity plot in the base model (Fig.6) illustrates recirculation zones (Velocity gradient at the section) in the vibrating zone. Horizontal Divider avoids recirculation zones only at few locations. Even though vertical divider avoids recirculation zones, Velocity becomes minimal at sharp corner. In Distributor plate velocity becomes maximum at Distributor section, and stream lined in further zones.

4. Conclusion:

Three Dimensional Computational Fluid Dynamic analysis of Base Ducting, Modified horizontal Divider with base duct, Vertical divider with base duct, Distributor plate with Base duct was done using Gambit-Fluent for the turbulent intensity level of five, Ten, Fifteen and Twenty percent . From the analysis it is seen that Distributor plate breaks eddies and avoid recirculation zones. This pattern is repeated for all the turbulent intensity level of Five percent, Ten percent, Fifteen percent and Twenty percent. Further Distributor plate requires minimum material, easy to attach to the existing system. Hence Distributor plate model is selected.

References:

[1] A. Leonard And A. Roshko , Aspects Of Flow-induced Vibration, *Journal of Fluids and Structures (2001) 15, 415-425.*

[2] Peter Vasilyev, Leonid Fromzel,Published, Analytical Study of Piping Flow-induced Vibration. Example of Implementation, Transactions of the 17th International Conference on Structural Mechanics in Reactor Technology (SMiRT 17) Prague, Czech Republic, August 17 –22, 2003

[3] Y.S.Choy, J.Huang, L.Huang,Y.Zhou, An Experimental Study of Flow Induced Vibration on a Tensioned Membrane,Journal of Mechanical Science and Technology 21 (2007) 1359-1366.

[4] Benny KUAN, William YANG ,Chris SOLNORDAL, CFD Simulation And Experimental Validation of dilute particulate turbulent flows in a 90^0 Duct Bend, Third International Conference on CFD in the Mineral and Process Industries CSIRO, Meibourne, Australia.

[5] ArindamMandal, SomnathBhattecharjee, Rabin Debnath, Debasish Roy, SnehamoyMajumder, Experimental Investigation of Turbulent Fluid Flow through a Rectangular Elbow ,International Journal of Engineering Science and Technology Vol. 2(6), 2010, 1500-1506"

[6] Bing Yang, Fuping*Gao, Yingxiang Wu,* Experimental Study on Flow Induced Vibration of a Cylinder with Two Degrees of Freedom Near a rigid Wall,Proceedings of the Eighteenth (2008) International Offshore and Polar Engineering Conference Vancouver, *BC, Canada, July 6-11, 2008 "*

[7] Stappenbelt B, Flow-induced vibration mitigation using attached splitter-plates , "2009 Annual Bulletin of the Australian Institute of High Energetic Materials v.l (20 I0) pp. 23-33

[8] S.Mittal, V.Kumar, Finite Element Study of Vortex-Induced Cross-Flow and in-Line Oscillations of Circular cylinder at Low Reynolds Number , International Journal for Numerical methods in Fluids,Int.J.Number.Meth.Fluids 31 : 1087-1120(1999)

[9] R. T. FAAL, D. DERAKHSHAN , Flow-Induced Vibration of Pipeline on Elastic Support, The Twelfth East Asia-Pacific Conference on Structural Engineering and Construction , Procedia Engineering 14 (2011) 2986–2993" Available in Science Direct.

[10] Ruth MOSSAD, William YANG, M. Philip SCHWARZ, NUMERICAL PREDICTION OF AIR FLOW IN A SHARP 90º ELBOW,Seventh International Conference on CFD in the Mineral and Process Industries CSIRO, Meibourne, Australia 9-11 December 2009".

[11] I.ChienLee,Kun Yu Chen, Jing Wang yu, Vibration reduction of the flue gas duct system on the site of TAICHUNG NO. 9 Power Plant ,18^{th} Conference of the Electric Power supply Industry

[12] Cyril M.Harris,Allan G.Piersol,R.D.Blevins, Harris' Shock and Vibration Handbook, Mcgraw Hill, pp 29.1-29.67

Location Aware Routing in Intermittently Connected MANETs

Sadhana V, Ishthaq Ahmed K
CSE Department, JNTU University

Abstract
Existing mobile ad hoc routing protocols like AODV, DSR and GPSR allow nodes to communicate with one another with an assumption that there exists a connected path from source to destination. Due to limited transmission range, power limitations, mobility of nodes, and the wide physical conditions over which ad hoc networks must be deployed; in some scenarios it is likely that this assumption is invalid leading to intermittent connectivity and absence of end-to-end connections. In this work, we propose a geographical routing algorithm called location-aware routing for delay-tolerant networks (LAROD), enhanced with a location service, location dissemination service (LoDiS), which together are shown to suit an intermittently connected MANET (IC-MANET). LAROD uses a beaconless strategy combined with a position-based routing for forwarding the packets resulting in less overhead. LoDiS maintains a local database of node locations, which is updated using broadcast gossip combined with routing overhearing.

Keywords— Delay-tolerant networks, location service, mobile ad hoc networks (MANETs), routing protocols, intermittent connectivity.

I. INTRODUCTION
Intermittently connected mobile ad hoc networks (IC-MANET) are wireless networks where the nodes do not form a completely connected network. Instead, they will form connected partitions that changes their topology often. This kind of intermittent connectivity may happen when the network is quite sparse, in which case it can be viewed as a set of disconnected, time-varying clusters of nodes. Intermittently connected mobile ad hoc networks is a type of Delay Tolerant Networks (DTN) [1], that is, networks were incurred delays can be very large and unpredictable. There are many real networks that fall into this category. Examples include disaster scenarios and military operations, wildlife tracking and habitat monitoring sensor networks (IPN) etc.

Since in the IC-MANET model there may not exist an end-to-end path between a source and a destination, existing ad-hoc network routing protocols, such as GPSR, DSR, AODV etc., would fail. To overcome the disconnected nature of IC-MANETs and to successfully route the packets under such conditions, a store-carry forward technique is used. Mobility can be exploited when wireless nodes cannot forward the packet.

In this paper we present a geographical routing protocol called Location Aware Routing for Opportunistic Delay-Tolerant networks (LAROD) which relies on position information of the nodes. LAROD is a beaconless protocol that greedily forwards packets towards the destination. When greedy forwarding is not possible a packet is temporarily stored by the current custodian until a suitable forwarding node comes up. Routing of packets toward the geographical location has shown to work well in IC-MANETs.

Clearly, a geographical routing protocol needs to be supplemented by a location service [2] that can provide the current physical location of the destination node for a packet. A location service can range from simple flooding-based services to hierarchical services. There have been many suggestions on how a location service can be provided in MANETs, but there have been no suggestions on how this service can be provided in an IC-MANET or DTN setting. The location dissemination service (LoDiS) is the first location service for IC-MANETs which disseminates node locations in the network using a Brownian gossip technique.

In the next section we go over some existing routing algorithms for IC-MANETs and location services. Section III presents LAROD and LoDiS protocol. Section IV, presents our evaluation of LAROD with LoDiS and compare the results with spray and wait. Finally in section V we end the paper with some conclusions and ideas on future work.

II. BACKGROUND AND RELATED WORK
Proposals on how we can route packets in fully connected MANETs have been studied to a great extent. In the last decade, this interest has broadened into networks with intermittent connectivity. In this section, we give an overview of IC-MANET routing and location services.

A. Routing in IC-MANET
In a wireless mobile ad hoc network where an end-to-end path can never be assumed to exist between any two nodes, mobility can be used to bridge the partitions. When there is no suitable forwarding node, a routing node can choose to

temporarily store a packet until node mobility presents a suitable forwarding node. This routing principle is called store–carry–forward.

The design of an IC-MANET routing protocol depends on the amount of contact information available with the node. The mobility of the nodes will constantly change the network topology and that nodes constantly come in contact with new nodes and leave the communication range of others. Node contacts can be classified based on their predictability into scheduled, predicted and opportunistic contacts. In scheduled contacts, the nodes know when they will be able to communicate with a specific node. In predicted contacts, nodes can estimate likely meeting times or meeting frequencies with specific nodes. If no such contact information is available with node then the contacts are opportunistic. LAROD neither requires scheduled contacts nor predicted contacts and is thus well suited for networks with opportunistic contacts.

Routing in IC-MANETs with opportunistic contacts is challenging since contact information is not known in advance. Three simple location unaware routing protocols for this environment are Randomized Routing, Epidemic Routing and Spray and Wait. Randomized Routing [3] is a single copy routing scheme in which a packet randomly moves around the network until it reaches the destination. Epidemic routing [6] extends the concept of flooding in IC-MANETs where every node in the network receives a copy of the packet. Spray and Wait [5] routing protocol "sprays" a limited number of copies into the network, and then "waits" until one of these nodes meets the destination.

If nodes are location-aware, then the relative position of the nodes can be used to make the forwarding decision. This is a property used by LAROD. In addition to LAROD there are two other delay-tolerant geographical routing protocols published. These protocols are motion vector (MoVe) and GeoDTN+Nav. Both these protocols are used in vehicular ad hoc networks (VANETs) and assume the destination to be static.

Most of the proposed MANET routing protocols transfer packets between nodes in a unicast transfer mode and thus does not exploit the broadcast nature of wireless transmissions. Opportunistic routing (OR) [8] fully embraces the broadcast nature of wireless medium and thus an optimal route is constructed between the source and the destination by selecting the "best" next forwarder. One way of selecting the best forwarder is by geographical selection that is the selection depends on closeness to the destination. This approach is used in contention-based forwarding (CBF) [11] and beaconless routing (BLR) [10]. LAROD is built on these principles and extends them to meet the requirements of an IC-MANET.

B. Location Services

A geographical routing protocol must be complemented by a location service that can provide position information for all potential destinations. In this section, we will give an overview of the location services [2] used in MANETs and discuss why most of them are not directly applicable to an IC-MANET.

Fig 1 shows taxonomy of the location services. At the top level, location services can be divided into flooding-based and rendezvous-based or mapping-based approaches. A major difference between the flooding-based location services and the mapping-based services lies with the number of nodes that act as location servers.

In the flooding-based services, all nodes in the network act

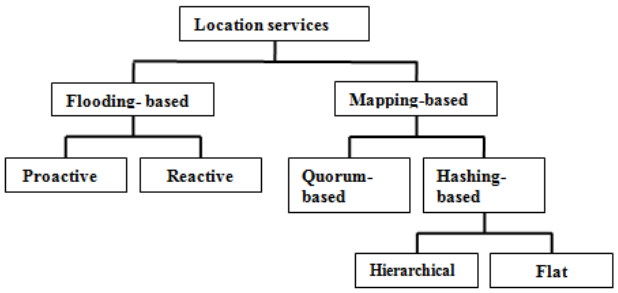

Fig. 1 Taxonomy of location services

as location servers. In the mapping-based services, only a subset of the nodes in the network act as location servers and the location queries must be routed to one of these location servers.

In a mapping-based location service, the node that needs the location information of the destination node sends the request to one of the node that act as location servers. In a delay-tolerant perspective, this case will significantly delay the time until a message can be sent toward its destination due to the transport time for a location request and its response.

In the flooding-based services, the location information is located in the source node itself so there is no delay for reaching the location service, but the time to acquire the location information differs between proactive and reactive location services. A reactive location service tries to obtain the destination position information only when needed. If the required information is not available in the local cache, then the location server broadcasts a location query over the

network. Due to the disconnected nature of the network, the reactive location services will result in delays as for the mapping-based location services. To limit the cost of a location request the location service uses a Brownian gossip [13] technique. In Brownian gossiping, nodes exchange information on previous encounters when two nodes meet. This information can be used to guide a location request toward the destination node's position.

In the proactive location service, each node periodically distributes its location information to other nodes in the network, which means that location information is immediately available when needed in the source node. Examples of proactive location services are: 1) the DREAM location service (DLS) [9] and 2) the simple location service (SLS) [9]. In DLS, a node broadcasts its location to nearby nodes at a given rate and to nodes far away at a lower rate. The rates depend on a node's speed. In SLS, location data are only exchanged between neighbors. This exchanging of location tables between neighbors keeps the communication local while permitting the location data to be distributed globally in the system. In both DLS and SLS, if the required location data are not available in the source node, they inquire a node location by broadcasting a request. As previously discussed, these systemwide broadcasts are problematic in an IC-MANET.

In order to minimize routing delays in an IC-MANET, all nodes must have a location service that has location data for all other nodes in the network. Due to the disconnected nature of IC-MANETs, this information provided by the location service might be old for some nodes. Even such inaccurate data can be used to route the packets successfully with a proper design of the routing protocol. LoDiS is based on SLS and modify the concept as required to meet the demands of an IC-MANET environment.

III. LOCATION AWARE ROUTING

This section describes the IC-MANET geographical routing protocol LAROD [4], followed by a description of the IC-MANET location service LoDiS.

A. LAROD

LAROD is a geographical routing protocol for IC-MANETs that use greedy packet forwarding when possible. When greedy forwarding is not possible, the node that currently holds the packet (the custodian) waits until node mobility makes it possible to resume greedy forwarding. It is a beaconless protocol that combines geographical routing with the store–carry–forward principle.

A custodian forwards a message toward the destination by simply broadcasting it. All nodes within a predefined forwarding area are called tentative custodians and are eligible to forward the packet. All tentative custodians set a delay timer *td* specific for each node, and the node whose delay timer expires first is selected as the new custodian. The new custodian forwards the message in the same manner as the previous custodian. The old custodian that forwarded the message and other tentative custodians will overhear this broadcast and conclude that a new node has taken over custody of the packet. If the current custodian does not overhear any such broadcast within an interval of *tr* (rebroadcast time), it repeats the broadcast of the message until a new custodian becomes available due to node mobility.

It is also possible that all nodes in the forwarding area may not overhear the transmission made by the new custodian, thereby producing packet duplicates. This case will not only increase the load in the system but results in exploration of multiple paths toward the destination. When the paths of two copies cross, only one copy will continue to be forwarded. When the time to live *tTTL* for a packet, which is expressed as duration, expires, a packet is deleted by its custodian. This is done to prevent a packet from indefinitely trying to find a path to its destination.

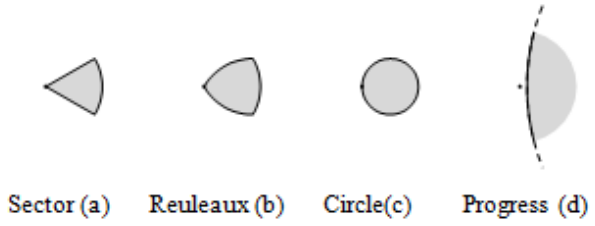

Fig 2 LAROD forwarding areas

```
Source node at data packet generation
   Get location data for destination from location service
   Broadcast data packet
   Set up the timer for rebroadcast to tr

Destination node at data packet reception
   If the packet is received for the first time
      Deliver data packet to application
      Broadcast ack packet
   Else
      Broadcast ack packet

All intermediate (non-destination)  nodes at data packet
reception
   Update location service with location information of the
   data packet
   //Packet has been received by the destination
   If an ack has been received for the packet
      Broadcast ack packet
   //The node is a tentative custodian
   If the node is the forwarding area
      If the node has an active copy of the packet
         Set up timer for rebroadcast to td
      Else
         Do nothing
   Else
      Remove active copy of the packet if it has one

At ack packet reception
   Update location service with location information of the
   ack packet
   If the node has an active copy of the packet
      Broadcast ack packet
      Remove data packet
   Else
      Do nothing

When a data packet rebroadcasting timer expires
   If the packet's TTL has expired
      Remove packet
   Else
      Update data packet's location information with
       location server data
       Broadcast data packet
       Set up the timer for rebroadcast to tr
```

Fig 3 LAROD pseudo code

The forwarding area can have many shapes as shown in fig 2. Examples of shapes include a 60◦ circle sector, a Reuleaux, triangle, or a circle [Fig. 2(a)–(c)]. The longest distance between two points within these shapes must be the assumed radio range. If we want to maximize the probability of determining a new custodian, then the forwarding area should include all nodes that guarantee progress toward the destination [Fig. 2(d)]. In this paper, we have chosen progress forwarding area.

When a packet has been received by the destination, it sends an acknowledgement packet (ack) to stop further transmission of a packet by custodians and tentative custodians. All nodes that hear an acknowledgement will store the acknowledgement information until the packet times out. If a node receives a packet for which it previously has received an acknowledgement, then it broadcasts an acknowledgement packet to stop further transmission of the packet.

LAROD inquires the location service at each packet hop to overcome the inaccuracies of an IC-MANET location service, and if more recent position data are available, then the routed packet is updated. In this way, the location data is incrementally updated with accurate data as the packet approaches the destination. To still improve the quality of the location data in the location service, LAROD routing protocol provides it with the location data available in received packets. Fig. 3 shows the pseudocode for LAROD routing protocol.

B. LoDiS

Due to the network partitioning of an IC-MANET environment, the information exchanged between the nodes can be delayed, which means that any time-dependent information that is received is more or less inaccurate. This indicates that any location service in an IC-MANET will generally provide inaccurate location data. This may be due to the time taken for a location update to reach the location server and/or the time taken for a location request to be answered by a location service. To avoid such delays, in LoDiS, every node acts as a location server, and location updates are made by data exchanges as nodes encounter each other. The reason for treating all nodes as location servers is to avoid delaying the packet at the source node.

When the routing protocol requests a location from the location service, LoDiS, the location data provided by LoDiS will be wrong due to the mobility of the nodes, but if the provided location points the data packet in the approximate right direction, it should be possible to use it as an initial estimate. To limit the location error, the geographical routing protocol should update the packet's location information for each node that the packet traverses. This is carried out by inquiring the node's local location server whether it has more accurate location information for the destination. This is based on the fact that nodes closer to the destination should have correct information on the destination's location. Thus the accuracy of the destination location is incrementally increased.

LoDiS is built on the conceptual solution used by SLS. A LoDiS location server periodically broadcasts the information it has in its location table. Any node receiving this broadcast compares the information with the one it has, and the most recent information will be propagated when that node makes its LoDiS broadcast. In this way, the location information is distributed throughout the network. In addition to this

```
Broadcast location data at a set interval
   Select location data vector with elements(node, location,
   timestamp)
   Broadcast location data

When a LoDiS broadcast is received
   If the received location data is more recent
      Update the entry in the LoDiS server

When the location data is received from the routing protocol
   If the data received is more recent
      Update the entry in the LoDiS server
```

Fig 4 LoDiS pseudocode

routing protocol. The geographical routing protocol provides the location service with location information present in the packet that it routes, which helps to improve the data in the location service. The pseudocode for LoDiS is shown in Fig.4.

IV. EVALUATION

In this section, the results from the evaluations of LAROD–LoDiS are shown. The routing protocols have been evaluated in the network simulator ns-2. The LAROD–LoDiS scheme is compared with an efficient delay-tolerant routing algorithm called spray and wait and is shown to have a competitive edge, both in terms of delivery ratio and overhead.

Delivery ratio and effort required for each generated data packet (overhead) are the two main evaluation metrics used. The delivery ratio determines the quality of service as perceived by the user or application and it is the most important evaluation criterion. The effort will be measured as the number of transmissions performed per generated data packet.

Comparing the delivery ratio and overhead of LAROD–LoDiS with spray and wait, a leading nongeographic delay tolerant routing scheme, we see that the benefit of using geographical information and active forwarding is very high (see Figs. 5–8). Fig. 5 shows the impact of the packet lifetime on the delivery ratio. As shown, both routing protocols benefit from having more time to find a path from the source to the destination. The performance of LAROD is high compared to spray and wait because spray and wait mainly uses node mobility to forward packets, whereas LAROD actively forwards the packet through peers toward the destination. Due to frequent node encounters, the protocols that actively forward the packets outperform protocols that rely on node mobility. As shown in fig. 6, the overhead for spray and wait is about double that of LAROD–LoDiS. Overhead in spray and wait are due to the beacons and the query and response packets, i.e., packets not present in LAROD–LoDiS.

Comparing the two routing protocols with respect to varying node densities, we can make some interesting observations. For both routing protocols, the delivery ratio improves with increased node density (see Fig. 7). Looking at

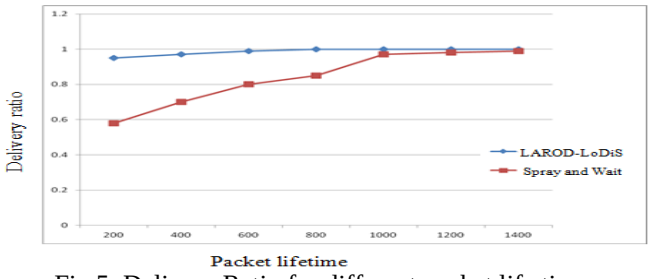

Fig 5 Delivery Ratio for different packet life times

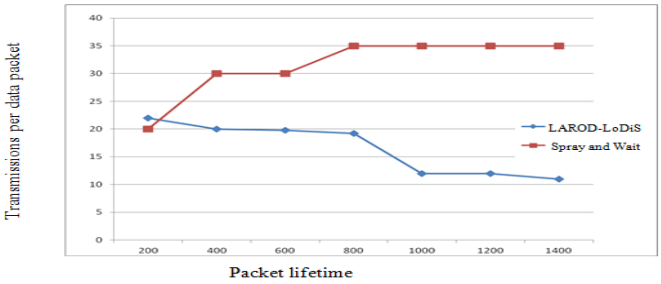

Fig 6 Overhead for different packet lifetimes

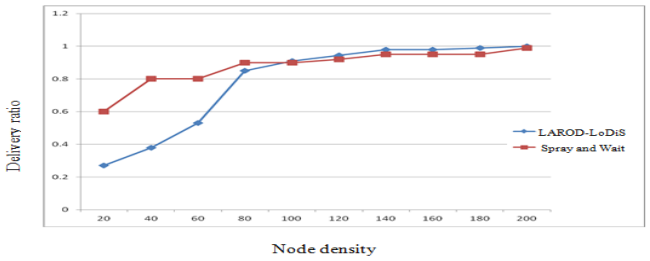

Fig 7 Delivery ratio for different node densities

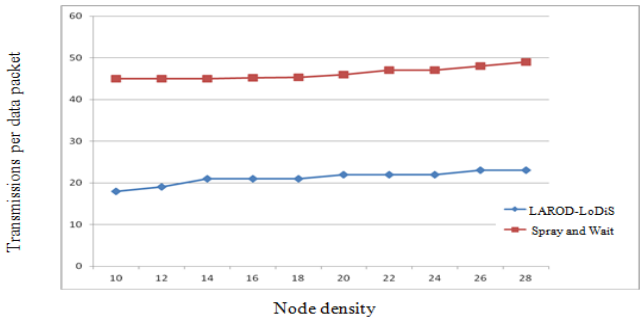

Fig 8 Overhead for different node densities

the overhead in Fig. 8, we observe that the overhead for LAROD-LoDiS is less compared to spray and wait.

V. CONCLUSION

Geographical routing protocols works efficiently in MANETs and IC-MANETs due to the availability of node location information. One major criterion for a geographical routing protocol is a well-performing location service. The location service provides the location information of the destination to route a packet toward.

This paper has shown that, by continuous updation of packet‘s location information, geographical routing in IC-MANETs is possible. The location service (LoDiS) has then been integrated with a routing protocol (LAROD) and thoroughly studied in comparison with a high-performance baseline.

Further studies can be done on different location services for MANETs and IC-MANETs. Performance metrics can be evaluated for LAROD-LoDiS based on the location service chosen.

LAROD-LoDiS routing algorithm handles intermittent connectivity but it is not suitable for systems with varying density (sparse and dense areas). For sparse systems, distribution of location information takes much time. For very large systems with thousands of nodes, the difficulty will be to distribute the location information to all the nodes in the system. The transfer of location information in such dense systems consumes much bandwidth of the network. In such scenarios, one can probably employ the density based techniques to overcome the density variation problem. The basic idea behind this technique is to detect the density of the network and defining the broadcast rate based on density.

REFERENCES

[1] F. Warthman, Delay-Tolerant Networks (DTNs): A Tutorial v1.1. Warthman Assoc., Mar. 2003. [Online]. Available: http://www.dtnrg.
org/docs/tutorials/warthman-1.1.pdf

[2] S. M. Das, H. Pucha, and Y. C. Hu, “Performance comparison of scalable location services for geographic ad hoc routing,” in *Proc. IEEE 24th Annu. Joint Conf. IEEE Comput. Commun. Soc.*, 2005, pp. 1228–1239.

[3] T. Spyropoulos, K. Psounis, and C. S. Raghavendra, “Efficient routing in intermittently connected mobile networks: The single-copy case,” *IEEE/ACM Trans. Netw.*, vol. 16, no. 1, pp. 63–76, Feb. 2008.

[4] E. Kuiper and S. Nadjm-Tehrani, “Geographical routing in intermittently connected ad hoc networks,” in Proc. 1st IEEE Int.Workshop Opportunistic *Netw.*, 2008, pp. 1690–1695.

[5] T. Spyropoulos, K. Psounis, and C. S. Raghavendra, “Spray and wait: An efficient routing scheme for intermittently connected mobile networks,” in Proc. ACM SIGCOMM Workshop Delay-Tolerant Netw., 2005, pp. 252–259.

[6] A. Vahdat and D. Becker, “Epidemic routing for partially connected ad hoc networks,” Duke Univ., Durham, NC, Tech. Rep. CS-2000-06, 2000.

[7] V. Cerf, S. Burleigh, A. Hooke, L. Torgerson, R. Durst, K. Scott, K. Fall, and H.Weiss, Delay-tolerant networking architecture. RFC 4838. [Online]. Available: ftp://ftp.rfc-editor.org/in-notes/rfc4838.txt

[8] R. Bruno and M. Nurchis, “Survey on diversity-based routing in wireless mesh networks: Challenges and solutions,” *Comput. Commun.*, vol. 33, no. 3, pp. 269–282, Feb. 2010.

[9] T. Camp, J. Boleng, and L. Wilcox, “Location information services in mobile ad hoc networks,” in *Proc. IEEE Int. Conf. Commun.*, 2002, pp. 3318–3324.

[10] M. Heissenbüttel, T. Braun, T. Bernoulli, and M. Wälchi, “BLR: Beaconless routing algorithm for mobile ad hoc networks,” *Comput. Commun.*, vol. 27, no. 11, pp. 1076–1086, Jul. 2004.

[11] H. Füler, J. Widmer, M. Käsemann, M. Mauve, and H. Hartenstein, “Contention-based forwarding for mobile ad hoc networks,” *Ad Hoc Netw.*, vol. 1, no. 4, pp. 351–369, Nov. 2003.

[12] D. Johnson and D. Maltz, “Dynamic source routing in ad hoc wireless networks,” in *Mobile Computing*. Norwell, MA: Kluwer, 1996, pp. 153–181.

[13] R. R. Choudhury, “Brownian gossip: Exploiting node mobility to diffuse information in ad hoc networks,” in Proc. Int. Conf. Collaborative Comput.: *Netw., Appl. Worksharing*, 2005, pp. 1–5.

Three Bad Assumptions: Why Technologies for Social Impact Fail

[1]S. Revi Sterling [2]John K. Bennett
[1,2]ATLAS Institute University of Colorado Boulder, USA

Abstract
While an increasing number of technologists want to develop humanitarian technologists, most projects suffer from mismatched expectations between the technologist and target community. There are methods to promote "correct" community engagement, but the majority of humanitarian technologists do not have the time or resources to learn relevant social science theory and practice. From practical experience and research, we suggest five strategies and corresponding tactics to help address this problem.
Keywords-humanitarian technology, community development

I. INTRODUCTION: HOW THE CHASM IS CREATED

Although humanitarian technologies often support particular traditional development sectors such as agriculture or health, the communities with whom we work do not self-arrange in this manner. People do not live in sectors. This simple statement helps explain decades of development inefficiencies, competing efforts, and gaps in services and programs. With the best of intentions, humanitarian technologists continue to perpetuate myopic development initiatives. Contradictions underlie both engineering as a discipline and humanitarianism as a goal. The developing world is littered with the vestiges of failed technology-for-development projects. Communities are increasingly skeptical of visitors who over-promise, under deliver, and rarely return. People in the developing world are tired of being research subjects.

There is a growing awareness of the ubiquity of failure in humanitarian technology. FailFaires are becoming must-attend events where we admonish ourselves for our short-sightedness, and praise ourselves for acknowledging suboptimal outcomes [1]. Exposés on the downsides of the "Playpump" [2] and the hyperbole of Three Cups of Tea [3] are intended to keep us honest as practitioners, as are EWB Canada's excellent Failure Report [4]. Recent efforts have attempted to develop a taxonomy of technology failure [5]. Three errant assumptions continue to lead many NGO and academic efforts toward failures, and many developing communities to a rejection of technology as a viable development strategy. Communities have gone so far as to tell their well-meaning humanitarian technology visitors to never return.

II. THE THREE BAD ASSUMPTIONS

A. Because a community did not have a certain technology before, the community will certainly be better off now that the project has been implemented.

The thinking (perhaps reasonable to us) is that "they had nothing of this sort, and now they at least have something that has to be better than nothing." Creating and deploying a novel technology may feel like it will inevitably move the development needle – until we see that the project does not actually meet a real community need, is deemed useless or cumbersome by community, or worse, exacerbates or introduces discord in the community.

B. The quality bar for humanitarian technologies is low.

While it is of course necessary to consider sustainability concerns such as local sources of materials and the capacity of the community to maintain the technology, simple design does not mean poor design. Time is the enemy of quality of projects for development projects. A student or team that only has Spring Break to visit a field site and install a working prototype is likely to cut corners to meet a deadline. In mature markets, this is forgivable, even standard operating procedure – we like to alpha- and beta-test new technologies; we understand that the software will have service packs and fixes after its release. But prototypes and early adopters have no place in humanitarian technology. When it comes to field deployment, testing should not happen in communities where livelihoods are at stake. It is usually wrong to offer a community a "proof of concept" technology that we would not offer paying customers in the developed world.

C. Install and forget works in development.

Very few development efforts make a truly long-term commitment to the communities they seek to serve. We have yet to visit a community anywhere in the developing world that does not have a story about an NGO or student group that promised to come back and never did. We know the value of long-term relationships with communities, and no one wants to tell community members that they will not likely return, We often justify not returning because we have left the community with a technology – something they didn't have before. After all, we have done the important part of the job, which is the project itself. Perhaps we have even left some training and repair manuals and some spare parts. Anything beyond that is simply relationship building and PR. There are two flaws with this thinking. First, is a community loses its

trust in our intentions; any future work is a non-started. Second, our primary goal is to actually improve the quality of someone's life. We should know if that goal is realized, and if not, we need to understand why not. Answering these questions requires an actual sustained presence in the community.

III. TECHNOLOGY VS. SOCIAL SCIENCE

Many organizations have created frameworks, checklists and top ten lists to ensure the soundness and credibility of their development projects. We point our students to the growing "mea culpa" literature and step them through such resources as BRIDGES.org's "Real Access / Real Impact criteria" and "12 Habits of Highly Effective Development Initiatives" [6]. These resources are unequivocally useful for class discussions and have unquestionable value. They remind us of the UN Millennium Development Goals themselves -- who could be against universal education and health [7]? Our students emphatically nod: of course they will do their research on the area; of course they will conduct community assessments. Of course they will be participatory, because we have said over and over again that community participation is the key to project success. What we fail to teach them, however, is that these activities are hard, time-consuming, and often lead to conflicting information.

It is unrealistic to expect to turn technologies and engineers into development experts and social scientists with a little in-class instruction. It is similarly unrealistic to teach social scientists to be computer scientists and engineers in a semester. Yet humanitarian technology initiatives require expertise – real expertise – in both fields.

We share an enthusiasm for the potential of technology to help address the complex challenges associated with development. Too often, however, we lead with the technology, focusing on our understanding of the solutions before we really understand the problem. Understanding a community's needs (and its priorities) is essential, but such assessment takes both time and expertise. We should expect to spend a lot of time listening to community members (especially dissenting voices), and, where appropriate, we should seek out colleagues whose knowledge and experience compliments our own.

With that focus in mind, we offer five principles that have helped us work successfully with communities. These suggestions represent practical advice that, in our experience, has helped obtain community participation, and the perception of projects as successful by both practitioners and community members.

IV. THE FIVE PRINCIPLES

These five principles have guided our work for several years. They have contributed to productive and participatory community engagement. These ideas are neither surprising nor unique, but they have helped the authors (a social scientist and a computer scientist) communicate honestly with each other and with the communities with whom we have worked. We believe the use of these principles lends to an engagement strategy that has a higher potential for success.

A. The community matters – your ideas don't

We are in the field of humanitarian technology because we are moved to action against inequity. We develop our foci around certain problem and community types – a region, a disease, a cause. Often, this agenda runs up against conflicting community perceptions. A humanitarian team focused on malaria reduction is in for a surprise when the community does not place malaria as its top priority. If the community identifies lack of education as its most pressing concern, this presents an option to link malaria reduction with school absence, likely requiring a shift in project design. Trying to convince a community that our priorities should be theirs is counterproductive at best.

There are many development anecdotes that describe the best of intentions gone wrong -- a community health post built upon land that no one in the community will walk on because of its bloody history, the well that is build closer to town -- to the dismay of women who now no longer get to enjoy their only time to chat with other women, the arsenic-free water pump whose water tastes unpalatable to those who prefer the poisonous water. If a family dislikes the taste of bread made in a solar oven, they are not going to use it just because we tell them it is better for the environment. Truly listening to community members about their perceptions and priorities will necessarily require changes to the project design that we have spent months or years developing. While that project may represent our "baby" (or our dissertation), we should not expect, and we cannot require, the community to adopt our priorities.

B. Don't use the community as a research subject

There is often discord when development practice and research abut in the field. Much has been written on the real goals of humanitarian technology, and active debate persists among development practitioners and researchers over objectives. Does "development" require an actual improvement in the quality of life of community members, or is it acceptable to conduct research that may not impact community development in the foreseeable future, but which may have a long-term potential for positive change? Our own thinking on this subject leans strongly toward development as positive impact. Pilot projects are particularly problematic in this instance, and should not be undertaken unless the community specifically understands that the pilot means short-term engagement and a low probability of immediate positive community impact.

Data collection and development are not the same. Using a community for project and usability data is only appropriate when explicit consent can be negotiated [8]. Otherwise, the implied promise of engagement and change is broken, which leaves a community without a usable technology and often with diminished trust of development initiatives in general. For this reason, we advocate that students go through the Institutional Review Board (IRB) process at their institution – not because it is a terribly useful tool in the field, but because the process of writing an IRB brings these questions and risks to the forefront, and makes evident what needs to be negotiated at the community level [9]. Many humanitarian technology projects eschew the IRB because they are not doing traditional research, but are project-based. The value of the IRB in humanitarian technology is not about research, but about respect for other people.

C. Buy-in from one community "champion" is not enough

This recommendation contradicts conventional development wisdom. Project leaders are often instructed to find a community champion to adopt and "sponsor" the technology being introduced. Usually, this is a mayor or equivalent – a chief, a group of elders. This idea stems from the belief that communities follow the example set by the persons in charge, especially in collective-oriented communities. While this may be true at least to some extent, it fails to recognize that those in power often do not share power. Many humanitarian technology failures, even those developed by the most engaged technology companies, stem from giving community leaders control of the technology. Follow-up visits to such communities frequently demonstrate that the dominant family or group in the community is the primary beneficiary of the initiative.

We have found our projects are much more sustainable and equitably used when we have transferred project or technology management to those who are already on the margins of the community – women, the elderly – especially widows, and those with disabilities. These groups of people understand the power relations in the community, and often appreciate the opportunity to work outside the dominant paradigm. Due to the cachet of an NGO or university, those in charge rarely challenge this unorthodox deployment; likewise, these unlikely champions enjoy a shift in status and recognition, which serves as a form of development in itself. Widows, who are often the most ostracized members of a community, set a powerful example. If they, as outcasts, can use and benefit from the technology, the perception is often that everyone can. Women and those with disabilities are often the least mobile and least likely to leave a community, unlike those in more powerful positions; thus, a project can enjoy consistency and a greater chance of sustainability.

D. Poor people are not monolithic

Because many humanitarian technologists do not have the luxury of getting to know the community well, they have a difficult time recognizing the power differentials in a community based on class/caste, race, gender and religion. We tend instead to lump "poor people" together as a self-organized unit with little internal differentiation. After all, they share many characteristics that we aim to impact; they are all without the options and opportunities afforded to those in higher socioeconomic strata. We have a tendency to also present "the poor" as a virtuous and grateful group that is happy we are willing to help, and who will do the right thing with the technology presented to them. This is frequently a misperception. Often, outsiders are viewed with suspicion, especially in communities with a colonial past, or those that have been disappointed by previous encounters with development efforts. Gratitude is not a given – often, we are simply brining the living standard of a community up to the most basic level. It is also presumptuous to assume that those in dire straits will use new resources in the way that we think they should. Project members are often disappointed when people use the donated laptop to read about movie stars rather than find employment or health information, or that a family will chose to go to a Bollywood film rather than pay back a loan. The poor are like all of us in this regard; we sometimes chose to act on taste and preference rather than logic. We should not be surprised when people do not drink the chlorine-treated water because they prefer the taste of untreated water or that they sell donated mosquito nets for a profit, any more that we should be surprised when our colleagues smoke, consume trans fatty acids, or collect debt on vanity items. We only have to look at the emerging body of literature in behavioral economics in development to realize that we are not the arbiters of judgment [10].

E. The customer is always right

It is condescending to view the beneficiaries of humanitarian technologies as anything other than customers. If our technology is being used in unanticipated ways, or not at all, it is because we have failed to correctly address human needs and wants with a technology. If we fail to serve our market, our project will become another failure. If we fail to understand the market for our produce, or if the market is already flooded with a competing product, we are likely to fail. If we fail to embrace existing standards, or if we develop a product of poor quality, we should not be surprised when our customers look elsewhere. Instead of being a standards-free zone, humanitarian technology should be governed by the same standards that we employ at home. The use of community devices, technologies and protocols is almost a more cost-effective and more success-prone approach that developing a custom solution. Our efforts should attempt to amplify existing community practices, rather than replace them.

V. CONCLUSION

The history of humanitarian technology is replete with mismatched expectations between the practitioner and the community intended to benefit from the provided technology. Recent work examining the failures that result from this mismatch shows promise, but few actionable recommendations for closing the chasm between practitioner and community have emerged. We have offered a few ideas that have worked for us. They are based upon several years of experience and practice. We encourage our colleagues to test these ideas.

REFERENCES

[1] Failfaire. (2011). [Online]. Available: http://failfaire.org.

[2] L. Freschi. (2011). Some NGOs CAN adjust to Failure: The PlayPumps Story [Online]. Available: http://aidwatchers.com/2010/02/some-ngos-can-adjust-to-failure-the-playpumps-story/.

[3] N. Kristof. (2011). Three Cups of Tea, Spilled [Online]. Available: http://www.nytimes.com/2011/04/21/opinion/21kristof.html.

[4] Engineers withouth Borders Canada. (2010). Failure Reports [Online]. Available: http://www.ewb.ca/en/whoweare/accountable/failure.html.

[5] L. Dodson, unpublished work.

[6] Bridges.org. (2006). 12 Habits of Highly Effective ICT-Enabled Development Initiatives and Real Access / Real Impact criteria [Online]. Available: http://www.bridges.org/12_habits and http://www.bridges.org/Real_Access.

[7] Millenium Development Goals. (2005). [Online]. Available: http://www.un.org/millenniumgoals/.

[8] S.R. Sterling and N. Rangaswamy, "Constructing Informed Consent in ICT4D Research," in Proceedings of the 4th ACM/IEEE Conference on Information and Communication Technology. London, UK, 2010.

[9] Ibid.

[10] A. Banerjee and E. Duflo, Poor Economics: A Radical Rethinking of the Way to Fight Global Poverty, NewYork, NY: PublicAffairs, 2011.

Solution of Fuzzy Games with Interval Data Using Approximate Method

Dr.C.Loganathan
Department of Mathematics
Maharaja Arts and Science College
Coimbatore – 641407, India

M.S.Annie Christi
Department of mathematics
Providence College for Women,
Coonoor-643104, India

Abstract
In this paper, we evaluate the value of the fuzzy game matrix with interval data using the approximate method. This method gives an approximate solution for the value of the game and the true value can be determined to any degree of accuracy. This method assumes that each player will play in such a manner so as to maximize the expected gain or to minimize the expected loss.

Keywords: Approximate method, Interval data, matrix game, value of the game.

1. Introduction

The solution methods of interval matrix games are studied by many authors. Most of the solution techniques are based on linear programming methods for interval numbers. We present, in this paper an approximate method for solving 3x3 or higher interval matrix games and illustrate this with a numerical example.The algebraic method is generally adopted to solve the game for which the graphical method cannot be applied, but the games with large payoff matrices are extremely tiresome to solve by algebraic method. For such large games the iterative method is very powerful to hand as well as machine computations.

1.1 Interval Numbers:

An interval number is of the form $\bar{a}$ = [L (a), U (a)] = {x∈ R: L (a) ≤x≤U (a)}.

If L (a) = U (a) then $\bar{a}$ is a real number. Mid point of $\bar{a}$ m ($\bar{a}$) and range of $\bar{a}$ r ($\bar{a}$) is defined as

m ($\bar{a}$) = $\frac{L(a)+U(a)}{2}$ and r ($\bar{a}$) = $\frac{U(a)-L(a)}{2}$ respectively.

The basic operations are defined as follows:

Let $\bar{a}$ = [L (a), U (a)], $\bar{b}$ = [L (b), U (b)], be two intervals. Then,

(i) $\bar{a}+\bar{b}$ = [L (a) +L (b), U (a) +U (b)],

(ii) $\bar{a}$ _ $\bar{b}$ = [L (a)-L (b), U (a)-U (b)],

(iii) $\bar{a}$ $\bar{b}$ =[min{L(a).L(b), L(a).U(b), U(a).L(b), U(a).U(b), },
max{ L(a).L(b), L(a).U(b), U(a).L(b), U(a).U(b),}],

(iv) λ $\bar{a}$ = [λ L(a), λ U(a)] if λ > 0.
= [λ U (a), λ L (a)] if λ <0.

Similarly the other binary operations are defined.

1.2 Comparison Of Intervals:

Comparison of intervals is very important problem in interval analysis. Comparison on interval numbers is given by Nayak and Pal[8].

Disjoint Intervals:

Let $\bar{a}$ = [L (a), U (a)], $\bar{b}$ = [L (b), U (b)], be two intervals. Then $\bar{a}<\bar{b}$ if

U (a) < L (b).

Example: Let $\bar{a}$ = [2, 5] and $\bar{b}$ = [6, 8] then $\bar{a} < \bar{b}$.

Nested Sub-Intervals:

Let $\bar{a}$ = [L (a), U (a)], $\bar{b}$ = [L (b), U (b)], be two intervals. If L(a)≤L(b)≤U(b)≤U(a), then $\bar{b}$ is contained in $\bar{a}$,which is the concept of inclusion. The extension of the set inclusion here only describes the condition that the interval $\bar{b}$ is nested in $\bar{a}$ but it cannot order $\bar{a}$ and $\bar{b}$ in terms of its value.

2. Matrix Games:

Given a matrix game A= ($\overline{a_{ij}}$), the element $\overline{a_{ij}}$ is called a saddle interval of A if

$$\overline{a_{ij}} \leq \overline{a_{il}} \quad \forall \ l=1, 2\ldots n$$

$$\overline{a_{ij}} \geq \overline{a_{kj}} \quad \forall \ k=1, 2\ldots m.$$

(i.e.) the element $\overline{a_{ij}}$ is simultaneously a minimum interval in its row and a maximum interval in its column.

When there is no saddle interval in a matrix game, an iterative method can be used to get an approximate solution

3. Procedure:

STEP: 1

Let the player A arbitrarily selects a row which will be the superior one of his other strategies and places it under the matrix.

STEP: 2

Player B examines this row and chooses a column corresponding to the smallest interval in the row and places to the right of the matrix.

STEP: 3

Player A now examines this column and chooses a row corresponding to the largest interval in this column. This row is added to the row last chosen and is placed under the previous row chosen.

STEP: 4

Player B then chooses the column corresponding to the smallest number in the new row and adds this column to the column chosen. In case of a tie, the player will select that row or column which is different from his last choice.

STEP: 5

The procedure is repeated for a finite number of iterations.

STEP: 6

The smallest elements in each succeeding row with the largest elements in each succeeding column are encircled.

STEP: 7

The approximate strategies after a certain number of iterations are found by dividing the number of encircled intervals in each row or column by total number of iterations.

STEP: 8

The upper bound for the value of the game can be determined by dividing the largest interval in the last column by the total number of iterations. Likewise the lower bound can be determined by dividing the smallest element in the last row by the total number of iterations. Thus the approximate value of game and the optimal strategies are evaluated.

4. Illustration:

$$\begin{bmatrix} [-4,-1] & [0,1] & [3,4] \\ [5,6] & [-2,0] & [1,2] \\ [0,1] & [3,6] & [-1,2] \end{bmatrix}$$

[0,1] [3,5] [6,9] [9,13] [5,12] [8,16] [4,15] [4,16] [4,17] [4,8] $q_1 = \frac{2}{10}$

[-2,0] [-1,2] [0,4] [1,6] [6,12] [7,14] [12,20] [10,20] [8,20] [6,20] $q_2 = \frac{3}{10}$

[3,6] [2,8] [1,10] [0,12] [0,13] [-1,15] [-1,16] [2,22] [5,28] [8,34]

$q3 = \frac{5}{10}$

[5, 6] [-2, 0] [1, 2]

[5, 7] [1, 6] [0, 4]

[5, 8] [4, 12] [-1, 6]

[5, 9] [7, 18] [-2, 8]

[1, 8] [7, 19] [1, 12]

6, 14] [5, 19] [2, 14]

[2, 13] [5, 20] [5, 18]

[7, 19] [3, 20] [6, 20]

[12, 25] [1, 20] [7, 22]

[12, 26] [4, 26] [6, 24]

$p_1 = \frac{2}{10}$ $p_2 = \frac{4}{10}$ $p_3 = \frac{4}{10}$

The strategies are approximate values. Hence they were taken as fuzzy strategies so that we have the expected pay-offs as

$p_1[-4,-1] + p_2[5, 6] + p_3[0, 1] = [\frac{12}{10}, \frac{22}{10}]$

$p_1[0, 1]+ \ p_2[-2, 0] + \ p_3[3, 4] = [\frac{4}{10}, \frac{18}{10}]$

$p_1[3, 4]+ \ p_2[1, 2] + \ p_3[-1, 2] = [\frac{6}{10}, \frac{24}{10}]$

$q_1[-4, -1] + \ q_2[0, 1] + \ q_3[3, 4] = [\frac{7}{10}, \frac{21}{10}]$

$q_1[5, 6]+ \ q_2[-2, 0] + \ q_3 \ [1, 2] = [\frac{9}{10}, \frac{22}{10}]$

$q_1[0, 1]+ \ q_2[3, 6] + \ q_3[-1, 2] = [\frac{4}{10}, \frac{28}{10}]$

These values lie around 4.5. Hence the value of the fuzzy game is approximately equal to $\bar{v}$ = [3, 6]. It lies between [-4, -1] and [5, 6] with R($\bar{v}$) = 4.5.

Conclusion:

An approximate method is applied to find out the value of the game matrix with interval data.Defuzzification is done to convert the fuzzy values to crisp values. These ideas can be applied to other fuzzy problems

References:

[1] Bellman, R.E., Zadeh, L.A., (1970). Decision making in a fuzzy environment, management science, vol, 17, No.4, B-141-B-164.

[2] Chen S.M., Hsiao. W.H. and Hong Y.J, knowledge based method for fuzzy quary processing for document retrieval, Cybernetics and Systems, Vol.28, No. 1, pp.99-119, (1997).

[3] Dubois., and Prade, H., (1978). Operations on fuzzy numbers, int.J.Systems.Sci. Vol.9, 613-626.

[4] Dubois., and Prade, H., (1978). The mean value of a fuzzy number, Fuzzy sets and systems 24, 279-300.

[5] Martyin Shubik, (1957). The uses and Methods of Game Theory, New York, American Elsevier

[6] Paul R. Thie, (1988). An introduction to linear programming and game theory, John Wiley & Sons, New York..

[7] Porchelvi, T., Stephen Dinagar, D.,(2010). An approximate Method for Solving Fuzzy Games, Advances in Fuzzy Mathematics, Vol.5, No.4, pp.295-300.

[8] Nayak, P.K., Madhumangal Pal, (2007).Solution Rectangular Fuzzy Games, OPSEARCH, Vol.44, No.3.

Low Power Glitch Free Modeling in Vlsi Circuitry Using Feedback Resistive Path Logic

Dr M.ASHARANI[1], N.CHANDRASEKHAR[2], R.SRINIVASA RAO[3]

[1]ECE Department, Professor, JNTU, Hyderabad
[2,3]ECE Department, Associate Professor, Khammam Institute of Technology and Sciences, Khammam

Abstract
Low power has emerged as a principal theme in today's electronics industry. This work focus on the development of low power VLSI design methodology on system level modeling and circuit level modeling for power optimization. This work develops a power optimization approach in bus transitions using hamming coding scheme called 'Unbounded Lagger algorithm' for transition power reduction in VLSI design. The developed transition optimization approach further merged with circuit level power optimization using Glitch minimization technique. A resistive feed back method is developed for the elimination of glitches in the CMOS circuitry which result in power consumption and reducing performance of VLSI design. The proposed system is developed on Active HDL for designing a Bus transition Optimization algorithm using Unbounded Lagger algorithm, where an encoder and decoder units are designed for the minimization of transition for parallel bus transition in data transfer**.**

Introduction
In past, the major concerns of the VLSI designer were area, performance, cost and reliability; power consideration was mostly of only secondary importance. With advanced Nickel-Metal-Hydride (secondary) battery technologies offering around 65 watt W hours/kilograms, this terminal would require an unacceptable 6 kilograms of batteries for 10 hours of operation between recharges. Even with new battery technologies such as rechargeable lithium ion or lithium polymer cells, it is anticipated that the expected battery lifetime will increase to about 90-110 watt-hours/kilogram over the next 5 years which still leads to an unacceptable 3.6-4.4 kilograms of battery cells. In the future, it can be extrapolated that a large microprocessor, clocked at 500 MHz (which is a not too aggressive estimate for the next decade) would consume about 300 W. Every 10^0C increase in operating temperature roughly doubles a component's failure rate.

Low-Power Vlsi Design
Power dissipation in CMOS circuits is caused by three sources:

1) The leakage current which is primarily determined by the fabrication technology, consists of reverse bias current in the parasitic diodes formed between source and drain.
2) The short-circuit (rush-through) current which is due to the DC path between the supply rails during output transitions and
3) The charging and discharging of capacitive loads during logic changes.
4) The dynamic power dissipation and is given by:

$$P = 0.5CV_{dd}^{2}E(sw)f_{clk}$$

Where C is the physical capacitance of the circuit, V_{dd} is the supply voltage, E(sw) referred as the switching activity is the average number of transitions in the circuit per $1/f_{clk}$ time, and f_{clk} is the clock frequency.

Low power design space

Optimizing for power entails an attempt to reduce one or more of these factors.

Voltage

Because of these factors, designers are often willing to sacrifice increased The limit of how low the Vt can go is set by the requirement to set adequate noise margins and control the increase in sub threshold leakage currents. The optimum Vt must be determined based on the current drives at low supply voltage operation and control of the leakage currents. Since the inverse threshold slope (S) of a MOSFET is invariant with scaling, for every 80-100 mV (based on the operating temperature) reduction in Vt, the standby current will be increased by one order of magnitude. This tends to limit Vt to about 0.3 V for room temperature operation of CMOS circuits. Basically, delay increases by 3x for a delta V_{dd} of plus/minus 0.15 V at V_{dd} of 1 V.

Physical capacitance

Dynamic power consumption depends linearly on the physical capacitance being switched. Approximate estimates can be obtained by using information derived from a companion placement solution or by using stochastic procedural interconnect models. As with voltage, however, we are not free to optimize capacitance independently.

Switching Activity

There are two components to switching activity: f_{clk} which determines the average periodicity of data arrivals and E(sw) which determines how many transitions each arrival will generate. For circuits that do not experience glitching, E(sw) can be interpreted as the probability that a power consuming transition will occur during a single data period. Even for these circuits, calculation of E(sw) is difficult as it depends not only on the switching activities of the circuit inputs and the logic function computed by the circuit, but also on the spatial and temporal correlations among the circuit inputs.

Calculation Of Switching Activity

Delay model

Based on the delay model used, the power estimation techniques could account for steady-state transitions (which consume power, but are necessary to perform a computational task) and/or hazards and glitches (which dissipate power without doing any useful computation). Sometimes, the first component of power consumption is referred as the functional activity while the latter is referred as the spurious activity. It is shown that the mean value of the ratio of hazardous component to the total power dissipation varies significantly with the considered circuits (from 9% to 38% in random logic circuits) and that the spurious power dissipation cannot be neglected in CMOS circuits.

Power Estimation Techniques

In the following section, various techniques for power estimation at the circuit, logic and behavioral levels will be reviewed. These techniques are divided into two general categories: simulation based and no simulation based.

Simulative Approaches

A. Brute force simulation

Power Mill is a transistor-level power simulator and analyzer which applies an event-driven timing simulation algorithm (based on simplified table-driven device models, circuit partitioning and single-step nonlinear iteration) to increase the speed by two to three orders of magnitude over SPICE. Switch-level simulation techniques are in general much faster than circuit- level simulation techniques, but are not as accurate or versatile. Standard switch-level simulators (such as IRSIM) can be easily modified to report the switched capacitance (and thus dynamic power dissipation) during a simulation run.

B. *Hierarchical simulation*

A simulation method based on a hierarchy of simulators are presented in past. The idea is to use a hierarchy of power simulators (for example, at architectural, gate-level and circuit-level) to achieve a reasonable accuracy and efficiency tradeoff. Another good example is Entice-Aspen. This power analysis system consists of two components: Aspen which computes the circuit activity information and Entice which computes the power characterization data.

C. *Monte Carlo simulation*

A Monte Carlo simulation approach for power estimation which alleviates the input pattern dependence problem were also suggested. This approach consists of applying randomly generated input patterns at the circuit inputs and monitoring the power dissipation per time interval T using a simulator. Based on the assumption that the power consumed by the circuit over any period T has a normal distribution, and for a desired percentage error in the power estimate and a given confidence level, the number of required power samples is estimated.

Non-Simulative Approaches

A. Behavioral level

The power model for a functional unit may be parameterized in terms of its input bit width. For example, the power dissipation of an adder (or a multiplier) is linearly (or quadratically) dependent on its input bit width.The library thus contains interface descriptions of each module, description of its parameters, its area, delay and internal power dissipation (assuming pseudo-random white noise data inputs).

B. *Logic level*

Estimation under a Zero Delay Model Most of the power in CMOS circuits is consumed during charging and discharging of the load capacitance. Methods of estimating the activity factor E n (sw) at a circuit node n involve estimation of signal probability prob(n), which is the probability that the signal value at the node is one. Under the assumption that the values applied to each circuit input are temporally independent (that is, value of any input signal at time t is independent of its value at time t-1), we can write:

$$E_n(sw) = 2\ prob(n)\ (1 - prob(n)).$$

(2)

Computing signal probabilities has attracted much attention. In the recent years, a computational procedure based on Ordered Binary-Decision Diagrams (OBDDs) has become widespread. In this method, which is known as the OBDD-based method, the signal probability at the output of a node is calculated by first building an OBDD corresponding to the global function of the node and then performing a post order traversal of the OBDD using equation:

$$prob(y) = prob(x)\,prob(f_x) + prob(\bar{x})\,prob(f_{\bar{x}})$$

(3)

This leads to a very efficient computational procedure for signal probability estimation. The activity factor of line x can be expressed in terms of these transition probabilities as follows:

$$E_x(sw) = prob(x_{0\to 1}) + prob(x_{1\to 0})$$

(4)

The various transition probabilities can be computed exactly using the OBDD representation of the logic function of x in terms of the circuit inputs. A mechanism for propagating the transition probabilities through the circuit which is more efficient as there is no need to build the global function of each node in terms of the circuit inputs. This work has been extended to handle highly correlated input streams using the notions of conditional independence and isotropy of signals. . Given these waveforms, it is straight-forward to calculate the switching activity of x which includes the contribution of hazards and glitches, that is:

$$E_x(sw) = \sum_{t\in\, eventlist(x)} \left(prob\left(x^t_{0\to 1}\right) + prob\left(x^t_{1\to 0}\right)\right)$$

(5)

Given such waveforms at the circuit inputs and with some convenient partitioning of the circuit, the authors examine every sub-circuit and derive the corresponding waveforms at the internal circuit nodes.

Cmos Device And Voltage Scaling

In the future, the scaling of voltage levels will become a crucial issue. The main force behind this drive is the ability to produce complex, high performance systems on a chip. Two CMOS device and voltage scaling scenarios are described, one optimized for the highest speed and one trading off high performance for significantly lower power (the speed of the low power case in one generation is about the same as the speed of the high-performance case of the previous generation, with greatly reduce power consumption). It is shown that the low power scenario is very close to the constant electric-field (ideal) scaling theory.

Cad Methodologies And Techniques

Behavioral synthesis

The behavioral synthesis process consists of three steps: allocation, assignment and scheduling. These steps determine how many instances of each resource are needed, on what resource each operation is performed and when each operation is executed. This approach requires various support circuitry including level-converters and DC/DC converters. Consider a module M in an RTL circuit that performs two operations A and B. Hence, the power dissipation depends on the module binding. Similarly, consider a register R that is shared between two data values X and Y. The switching activity of R depends on the correlations between these two variables X and Y.

Logic synthesis

Logic synthesis fits between the register transfer level and the netlist of gate specification. It provides the automatic synthesis of netlists minimizing some objective function subject to various constraints. Depending on the input specification (combinational versus sequential, synchronous versus asynchronous), the target implementation (two-level versus multi-level, unmapped versus mapped, ASICs versus FPGAs), the objective function (area, delay, power, testability) and the delay models used (zero-delay, unit-delay, unit-fanout delay, or library delay models), different techniques are applied to transform and optimize the original RTL description.

Physical design

Physical design fits between the netlist of gates specification and the geometric (mask) representation known as the layout. It provides the automatic layout of circuits minimizing some objective function subject to given constraints. Depending on the target design style (full-custom, standard-cell, gate arrays, FPGAs), the packaging technology (printed circuit boards,

multi-chip modules, wafer-scale integration) and the objective function (area, delay, power, reliability), various optimization techniques are used to partition, place, resize and route gates.

Power Management Strategies

In many synchronous applications a lot of power is dissipated by the clock. The clock is the only signal that switches all the time and it usually has to drive a very large clock tree. Moreover in many cases the switching of the clock causes a lot of additional unnecessary gate activity. For that reason, circuits are being developed with controllable clocks.

TRANSITION POWER OPTIMIZATION USING LAGGER ALGORITHM

Bus transition logic

Activation of external buses consumes significant power as well, because many input–output (I/O) pins and large I/O drivers are attached to the buses. Typically, 50% of the total power is consumed at the I/Os for well-designed low-power chips by R.Wilson. Thus, reducing the power dissipated by buses becomes one of the most important concerns in low-power VLSI design. The dynamic power dissipated in a bus is expressed as the following;

$$P_{\mathrm{BUS}} = \sum_{\mathrm{line}} C_{\mathrm{load}} V_{\mathrm{DD}}^2 N_{\mathrm{trans}}$$

Where C_{load} is the total load capacitance attached to a bus line, V_{DD} is the voltage swing at operation, and N_{trans} is the number of transitions per second. There are two approaches to reduce the dynamic power of buses. One is to save the dynamic power per activation by reducing either C_{load} or V_{DD}.

Sequence-switch coding

The I/O data are transferred consecutively at a relatively constant rate. This kind of transfer pattern gives us a new opportunity to reduce the number of bus and I/O) transitions during data transmission. When a sequence of data moves through a bus, its transmission sequence can be chosen to minimize the number of bus transitions. For example, the effect of the sequence on the number of bus transitions is illustrated in Fig. 1. Let us assume that there are eight data to be sent via a bus, and Fig. 3.1(a) is the waveform of the bus when these are transmitted without any modification.

Resistive Feedback Power Optimization

Logical modeling

The formulation might become non-linear, since changing the W/L ratio of a MOSFET changes the channel resistance as well as the associated parasitic capacitances Thus, an n-diffusion capacitor and a resistor wire with a blocking mask is developed. The blocking mask increases the resistivity of the polysilicon resistor. To simulate a realistic situation, each delay element is driven by an inverter gate and is also loaded with an inverter. The circuit set up is shown in Figure1.The inverter and the transmission gate cells are made of transistors with minimum sizes.

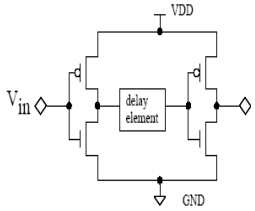

Figure 1. Circuit setup for resistive load placement

The delay/power (metric 1) and delay/area (metric 2) are used as the referencing values for power minimization. The delay values used to calculate both metrics are given in column 2 of the table 1. The power consumption values used to calculate metric 1 are expressed in μW. Since the delay elements are implemented as standard cells with fixed height, the area is measured in terms of the number of grid units along the width. This delay element is called as resistive feedthrough logic. The resistance of a rectangular slab of length L, width W and thickness t can be calculated in terms of a material specific constant called resistivity ρ, as R=ρL/(Wt).

Glitch free physical design

The resistances found from the lookup table are automatically designed as standard cells. These feedthrough cells are inserted into the original circuit by modifying a HDL netlist of the circuit. The place-and-route layout of the modified netlist is then done using a commercial tool such as Tanner.

DESIGN IMPLEMENTATION

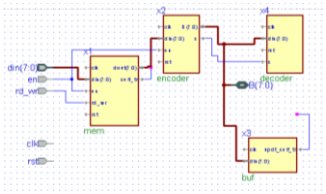

Figure 2. Implemented system diagram on Aldec's Block diagram

Result Analysis

For the evaluation of the suggested approach an simulation is carried out in Active HDL tool and then the units are developed on tanner tool for the glitch minimization. The obtained simulation results are as shown below,

With stray capacitance:

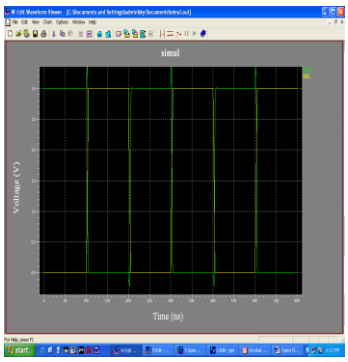

Figure 3. Simulation observation with stray capacitance

After feed-back path offered:

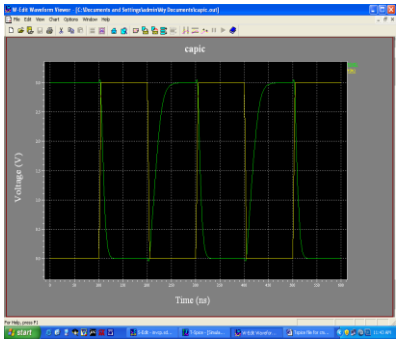

Figure 4. Spice simulation showing the glitch minimization

DEVICE UTILIZATION SUMMARY

Selected Device: 2vpx70ff1704-7

Number of Slices	: 11533 out of 33088	34%
Number of Slice Flip Flops	: 571 out of 66176	0%
Number of 4 input LUTs	: 20312 out of 66176	30%
Number of bonded IOBs	: 326 out of 996	32%

Number of GCLKs : 1 out of 16 6%

CONCLUSION

The Low power-designing objective is successfully developed based circuit level and behavioral level design flow. This was done without re-design of the CMOS logic with resister feedback. The new design flow is effective in designing minimum transient energy standard cell based digital CMOS circuits. The objective is achieved with CMOS level developing on Tanner CAD tool and simulating it on Spice simulator. The power optimization is also achieved by using Bus transition minimization where a Lagger algorithm is realized for the minimization of transitions to reduce power consumption in Bus architecture.

References

[1] M.Alidina, J. Monteiro, S. Devadas, A. Ghosh, and M. Papaefthymiou." Pre computation- based sequential logic optimization for low power. "*In Proceedings of the 1994 International Workshop on Low Power Design*, pages 57-62, April 1994.

[2] W.C.Athas, L. J. Svensson, J.G.Koller, N.Thartzanis and E. Chou. " Low-Power Digital Systems Based on Adiabatic-Switching Principles. " *IEEE Transactions on VLSI Systems*, 2(4)398-407:, December 1994

[3] H. Bakoglu, Circuits, Interconnections, and Packaging for VLSI, Addison-Wesley, Menlo Park, CA, 1990.

[4] L . Benini, M. Favalli, and B. Ricco. *"Analysis of hazard contribution to power dissipation in CMOS IC's."* In Proceedings of the 1994 International Workshop on Low Power Design, pages 27–32, April 1994.

[5] M. Berkelaar and J. Jess. "*Gate sizing in MOS digital circuits with linear programming*" In Proceedings of the European Design Automation Conference, pages 217-221, 1990.

[6] R. Bryant. "Graph-based algorithms for Boolean function manipulation." *IEEE Transactions on Computers*, volume C-35, pages 677–691, August 1986.

To Find Strong Dominating Set and Split Strong Dominating Set of an Interval Graph Using an Algorithm

Dr. A. Sudhakaraiah[*], V. Rama Latha[1], E. Gnana Deepika[2], T.Venkateswarulu[3]
Department of Mathematics, S.V . University, Tirupati-517502, Andhra Pradesh, India.

Abstract:
Strong and weak domination arise naturally in certain practical situations. For example, consider a network of roads connecting a number of locations. In such a network, the degree of a vertex v is the number of roads meeting at v. Suppose $\deg u \geq \deg v$. Naturally, the traffic at u is heavier than that at v. If we consider the traffic between u and v, preference should be given to the vehicles going from u to v. Thus, in some sense, u strongly dominates v and v weakly dominates u. In this paper we present an algorithm to find a strong dominating set and split strong dominating set of an interval graph which is connected.

Keywords: domination number, dominating set, Interval family, Interval graph, strong domination number , split dominating set, spit strong dominating set, strong dominating set.

1. Introduction

We have defined a graph as a set and a certain relation on that set. It is often convenient to draw a "picture" of the graph. This may be done in many ways usually one draws an interval graph corresponding to I for each vertex and connects vertex u and vertex v with a directed arrow whenever uv is an edge. If both uv and vu are edges then some times a single line joints u and v without arrows.

Let $I = \{I_1, I_2, ..., I_n\}$ be the given interval family. Each interval i in I is represented by $[a_i, b_i]$, for $i = 1, 2, ..., n$. Here a_i is called the left endpoint and b_i the right endpoint of the interval I_i. Without loss of generality we may assume that all end points of the intervals in I which are distinct between 1and 2n. The intervals are labelled in the increasing order of their right endpoints. Two intervals i and j are said to intersect each other, if they have non-empty intersection. Interval graphs play important role in numerous applications, many of which are scheduling problems. They are a subset of perfect graphs [1]. A graph $G = (V, E)$ is called an interval graph if there is a one-to-one correspondence between V and I such that two vertices of G are joined by an edge in E if and only if their corresponding intervals in I intersect. That is, if $i = [a_i, b_i]$ and $j = [a_j, b_j]$, then i and j intersect means either $a_j < b_i$ or $a_i < b_j$.

Let G be a graph, with vertex set V and edge set E. The open neighbourhood set of a vertex $v \in V$ is

$$nbd(v) = \{u \in V / uv \in E\}$$

The closed neighbourhood set of a vertex $v \in V$ is

$$nbd[v] = nbd(v) \cup \{v\}$$

A vertex in a graph G dominates itself and it's neighbours. A set $D \subseteq V$ is called dominating set if every vertex in $<V - D>$ is adjacent to some vertex in D. The domination studied in [2-3]. The domination number γ of G is the minimum cardinality of a dominating set. The domination number is well-studied parameter. We can see this from the bibliography [4] on domination. In [5] , Sampathkumar and Pushpa Latha have introduced the concept of strong domination in graphs. Strong domination has been studied [6-67]. Kulli.V.R. et all [8] introduced the concept of split and non-split domination in graphs. A dominating set D is called split dominating set if the induced subgraph $<V - D>$ is disconnected. The split domination number of γ_s of G is the minimum cardinality of a split dominating set. Let $G = (V, E)$ be a graph and $u, v \in V$. Then u strongly dominates v if

(i) $uv \in E$
(ii) $\deg v \leq \deg u$.

A set $D_{st} \subseteq V$ is a strong dominating set of G if every vertex in $V - D_{st}$ is strongly dominated by atleast one vertex in D_{st}. The strong domination number $\gamma_{st}(G)$ of G is the minimum cardinality of a strong dominating set. Define

$NI(i) = j$, if $b_i < a_j$ and there do not exist an interval k such that $b_i < a_k < a_j$. If there is no such j, then define $NI(i) = null$. N_{sd} (i) is the set of all neighbours whose degree is greater than degree of i and also greater than i. If there is no such neighbor then define $N_{sd}(i) = null$. M (S) is the largest highest degree vertex in the set S. nbd^+ (i) is the set of all adjacent vertices which are greater than i. nbd^- (i) is the set of all adjacent vertices which are less than i. d^+ (i) is the number of adjacent vertices which are greater than i. d^- (i) is the number of adjacent vertices which are less than i.

3. Algorithms

3.1. To find a Strong dominating set of an interval graph using an algorithm

Input: Interval family $I = \{I_1, I_2, ..., I_n\}$.

Output: Strong dominating set of an interval graph of a given interval family.

Step 1 : $S_1 = nbd\ [1]$.

Step 2 : S = The set of vertices in S_1 which are adjacent to all other vertices in S_1.

Step 3 : D_{st} = The largest highest degree interval in S.

Step 4 : LI = The largest interval in D_{st}.

Step 5 : If $N_{sd}(LI)$ exists

Step 5.1 : a = M($N_{sd}(LI)$) .

Step 5.2 : b = The largest highest degree interval in nbd [a].

Step 5.3 : $D_{st} = D_{st} \cup \{b\}$ goto step 4.

end if

else

Step 6 : Find $NI(LI)$

Step 6.1: If $NI(LI) = null$ goto step 7.

Step 6.2 : $S_2 = nbd[NI(LI)]$.

Step 6.3 : S_3 = The set of all neighbors of $NI(LI)$ which are greater than or equal to $NI(LI)$.

Step 6.4 : S_4 = The set of all vertices in S_3 which are adjacent to all vertices in S_3.

Step 6.5 : c = The largest highest degree interval in S_4.

Step 6.6 : $D_{st} = D_{st} \cup \{c\}$ goto step 4.

Step 7 : End

3.2. To find a split strong dominating set(sd_{st}) of an interval graph using an algorithm.

Input : Interval family $I = \{I_1, I_2, ..., I_n\}$.

Output : Split strong dominating set of an interval graph of an interval family I.

Step 1 : $S_1 = nbd\ [1]$.

Step 2 : S_2 =The set of all vertices in S_1 which are adjacent to all other vertices in S_1.

Step 3 : $SD_{st} = \{a\}$, where 'a' is the largest highest degree interval in S_2.

Step 4 : Count = The number of pendent vertices or number of vertices with degree one in G.

Step 5 : If Count > 0 then goto step 7

Else

Step 6 : If there exists at least one edge (u, v) such that $u \in nbd^-(a)$ & $v \in nbd^+(a)$

Step 6.1 : Count = Count + 1.

Step 6.2 : Take largest v.

Step 6.3 : $SD_{st} = SD_{st} \cup \{v\} = \{a, v\}$.

Endif

Step 7 : LI = The largest interval in SD_{st}.

Step 8 : If $d^+(LI)=1$ then (If already checked this condition for the same vertex skip)

Step 8.1 : Count = Count + 1.

Step 9 : If $Count \geq 1$ then goto step 12

Else

Step 10 : If there exists atleast one edge (w,x) such that $w \in nbd^-(LI)$ & x $\in$ nbd$^+(LI)$

Step 10.1 : Count = Count + 1.

Step 10.2 : Take largest x .

Step 10.3 : $SD_{st} = SD_{st} \cup \{x\}$.

Endif

Step 11 : If $d^+(x)=1$

Step 10.1 : Count = Count + 1.

Step 12 : If $N_{sd}(LI)$ exists

Step 12.1 : a = M($N_{sd}(LI)$).

Step 12.2 : b = The largest highest degree interval in nbd [a].

Step 12.3 : $SD_{st} = SD_{st} \cup \{b\}$ goto step 7.

end if

else

Step 13 : Find $NI(LI)$

Step 13.1: If $NI(LI) = null$ goto step 14.

Step 13.2 : $S_2 = nbd[NI(LI)]$.

Step 13.3 : S_3 = The set of all neighbors of $NI(LI)$ which are greater than or equal to $NI(LI)$.

Step 13.4 : S_4 = The set of all vertices in S_3 which are adjacent to all vertices in S_3.

Step 13.5 : c = The largest highest degree interval in S_4 .

Step 13.6 : $D_{st} = D_{st} \cup \{c\}$ goto step 7.

Step 14 : End

4. Main Theorems.

Theorem 4.1 : Let G be an interval graph corresponding to an interval family $I = \{I_1, I_2, ..., I_n\}$. If i and j are any two intervals in I such that $i \in D_{st}$, where D_{st} is a minimum strong dominating set of the given interval graph G, $j \neq 1$ and j is contained in i and if there is at least one interval to the left of j that intersects j and at least one interval $k \neq i$ to the right of j that intersects j then $\gamma_{st}(G) < \gamma_{sst}(G)$.

Proof : Let G be an interval graph corresponding to an interval family $I = \{I_1, I_2, ..., I_n\}$. Let i and j be any two intervals in I such that $i \in D_{st}$, where D_{st} is a minimum strong dominating set of the given interval graph G, $j \neq 1$ and j is contained in i and Suppose there is at least one interval to the left of j that intersects j and at least one interval $k \neq i$ to the right of j that intersects j. Then it is obviously we know that j is adjacent to k in the induced sub graph $< V - D_{st} >$. Then there will be a connection in $< V - D_{st} >$. Since there is at least one interval to the left of j that intersects j, there will be a connection in $< V - D_{st} >$ to it's left. In this connection we introduce another interval 'h', which is to the right of j and i and also interest i and j to D_{st} for disconnection in the induced subgraph $< V - D_{st} >$. We also formulated Split strong dominating set as follows

$$SD_{st} = D_{st} \cup \{h\} \Rightarrow |SD_{st}| = |D_{st} \cup \{h\}| .$$

Since D_{st}, h are disjoint $\Rightarrow |SD_{st}| = |D_{st}| + |\{h\}|$ Or $|D_{st}| + |\{h\}| = |SD_{st}|$.

$$\Rightarrow \gamma_{st}(G) + |\{h\}| = \gamma_{sst}(G) .$$

$\Rightarrow \gamma_{st}(G) < \gamma_{sst}(G)$.

ILLUSTRATION

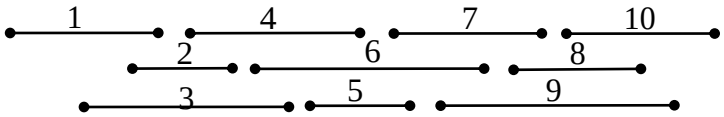

Figure 1. Interval Family

As follows an algorithm with illustration for neighbours as given interval family I.
We construct an interval graph G from an interval family I={1, 2,……,10}as follows

$\text{nbd}[1]=\{1,2,3\}$, $\text{nbd}[2]=\{1,2,3,4\}$, $\text{nbd}[3]=\{1,2,3,4,6\}$, $\text{nbd}[4]=\{2,3,4,5,6\}$,
$\text{nbd}[5]=\{4,5,6,7\}$, $\text{nbd}[6]=\{3,4,5,6,7,9\}$, $\text{nbd}[7]=\{5,6,7,8,9\}$, $\text{nbd}[8]=\{7,8,9,10\}$,
$\text{nbd}[9]=\{6,7,8,9,10\}$, $\text{nbd}[10]=\{8,9,10\}$.

$N_{sd}(1)=\{2,3\}$, $N_{sd}(2)=\{3,4\}$, $N_{sd}(3)=\{6\}$, $N_{sd}(4)=\{6\}$, $N_{sd}(5)=\{6\}$, $N_{sd}(6)=\text{null}$, $N_{sd}(7)=\text{null}$,
$N_{sd}(8)=\{9\}$, $N_{sd}(9)=\text{null}$, $N_{sd}(10)=\text{null}$.

$NI(1)=4$, $NI(2)=5$, $NI(3)=5$, $NI(4)=7$, $NI(5)=8$, $NI(6)=8$, $NI(7)=10$,
$NI(8)=\text{null}$, $NI(9)=\text{null}$, $NI(10)=\text{null}$.

Procedure for finding a strong dominating set(D_{st}) of an interval graph using an algorithm.

Input : Interval family $I=\{1,2,.....,10\}$.

Step 1 **:** $S_1=\{1,2,3\}$.

Step 2 : $S=\{1,2,3\}$.

Step 3 : $D_{st}=\{3\}$.

Step 4 : $LI=3$.

Step 5 : $N_{sd}(3)=\{6\}$.

Step 5.1 : $a=M(N_{sd}(3))=M(\{6\})=6$.

Step 5.2 : $b=6$.

Step 5.3 : $D_{st}=\{3\}\cup\{6\}=\{3,6\}$.

Step 6 : $LI=6$.

Step 7 : $NI(6)=8$.

Step 7.1 : $S_2=nbd[8]=\{7,8,9,10\}$.

Step 7.2 : $S_3=\{8,9,10\}$.

Step 7.3 : $S_4=\{8,9,10\}$.

Step 7.4 : $c=9$.

Step 7.5 : $D_{st}=D_{st}\cup\{9\}=\{3,6\}\cup\{9\}=\{3,6,9\}$.

Step 8 : $LI=9$.

Step 9 : $N_{sd}(9)$ = null and NI (9) = null.

Step 10 : End.

Output : {3,6,9} is the strong dominating set of an interval graph of given interval family.

Procedure for finding a split strong dominating set(SD_{st}) of an interval graph using an algorithm.

Input : Interval family $I=\{1,2,.....,10\}$.

Step 1 **:** $S_1=\{1,2,3\}$.

Step 2 : $S_2=\{1,2,3\}$.

Step 3 : $SD_{st}=\{3\}$.

Step 4 : Count = 0.

Step 5 : There exists (2,4) such that $2\in nbd^{-}(3)=\{1,2\}$ and $4\in nbd^{+}(3)=\{4,6\}$.

Step 5.1 : Count = Count +1 .

Step 5.2 : $SD_{st} = \{3\} \cup \{4\} = \{3,4\}$.

Step 6 : $LI = 4$.

Step 7 : $N_{sd}(4) = \{6\}$.

Step 5.1 : $a = M(N_{sd}(4)) = M(\{6\}) = 6$.

Step 5.2 : $b = 6$.

Step 5.3 : $SD_{st} = \{3,4\} \cup \{6\} = \{3,4,6\}$.

Step 8 : $LI = 6$.

Step 9 : $NI\ (6) = 8$.

Step 9.1 : $S_2 = nbd\ [8] = \{7,8,9,10\}$.

Step 9.2 : $S_3 = \{8,9,10\}$.

Step 9.3 : $S_4 = \{8,9,10\}$.

Step 9.4 : $c = 9$.

Step 9.5 : $D_{st} = D_{st} \cup \{9\} = \{3,6\} \cup \{9\} = \{3,6,9\}$.

Step 10 : $LI = 9$.

Step 11 : $N_{sd}(9)$ = null and NI (9) = null.

Step 12 : End.

Output : {3,4,6,9} is the split strong dominating set of an interval graph of given interval family.

$D_{st} = \{3,6,9\}$.

$SD_{st} = \{3,4,6,9\}$.

$|D_{st}| < |SD_{st}|$.

$\therefore \gamma_{st}(G) < \gamma_{sst}(G)$.

Theorem 4.2 : Let D_{st} be a strong dominating set of the given interval graph G corresponding to an interval family $I = \{I_1, I_2, ..., I_n\}$. If i and j are any two intervals in I such that j is contained in i and if there is no other interval $k \neq i$ that intersects j then the strong dominating set D_{st} is also a split strong dominating set of an interval graph G.

Proof : Let $I = \{I_1, I_2, ..., I_n\}$ be an interval family and G is an interval graph corresponding to I . Let i and j be any two intervals in I such that j is contained in i . If there is no interval $k \neq i$ that intersect j . Then clearly i lies in the strong dominating set D_{st} . Further in induced subgraph $< V - D_{st} >$ the vertex j is not adjacent to any other vertex and then j becomes as an solated vertex in induced sub graph $< V - D_{st} >$. There is a disconnection in $< V - D_{st} >$ .Hence the strong dominating set, which we considered is split strong dominating set.Hence we follows an algorithm to find strong dominating set and split strong dominating set of an interval graph with an illustration.

ILLUSTTRATION

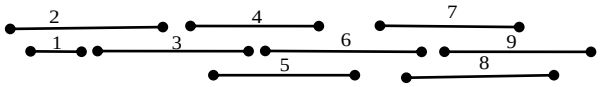

Figure 2.Interval Family

As follows an algorithm with illustration for neighbours as given interval family I.

We construct an interval graph G from an interval family I={1, 2,……,9}as follows

$nbd[1] = \{1,2\}$, $nbd[2] = \{1, 2, 3\}$, $nbd[3] = \{2,3,4,5\}$, $nbd[4] = \{3,4,5,6\}$, $nbd[5] = \{3,4,5,6\}$,

$nbd[6] = \{4,5,6,7,8\}$, $nbd[7] = \{6,7,8,9\}$, $nbd[8] = \{6,7,8,9\}$, $nbd[9] = \{7,8,9\}$

$N_{sd}(1) = \{2\}$, $N_{sd}(2) = \{3\}$, $N_{sd}(3) = null$, $N_{sd}(4) = \{6\}$, $N_{sd}(5) = \{6\}$, $N_{sd}(6) = null$,

$N_{sd}(7) = null$, $N_{sd}(8) = null$, $N_{sd}(9) = null$.

$NI(1) = 3$, $NI(2) = 4$, $NI(3) = 6$, $NI(4) = 7$, $NI(5) = 7$, $NI(6) = 9$, $NI(7) = null$,

$NI(8) = \text{null}, \quad NI(9) = \text{null}.$

Procedure for finding a strong dominating set(D_{st}) of an interval graph using an algorithm.

Input : Interval family $I = \{1, 2, ..., 9\}$.

Step 1 : $S_1 = nbd[1] = \{1, 2\}$.

Step 2 : $S = \{1, 2\}$.

Step 3 : $D_{st} = \{2\}$.

Step 4 : $LI = 2$.

Step 5 : $N_{sd}(2) = \{3\}$.

Step 5.1 : $a = M(N_{sd}(2)) = M(\{3\}) = 3$.

Step 5.2 : $b = 5$.

Step 5.3 : $D_{st} = \{2\} \cup \{5\} = \{2, 5\}$.

Step 6 : $LI = 5$.

Step 7 : $N_{sd}(5) = \{6\}$.

Step 7.1 : $a = M(N_{sd}(5)) = M(\{6\}) = 6$.

Step 7.2 : $b = 6$.

Step 7.3 : $D_{st} = \{2, 5\} \cup \{6\} = \{2, 5, 6\}$.

Step 8 : $LI = 6$.

Step 9 : $NI(6) = 9$.

Step 9.1 : $S_2 = nbd\ [9] = \{7, 8, 9\}$.

Step 9.2 : $S_3 = \{9\}$.

Step 9.3 : $S_4 = \{9\}$.

Step 9.4 : $c = 9$.

Step 9.5 : $D_{st} = D_{st} \cup \{9\} = \{2, 5, 6\} \cup \{9\} = \{2, 5, 6, 9\}$.

Step 10 : $LI = 9$.

Step 11: $N_{sd}(9)$ = null and NI (9) = null.

Step 12 : End.

Output : {2,5,6,9} is the strong dominating set of an interval graph of given interval family.

Procedure for finding a split strong dominating set(SD_{st}) of an interval graph using an algorithm.

Input : Interval family $I = \{1, 2, ..., 9\}$.

Step 1: $S_1 = nbd[1] = \{1, 2\}$.

Step 2 : $S = \{1, 2\}$.

Step 3 : $SD_{st} = \{2\}$.

Step 4 : Count = 1.

Step 5 : $LI = 2$.

Step 6 : $d^+(2) = 1$.

Step 6.1 : Count = 1 + 1 = 2.

Step 7 : $N_{sd}(2) = \{3\}$.

Step 7.1 : $a = M(N_{sd}(2)) = M(\{3\}) = 3$.

Step 7.2 : $b = 5$.

Step 7.3 : $D_{st} = \{2\} \cup \{5\} = \{2, 5\}$.

Step 8 : $LI = 5$.

Step 9 : $N_{sd}(5) = \{6\}$.

Step 9.1 : $a = M(N_{sd}(4)) = M(\{6\}) = 6$.

Step 9.2 : $b = 6$.

Step 9.3 : $SD_{st} = \{2,5\} \cup \{6\} = \{2,5,6\}$.

Step 10 : $LI = 6$.

Step 11 : $NI\ (6) = 9$.

Step 11.1 : $S_2 = nbd\ [9] = \{7,8,9\}$.

Step 11.2 : $S_3 = \{9\}$.

Step 11.3 : $S_4 = \{9\}$.

Step 11.4 : $c = 9$.

Step 11.5 : $D_{st} = D_{st} \cup \{9\} = \{2,5,6\} \cup \{9\} = \{2,5,6,9\}$.

Step 12 : $LI = 9$.

Step 13 : $N_{sd}(9)$ = null and NI (9) = null.

Step 14 : End.

Output : {2,5,6,9} is the split strong dominating set of an interval graph of given interval family.

$D_{st} = \{2,5,6,9\}$, $SD_{st} = \{2,5,6,9\}$.

$D_{st} = SD_{st}$.

Theorem 4.3 : Let $I = \{I_1, I_2, ..., I_n\}$ be an interval family and D_{st} is a strong dominating set of the given interval graph G. If i, j, k are any three consecutive intervals such that $i < j < k$ and if $j \in D_{st}$, and i intersects j, j intersect k and i does not intersect k then $D_{st} = SD_{st}$.

Proof : Suppose $I = \{I_1, I_2, ..., I_n\}$ be an interval family . If i, j, k be three consecutive intervals such that $i < j < k$ and i intersect j, j intersect k, but i does not intersect k. Suppose $j \in D_{st}$, where D_{st} is a strong dominating set. Then i and k are not adjacent in the induced subgraph $< V - D_{st} >$. There exists a a disconnection between i and k. That is, there is no $m \in I$, $m < k$ such that m intersects k. If possible suppose that such an m exists, then since $m < k$ we must have $m < i < j < k$ ($\because m < k$). Now m intersects k implies i and j also intersect. Then there is a path between i and k and are adjacent. This is a contradiction to hypothesis. So such a m does not exists. Hence we get disconnection. Hence D_{st} is also a split strong dominating set of the given interval graph G. As usual as follows an algorithm to find a strong dominating set and split strong dominating set of an interval graph G.

ILLUSTRATION

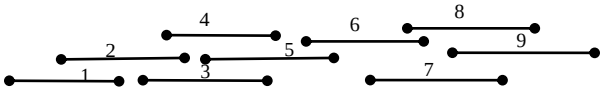

Figure 3.Interval Family I.

We construct an interval graph from an interval family I={1,2,3,4,5,6,7,8,9} as follows.

$nbd[1] = \{1,2\}$, $nbd[2] = \{1,2,3,4\}$, $nbd[3] = \{2,3,4,5\}$, $nbd[4] = \{2,3,4,5\}$, $nbd[5] = \{3,4,5,6\}$,

$nbd\ [6] = \{5,6,7,8\}$, $nbd\ [7] = \{6,7,8,9\}$, $nbd[8] = \{6,7,8,9\}$, $nbd[9] = \{7,8,9\}$.

$N_{sd}(1) = \{2\}$, $N_{sd}(2) = null$, $N_{sd}(3) = null$, $N_{sd}(4) = null$, $N_{sd}(5) = null$, $N_{sd}(6) = null$,

$N_{sd}(7) = null$, $N_{sd}(8) = null$, $N_{sd}(9) = null$.

$NI\ (1) = 3$, $NI\ (2) = 5$, $NI\ (3) = 6$, $NI\ (4) = 6$, $NI(5) = 7$, $NI\ (6) = 9$, $NI\ (7) = null$,

$NI\ (8) = null$, $NI\ (9) = null$.

Procedure for finding a strong dominating set(D_{st}) of an interval graph using an algorithm.

Input : Interval family $I = \{1, 2, ..., 9\}$.

Step 1 : $S_1 = nbd[1] = \{1,2\}$.

Step 2 : $S = \{1,2\}$.

Step 3 : $D_{st} = \{2\}$.

Step 4 : $LI = 2$.

Step 5 : $NI(2) = 5$.

Step 5.1 : $S_2 = nbd\ [5] = \{3,4,5,6\}$.

Step 5.2 : $S_3 = \{5,6\}$.

Step 5.3 : $S_4 = \{5,6\}$.

Step 5.4 : $c = 6$.

Step 5.5 : $D_{st} = D_{st} \cup \{6\} = \{2\} \cup \{6\} = \{2,6\}$.

Step 6 : $LI = 6$.

Step 7 : $NI(6) = 9$.

Step 7.1 : $S_2 = nbd\ [9] = \{7,8,9\}$.

Step 7.2 : $S_3 = \{9\}$.

Step 7.3 : $S_4 = \{9\}$.

Step 7.4 : $c = 9$.

Step 7.5 : $D_{st} = D_{st} \cup \{6\} = \{2,6\} \cup \{9\} = \{2,6,9\}$.

Step 8 : $LI = 9$.

Step 9: $N_{sd}(9)$ = null and NI (9) = null.

Step 12 : End.

Output : {2,6,9} is the strong dominating set of an interval graph of given interval family.

Procedure for finding a split strong dominating set(SD_{st}) of an interval graph using an algorithm.

Input : Interval family $I = \{1,2,.....,9\}$.

Step 1 : $S_1 = nbd[1] = \{1,2\}$.

Step 2 : $S = \{1,2\}$.

Step 3 : $SD_{st} = \{2\}$.

Step 4 : Count = 1.

Step 5 : $LI = 2$.

Step 6 : $d^+(2) = 1$.

Step 6.1 : Count = 1 + 1 = 2.

Step 7 : $N_{sd}(2) = \{3\}$.

Step 7.1 : $a = M(N_{sd}(2)) = M(\{3\}) = 3$.

Step 7.2 : $b = 5$.

Step 7.3 : $D_{st} = \{2\} \cup \{5\} = \{2,5\}$.

Step 8 : $LI = 5$.

Step 9 : $N_{sd}(5) = \{6\}$.

Step 9.1 : $a = M(N_{sd}(4)) = M(\{6\}) = 6$.

Step 9.2 : $b = 6$.

Step 9.3 : $SD_{st} = \{2,5\} \cup \{6\} = \{2,5,6\}$.

Step 10 : $LI = 6$.

Step 11 : $NI\ (6) = 9$.

Step 11.1 : $S_2 = nbd\ [9] = \{7,8,9\}$.

Step 11.2 : $S_3 = \{9\}$.

Step 11.3 : $S_4 = \{9\}$.

Step 11.4 : $c = 9$.

Step 11.5 : $D_{st} = D_{st} \cup \{9\} = \{2,5,6\} \cup \{9\} = \{2,5,6,9\}$.

Step 12 : $LI = 9$.

Step 13 : $N_{sd}(9)$ = null and , NI (9) = null.

Step 14 : End.

Output : {2,5,6,9} is the split strong dominating set of an interval graph of given interval family.

$D_{st} = \{2,5,6,9\}$

$SD_{st} = \{2,5,6,9\}$.

$\therefore D_{st} = SD_{st}$.

5. Conclusions

In this paper we introduced an algorithm for finding strong dominating set and split strong dominating set of an interval graph which is connected.

6. Acknowledgements

The authors are very grateful to the referees for many valuable suggestions and corrections which have helped to significantly improve the quality of the presentation of the paper.. This work was supported by S.V. University, Tirupati-517502, Andhra Pradesh, India.

References

[1] M.C. Golumbic, "Algorithmic graph theory and perfect graphs" ,Academic press ,1980.

[2] T. W. Haynes, S.T. Hedetniemi and P.J.Slater, Fundamentals of domination in graphs, Marcel Dekker, Inc., New York (1998).

[3] **T**. W. Haynes, S.T. Hedetniemi and P.J.Slater, Domination in Graphs: advanced topics , , Marcel Dekker, Inc., New York (1998).

[4] S.T. Hedetniemi and R.C. Laskar, 1990, 86, 257-277

[5] E. Sampathkumar, L.Pushpa Latha , 1996, 161, 235-242

[6] J.H. Hahingh, M.A.Henning, 1998, 26 ,73-92.

[7] D.Rautenbach, 2000, 215 , 201-212.

[8] Kulli.V. R. and Janakiram . B, 2000,Vol.19. No.2, pp. 145-156.

A Compact Printed Antenna For Wimax, Wlan & C Band Applications

Barun Mazumdar
Assistant Professor, ECE Department, AIEMD, West Bengal, India

Abstract:
A single feed compact microstrip antenna is proposed in this paper. One L slit & one H slit are introduced on the right edge of the patch to study the effect of the slit on radiation behaviour with respect to a conventional microstrip patch. An extensive analysis of the return loss, radiation pattern and efficiency of the proposed antenna is shown in this paper. For the optimize value of the slit parameters antenna resonant frequencies are obtained at 2.53, 4, 5.73 & 7.54 GHz with corresponding bandwidth 12.48 MHz, 37.97 MHz, 80.68 MHz , 230.67 MHz and return loss of about -17.4, -32.5, -12.4 & -29.7 dB respectively. The antenna size has been reduced by 75% when compared to a conventional microstrip patch. The characteristics of the designed structure are investigated by using MoM based electromagnetic solver, IE3D. The simple configuration and low profile nature of the proposed antenna leads to easy fabrication and make it suitable for the applications in Wireless communication system. Mainly it is developed to operate in the WiMAX & WLAN application.

Keywords: Compact, patch antenna, Quad band, slit.

1. Introduction:

Microstrip patch antennas [1] are popular in wireless communication, because they have some advantages due to their conformal and simple planar structure. They allow all the advantages of printed-circuit technology. There are varieties of patch structures available but the rectangular, circular and triangular shapes [2] are most frequently used. Design of WLAN antennas also got popularity with the advancement of microstrip antennas. Wireless local area network (WLAN) requires three bands of frequencies: 2.4GHz (2400-2484MHz), 5.2GHz (5150-5350MHz) and 5.8GHz (5725-5825MHz). WiMax [7] (Worldwide Interoperability for Microwave access) has three allocated frequency bands. The low band (2.5-2.69 GHz), the middle band (3.2-3.8 GHz) and the upper band (5.2-5.8 GHz).The size of the antenna are effectively reduced by cutting slot in proper position on the microstrip patch. It has a gain of 4.60 dBi at 4 GHz, 4.35 dBi at 5.73GHz & 3.49 dBi at 7.54 GHz presents a size reduction of about 75% when compared to a conventional microstrip patch. Due to the Small size, low cost and low weight this antenna is a good candidate for the application of wireless communication systems [4-6], mobile phones and laptops.

2. Antenna Design: The configuration of the proposed antenna is shown in the fig 1. The antenna is an 18mm x 14mm rectangular patch. The dielectric material selected for this design is an FR4 epoxy with dielectric constant (ε_r) =4.4 and substrate height (h) =1.6 mm.

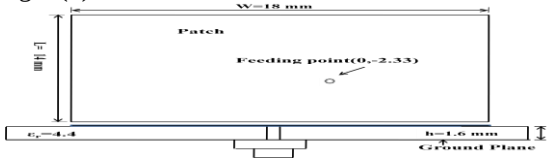

Fig 1. Antenna 1 configuration.

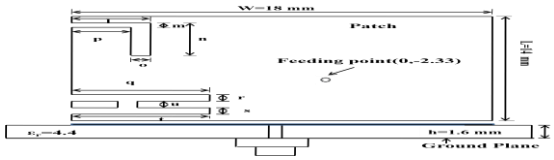

Fig 2. Antenna 2 configuration.

The optimal parameter values of the L slits & H slits are listed in Table:

Table:

Parameters	l	m	n	o	p	q	r	s	t	u
Values (mm)	4.45	.45	9.85	1.2	3.25	7.5	1	.8	7.5	1

3. Simulated Results & Discussion: Simulated (using IE3D [9]) results of return loss of the Conventional & proposed antenna are shown in Figure 3 & 4. In Conventional antenna only one frequency is obtained below -10 dB which is 4.73 GHz & return loss is found about -20.43 dB with 103.09 MHz bandwidth. For the proposed antenna resonant frequencies are 2.53 GHz, 4GHz, 5.73 GHz, 7.54 GHz and their corresponding return losses are -17.4 dB, -32.5 dB, -12.4 & -29.7 dB respectively. Simulated 10 dB bandwidths are 12.48 MHz, 37.97 MHz 80.68 & 230.67 MHz respectively.

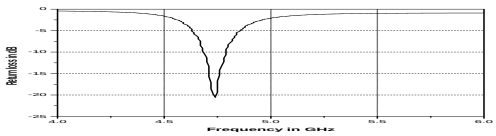

Fig 3. Return loss of the Conventional antenna

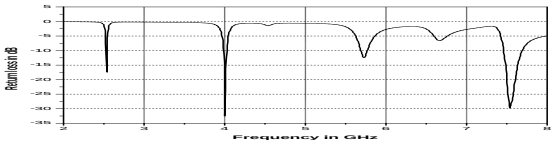

Fig 4. Return loss of the proposed antenna

Simulated radiation pattern

The simulated E –H plane radiation patterns for antenna 2 are shown in Figure 5-12**.**

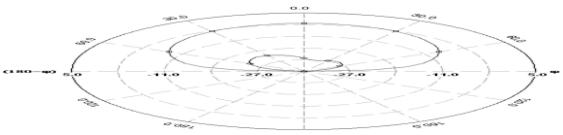

Fig 5. E plane Radiation Pattern of the antenna for 2.51 GHz

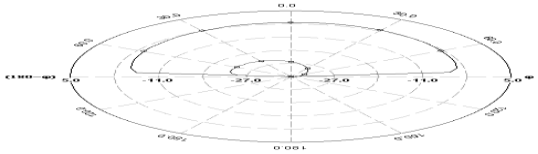

Fig 6. H plane Radiation Pattern of the antenna for 2.51 GHz

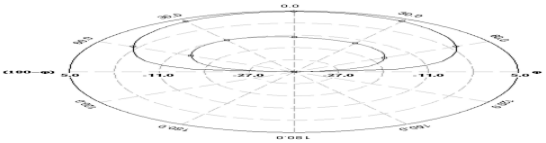

Fig 7. E plane Radiation Pattern of the antenna for 4 GHz

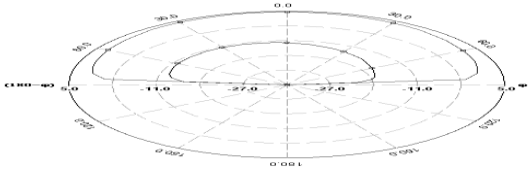

Fig 8. H plane Radiation Pattern of the antenna for 4 GHz

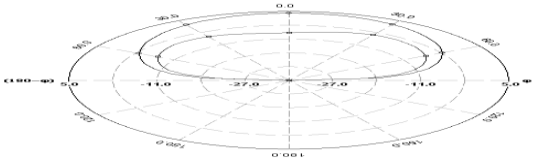

Fig 9. E plane Radiation Pattern of the antenna for 5.73 GHz

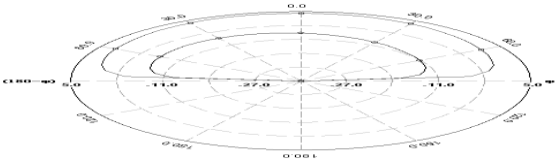

Fig 10. H plane Radiation Pattern of the antenna for 5.73 GHz

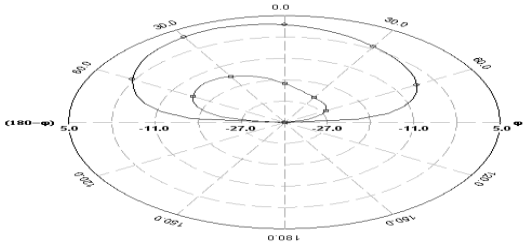

Fig 11. E plane Radiation Pattern of the antenna for 7.54 GHz

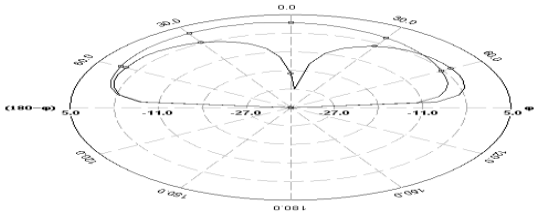

Fig 12. H plane Radiation Pattern of the antenna for 7.54 GHz

Figure 13 shows the Gain versus frequency plot for the antenna 2.It is observed that gain is about 4.6 dBi for 4GHz, 4.35 dBi for 5.73 GHz & 3.49 dBi for 7.54 GHz.

Efficiency of the antenna 2 with the variation of frequency is shown in figure 14. It is found that antenna efficiency is about 67.52 % for 4 GHz, 61.94 % for 5.73 GHz & 46.06 % for 7.54 GHz

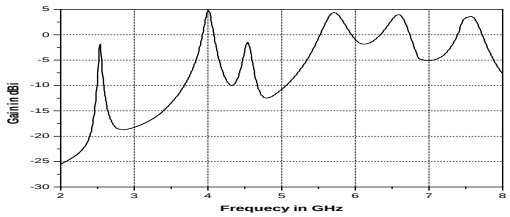

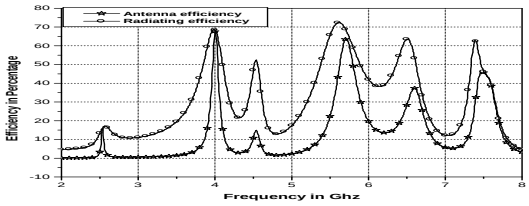

Fig 13. Gain versus frequency plot for the proposed antenna.

Fig14. Antenna efficiency versus frequency plot for the proposed antenna.

4. Experimental results: Comparisons between the measured return losses with the simulated ones are shown in Fig. 15 & Fig.16. All the measurements are carried out using Vector Network Analyzer (VNA) Agilent N5 230A.The agreement between the simulated and measured data is reasonably good. The discrepancy between the measured and simulated results is due to the effect of improper soldering of SMA connector or fabrication tolerance.

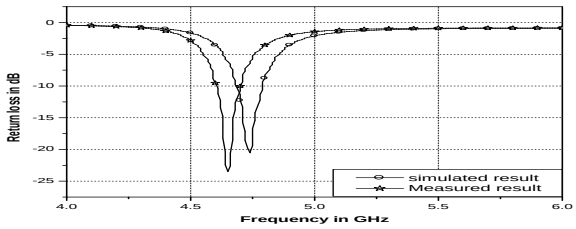

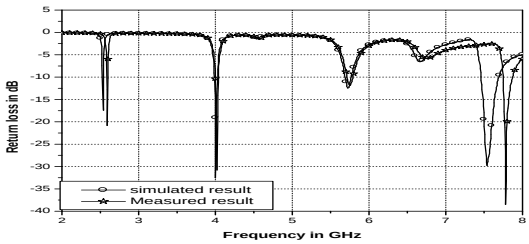

Fig 15. Comparison between measured and simulated conventional antenna.

Fig 16. Comparison between measured and return losses for simulated return losses for proposed antenna.

5. Conclusions: A single feed single layer microstrip antenna has been proposed in this paper. It is shown that the proposed antenna can operate in four frequency bands. The slits reduced the size of the antenna by 75 % and increase the bandwidth up to 230.67 MHz with a return loss of -29.7 dB, absolute gain about 3.49 dBi. Efficiency of antenna has been achieved 67.52 %. An optimization between size reduction and bandwidth enhancement is maintained in this work.

6. References:

1. R. L. Li, B. Pan, T. Wu, J. Laskar, and M. M.Tentzeris "A Triple-Band Low-Profile Planar Antenna for Wireless Applications" December15, 2008, IEEE Xplore.R. K. Gupta "Printed TRI-BAND Monopole Antenna Structures For Wireless Applications" Issue 2, Vol I, Apr 2010.
2. S. Bhunia, M.-K. Pain, S. Biswas, D. Sarkar, P. P. Sarkar, and B. Gupta, "Investigations on Microstrip Patch Antennas with Different slots and Feeding Points" , *Microwave and Optical Technology Letters*, VOL 50, NO. 11, November 2008 pp 2754-2758.
3. F. Yang, X. -X. Zhang, X. Ye, and Y. Rahmat-Samii, " Wide-Band Eshaped Patch Antennas for Wireless Communications," *IEEE Trans. Antennas Propagat.*, vol. 49, no. 7, pp. 1094-1100, July. 2001.
4. D. N. Elsheakh, H. A. Elsadek, and E. A. Abdallah "Reconfigurable Single and MultiBand Inset Feed Microstrip Patch Antenna For Wireless Communication Devices" Progress In Electromagnetics Research C, Vol. 12, 191{201, 2010}.
5. B.Mazumdar, U.Chakraborty, S. K. Chowdhury, and A. K. Bhattacharjee, "A Compact Microstrip patch Antenna for Wireless Communication," Global Journal Of Researches in Engineering (F) Volume XII Issue V Version I April, 2012.
6. B. Mazumdar, A.Kumar "A compact dual band printed antenna for WiMAX & HIPERLAN applications", IJECCE journal, Vol-3, Issue-3, June 2012.
7. C.A.Balanis, "Advanced Engineering Electromagnetics", John Wiley & Sons., New York, 1989.

   Zeland Software Inc. IE3D: MoM-Based EM Simulator.Web: http://www.zeland.com

Declined Tank Irrigated Area Due ToInactive Water User's Association

B.Anuradha[1], V.Mohan[2], S.Madura[3], T.Ranjitha[4] and C.Babila Agansiya[5]
[1, 2, 3, 4,5]Department of Civil Engineering, Madha Engineering College, Chennai-69, India

Abstract
The rainfed tank sector has traditionally been an important mainstay of Tamilnadu rural economy. In the years following independence, the performance of the sector declined for a number of economic and institutional reasons one among the predominant is inactive Water user's Association (WUA) in villages. WUA is a group of water users, such as irrigation, who pool their financial, technical, material and human resources for the operation and maintenance of a water system. Due to absence of WUA agricultural productivity is drastically reduced in terms of decreased cropping season and change in cropping pattern. Water scarcity from the sources (tank) due to irregular usage is the main reason for less crop production. Hence two tanks namely, Kolathur and Vellarai of Kancheepuram district, Sriperambathur taluk in Tamilnadu were selected for this study to probe the impact of inactive WUA on total land holding and cultivated land in command area by the respondents. Primary data were collected through interview schedule and was analysed using Statistical Package for Social Science. Expected result will give the regression equation for farm size, income and expenditure.

Keywords : Irrigation, tank, water user's association, agriculture, crop production, SPSS

Introduction
There was a large variety of community managed irrigation system in ancient India. Tank irrigations one of the oldest sources of irrigation and is particularly important in South India, where it accounts for about one-third of the rice irrigated area. Now it is necessary to take up a programme of revising local water management groups and water rights, the law should recognize those existing water user group as in effects having control and consider irrigation management as a socio-technical system. (Murthy 1997). Tank systems, developed ingeniously and maintained over the centuries, have provided insulation from recurring droughts, floods due to vagaries of the monsoon and offered the much-needed livelihood security to the poor living in fragile semi-arid regions (Sakthivadivel and Gomathinayagam 2004b). Almost all monsoon countries in the semi-arid tropics have small water bodies like tanks (Vaidyanathan 2001; Sengupta 1985). Problems involved in the formation of WUA are lack of cooperation among the farmers, crop diversification in the field and identifying and promoting leadership can prove to be a major crisis in the formation of WUA's. But if devoted leaders are identified properly with the help of some socio-metric analysis, further work goes ahead smoothly. Reorientation training will be necessary for active participation of WUA in water management. Improving the tank management will enhance tank supplies which in turn will reduce the demand for more number of wells in the tank command area and hence efforts should be made to improve the system efficiencies through tank modernisation strategies involving the water users organisations / associations (Palanisami et al 2008). Multiple uses of tanks make village community including landless to become members of the water users group (Sakthivadivel 2000). According to Makombe et al (2007) high, average and marginal productivities of land under irrigation suggest that expanding irrigation development with WUA, as articulated by Government ambitious plans, may be a viable development strategy.

Sakthivadivel (2005) studied the estimation of water and land productivities in tank commands and its temporal and spatial values. His study has indicated that water productivity was low when tank water alone is used for irrigating crops in the command area especially in the absence of WUA parcitipation. Sustainable institution for management of the tank and ground water systems are the prerequisites to enhance tank water productivity. Palanisami and Flinn (1989) estimated the direct and indirect impacts of varying irrigation water supplies on rice yields for a set of tank irrigation systems in south India through a simultaneous equation model. The model captured the direct effect of varying water supplies on rice yield through the influence of moisture stress on crop growth and indirect effects through its influence on farmer's use of complementary input such as fertiliser and crop management.

Methodology
From the fig 1 it is clear that two villages which do not possess Water user's Association were selected as study areas. They are stratified in to three categories such as reach, source and size of land holding by the farmers. In case of reach, lands located closer to the tank is considered as head reach and farther away is taken as tail reach and the remaining portion is middle reach. Also famers using only well and only tank water for irrigating their fields are classified under source. With respect to size of land holding, farmers owning land less than 1 ha are marginal farmers, from 1 to 2 ha are small farmers and

above 2 ha are big farmers. With the matrix of above stratification, thirty respondents of each village were selected and interview schedule was used to collect primary data.

Fig 1 Frame work for methodology adopted

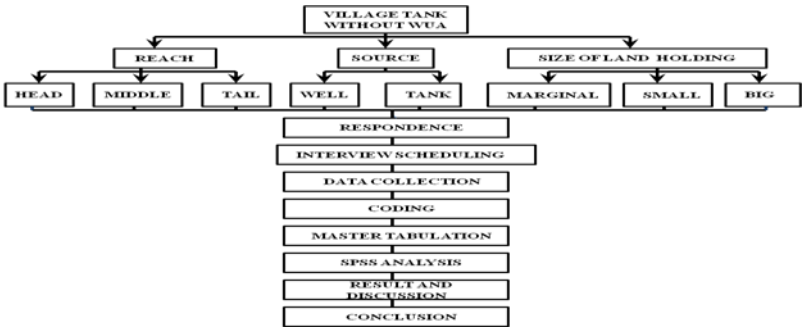

The gathered information was coded, master tabulated and analysed using Statistical Package for Social Science. The results are given in the form of regression equation interms of farm size, income and expenditure.

STUDY AREA

Kolathur village is located at latitude of 12^{o} 9' N and at longitude of 79^{o} 9' E. The total village area is 422.66hectares and consists of 451 households. The total irrigated land is 376.27hectares and rain fed land is 68.41hectares. The only source of irrigation for this village is tank (Kolathur big tank). The irrigation schemes are not available in this village, i.e., no Water users association (WUA) exists. There are four sluices present in the tank. Depth of water stored in the tank is about 3.55 meters.

Vellarai village

is located at latitude of 12^{o} 9' N and at longitude of 80^{o} 0'E with a total area of 191.16hectares. This village has only tank irrigation system (Vellarai tank) and the length of the tank is 1760 meters. Water users association was formed earlier and was not successfully functioned later due to various conflicts raised among the members. Total irrigated area is 94.42hectares and rain fed land is 14.27hectares. The soil type found here is clay. There are only three sluices present in the village tank.

A total income and expenditure detail for one acre of paddy cultivation is clearly shown in Table1. From nursery to harvest, crop grown period is 120 days. Different varieties of paddy cultivated in Tamilnadu are Ponni, Super ponni, ADT-43, ADT-45, Bapatlal etc. In study villages, Ponni is cultivated widely. The final produce is 25 bags/acre at the cost of Rs.850/bag (each bag weighs 75kg). Hence the total gross income from one acre of paddy cultivation is Rs.21,250. On the other hand the expenses constitutes various activities like nursery, ploughing, sapling, fertilizer and pesticide application, weeding, harvesting, transportation, marketing etc. Approximately 20 kg of seeds are required for one acre of paddy cultivation at the cost of Rs.25/kg. Two persons are in need of nursery work at Rs 300/person.

For transplantation 10 labours are necessary at Rs 200/person as wage rate. DAP, urea, potash and gypsum are applied as fertilizer and Prudon is sprayed three times as insecticide. Removal of weed needs 9 workers at Rs 100/person. Machine harvest is carried out at the cost of Rs 1500/acre for 2.30 hours. While marketing, 25 bags of paddy will be transported from field to market at the cost of Rs 300/acre. Mediator cost is approximately 2% of gross income. Hence the total expenditure is Rs 13,440/-. Net profit is arrived by deducting total expenses from gross income.

Table 1 Total income and Expenditure details for one acre of paddy cultivation in study villages

S.No	Descriptions	Particulars
1	Total Cultivated land in acre	1
2	Crop	Paddy
3	Variety	Ponni
4	Period in days	120
5	No. of bags/acre	25
6	Rate per bag (Rs.)	850
9	Cost of total bags (Rs.)	21250
11	**Gross Amount (Rs.)**	**21,250**
12	Required seed quantity in kg for 1 acre	20
13	Rate of Seed(Rs./Kg.)	25
14	Cost of Seed (Rs.) for 1 acre	500
15	Amount spent on nursery (Rs.) for 1 acre	600
16	Ploughing charges/acre in Rs	2,500

Analysis and Interpretation

In statistics, regression analysis includes any techniques for modeling and analyzing several variables, when the focus is on the relationship between a dependent variable and one or more independent variables. More specifically, regression analysis helps to understand how the typical value of the dependent variable changes when any one of the independent variables is varied, while the other independent variables are held fixed. In all cases, the estimation target is a function of the independent variables called the regression function.

Regression Analysis for Total Land Holding by the Respondents

1. Dependent Variable : Farming Expenditure (Y)
2. Independent Variable : Income in Rs (X1) and Size of land in acres (X2)
3. Multiple R Value : 0.841
4. R Square Value : 0.707
5. Adjusted R Square Value : 0.695
6. F Value : 61.517
7. P Value : 0.000**

*Note: ** refers it is more significant at 1 % level***.**

Here the dependent variable is farming expenditure and independent variables are income in rupees and size of land in acres. Multiple R values show the correlation coefficient between actual value of Y and the predicted value of Y. Since R^2=0.841 which is greater than 0.5, it is highly correlated. R^2 value is the coefficient of determination. Here 70.7% information about farming expenditure is extracted from income and size of land holding. Adjusted R^2 value is 0.695 and R^2 value is 0.707, which means sample number is higher than Y. Since P-value is less than 0.01, R^2 is highly correlated at 1% level in case of total land holding by the respondents.

Table 2 Regression Analysis for Total Land Holding by the Respondents

Model	Unstandardised Coefficients		Standardised Coefficients	t- Value	p-Value
	B	Std.Error	Beta		
Constant	2.971	0.410	-	7.246	0.000
Net income (X1)	0.400	0.185	0.318	2.164	0.035
Total land holding (X2)	0.292	0.078	0.552	3.752	0.000

Regression Equation for Total Land Holding by the Respondents

Y = 2.971 + 0.400 X1 + 0.292 X2

It is proved from the Table 2, if income is increased by Rs.1000, then the expenditure is increased by Rs.318 and if 1 acre of land is cultivated by the respondents, then expected increase in expenditure is Rs.552.

Regression Analysis for Total Cultivated Land by the Respondents:

1. Dependent Variable : Farming Expenditure (Y)
2. Independent Variable : Income (X1) in Rs and Size of Land in acres (X2)
3. Multiple R Value : 0.860
4. R Square Value : 0.739
5. Adjusted R Square Value : 0.729
6. F-Value : 72.350
7. P-Value : 0.000**

*Note: ** refers it is more significant at 1 % level***.**

Here the dependent variable is farming expenditure and independent variables are income in rupees and size of land in acres. Multiple R values shows the correlation coefficient between actual value of Y and the predicted value of Y. Since R^2=0.860 which is greater than 0.5, it is highly correlated. R^2 value is the coefficient of determination. Here 73.9% information about farming expenditure is extracted from income and size of land holding. Adjusted R^2 value is 0.729 and R^2 value is 0.739, which means sample number is higher than Y. Since P-value is less than 0.01, R^2 is highly correlated at 1% level in case of total cultivated land by the respondents.

Table 3 Regression Analysis for Total Cultivated Land by the Respondents

Model	Un-standardized Coefficients		Standardized Coefficients	t- Value	p -Value
	B	Std.Error	Beta		
Constant	3.354	0.412	-	8.314	0.000
Net income (X1)	0.011	0.227	0.900	0.500	0.096
Total cultivable land (X2)	0.358	0.076	0.851	4.709	0.000

Regression Equation (For Total Cultivated Land):

$Y = 3.354 + 0.011 X1 + 0.358 X2$

It is proved from the Table 3, if income is increased by Rs.1000, then the expenditure is increased by Rs.900 and if 1 acre of land is cultivated by the respondents, then expected increase in expenditure is Rs.851.

Discussion And Conclusion

The functioning of Water User's Association is never an easy job since those are formed by the farmers and are expected to run practically on their own contributions both in terms of finance and manpower. If it is not performing properly, the available water in the storage structure will not be efficiently utilized by the farmers for irrigating their land. Unplanned distribution of water leads to wastage of water and the end result will be the declining tank irrigated area. For example if the farmer owns 5ha of land, he could not cultivate the whole area, rather he will cultivate only 2ha by leaving the remaining land fallow. Most of the time he will go in for only one paddy cultivation season among three seasons. Expenditure interms of agriculture labour, machine harvesting, fertilizer and pesticide cost, transportation of manure to the field and produce to the market, mediator charge will be less when large area is cultivated by a single owner. Incase of agricultural labour, wage rate is less for larger area compared to less cultivated area. Because if land extent is high, labours will adjust their job timing and complete the work with nominal rate since they can get more number of days with a single owner. Otherwise their demand will be high inorder to compensate the income until they get next opportunity. Carrying fertilizer to land, final produce to market, collection of straw from field after harvest etc is done with the help of bullock cart or small truck. For large area, transportation is easy which leads to nominal charge/acre. But for smaller area it is very difficult to reach the field. Drivers are demanding huge amount from the land owners which will reduce their net income. Mediator for marketing the produce is felt necessary by farmers for getting good rate/bag. Mediators charge is high incase of less produce. If they get produce in mass, their work will become effortless to earn more money in a short period. Therefore it is very clear that cultivating larger extent of land by farmers will reduce the expenditure and increase the net income. Efficient use of available water in storage structure by Water User's Association helps farmers to plan for cultivating the entire area they possess. So it is necessary to form a new WUA in the villages where it does'nt exist so far. Also WUA should be revived in a place where it is not functioning well.

Reference

1. Makombe G., Kelemework D. and Aredo D. (2007), 'A comparative analysis of rainfed and irrigated agricultural production in Ethiopia', Irrigation and Drainage System, Vol. 21, pp. 35-44.
2. Narasihma Murthy (1997), "Water User's Association – Formation and function", National seminar on Farmers participation in Tank Rehabilitation and Management, IMTI.
3. Palanisami K. and Flinn. J.C. (1989), 'Impact of varying water supply on input use and yield of tank – Irrigated Rice', Agricultural Water Management, Vol. 15, pp. 347-359.
4. Palanisami K., Gemma M. and Ranganathan C.R. (2008), 'Stabilisation value around water in Tank Irrigation systems', Indian Journal of Agricultural Economics, Vol. 63, No.1, Jan – March.
5. Sakthivadivel (2005), 'Tank water productivity in Palar basin', Report of the Fourth IWMI Tata Annual Partner's Meet, February.
6. Sakthivadivel R. (2000), 'Two decades of tank rehabilitation in India: Investment, Institutional and policy issues IWMI', Tata Water Policy Research Program, and Annual Partners Meet 2000.
7. Sakthivadivel R. and Gomathinayagam P. (2004a), 'Institutional analysis of best performing locally managed tanks in India', Third IWMI-Tata Annual Partners Meet, Anand, February 2004.
8. Sengupta N. (1985), 'Irrigation: Traditional vs moderns', Economic and Political Weekly, Vol. 20, pp. 1919-1938.
9. Vaidyanathan A. (Ed.) (2001), 'Tanks of South India', Center for Science and Environment, New Delhi.

Performance of Steel Fiber Reinforced Self Compacting Concrete

Dr. Mrs. S.A. Bhalchandra
Associate Professor, Department of Applied Mechanics
Govt. College of Engineering, Aurangabad (M.S.) India
Pawase Amit Bajirao
Post Graduate Student
Govt. College of Engineering, Aurangabad (M.S.) India

Abstract:
Construction of durable concrete structures requires skilled labor for placing and compacting concrete. Self Compacting Concrete achieves this by its unique fresh state properties. In the plastic state, it flows under its own weight and homogeneity while completely filling any formwork and passing around congested reinforcement. In the hardened state, it equals or excels standard concrete with respect to strength and durability.

This work is aimed to study the performance of steel fiber reinforced self compacting concrete as plain self compacting concrete is studied in depth but the fiber reinforced self compacting concrete is not studied to that extent.

Key words: Self compacting concrete, fibers, compressive strength, flexure strength.

I Introduction

Though concrete possess high compressive strength, stiffness, low thermal and electrical conductivity, low combustibility and toxicity but two characteristics limited its use are, it is brittle and weak in tension. However the developments of Fiber Reinforced Composites (FRC) have provided a technical basis for improving these deficiencies. Fibers are small pieces of reinforcing materials added to a concrete mix which normally contains cement, water, fine and course aggregate.[1] Among the most common fibers used is steel, glass, asbestos, polypropylene etc. When the loads imposed on the concrete approach that for failure, crack will propagate, sometimes rapidly, fibers in concrete provides a means of arresting the crack growth. If the modulus of elasticity of fiber is high with respect to the modulus of elasticity of concrete or mortar binder the fiber helps to carry the load, thereby increasing the tensile strength of the material. Fibers increase the toughness, the flexural strength, and reduce the creep strain and shrinkage of concrete. [2] Several European countries recognized the significance and potentials of SCC developed in Japan. During 1989, they founded European federation of natural trade associations representing producers and applicators of specialist building products (EFNARC). The utilization of SCC started growing rapidly. EFNARC, making use of board practical experiences of all members of European federation with SCC, has drawn up specification and guide lines to provide a framework for design and use of high quality SCC, during 2002[3].

Self Compacting Concrete has been desired as “The Most Revolutionary Development in Concrete Construction for Several Decades”.

Ii Objective

The objective of this study is to optimize the Steel Fiber Reinforced Self Compacting Concrete (SFRSCC) in the fresh and in hardened state. But the literature indicates that some studies are available on plain SCC but sufficient literature is not available on SFRSCC with different mineral admixtures. Hence an attempt is made in this work to study the mechanical properties of both plain SCC and SFRSCC.

Iii Materials Used

For the present study ordinary Portland cement of 53 Grade, Natural sand from river Godavari (Paithan) confirming IS 383-1970 along with potable water and natural aggregates were used for preparation of concrete.

The super plasticizer used for the present study was supplied by the manufacturer Sika India Pvt. Ltd., Mumbai complies IS: 9103- 1999 (Amended 2003).

The viscosity modifying agent (VMA)was also supplied by the manufacturer Sika India Pvt. Ltd.

Dramix steel fibers conforming to ASTM A820 type-I are used for experimental work. Dramix RC - 80/60 - BN are high tensile steel cold drawn wire with hooked ends, glued in bundles & specially engineered for use in concrete. Fibers are made available from Shakti Commodities Pvt. Ltd., New Delhi.

Fly Ash (FLA) which is available in dry powder form and is procured from Dirk India Pvt. Ltd., Nashik. It is available in 30Kg bags, color of which is light gray under the product name "**Pozzocrete 60**" was used for the present study.

Iv Methodology

After performing all required tests on the ingredients of concrete such as cement, sand, coarse aggregates etc. mix design for SCC was done.

Mix Design For Scc:-

Rational method is used for mix design of M-30 grade of concrete. The optimum percentage of fly ash to give maximum compressive strength was achieved by making trial mixes with fly ash at a constant interval of 3% by weight of cement. The trial mixes were made for fly ash from 12% to 36%. The compressive strength went on increasing up to 33% at it decreased at 36%. The maximum compressive strength was achieved at 33%. Hence, fly ash at 33% by weight of cement was added to concrete in this experiment. A

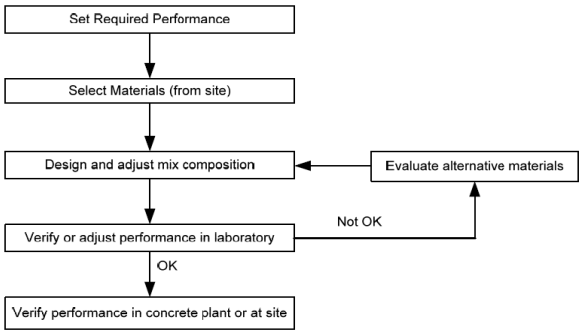

Flow-chart describing the procedure for design of SCC mix is shown in figure No.1

Figure 1: SCC Mix Design Procedure (EFNARC, 2005) [3].

At the end after performing the entire test following mix proportion was used for the present study.

The quantity of ingredient materials and mix proportions as per EFNARC guide lines is shown in the Table No.1.

Table1 Quantity of Materials per Cubic Meter of Concrete

Material	Proportion by Weight	Weight in Kg/m^3
Cement	1	450.00
F.A.	2.18	983.63
Fly ash	0.33	148.50
C.A. (<12 mm)	1.78	803.00
W/C	0.40	180.00

After finalizing the proportion of ingredients following mix proportions with different designations according to Steel Fiber content were used. The details are shown in Table No.2

Table No.2 Mix Designations Used

Sr.no.	Mix designation	FLA (%)	Steel Fiber content (%)	W/C ratio
01.	M0	33.0	0.0	0.40
02.	M1	33.0	0.5	0.40
03.	M2	33.0	1.0	0.40
04.	M3	33.0	1.25	0.40
05.	M4	33.0	1.5	0.40
06.	M5	33.0	1.75	0.40
07.	M6	33.0	2.0	0.40
08.	M7	33.0	2.25	0.40
09.	M8	33.0	2.5	0.40
10.	M9	33.0	2.75	0.40
11.	M10	33.0	3.0	0.40

TEST SPECIMENS USED FOR THE STUDY:-

The specimens used were cubes, beam specimens. Dimensions of each test specimen are as under:
Cube: 100 mm x 100 mm x 100 mm
Beam: 100 mm x 100 mm x 500 mm
Above specimens were used to determine the compressive strength test and flexural strength test respectively.

V Test Results and Discussion.

Compressive Strength Test on Cube

A cube compression test was performed on standard cubes of plain and SFRSCC of size 100 x 100 x 100 mm after 7 days and 28 days of immersion in water for curing. Results are shown in Table No.3 and graphical presentation between compressive strength and percentage fiber volume fraction is shown in graph No.1.(Appendix I)

Table N0.3 Compressive Strength of Normal SCC and SFRSCC, MPa

Sr. No.	Fiber Content (%)	Compressive Strength (f_{cu}) MPa		% Variation in Compressive Strength Over Control Concrete	
		7 Days	28 Days	7 Days	28 Days
01.	0	35.55	45.63	00.00	00.00
02.	0.5	35.75	48.41	0.619	6.092
03.	1.0	36.92	50.33	3.854	10.256
04.	1.25	37.03	52.14	4.163	14.267
05.	1.5	37.85	54.95	6.469	20.425
06.	1.75	38.92	57.38	9.479	25.751
07.	2.0	39.49	61.75	11.083	35.328
08.	2.25	39.68	63.82	11.617	39.864
09.	2.5	40.84	65.89	14.880	44.401
10.	2.75	41.97	68.97	18.059	51.151
11.	3.0	43.14	70.04	21.350	53.496

Flexural Strength Test on Beam:

Flexural strength is obtained for various fiber volume fractions and results are presented in Table No. 4 and the variation of flexural strength with respect to fiber volume fraction is shown in Graph
No.2 (Appendix I)

Table No.4 Variation of Flexural Strength Normal SCC and SFRSCC, MPa

Sr. No.	% of Steel Fiber	Flexural Strength in N/mm^2		% variation in Flexural Strength Over Control Concrete	
		7 days	28 days	7 days	28 days
01	0	4.31	5.29	0.000	0.000
02	0.5	4.46	5.55	3.48	4.91
03	1.0	4.63	5.86	7.42	10.77
04	1.25	4.74	5.94	9.97	12.28
05	1.5	5.02	6.13	16.47	15.87
06	1.75	5.41	6.32	25.52	19.47
07	2.0	5.45	6.44	26.45	21.73
08	2.25	5.60	6.48	29.93	22.49
09	2.5	5.74	6.68	33.17	26.27
10	2.75	6.02	6.97	39.67	31.76
11	3.0	6.11	7.14	41.76	34.97

Discussion on Test Results:

Results of compressive strength are shown in Table 3. It indicates the optimum volume fraction of fibers which gives maximum strength at 28 days is 3.0%. The percentage increase in strength at this volume fraction of fibers over normal SCC at 7 and 28 days is 21.35% and 53.49% respectively. Cracks occur in microstructure of concrete and fibers reduce the crack formation and propagation. Also fly ash improves the microstructure of concrete. Here, this might be the reason for the enhancement of compressive strength.

From above Table 4, it is observed that the flexural strength increases with increase in fiber content up to 3.0%. The maximum values at 7 and 28 days are 6.11 and 7.14 respectively. Thus, there is enhancement in flexural strength of concrete from 3.48% to 41.76% at 7 days and from 4.91% to 34.97% at 28 days.

Vi Conculsions

Following conclusion are drawn based on the result discussed above

1. In general, the significant improvement in various strengths is observed with the inclusion of Hooked end steel fibres in the plain concrete. However, maximum gain in strength of concrete is found to depend upon the amount of fibre content. The optimum fibre content to impart maximum gain in various strengths varies with type of the strengths.
2. In general the compressive strength and the flexural strength increase with increase in the percentage of fibre content.
3. In addition to the compressive strength and the flexural strength on the concrete split tension test was also performed on the SFRSCC the results of which are not mentioned in the paper (because the scope is limited to compressive and flexural strength of the SFRSCC) and it was found that the split tensile strength went on increasing with the addition of fibers. The optimum fiber content for increase in split tensile strength is 1.75% and percentage increase is 24.49% of SFRSCC over normal SCC.
4. The increase in compressive strength is 25.75% and increase in flexural strength is 19.47% of SFRSCC over normal SCC for the fibre content of 1.75%.
5. Satisfactory workability was maintained with increasing volume fraction of fibers by using super plasticizer.
6. With increasing fiber content, mode of failure was changed from brittle to ductile failure when subjected to compression and bending.

References

1. Hajime Okamura and Masahiro Ouchi, "Self Compacting Concrete", Journal of Advanced Concrete Technology Vol. 1, No. 1, April 2003, pp. 5-15.
2. Khayat K. H., "Workability, Testing and Performance of Self Consolidating Concrete", ACI Materials Journal, Vol. 96, No. 3, May-June 1999, pp.346-354.
3. EFNARC, "The European Guidelines for Self Compacting Concrete Specification, Production and Use", May 2005.
4. Jacek K.," Steel Fiber and Steel Fiber Reinforced Concrete in Civil Engineering", The Pacific Journal of Science And Technology, Vol. 7, No. 1, May2006, pp.53-58.
5. Chuan Mein Wong, "Use of Short Fibres in Structural Concrete to Enhance Mechanical Properties", University of Southern Queensland, November 2004.
6. Vítor M.C.F. Cunha, Joaquim A.O. Barros, José M. Sena-Cruz, "Pullout Behaviour of Hooked End Steel Fibres in Self Compacting Concrete", University of Minho, Portugal, April 2007.
7. Joaquim A.O.B., Lucio A.P., Varma R.K. and Delfina M.F., "Cost Competitive Steel Fiber Reinforced SCC for Structural Applications", The Indian Concrete Journal published by ACC limited, Vol.83, No.8, August 2009, pp.15-26.
8. Jain M.K., Govilkar S.D. and Bhandare U., "High-early Strength SCC for Flyover Project in Mumbai", The Indian Concrete Journal published by ACC limited, Vol.83, No.8, August 2009, pp.33-37.
9. Rame G. M., Narasimhan M.C., Karisddappa and Rajeeva S. V., "Study of the Properties of SCC with Quarry Dust", The Indian Concrete Journal published by ACC limited, Vol.83, No.8, August 2009, pp.54-60.
10. Lakshmipathy M., Satyanarayanan K.S., Jayasree G. and Mageshwaran V., "Reinforced Cement Concrete Pipes Made with SCC Technology", The Indian Concrete Journal, August 2009, pp.38-44.
11. Subramania B. V., Ramasamy J.V., Ragupathy R. and Seenivasan, "Workability and Strength Study of High Volume Fly Ash Self Compacting Concrete" The Indian Concrete Journal published by ACC limited, March 2009, pp. 17-22.
12. Mattur C. Narasimhan, Gopinatha Nayak, Shridhar K.C., "Strength and Durability of High-Volume Fly-ash Self-compacting Concrete", ICI Journal, January-March 2009, pp. 7-16.
13. Liberato Ferrara, Yon-Dong Park, Surendra P. Shah, "A Method for Mix-Design of Fiber-Reinforced Self Compacting Concrete", Cement and Concrete Research, Vol. 37, March 2007, pp.957-971.
14. Pai B.V.B., "How Economic is Self-Compacting Concrete", The Indian Concrete Journal published by ACC limited, June2004, pp.58-59.
15. Buquan Miao, Jenn-Chuan Chern and Chen-An Yang "Influences of Fiber Content on Properties of Self-Compacting Steel Fiber Reinforced Concrete", Journal of the Chinese Institute of Engineers, Vol. 26, No. 4, 2003, pp. 523-530.
16. Eduardo N.B., Pereira, Joaquim A.O., Barros and Aires Cameos, "Steel Fibre Reinforced Self Compacting Concrete; Experimental Research and Numerical Simulation, Journal of Structural Engineering", ASCE, Auguest-2008, pp.1310-1315.

17. Cumba, J.A. Barros, Sena, Cruz J., V.M.C.F., "Modelling the Influence of Age of Steel Fiber Reinforced Self Compacting Concrete on Its Compressive Behaviours Material And Structure", pp. 465-478.
18. Dossland A. and Kanstad, "T. Full Scale Experiments with Fiber Reinforced SCC", to be presented at Nordic Concrete Research Project, Sandefjiord, June 2005.
19. Joaquim Barros, Eduardo Pereira and Simão Santos, "Light Weight Panel of Steel Fiber Reinforced Self Compacting Concrete", Journal of Material in Civil Engineering, ASCE, pp.295-304.
20. Pereira E.B., Barros J.A.O., Cunha V.M.C.F. and Santos S.P.F., "Compression and Bending Behaviour of Steel Fiber Reinforced Self-Compacting Concrete", University of Minho, Guimarães, Portugal, 2004.
21. Seung-Hee Kwon, Raissa P. Ferron, Yilmaz Akkaya, and Surendra P. Shah, " Cracking of Fiber Reinforced Self Compacting Concrete due to Restrained Shrinkage", International Journal of Concrete Structures and Materials,Vol.1,No.1,pp3-9.
22. Grunewald S., Walraven J.C., "Self Compacting Fiber Reinforced Concrete", HERON, Vol.46, No.3, 2001, pp.201-206.
23. Joanas Gustafssons, Betongindustri AB, Pratik Groth, "Self Compacting Fiber Reinforced Concrete on Ground", LTU, Task 6, pp.1-33.

APPENDIX-I

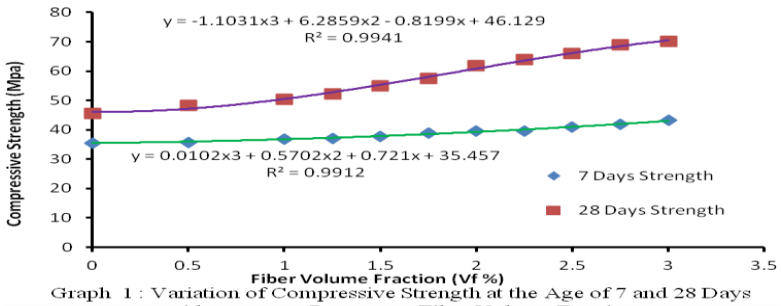

Graph 1 : Variation of Compressive Strength at the Age of 7 and 28 Days with respect to Percentage Fiber Volume Fraction

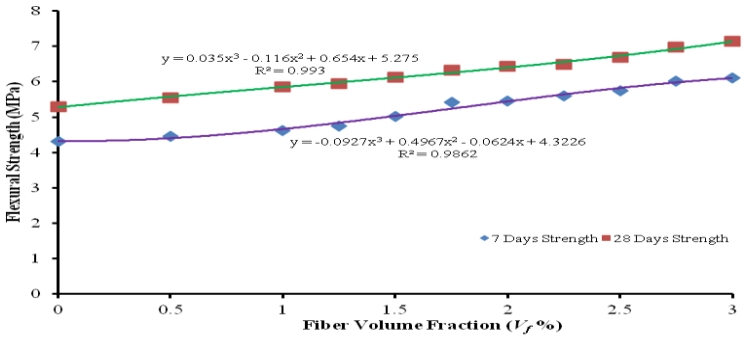

Graph 2 : Variation of Flexural Strength at The Age of 7 and 28 Days with respect to Percentage Fiber Volume Fraction

STUDY OF COLOR VISUAL CRYPTOGRAPHY

ASMITA KAPSEPATIL, APEKSHA CHAVAN
Pillai's Institute of Information Technology, New Panvel, India 410206

Abstract:
This paper shows the study on the concept of color visual cryptography. This paper includes study of color visual cryptography which involves visual information pixel (VIP) synchronization and error diffusion technique applicable for color visual cryptography. VIP carries visual information of original image and VIP synchronization helps to keep the same position of pixels throughout the color channels. Error diffusion generates shares which are clear and visible to human eyes and it improves the visibility of shares. With the help of these two concepts it results in visual quality improvement of images. It also includes a brief description of color model used for the process color visual cryptography.

Keywords: error diffusion, visual cryptography, visual information pixel, visual information pixel synchronization

Introduction
Visual cryptography, is an emerging cryptography technology, uses the characteristics of human vision to decrypt encrypted images. It needs neither cryptography knowledge nor complex computation. For security concerns, it also ensures that hackers cannot perceive any clues about a secret image from individual cover images. There have been many published studies of visual cryptography. Most of them, however, have concentrated on discussing black-and-white images, and just few of them have proposed methods for processing gray-level and color images. Based on previous study in binary image and grey level images this analyzed concept gives a better visual cryptography method for color images and it provides pleasant feel of shares and high visual quality to human eye using Visual Information Pixel and Error Diffusion Technique.

Visual Cryptography for Color Images
In visual cryptography the secret information that is an image is split into shares such that the decryption can be performed by the human visual system by simply superimposing the shares. No computations are involved in the reconstruction of images. This section provides an overview on a color visual cryptography which is simple and good. This method involves C, M, Y subtractive color model in which the color is represented by applying the combinations of colored lights reflected from the surface of an object because most of the objects do not radiate by them [1].

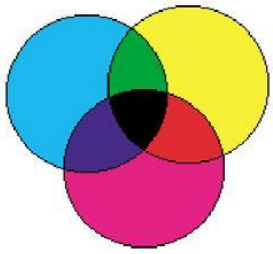

Fig 1. Subtractive color model [1]

This proposed method includes the concept of visual pixel information synchronization and error diffusion.
Error Diffusion: This is simple but efficient method for image halftone generation. The quantization error is filtered and fed to future inputs. The error filter is designed in a way that the low frequency differences between the input and output images are minimized and it produces pleasing halftone images to human vision.
VIP synchronization: Synchronization of the visual information pixel across the color channels improves visual contrast of shares. In color VC schemes the colors of encrypted pixels and the contrast can be degraded due to random matrix permutation. Random matrix permutations are key security features in VC schemes [3]. In gray scale VC schemes it does not affect the visual schemes however in color schemes, independent execution of random matrix permutation for each color channel can cause color distortion by placing VIPs at random positions in sub pixels which finally degrades the visual quality. VIP synchronization prevents the color and contrast of original images from degradation even with matrix permutations. In this concept it derives basis matrices from the given set of matrices which is used in standard VCS.

VIP pixels include the color information of original image which helps in making encrypted shares meaningful. In this process a set of basis matrices $S_c^{c1,c2,,cn}$ (c,c1,c2,,,cn € {0,1}) is generated where c is a pixel bit of message and c1,,,,cn indicates the corresponding pixel bits from the shares. In each row of $S_c^{c1, c2, cn}$ there are q number of VIPs which are denoted as c_i and the values are defined by halftone process. The actual bit values of c_i are defined by referring the pixel values of original shares which are not known at the matrix derivation stage and then errors are diffused away. In this analyzed method each pixel carries visual information as well as message information [3], while other method used needs extra pixels in addition to the pixel expansion to produce meaningful shares. Since each VIP is placed at the same position in sub pixels across three color channels, VIP represents accurate colors of original image. In this method ω ($S_c[i]$) is a hamming weight of 'OR' -ed row vector up to i^{th} rows in $S_c^{c1, c2, cn}$. This row vector should not contain any c_i as elements. Since the values of ci are undefined, it can be represented as 0 or 1 in the halftone stage which ensures the placement of c_i at the same position in each row of S_c [3].

Thus each encrypted sub pixel has the same VIP positions across three channels which mean that these sub pixels carry accurate visual information of the original image and this result in high visual quality in encrypted shares.

EXAMPLE FOR ANALYZED METHOD

Fig. 2 Secret Image [2]

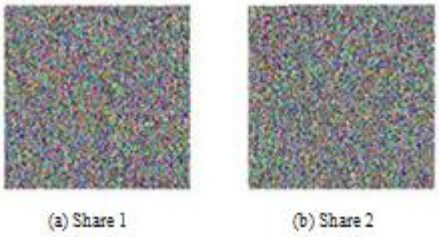

Fig. 4 Shares of original image [2]

Fig. 5 Reconstruction of shares [2]

Conclusion

Review of this proposed method provides a study on a better visual cryptography for color images and it provides pleasant feel with high visual quality.

References

1. Young Chang Hou,2003,vol 36,pp 1619-1629
2. Duo Jin, Wei-Qi Yan, Mohan S. Kankanhalli ,"Progressive Color Visual Cryptography " , JEI,2004
3. InKoo Kang, Gonzalo R Arce, Heung Kyu Lee, "Color Extended Visual Cryptography using Error Diffusion" , 2009

Laplace Substitution Method for Solving Partial Differential Equations Involving Mixed Partial Derivatives

Sujit Handibag[1], B. D. Karande[2]
[1]Department of Mathematics, Mahatma Basweshwar Mahavidyalaya, Latur-413 512, Maharashtra, India.
[2]Department of Mathematics, Maharashtra Udaygiri Mahavidyalaya, Udgir, India.

Abstract:
In this paper we introduced a new method, named Laplace substitution method (LSM), which is based on Lapalce transform. This new method with a convenient way to find exact solution with less computation as compared with Method of Separation of Variables(MSV) and Variational iteration method (VIM). The proposed method solves linear partial differential equations involving mixed partial derivatives.

Keywords: Approximate solution, Adomian decomposition method, Laplace decomposition method, Nonlinear partial differential equations.

Introduction:

Nonlinear ordinary or partial differential equations involving mixed partial derivatives arise in various fields of science, physics and engineering. The wide applicability of these equations is the main reason why they have gained so much attention from many mathe- maticians and scientists. Unfortunately they are sometimes very difficult to solve, either Numerically or theoretically. There are many methods to obtain approximate solutions of these kinds of equations. Partial differential equations (PDE) are differential equations that contain unknown multi variable functions and their partial derivatives. PDEs are used to formulate problems involving functions of several variables, and are either solved by hand, or used to create a relevant computer model. The Method of separation of variables [8] and Variational iteration method [2-4] has been extensively worked out for many years by numerous authors. Starting from the pioneer ideas of the Inokuti -Se kine- Mura method [5], JI-Huan He [4] developed the Variational iteration method (VIM) in 1999. The variational iteration method , has been widely applied to solve nonlinear problems, more and more merits have been discovered and some modifications are suggested to overcome the demerits arising in the solution procedure. For example, T.A.Abassy. et al [6,7] also proposed further treatments of these modification results by using Pade approximants and the Laplace transform. The Laplace transform is a widely used integral transform. The Laplace transform has the useful property that many relationships and operations over the originals f(t) correspond to simpler relationships and operations over the images F(s). It is named for Pierre-Simon Laplace (1749-1827) [1], who introduced the transform in his work on probability theory.

The main goal of this paper is to describe new method for solving linear partial Differential equations involving mixed partial derivatives. This powerful method will be proposed in section 2; in section 3 we will apply it to some examples and in last section we give some conclusion.

2. Laplace Substitution Method:

The aim of this section is to discuss the Laplace substitution method. We consider the general form of non homogeneous partial differential equation with initial conditions is given below

$$Lu(x,y) + Ru(x,y) = h(x,y) \qquad (2.1)$$

$$u(x, 0) = f(x), \qquad u_y(0, y) = g(y) \qquad (2.2)$$

Where $L = \frac{\partial}{\partial x \partial y}$, $Ru(x,y)$ is the remaining linear terms in which contains only first order partial derivatives of u(x, y) with respect to either x or y and h(x, y) is the source term. We can write equation (2.1) in the following form

$$\frac{\partial^2 u}{\partial x \partial y} + Ru(x,y) = h(x,y)$$

$$\frac{\partial}{\partial x}\left(\frac{\partial u}{\partial y}\right) + Ru(x,y) = h(x,y) \qquad (2.3)$$

Substituting $\frac{\partial u}{\partial y} = U$ in equation (2.3), we get

$$\frac{\partial U}{\partial x} + Ru(x,y) = h(x,y) \qquad (2.4)$$

Taking Laplace transform of equation (2.4) with respect to x, we get

$$U(s,y) = \frac{1}{s}U(0,y) + \frac{1}{s}L_x[h(x,y) - Ru(x,y)]$$

$$U(s,y) = \frac{1}{s}u_y(0,y) + \frac{1}{s}L_x[h(x,y) - Ru(x,y)]$$

$$U(s,y) = \frac{1}{s}g(y) + \frac{1}{s}L_x[h(x,y) - Ru(x,y)] \qquad (2.5)$$

Taking inverse Laplace transform of equation (2.5) with respect to x, we get

$$U(x,y) = g(y) + L_x^{-1}\{L_x[h(x,y) - Ru(x,y)]\} \qquad (2.6)$$

Re-substitute the value of U(x, y) in equation (2.6), we get

$$\frac{\partial u(x,y)}{\partial y} = g(y) + L_x^{-1}\{L_x[h(x,y) - Ru(x,y)]\} \qquad (2.7)$$

This is the first order partial differential equation in the variables x and y. Taking the Laplace transform of equation (2.7) with respect to y, we get

$$su(x,s) = f(x) + L_y\left[g(y) + L_x^{-1}\left[\frac{1}{s}L_x[h(x,y) - Ru(x,y)]\right]\right]$$

$$u(x,s) = \frac{1}{s}f(x) + \frac{1}{s}L_y\left[g(y) + L_x^{-1}\left[\frac{1}{s}L_x[h(x,y) - Ru(x,y)]\right]\right] \qquad (2.8)$$

Taking the inverse Laplace transform of equation (2.8) with respect to y, we get

$$u(x,y) = f(x) + L_y^{-1}\left\{\frac{1}{s}L_y\left[g(y) + L_x^{-1}\left[\frac{1}{s}L_x[h(x,y) - Ru(x,y)]\right]\right]\right\} \qquad (2.9)$$

The last equation (2.9) gives the exact solution of initial value problem (1.1).

3. Applications:

To illustrate this method for coupled partial differential equations we take three examples in this section.

Example 1: Consider the partial differential equation

$$\frac{\partial^2 u}{\partial x \partial y} = e^{-y}\cos x \qquad (3.10)$$

with initial conditions $u(x, 0) = 0$, $u_y(0, y) = 0$ (3.11)

In the above initial value problem $Lu(x, y) = \frac{\partial^2 u}{\partial x \partial y}$, $h(x,y) = e^{-y}\cos x$ and general linear term Ru(x,y) is zero.

Equation (3.10) we can write in the following form

$$\frac{\partial}{\partial x}\left(\frac{\partial u}{\partial y}\right) = e^{-y}\cos x \qquad (3.12)$$

Substituting $\frac{\partial u}{\partial y} = U$ in equation (3.12), we get

$$\frac{\partial U}{\partial x} = e^{-y}\cos x \qquad (3.13)$$

This is the non homogeneous partial differential equation of first order. Taking Laplace transform on both sides of equation (3.13) with respect to x, we get

$$sU(s,y) - U(0,y) = L_x[e^{-y}\cos x]$$

$$U(x,y) = e^{-y}\frac{1}{s}\frac{s}{(1+s^2)}$$

Taking inverse Laplace transform of equation (3.13) with respect to x, we get

$U(x,y) = e^{-y}\cos x$

$$\frac{\partial u(x,y)}{\partial y} = e^{-y}\cos x \qquad (3.14)$$

This is the partial differential equation of first order in the variables x and y. Taking Laplace transform of equation (3.14) with respect to y, we get

$$su(x,s) - u(x,0) = \sin x\frac{1}{1+s}$$

$$u(x,s) = \sin x\frac{1}{s(1+s)} \qquad (3.15)$$

Taking inverse Laplace transform of equation (3.15) with respect to y, we get

$$u(x,s) = \sin x(1 - e^{-y}) \qquad (3.16)$$

This is the required exact solution of equation (3.10). Which can be verify through the substitution. Which is same the solution obtained by (MSV) and (VIM).

Example 2: Consider the partial differential equation

$$\frac{\partial^2 u}{\partial y\,\partial x} = \sin x \sin y \qquad (3.17)$$

with the inital conditions

$$u(x, 0)=1+\cos x \ , \quad u_y(0, y)= -2\sin y \qquad (3.18)$$

In the above example assume that ux(x, y) and uy(x, y) both are differentiable in the domain of definition of function u(x, y) [Young's Theorem]. This implies that $\frac{\partial^2 u}{\partial y\partial x} = \frac{\partial^2 u}{\partial x\partial y}$. Given initial conditions (3.18) force to write the equation (3.17) in following form and use the substitution $\frac{\partial u}{\partial y} = U$

$$\frac{\partial}{\partial x}\left(\frac{\partial u}{\partial y}\right) = \sin x \sin y \qquad (3.19)$$

$$\frac{\partial U}{\partial x} = \sin x \sin y \qquad (3.20)$$

Taking Laplace transform of equation (3.20) with respect to x, we get

$$U(x,y) = \frac{-2\sin y}{s} + \sin y\left[\frac{1}{s} - \frac{s}{1+s^2}\right] \qquad (3.21)$$

Taking inverse Laplace transform of equation (3.21) with respect to x, we get

$$U(x,y) = -2\sin y + \sin y[1 - \cos x]$$

$$\frac{\partial u(x,y)}{\partial x} = -2\sin y + \sin y[1 - \cos x] \qquad (3.22)$$

Taking Laplace transform of equation (3.22) with respect to y, we get

$$su(x,s) - u(x,0) = \frac{1}{1+s^2}[-1 - \cos x]$$

$$su(x,s) = (1+\cos x) - \frac{1}{1+s^2}[1 + \cos x]$$

$$u(x,s) = (1+\cos x)\left[\frac{1}{s} - \frac{1}{s(1+s^2)}\right] \qquad (3.23)$$

Taking inverse Laplace transform of equation (3.23) with respect to y, we get

$$u(x, y)=(1+\cos x)\cos y \qquad (2.24)$$

This is the required exact solution of equation (3.17). Which can be verify through the substitution. Which is same the solution obtained by (MSV) and (VIM).

Example 3: Consider the following partial differential equation with $Ru(x,y) \neq 0$

$$\frac{\partial^2 u}{\partial x\,\partial y} + \frac{\partial u}{\partial x} + u = 6x^2 y \qquad (3.26)$$

With initial conditions

$$u(x, 0)=1, \qquad u(0, y)=y \ , \quad u_y(0, y)=0 \qquad (3.26)$$

In the above example Ru(x, y) = $\frac{\partial^2 u}{\partial x \partial y} + u(x,y)$. Use the substitution $\frac{\partial u}{\partial y} = U(x,y)$ in equation (3.25), we get

$$\frac{\partial U}{\partial x} + \frac{\partial u}{\partial x} + u = 6x^2 y \qquad (3.27)$$

Taking Laplace transform of equation (3.27) with respect to x, we get

$$sU(s,y) - U(0,y) + su(s,y) - u(0,y) + L_x[u(x,y)] \frac{12y}{s^2}$$

$$U(s,y) = -u(s,y) - \frac{1}{s} L_x[u(x,y)] + \frac{12y}{s^4} \qquad (3.28)$$

Taking inverse Laplace transform of equation (3.28) with respect to x, we get

$$U(x,y) = -u(x,y) - L_x^{-1}\left[\frac{1}{s} L_x[u(x,y)]\right] + 2yx^3$$

$$\frac{\partial u(x,y)}{\partial x} = -u(x,y) - L_x^{-1}\left[\frac{1}{s} L_x[u(x,y)]\right] + 2yx^3 \qquad (3.29)$$

Taking Laplace transform of equation (3.29) with respect to y, we get

$$su(x,s) - u(x,0) = -L_y\left[u(x,y) + L_x^{-1}\left[\frac{1}{s} L_x[u(x,y)]\right]\right] + 2x^3 \frac{1}{s^2}$$

$$u(x,s) = \frac{1}{s} - L_y\left[u(x,y) + L_x^{-1}\left[\frac{1}{s} L_x[u(x,y)]\right]\right] + 2x^3 \frac{1}{s^2} \qquad (3.30)$$

Taking inverse Laplace transform of equation (3.30) with respect to y, we get

$$u(x,y) = 1 - L_y^{-1}\left[\frac{1}{s} L_y\left[u(x,y) + L_x^{-1}\left[\frac{1}{s} L_x[u(x,y)]\right]\right]\right] + x^3 y^2 \qquad (3.31)$$

We cannot solve the equation (3.31) because our goal u(x, y) is appeared in both sides of equation (3.31). Therefore the equation (3.25) we cannot solve by using LSM because of $Ru(x,y) \neq 0$.

3. Conclusion

In this paper, we proposed Laplace Substitution Method (LSM) is applicable to solve partial differential equations in which involves mixed partial derivatives and general linear term Ru(x, y) is zero. The result of first two examples compared with (MSV) and (VIM), tell us that these methods can be use alternatively for the solution of higher order initial value problem in which involves the mixed partial derivatives with general linear term Ru(x, y) is zero. But the result of example number three tell us that (LSM) is not applicable for those partial differential equations in which R u(x, y) ≠ 0.Consequently the (LSM) is promising and can be applied for other equations that appearing in various scientific fields.

References

[1] Joel L. Schiff, The Laplace Transform: Theory and Applications, Springer

[2] J. H. He, Approximate analytical solution for seepage ow with fractional derivatives in porous media, Comput. Methods Appl. Mech. Engrg. 167(1998)57-68.

[3] J. H. He, Approximate solution of nonlinear differential equations with convolution product nonlinearities, Comput. Methods Appl. Mech. Engrg. 167(1998)69-73.

[4] J.-H. He, Variational iteration method- a kind of non-linear analytical technique: some examples, Internat. J. Non-Linear. Mech. 34 (1999) 699-708.

[5] M. Inokuti, H. Sekine, T. Mura, General use of the Lagrange multiplier in nonlinear mathematical physics, Variational Methods in the Mechanics of Solids, Pergamon Press, New York, 1978, pp. 156162.

[6] T. A. Abassy , M.A.El-Tawil ,H.El-Zoheiry, Solving nonlinear partial differential equations using the modified variational iteration Pade technique ,Journal of Computational and Applied Mathematics 207 (1)(2007)73-91.

[7] T. A. Abassy, M.A.El-Tawil ,H.El-Zoheiry, Exact solutions of some nonlinear partial diferential using the variational iteration method linked with Laplace transforms and the Pade technique, Computers and Mathematics with Applications,54 (7-8))(2007)940-954.

[8] Richard Jozsa, DAMTP Cambridge, PDEs on bounded domains: Separation of vari-ables, Part II, (2011).

ARkanoid: Development of 3D Game and Handheld Augmented Reality

[1]Markus Santoso, [2]Lee Byung Gook
[1]Ph.D Candidate, Visual Content Department, Dongseo University, South Korea.
[2]Professor, Visual Content Department, Dongseo University, South Korea.

Abstract
In this paper, researcher presents ARkanoid, a 3D Handheld Augmented Reality game. Through this project, researcher tried to remake the old 2D game and brought it into something new. This time, researcher chooses an Arkanoid game which was first introduced in 1986 and became very famous together with the raise of video game era on that moment. Not only makes it in the 3D version, but also researcher combines it with an Augmented Reality (AR) technology. And finally, this AR project is finalized through handheld devices so that it can be commercialized to the real world in the future. This paper discusses the technical aspect of the game, the design and development process and the result of user study. The goal of this research is to explore the affordances and constraints of handheld AR interfaces for 3D games. This project showed some promising results of handheld AR application in game. User feels that the game presentation with 3D and AR technology is more interesting than general 2D game, the immersion of virtual object in real world also brings unique game ambient and touch-screen gameplay makes the player becomes more engaged to the game. Researcher hopes this research can be the milestone and will inspire the further research of respected field. Researcher also hopes this Arkanoid AR game can educate the user of handheld device who mostly grew up in previous era of Arkanoid game, that they can easily get familiar with AR technology applications.

Keywords – Arkanoid game, 3D Game, Handheld AR

I. Introduction

These last decades, the 3D technology has been well developed and this knowledge has become more mature than before. We can see that 3D technology has been used in several fields in our daily life. However, to reach the end user or audience, this 3D technology needs to be displayed. In general, there are 4 types of 3D display, namely stereoscopic, augmented and virtual reality, integral image and holographic display. Figure 1 will display a simple graph of 3D technology display.

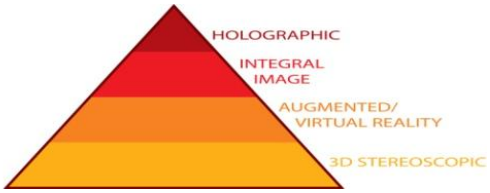

Figure 1. 3D Technology Display

Historically, 3D technology was developed based on 2D graphic. In the early of 90's 2D graphic technology got its popularity. Then, 3D technology became mature and started to be commercialized. Several fields had been reached by previous 3D technology. 3D technology then derived again become 3D stereoscopic that been massively used these days. After that, researchers tried to find another way to display 3D technology, and then augmented/virtual reality appeared. Recently, an augmented and virtual reality has reached certain level to bring them from research lab into real world. The core technology has been mature enough to be applied in several fields of human life, such as entertainment, education and others.

The integral image is starting to develop as well these days. It rose to overcome several disadvantages appeared from 3D stereoscopic technology, such as parallax problem. This technology is still in process to find their maturity in research lab. And finally, the most ideal 3D technology display is holographic display. The previous 3D display however is still covered by the screen. It is just the illusion of 3D display behind the screen. Holographic display will display the 3D object in the free-space and can interact directly with the user. Figure 2 will display the 3D display technology transition.

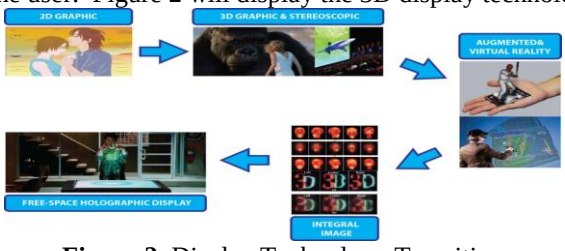

Figure 2. Display Technology Transition

In this paper, researcher decided to develop a project related to handheld augmented reality. Some expertise believed that an AR/VR is a proper bridge to reach an ideal 3D display, holographic. While the integral image is still in the research and development phase, an AR/VR technology has reached their maturity. Reaching more than 10 years since its first official conference, this research field has grown significantly. Based on this fact, lately several parties started to move this technology to real world so it can give benefit a lot of people. Previously this technology had several barriers related with the commercialization effort. But the invention of handheld devices happened recently and helped AR technology to reach end user easier than before. Based on these facts, researcher chose an augmented reality that is finalized in handheld device to display the 3D object in this game.

From this project, researcher would like to support the commercialization effort of AR technology. Several AR projects have been developed before in the various fields and now researcher wanted to represent one of the famous games in previous era, Arkanoid, and combined it with recent technology. This research is expected to be a proper milestone for further research and development of AR technology in various fields. It is the right time for AR technology to show its contribution to real human life.

II. Previous Work

The commercialization effort of AR technology has been appeared since several years ago. Various fields have been reached by AR technology but in general there are six types of applications, namely personal information system, industrial and military applications, medical applications, entertainment, office applications, education and training [1]. But, still it found some difficulties to reach end user in real world. The invention of handheld device, such as smart phone and computer tablet, which had been massively used by people recently really helped AR technology to reach real world application. It also had domino effect to the number of research in handheld AR. Survey found that the published papers about handheld AR has become more popular these days [2].

In education field, Markus et al had developed an AR edutainment content for Sungsan elementary school (SES) in Busan - South Korea[9]. The project name is EDUtangram and it combined conventional Tangram edutainment tool with AR technology. This project was also finalized using handheld devices, iPad2. An AR Tangram edutainment was then installed on 30 iPads belonged to SES and they used it regularly during their class session.

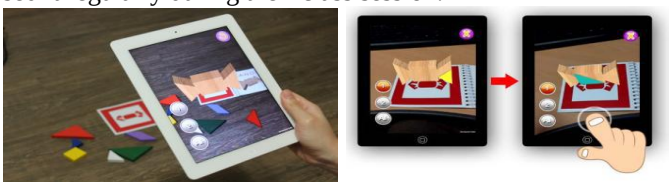

Figure 3. EDUtangram project.

In entertainment field, these days there are several great AR projects released. At least there are three big names in entertainment industry exploring AR technology for their activity. Transformer creates an AR application for iPad device to support their movie in the theater. This year Marvel Corp. also releases an AR application for one of their most famous hero characters, Iron Man. And lastly, to support the commercial release of newest Spiderman movie in theater, they also create AR application for handheld device. Together with conventional promotion media such as poster and website, this handheld AR application become an integrated and creative marketing tools.

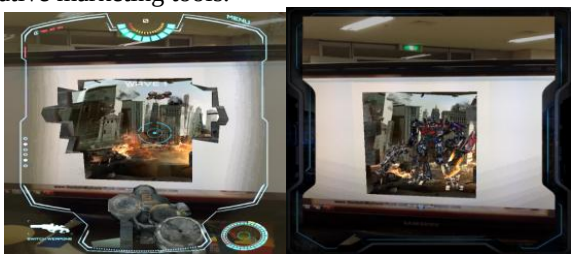

Figure 4. Transfomer Handheld AR Applications

Figure 5. Marvel Handheld AR Applications

Figure6. Spiderman 4 Handheld AR Applications.

Not only in entertainment field, increasing number of AR project also happened in game field. Several published plug-in or software for AR purpose had contribute to blooming number of AR applications in this field both for PC- based, handheld device-based and other possible device. One of the developers who develop 3D AR game for handheld device is Fuzzy Logic. They developed an Augmentron for iPad2 device.

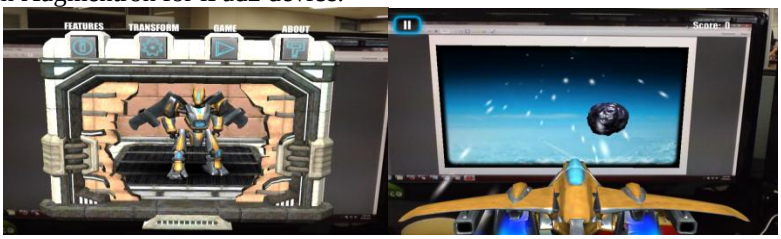

Figure7. Augmentron handheld AR applications

III. Game Description

ARkanoid was chosen as the main theme of this project. Arkanoid is an arcade game developed by Taito in 1986 and it first released for Atari consol. This game is well-known on that moment so that it reproduced again for several game consoles that released after Atari console era. In simple way, the player of Arkanoid will control the paddle and prevent a ball falling down from playing field. When the ball hit the paddle, it will bounce against the brick that are provided in the field. The objective is to finish all of the bricks, end the game and move to next stage. The objective is simple but the challenge is not that easy. It makes the player become addicted to this game. In 1989, Arkanoid was reviewed by Patricia Hartley and Kirk Lesser. In their "The Role of Computers" column, the reviewers gave this game 5 out of 5 stars.

Figure8. Arkanoid Game in Early Era.

Children who play an Arkanoid game in early released era had been grown up now, finished their higher education and some of them already maybe working. The most important thing is they are the user of the handheld devices recently. By combining the game that famous in their childhood era with AR technology, researcher tries to educate this generation to be familiar with this recent technology. So that, they will be able to get used with further AR application easily.

IV. Augmented Reality

Augmented reality topic was first introduced by Sutherland in 1960. Then it became an emerging research topic when Milgram and Kishino published their paper and introduce about the concept of "Virtuality Continuum"[7]. In this concept, they clarify the position of the augmented reality in the simple graph as seen in figure 9. This concept then became the milestone of the Augmented Reality development until these days.

Figure9. Virtual Continuum Concept

Augmented reality is technology which allows computer generated virtual imagery to exactly overlay physical objects in real time. AR allows user to interact with the virtual images using real objects in a seamless way [4]. Furthermore, Azuma provide commonly accepted definition of AR as a technology which combines real and virtual imagery, interactive in real time and registers the virtual imagery with the real world [8]. In order to provide an effective AR experience there are number of factors that must be developed, namely graphics rendering hardware and software, tracking techniques, tracker calibration and registration tools, display hardware, computer processing hardware and interaction techniques [2]. During the evolution of AR, there are various research topics appeared and developed extensively.

In general, there are 2 groups of AR research topic [2]. First group contains the main research areas of Tracking techniques, Interaction techniques, Calibration and Registration, AR Applications and Display techniques. This group represents the core AR technology areas which are needed to deliver an AR application. Second group of topic reflects more emerging research interest, including Evaluating/testing, Mobile/Handheld AR, AR Authoring, Visualization, Multimodal AR, Rendering [2]. Since the invention of handheld devices in our daily life, the number of research in mobile AR has been raised as well.

One of the main components for AR is display. There are three major types of AR displays, namely Head-Mounted Display (HMD), Spatial Display and Handheld Display [3]. HMD is a display device worn on the head or as part of helmet and that places both images of the real and virtual environment over the user's view of the world. Spatial Display makes use of video projector, optical elements, holograms, radio frequency tags and other tracking technologies to display graphical information directly onto physical object without requiring the user to wear it or carry the display. Handheld display employs small computing devices with a display that the user can hold in their hands. There are three distinct classes of commercially available handheld display that are being used for AR system, namely Smart-phones, PDA and Tablet PC [3].

The presence of handheld devices in AR field is expected to contribute more in commercialization effort of AR technology. The reason is because handheld AR is predicted to fulfill some requirements to be successful systems in the market. Carmigniani and Furht stated there are three requirements for systems to reach its success in market. First is socially acceptable, it means that is subtle, discrete and unobtrusive. Second is natural interaction which is needed to be able to interact with the system in a natural way. And last factor is fashionably acceptable so that user does not need to look strange while operating the system [3].

V. Design And Development Process

ARkanoid is a project that combines conventional Arkanoid game with Augmented Reality technology and installed on handheld device. The gameplay of Arkanoid itself will remain unchanged, still related to paddle, ball and brick. But this time, researcher represented Arkanoid game in 3D version.

To build this game, researcher used Unity3D game engine. Unity3D game engine right now has been widely used by game developer. There are tons of advantages offer by Unity3D, such as multi-platform device possibility (iOS, android, Xbox, Nintendo wii, PC), graphical advantages, simple user interface and others. Unity3D is supported by 3 common programming languages such as java, c# and boo. Unity3D also has a strong community to support each member in this area and it becomes another advantage for the various skill range of user (www.unity3d.com).

To build the AR session, researcher used Vuforia. Vuforia is the AR extension created by Qualcomm and it perfectly bundled with Unity3D software.Vuforia is a marker-based AR system and it enables vision detection and tracking functionality into Unity3D IDE, it also allows developers to easily create AR application and games. A Vuforia based AR application is composed of the following core components: camera, image converter, tracker, video background renderer, application code and target resources. Figure 10 is the data flow diagram of Vuforia Ar extension (http://ar.qualcomm.at).

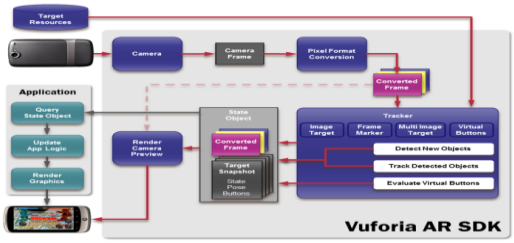

Figure10. Data Flow Diagram of the Vuforia AR Extension

Basically, Vuforia is Marker-based AR extension. Because of that, we need the marker so that the system can detect it, track it and then visualize the 3D object above the marker. Unlike the previous AR tool, Vuforia allow us to create colorful marker because they just extract the edge and contrast as a feature point. Figure 11 show the design of marker for ARkanoid project.

Figure11. ARkanoid Marker Design.

To play ARkanoid AR game, user needs to prepare and put the marker in the horizontal position. After that, they need to point device's camera into the marker. When the camera already capture the marker, 3D object will automatically appeared in the screen and audience can start to play the game. Figure 12 show the gameplay procedure of ARkanoid AR game.

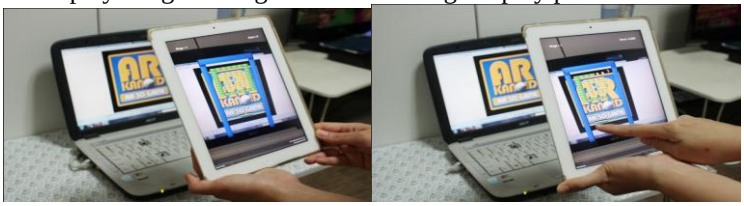

Figure12. ARkanoid Gameplay Procedure

Previously, player needs to use joystick, keyboard or any other 3rd parties to move the paddle. But, since this new ARkanoid is built on the handheld devices that had no additional button, researcher added slide function to move the paddle. Using this function, player can slide their finger on the device's screen to move the paddle to the respected direction. Figure 13 show the slide function of ARkanoid 3D game.

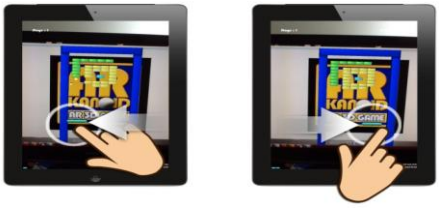

Figure13. Slide Function of ARkanoid 3D Game

In conclusion, researcher try to bring the same gameplay experience from the conventional while in the same time researcher should adjust some parts to fit the AR technology and handheld devices. The general gameplay is still remaining the same, but the 2D graphic display was changed into 3D graphic display. This game also created on marker-based AR technology. Finally, since it built on handheld devices, rather than using 3rd parties to interact with 3D object, player can directly touch and interact with the paddle on this game.

VI. User Study

4.1 Goals and Participant Recruitment

After complete ARkanoid game prototype, researcher conducted small user study with 10 participants. Specifically, researcher hoped to explore their opinion about the comparison of 3D AR game with the conventional 2D game, the augmented reality technology embedded with game and the gameplay of new Arkanoid. We were interested to find out their interest about an AR game and their feedback about the gameplay itself would be valuable information for the further research in AR game.

To recruit participants, we have several situations to be considered. First, the participant should have an experience playing an early Arkanoid game, no matter what game console they used at that time. Since we want to compare between conventional Arkanoid games with our new Arkanoid, so the previous experience of an early Arkanoid game should be fulfilled by participant. Second, we try to find participant from various background of knowledge as long as they can satisfy first requirement. They can be a student from various major, workers, housewife and other else. And last, we try to observe multi-nation participant. Rather than focusing in one nation or races, we open this research for participant from various nationalities.

Finally, we found 10 participants with the age range from late of 20's to mid of 30's. Since they spent their childhood in 1980's until early of 1990's, all of them definitely had an experience playing early Arkanoid game. 2 of them are the undergraduate students from non computer science major, 4 of them are graduate students from computer science major, 2 of them are workers, and 2 of them are housewife. The participants were from 5 countries, namely Korea, China, Malaysia, Indonesia and Russia. Except the graduate students, all of them do not have prior knowledge and experience in augmented reality games before. For the research in Indonesia, researcher sent the application installer to the participant and the survey was completed by skype chatting.

4.2 Procedure and Setting

The user study was divided into three parts. First, researcher gave a brief explanation about the gameplay procedure; in this case researcher already prepared the marker and handheld device. After that, researcher let the participant played the game directly and there was no game time limitation. Participant could decide by themselves when they wanted to stop playing the game. Except for the participant in Indonesia, all the research was done in the research lab with one condition should be considered, it should be indoor. Indoor place was chosen to prevent unexpected distraction to the tracking robustness ability. And last, researcher interviewed the participant to gather needed information, data and opinion.

The user study also conducts individually. It means that it separately from one participant to each other. Since mostly of user study were done by interviewing, it would be easier to explore their opinion when discussions were held individually. By using individual interview, not only we can observe more about participant opinion but also it can keep privacy from each recruited participant.

VII. Discussion

Through the user study, participants gave us valuable feedback about ARkanoid AR game. We interviewed the participants whether they like or dislike the new appearance of Arkanoid game. 8 of the participants were pros to the new ARkanoid AR game. Most of them explained that the using of 3D graphic and AR technology bring this game to the next level and it is more interesting than conventional 2D game. The rest participants choose to cons the new ARkanoid AR game since they felt there is no significant difference to early Arkanoid game and there is no urgency to use 3D and AR technology since they already like early Arkanoid format.

Next, we try to observe their opinion about the AR technology that embedded in this game. 6 of the participants said that they are excited and interested about the AR technology. Rather than playing a fully virtual game, the immersion of virtual object in the real world gave them a unique sensation during game session. The rest participants stand for cons position since they felt that AR technology made the gameplay become more difficult because they needed to point the camera to the marker during game session, the other else said that it was quite heavy to hold the device during game session.

Last, we observe their opinions about the gameplay of new ARkanoid game. 7 of the participants said that they like the new way of the ARkanoid gameplay. Previously, they need to move the paddle using 3rd parties' device such as joystick, keyboard and other else. But using handheld device and sliding function, participants could interact with the paddle directly from the screen. It made them comfortable and more engaged with the game itself. 2 of the participants said that using handheld device to play a game was fine and they give suggestion to put the virtual button in the screen to move the paddle rather than using slide function. And 1 of the participant said that playing with the joystick was better especially in controlling the paddle.

VIII. Conclusion

In this paper, we conducted research about the potential of combination 3D game and handheld AR technology then analyzed the user study from it. In contrast with the early design of Arkanoid game, researcher tried to represent it into 3D platform game and furthermore combine it with an AR technology. And finally, the new ARkanoid game was finalized in the recent handheld devices that already massively used these days.

Our research about the combination of 3D game and handheld AR technology found promising result and it can be the basic of the further research to bring this technology from research lab to the real world. We can conclude that users feel the game presentation with 3D graphic and AR technology is more interesting than general 2D game, the immersion of virtual object in real world also brings unique game ambient and touch-screen gameplay makes the gap between player and the game became closer and it makes them more engaged to the game.

As we move forward, researcher hope this research can be milestone and will inspire further research of respected field. Researcher also hopes can educate the user of handheld device who mostly grew up in the previous era of Arkanoid game, so that they can easily get familiar with AR technology applications. Since AR is pretty new technology in our daily life, we need to educate the people as end user so that they can get used and familiar with this technology. In the long run, we hope to explore an AR technology deeper and observe the application of AR technology in various fields, any other purposes and brings more benefit to people in the real world.

Acknowledgement

This research was supported by Basic Science Research Program through the National Research Foundation of Korea (NRF) funded by the Ministry of Education, Science and Technology (2010-0009003).

References

1. D.W.F. Van Krevelen, R. Poelman. A Survey of Augmented Reality Technologies, Applications and Limitations. In *The International Journal of Virtual Reality*, 2010, 9(2), pp1-20.
2. F. Zhou, H.B.L. Duh, M. Billinghurst. Trends in Augmented reality Tracking, Interaction and Display: A Review of Ten Years of ISMAR. In *International Symposium on Mixed and Augmented Reality (ISMAR'08).*
3. J. Carmigniani, B. Furht. Augmented Reality: An Overview. In *Handbook of Augmented Reality*. ISBN: 978-1-4614-0063-9. Springer Science, London.
4. M. Billinghurst. Augmented Reality in Education. *New Horizons for Learning*. Retrieved from: http://www.it.civil.aau.dk/it/education /reports/ar_edu.pdf.2002.
5. M. Billinghurst, A. Henrysson. Research Direction in Handheld AR. In *The International Journal of Virtual Reality*, 2006, 5(2), pp51-58.
6. M. Haller, M. Billinghurst, B. Thomas. Augmented Reality: Interfaces and Design. ISBN: 1-59904-066-2. Idea Group Publishing.
7. P. Milgram, F.Kishino. A Taxonomy of Mixed Reality Visual Displays. In *IEICE Transactions on Information Systems*, VolE77D, No. 12, December 1994.
8. R.T. Azuma. A Survey of Augmented Reality. In *Presence:Teleoperators and Virtual Environment*, 6:4, 355-385, August 1997.
9. S. Markus, F.Y. Wang, B.G. Lee. Development of Edutainment Content for Elementary School Using Mobile Augmented Reality. *Proceeding of ICCRD'12* (Chengdu, China, May 5-6, 2012).

A Selective Survey and direction on the software of Reliability Models

Vipin Kumar
Research Scholar, S.M. Degree College, Chandausi

Abstract:
Software development, design and testing have become very intricate with the advent of modern highly distributed systems, networks, middleware and interdependent application. The demand for complex software systems has increased more rapidly than the ability to design, implement, test, and maintain them and the reliability of software systems has become a major concern for our modern society. Software reliability modeling and measurements have drawn quite a bit of attention recently in various industries due to concerns about the quality of software. In few years of 21st century, many reported system outages or machine crashes were traced back to computer software failures.

In this paper, I have many challenges in getting wide spread use of software reliability models. I am focus on software reliability models and measurements. A software reliability model specifies the general form of the dependence of the failure process on the principal factors that affect it: fault introduction, fault removal and the operational environment. During the test phase, the failure rate of a software system is generally decreasing due to discovery and correction of software faults. With careful record-keeping procedures in place, it is possible to use statistical methods to analyze the historical record. The purpose of these analyses is twofold:(1) to predict the additional time needed to achieve a specified reliability objective; (2) to predict the expected reliability when testing is finished.

Key words: Dynamic model, Growth model, Reliability software, Static model, Telecommunication.

Introduction:

In few year of century, many reported system outages or machine crashes were traced back to computer software failures. Consequently, recent literature is replete with horror stories due to software problems. Software failure has impaired several high visibility programs in space, telecommunications and defense and health industries. The Mars Climate Orbiter crashed in 1999. The Mars Climate Orbiter Mission failure investigation Board [1] concluded that "The root cause of the loss of the spacecraft was the failed translation of English unit into metric units in a segment of ground based, navigation related mission software. Current versions of the Osprey aircraft, developed at a cost of billions of dollars, are not deployed because of software induced field failure. In the health industry [2], the Yherac-25 radiation therapy machine was hit by software errors in its sophisticated control systems and claimed several patients' lives in 1985 &1986. Even in the telecommunications industry, known for its five nines reliability, the nationwide long distance network of a major carrier suffered an embarrassing network outage on January 1990, due to software problem. In 1991, a series of local network outage occurred in a number of US cities due to software problems in central office switches [3].

Software reliability is defined as the probability of failure free software operations for a specified period of time in a specified environment [4]. The software reliability field discusses ways of quantifying it and using it for improvement and control of the software development process.. Software reliability is operationally measured by the number of field failures, or failures seen in development, along with a variety of ancillary information. The ancillary information includes the time at which the failure was found, in which part of the software it was found, the state of software at that time, the nature of the failure. ISO9000-3 [5] is the weakest amongst the recognized standards, in that it specifies measurement of field failures as the only required quality metric.

In this paper, I take a narrower view and just look at models that are used in software reliability-their efficacy and adequacy without going into details of the interplay between testing and software reliability models. Software reliability measurement includes two types of model: static and dynamic reliability estimation, used typically in the earlier and later stages of development respectively. These will be discussed in the following two sections. One of the main weaknesses of many of the models is that they do not take into account ancillary information, like churn in system during testing. Such a model is described in Growth reliability. A key use of the reliability models is in the area of when to stop testing. An economic formulation is discussed in next paragraph.

Static Models:

One purpose of reliability models is to perform reliability prediction in an early stage of software development. This activity determines future software reliability based upon available software metrics and measures. Particularly when field failure data are not available (e.g. software is in design or coding stage), the metrics obtained from the software development process and the characteristics of the resulting product can be used to estimate the reliability of the software

upon testing or delivery. I am discussing two prediction models: the phase based model by Gaffney and Davis [10] and a predictive development life cycle model from Telcordia Technologies by Dalal and Ho [11].

(a) Phase based Model:

Gaffney and Davis [10] proposed the phase based model, which divides the software development cycle into different phases (e.g. requirement review, design, implementation, unit test, software integration, system test, operation etc.) and assumes that code size estimates are available during the early phases follow a Raleigh density function when normalized by the lines of code. The idea is to divide the stage of development along a continuous time (i.e. t=0-1means requirements analysis and so on) and overlay the Raleigh density function with a scale parameter, known as fault discovery phase constant, is estimate by equating the area under the curve between earlier phases with observed error rates normalized by the lines of code. This method gives an estimate of the fault density for any later phase. The model also estimates the number of faults in a given phase by multiplying the fault density by the number of lines of code.

This method is clearly motivated by the corresponding model used in hardware reliability and the predictions are hardwired in the model based on one parameter. In spite of this criticism, this model is one of the first to leverage information available in earlier development life cycle phases.

(b) Predictive Development Life Cycle Model:

In this model the development life cycle is divided into the same phases as in Phase based method. However, it does not postulate a fixed relationship (i.e. Raleigh distribution) between the numbers of faults discovered during different phases. Instead, it leverages past releases of similar products to determine the relationships. The relationships are not postulated beforehand, but are determined from data using only a few releases per product. Similarity is measured by using an empirical hierarchical bays framework. The number of releases used as data is kept minimal and, typically, only the most recent one or two releases are used for prediction. The lack of data is made up for by using as many products as possible that were being developed in a software organization at around the same time. In that sense it is similar to meta analysis [12], where a lack of longitudinal data is overcome by using cross-sectional data.

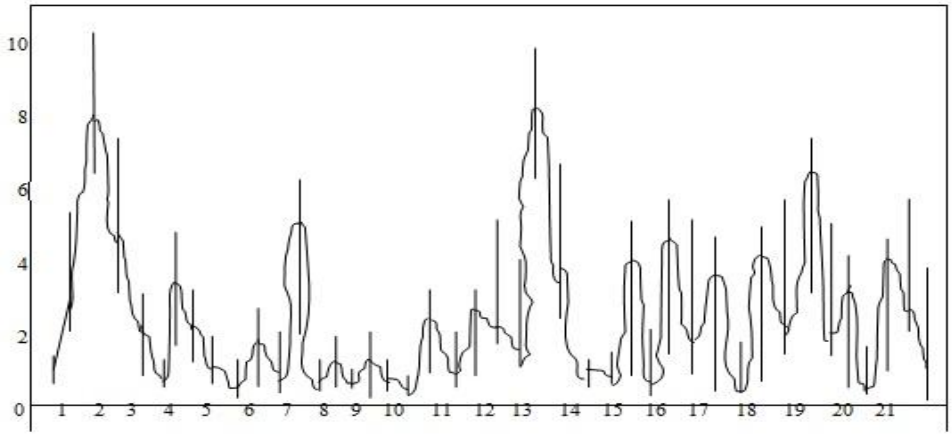

22 products and their releases versus observed (+) and predicted Fault Density connected by dash lines. Solid vertical lines are 90% predictive intervals for Faulty Density

Conceptually, the two basic assumptions behind this model are as follows that one is "*defect rates from different products in the same product life cycle phase are samples from a statistical universe of products coming from that development organization*" and the second is "*different releases from a given product are samples from a statistical universe of releases for that product".*

Dynamic Models: Reliability Growth Models

Software reliability estimation determines the current software reliability by applying statistical inference techniques to failure data obtained during system test or during system operation. Since reliability tends to improve over time during the software testing and operation periods because of removal of faults, the models are also called reliability growth models. They model the underlying failure process of the software, and use the observed failure history as a guideline, in order to estimate the residual number of faults in the software and the test time required to detect them. This can be used to make

release and development decisions. Most current software reliability models fall into this category. Details of these models can be found in Lyu [9], Musa et al. [8], Singpurwalla and Wilson [13], and Gokhale et al. [14].

Classes of Models:

I am describing a general class of models. In binominal models the total number of faults is some number N; the number found by time t has a binominal distribution with mean $\mu(t) = NF(t)$, where F (t) is the probability of a particular fault being found by time t. Thus, the number of faults found in any interval of time (including the interval (t, ∞) is also binominal. F (t) could be any arbitrary cumulative distribution function. Then, a general class of reliability models is obtained by appropriate parameterization of μ (t) and N.

Letting N be Poisson (with some mean υ) gives the related Poisson model; now, the number of faults found in any interval is Poisson, and for disjoint intervals these numbers are independent. Denoting the derivative of F by F′, rate at time t is $F'(t)$ /[1-F(t)]. These models are Markovian but not strongly Markoviaan, except when F is exponential; minor variations of this case were studied by Jelinski and Moranda [15], Shooman [16], Schneidewind [17], Musa [18], Moranda [19], and Goel and okomoto [20]. Schick and Wolverton [21] and crow [22] made F a Weibull distribution; Yamada et al. [23] made F a Gamma distribution; and Littlewood's model [24] is equivalent to aassuming F to be Pareto. Musa and Okumoto [25] assumed the hazard rate to be an inverse linear function of time; for this "Logarithmic Poisson" model the total number of failures is infinite. The success of a model is often judged by how well it fits an estimated reliability curve μ(t) to the observed "number of faults versus time" function.

Let us examine the real example plotted in above Figure from testing a large software system at a telecommunications research company. The system had been developed over years, and new releases were created and tested by the same development and testing groups respectively. In this figure, the elapsed testing time in staff day's t is plotted against the cumulative number of faults found for one of the releases. It is not clear whether there is some "total number" of bugs to be found, or whether the number found will continue to increase indefinitely. However, from data such as that in figure, an estimation of the tail of a distribution with a reasonable degree of precision is not possible. I also fit a special case of the general reliability growth model described above corresponding to N being Poisson and F being exponential.

Reliability Growth Modeling:

We have so far discussed a number of different kinds of reliability model of varying degrees of plausibility, including phase-based models depending upon a Raleigh curve, growth models like the Goel-okumoto model, etc. The growth models take us at input either failure time on failure count data, and fit a stochastic process model to reflect reliability growth. The differences between the models lie principally in assumptions made on the underlying stochastic process generating the data.

Most existing models assume that no explanatory variables are available. This assumption is assuredly simplistic, when the models are used to model a testing process, for all but small systems involving short development and life cycles. For large systems (e.g. greater than 100 KNCSL, i.e. thousands of non-commentary source lines) there are variables, other than time, that are very relevant. For example, it is typically assumed that the number of faults (found and unfound) in a system under test remains stable during testing. This implies that the code remains frozen during testing. However, this is rarely the case for large systems, since aggressive delivery cycles force the final phases of development to overlap with the initial stages of system test. Thus, the size of code and, consequently, the number of faults in a large system can vary widely during testing. If these changes in code size are not considered as a covariate, one is , at best, likely to have an increase in variability and a loss in predictive performance; at worst, a poor fitting model with unstable parameter estimates is likely. I briefly describe a general approach proposed by Dalal and McIntosh [28] for incorporating covariates along with a case study dealing with reliability modeling during product testing when code is changing.

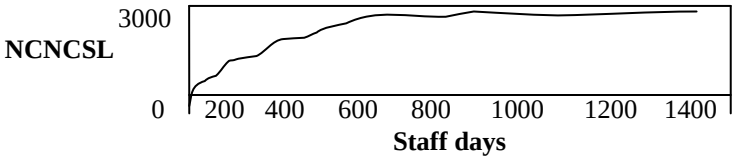

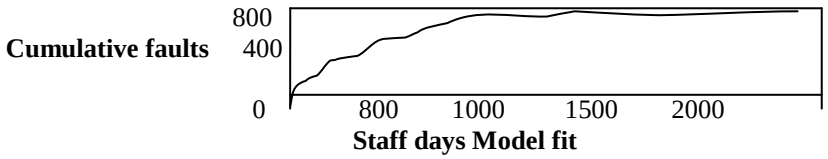

As an example, consider a new release of a large telecommunications system with approximately 7 million NCSL and 300 KNCNCSL (i.e. thousands of lines off non-commentary new or changed source lines). For a faster delivery cycle, the source code used for system test was updated every night throughout the test period. At the end of each of 198 calendar days in the test cycle, the number of faults found, NCNCSL, and thee staff time spent on testing were collected. Above figure portrays the growth of the system in terms of NCNCSL and of faults against staff time. The corresponding numerical data are providing in Dalal and McIntosh [28].

Assume that the testing process is observed at time t_i , i=0, 1,. . ., h, and at any given time the amount of time it takes to find specific bug is exponential with rate m. At time t_i, the total number of faults remaining in the system is Poisson with mean l_{i+1}, and NCNCSL is increased by an amount C_i. This change adds a Poisson number of faults with mean proportional to C, say qC_i, These assumption lead to the mass blance equation, namely that the expected number of faults in the system at t_i (after possible modification) is the expected number of faults in the system at t_{i-1} adjusted by the expected number found in the interval ($t_{i-1,}$ t_i) plus the faults introduced by the changes made at t_i:

$$l_{i+1} = l_i e^{-m(t_i - t_{i-1})} + qC_i$$

for i= 1, 2, 3….h. Note that q represent the number of new faults entering the system per additional NCNCSL, and l_1 represent the number of faults in the code at the starts of system test. Both of these parameters make it possible to differentiate between the new code added in the current release and the older code. For the example, the estimated parameters are q=0.025, m=0.002, and l_1=41. The fitted and the observed data are plotted against staff time in the given above figure (bottom). The fit is evidently very good. Of course, assessing the model on independent or new data is required for proper validation.

Now, I examine the efficacy of creating a statistical model. The estimate of q in the example is highly significant, both statistically and practically, showing the need for incorporating changes in NCNCSL as a covariate. Its numerical value implies that for every additional 10000 NCNCSL added to the system, 25 faults are being added as well. For these data, the predicted number of faults at the end of the test period is Poisson distributed with mean 145. Dividing this quantity by the total NCNCSL, gives 4.2 per 10000 NCNCSL as an estimated field fault density. These estimates of the incoming and outgoing quality are valuable in judging the efficacy of system testing and for deciding where resources should be allocated to improve the quality. Here, for example, system testing was effective, in that it removed 21 of every 25 faults. However, it raises another issue: 25 faults per 10000 NCNCSL entering system test may be too high and a plan ought to be considered to improve the incoming quality.

None of the above conclusion could have been made without using a statistical model. These conclusions are valuable for controlling and improving the process.

Conclusion:

In this paper, I am described key software reliability models for early stages, as well as for the test and operational phases and have given some examples of their uses. I have also proposed some new research directions useful to practitioners, which will lead to wider use of software reliability models.

References:

1. Mars Climate Orbiter Mishap Investigation Board Phase I Report, 1999, NASA.
2. Lee L. The day the phones stopped: how people get hurt when computers go wrong. New York: Donald I. Fine, Inc.; 1992
3. Dalal SR, Horgan JR, Kettenring JR. Reliable software and communication: software quality, reliability, and safety. IEEE J spec Areas Commun 1993; 12; 33-9.
4. Institute of Electrical and Electronics Engineers. ANSI/IEEE standard glossary of software engineering terminology, IEEE Std. 729-1991.
5. ISO 9000-3. Quality management and quality assurance standard- part 3: guidelines for the application of ISO 9001 to the development, supply and maintenance of software. Switzerland: ISO; 1991.
6. Paulk M, Curtis W, Chrises M, Weber C., Capability maturity model for software, version 1.1, CMU/SEI-93-TR-24.Carnegie Mellon University, Software engineering Institute, 1993.

7. Emam K, Jean Normand D, Melo W. Spice: the theory and practice of software process improvement and capability determination. IEEE computer Society Press; 1997.
8. Musa JD, Iannio A, Okumoto K. Software reliability measurement, prediction, application. New York: Mc Grawth-Hill; 1987.
9. Lyu MR, editor. Handbook of software reliability engineering. New York: MC Grawth- Hill; 1996.
10. Gaffney JD, Davis CF. An approach to estimating software errors and availability. SPC-TR-88-007, version 1.0,1988.
11. Dalal SR, and Ho YY. Predicting later phase faults knowing early stage data using hierarchical Bayes models. Technical Report, Telcordia Technologies, 2000.
12. Thomas D, Cook T, Cooper H, Cordray D, Hartmann H, Hedges L, Light R, Louis T, Mosteller F. Meta analysis for explanation: a casebook. New York: Russell Sage Fiundation; 1992.
13. Singpurwalla ND, Wilson SP. Software reliability modeling, Int Stat Rev 1994; 62 (3): 289-317.
14. Gokhale S, Marinos P, Trivedi K. Important milestones in software reliability modeling. In: Proceeding of software Engineering and knowledge Engineering (SEKE 96), 1996.p. 345-52.
15. Jelinski Z, Moranda PB. Software reliability research. In: Statistical computer performance evaluation. New York: Academic Press; 1972. P.465-84.
16. Shooman ML. Probabilistic models for software reliability prediction. In: Statistical computer performance evaluation. New York: Academic Press; 1972. P.485-502.
17. Schneidewind NF. Analysis of error processes in computer software. Sigplan Note 1975; 10(6): 337-46.
18. Mussa JD, A theory of software reliability and its application. IEEE Trans software Eng 1975; SE-1(3): 312-27.
19. Moranda PB. Predictions of software reliability during debugging. In: Proceeding of the Annual Reliability and Maintainability Symposium, Washington, DC, 1975.p 327-32.
20. Goal AL, Okumoto K. Time dependent error detection rate model for software and other performance measures. IEEE Trans Reliab 1979; R-28 (3): 206-11.
21. Schick GJ, Wolverton RW. Assessment of software reliability. In: Proceeding, Operation Research. Wurzburg Wien: Physica Verlag; 1973. P. 395-422.
22. Crow LH. Reliability analysis for complex repairable systems. In: Proschan F, Serfling RJ, editors. Reliability and biometry. Philadelphia: SIAM; 1974.p. 379-410.
23. Yamada S, Obha M, Osaki S. S-shaped reliability growth modeling for software error detection. IEEE Tran Reliab 1983; R-32 (5):475-8.
24. Littlewood B. Stochastic reliability growth: a model for fault removal in computer programs and hardware designs. IEEE Tran Reliab 1981; R-30 (4):313-20.
25. Musa JD, Okumoto K. A logarithmic Poisson executive time model for software reliability measurement. In: Proceeding seventh International conference on Engineering, Orlando (FL), 1984. p.230-8.
26. Miller D. Exponential order statistic models of software reliability growth. IEEE Trans software Eng 1986; SE-12(1):12-24.
27. Gokhale S, Lyu M, Trivedi K. Software reliability analysis incorporating debugging activities. In: Proceeding of International Symposium on software Reliability Engineering (ISSRE 98), 1998.P.202-11.
28. Dalal SR, Mcintosh AM. When to stop testing for large software system with changing code. IEEE Trans software Eng 1994; 20:318-23.

An Application of Linguistic Variables in Assignment Problem with Fuzzy Costs

[1]K.Ruth Isabels, Dr.G.Uthra[2]
Associate Professor
Department Of Mathematics
Saveetha Engineering College
Thandalam -602 105

Abstract
This paper presents an assignment problem with fuzzy costs, where the objective is to minimize the cost. Here each fuzzy cost is assumed as triangular or trapezoidal fuzzy number. Yager's ranking method has been used for ranking the fuzzy numbers. The fuzzy assignment problem has been transformed into a crisp one, using linguistic variables and solved by Hungarian technique. The use of linguistic variables helps to convert qualitative data into quantitative data which will be effective in dealing with fuzzy assignment problems of qualitative nature.
A numerical example is provided to demonstrate the proposed approach.

Key words: Fuzzy Assignment Problem, Fuzzy Numbers, Hungarian method, Ranking of Fuzzy numbers

Introduction

Much information that we need to deal with day to day life is vague, ambiguous, incomplete, and imprecise. Crisp logic or conventional logic theory is inadequate for dealing with such imprecision, uncertainty and complexity of the real world. It is this realization that motivated the evolution of fuzzy logic and fuzzy theory.
The fundamental concept of fuzzy theory is that any field X and theory Y can be fuzzified by replacing the concept of a crisp set in X and Y by that of a fuzzy set. Mathematically a fuzzy set [4] can be defined by assigning to each possible individual in the universe of discourse, a value representing its grade of membership in the fuzzy set. The membership function denoted by μ is defined from X to [0, 1].
An assignment problem (AP) is a particular type of transportation problem where n tasks (jobs) are to be assigned to an equal number of n machines (workers) in one to one basis such that the assignment cost (or profit) is minimum (or maximum). Hence, it can be considered as a balanced transportation problem in which all supplies and demands are equal, and the number of rows and columns in the matrix are identical.
Sakthi *et al* [1] adopted Yager's ranking method [2] to transform the fuzzy assignment problem to a crisp one so that the conventional solution methods may be applied to solve the AP. In this paper we investigate an assignment problem with fuzzy costs or times $\tilde{C}_{ij}$ represented by linguistic variables which are replaced by triangular or trapezoidal fuzzy numbers.

Definitions and Formulations

Triangular fuzzy number

A triangular fuzzy number $\hat{a}$ is defined by a triplet (a_1, a_2, a_3). The membership function is defined as

$\mu_{\hat{a}}(x) = \{ (x - a_1) / (a_2 - a_1)$ if $a_1 \le x \le a_2$
$(a_3 - x) / (a_3 - a_2)$ if $a_2 \le x \le a_3$
0 otherwise$\}$

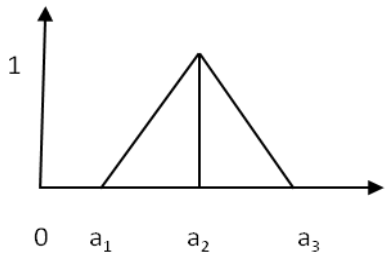

The triangular fuzzy number is based on three-value judgement: The minimum possible value a_1, the most possible value a_2 and the maximum possible value a_3

Trapezoidal fuzzy number

A trapezoidal fuzzy number â is a fuzzy number (a_1, a_2, a_3, a_4) and its membership function is defined as

$\mu_{â}(x) = \{ (x - a_1) / (a_2 - a_1)$ if $a_1 \le x \le a_2$

1 if $a_2 \le x \le a_3$

$(x - a_4) / (a_3 - a_4)$ if $a_3 \le x \le a_4$

0 otherwise$\}$

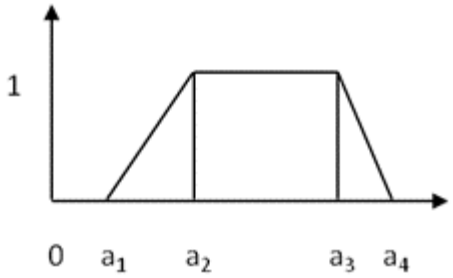

Linguistic Variable

A linguistic variable [3] is a variable whose values are linguistic terms. The concept of linguistic variable is applied in dealing with situations which are too complex or too ill-defined to be reasonably described in conventional quantitative expressions.

For example, '**height**; is a linguistic variable, its values can be very high, high, medium, low, very low etc., These values can also be represented by fuzzy numbers.

α-cut and strong α-cut

Given a fuzzy set A defined on X and any number $\alpha \in [0,1]$, the α- cut α_A, and the strong α-cut α_A+, are the crisp sets

$\alpha_A = \{x/A(x) \ge \alpha\}$

$\alpha_A+ = \{x/A(x) > \alpha\}$

The Proposed Method

The assignment problem can be stated in the form of n x n cost matrix $[c_{ij}]$ of real numbers as given in the following table:

Jobs → / Persons ↓	1	2	3	---j---	n
1	**c_{11}**	**c_{12}**	**c_{13}**	**--c_{1j}--**	**c_{1n}**
2	c_{21}	c_{22}	c_{23}	--c_{2j}--	c_{2n}
-	-	-	-	-	-
-	-	-	-	-	-
i	c_{i1}	c_{i2}	c_{i3}	--c_{ij}—	c_{in}
-	-	-	-	-	-
n	c_{n1}	c_{n2}	c_{n3}	c_{nj}	c_{nn}

Mathematically assignment problem can be stated as

Minimize $Z = \sum_{i=1}^{n}\sum_{j=1}^{n} c_{ij}x_{ij}$ i=1,2,……n: j=1,2,…….n

Subject to

$$\sum_{j=1}^{n} x_{ij} = 1, \quad i=1,2,\ldots\ldots n \qquad \ldots.(1)$$

$$\sum_{i=1}^{n} x_{ij} = 1, \quad j=1,2,\ldots\ldots n \qquad x_{ij} \in \{0,1\},$$

where x_{ij} = 1, if the i^{th} person is assigned the j^{th} job
0, otherwise
is the decision variable denoting the assignment of the person i to job j, C_{ij} is the cost of assigning the j^{th} job to the i^{th} person. The objective is to minimize the total cost of assigning all the jobs to the available persons. (One job to one person). When the costs $\tilde{C}_{ij}$ are fuzzy numbers, then the fuzzy assignment problem becomes

$$Y(\tilde{z}) = \sum_{i=1}^{n}\sum_{j=1}^{n} Y(\tilde{c}_{ij})x_{ij} \qquad \ldots\ldots(2)$$

subject to the same conditions (1).
We defuzzify the fuzzy cost coefficients into crisp ones by a fuzzy number ranking method. Yager's Ranking index [2] is defined by

$Y(\tilde{c}) = \int_0^1 0.5(c_\alpha^L + c_\alpha^U)$, where (c_α^L, c_α^U) is the α - level cut of the fuzzy number $\tilde{c}$.

The Yager's ranking index $Y(\tilde{c})$ gives the representative value of the fuzzy number $\tilde{c}$. Since $Y(\tilde{C}_{ij})$ are crisp values, this problem is obviously the crisp assignment problem of the form (1) which can be solved by Hungarian Method.
The steps of the proposed method are
Step 1: Replace the cost matrix C_{ij} with linguistic variables by triangular or trapezoidal fuzzy numbers.
Step 2: Find Yager's Ranking index.
Step 3: Replace Triangular or Trapezoidal numbers by their respective ranking indices.
Step 4: Solve the resulting AP using Hungarian technique to find optimal assignment.

Numerical Example
Let us consider a Fuzzy Assignment Problem with rows representing four persons W, X, Y, Z and columns representing the four jobs, Job1, Job2, Job3 and Job4 with assignment cost varying between 0$ to 50$. The cost matrix $[\tilde{C}_{ij}]$ is given whose elements are linguistic variables which are replaced by fuzzy numbers. The problem is then solved by Hungarian method to find the optimal assignment.

	1	2	3	4
W	extremely low	low	fairly high	extremely high
X	low	very low	high	very high
Y	medium	extremely high	very low	extremely low
Z	very high	low	fairly low	fairly low

Solution: The Linguistic variables showing the qualitative data is converted into quantitative data using the following table. As the assignment cost varies between 0$ to 50$ the minimum possible value is taken as 0 and the maximum possible value is taken as 50.

Extremely low	(0,2,5)
Very low	(1,2,4)
Low	(4,8,12)
Fairly low	(15,18,20)
Medium	(23,25,27)
Fairly High	(28,30,32)
High	(33,36,38)
Very High	(37,40,42)
Extremely High	(44,48,50)

The linguistic variables are represented by triangular fuzzy numbers
Now

$$\begin{array}{c} \\ \mathbf{W} \\ \mathbf{X} \\ \mathbf{Y} \\ \mathbf{Z} \end{array} \begin{array}{c} \begin{array}{cccc} \mathbf{1} & \mathbf{2} & \mathbf{3} & \mathbf{4} \end{array} \\ \begin{pmatrix} (0,2,5) & (4,8,12) & (28,30,32) & (44,48,50) \\ (4,8,12) & (1,2,4) & (33,36,38) & (37,40,42) \\ (23,25,27) & (44,48,50) & (1,2,4) & (0,2,5) \\ (37,40,42) & (4,8,12) & (15,18,20) & (15,18,20) \end{pmatrix} \end{array} \quad \ldots(3)$$

we calculate Y(0,2,5) by applying the Yager's Ranking Method.
The membership function of the triangular fuzzy number (0,2,5) is

$$\mu(x) = \begin{matrix} \frac{x-0}{2-0}, 0 \le x \le 2 \\ \frac{x-5}{2-5} 2 \le x \le 5 \end{matrix}$$

The α − cut of the fuzzy number (0,2,5) is $(c_\alpha^L, c_\alpha^U) = (2\alpha, 5-3\alpha)$ for which

$$Y(\tilde{c}_{11}) = Y(0,2,5) = \int_0^1 0.5(c_\alpha^L, c_\alpha^U)d\alpha = \int_0^1 0.5(2\alpha + 5 - 3\alpha)d\alpha = 2.25$$

Proceeding similarly, the Yager's indices for the costs $\tilde{c}_{ij}$ are calculated as:

$Y(\tilde{c}_{12}) = 8$, $Y(\tilde{c}_{13}) = 31$, $Y(\tilde{c}_{14}) = 47.5$, $Y(\tilde{c}_{21}) = 8$, $Y(\tilde{c}_{22}) = 1.75$, $Y(\tilde{c}_{23}) = 81.5$, $Y(\tilde{c}_{24}) = 79.5$, $Y(\tilde{c}_{31}) = 25$,

$Y(\tilde{c}_{32}) = 47.5$, $Y(\tilde{c}_{33}) = 1.75$, $Y(\tilde{c}_{34}) = 2.25$, $Y(\tilde{c}_{41}) = 79.5$, $Y(\tilde{c}_{42}) = 8$, $Y(\tilde{c}_{43}) = 35.5$, $Y(\tilde{c}_{44}) = 35.5$.

We replace these values for their corresponding $\tilde{c}_{ij}$ in (3) and solve the resulting assignment problem by using Hungarian method.

$$\begin{pmatrix} 2.25 & 8 & 31 & 47.5 \\ 8 & 1.75 & 35.75 & 39.75 \\ 25 & 47.5 & 1.75 & 2.25 \\ 39.75 & 8 & 17.75 & 17.75 \end{pmatrix}$$

Performing row reductions

$$\begin{pmatrix} 0 & 5.75 & 28.75 & 45.25 \\ 6.25 & 0 & 34 & 38 \\ 23.25 & 45.75 & 0 & 0.5 \\ 31.75 & 0 & 9.75 & 9.75 \end{pmatrix}$$

Performing column reductions

$$\begin{pmatrix} 0 & 5.75 & 28.75 & 44.75 \\ 6.25 & 0 & 34 & 37.5 \\ 23.25 & 45.75 & 0 & 0 \\ 31.75 & 0 & 9.75 & 9.25 \end{pmatrix}$$

The optimal assignment matrix is

$$\begin{pmatrix} 0 & 5.75 & 19.5 & 44.75 \\ 6.25 & 0 & 24.75 & 28.25 \\ 32.5 & 55 & 0 & 0 \\ 31.75 & 0 & 0.5 & 0 \end{pmatrix}$$

The optimal assignment schedule is $W \to 1, X \to 2, Y \to 3, Z \to 4$.

Conclusions:

In this paper, the assignment costs are considered as linguistic variables represented by fuzzy numbers. The fuzzy assignment problem has been transformed into crisp assignment problem using Yager's ranking indices. Hence we have shown that the fuzzy assignment problems of qualitative nature can be solved in an effective way. This technique can also be tried in solving other types of problems like Transportation problems, project scheduling problems, network flow problems etc.,

References

Journals

[1] Sakthi Mukherjee and Kajla Basu, "Application of Fuzzy Ranking Method for solving Assignment Problems with Fuzzy Costs", International Journal of Computational and Applied Mathematics, ISSN 1819-4966 Volume 5 Number 3(2010). Pp.359-368.

[2] Yager.R.R., "A procedure for ordering fuzzy subsets of the unit interval," Information Sciences, vol 24, pp. 143-161, 1981

[3] Zadeh, L. A., "The concept of a linguistic variable and its application to approximate reasoning", Part 1, 2 and 3, Information Sciences, Vol.8, pp.199- 249, 1975; Vol.9, pp.43-58, 1976.

[4] Zadeh L. A, Fuzzy sets, Information and Control 8 (1965) 338–353.

Book:

[1] Klir G. J, Yuan B, Fuzzy Sets and Fuzzy Logic: Theory and Applications, Prentice-Hall, International Inc., 1995.

[2] S.Baskar,Operations Research for Technical and Managerial courses, Technical Publishers.

Characterization of Paired Domination Number of a Graph

G. Mahadevan[1], A. Nagarajan[2] A. Rajeswari[3]

[1]Department of Mathematics, Anna University of Technology, Tirunelveli -627 002
[2]Department of Mathematics, V.O.Chidambaram College, Tuticorin- 628 008
[3]Aarupadai Veedu Institute of Technology, Paiyanoor, Chennai -603 104

Abstract:
Paired domination is a relatively interesting concept introduced by Teresa W. Haynes **[9]** recently with the following application in mind. If we think of each vertex s ∈ S, as the location of a guard capable of protecting each vertex dominated by S, then for a paired domination the guards location must be selected as adjacent pairs of vertices so that each guard is assigned one other and they are designated as a backup for each other. A set S ⊆ V is a paired dominating set if S is a dominating set of G and the induced subgraph <S> has a perfect matching. The paired domination number $\gamma_{pr}(G)$ is the minimum cardinality taken over all paired dominating sets in G. The minimum number of colours required to colour all the vertices so that adjacent vertices do not receive the same colour and is denoted by $\chi(G)$. In **[3]**, Mahadevan G proved that $\gamma_{pr} + \chi \leq 2n - 1$, and characterized the corresponding extremal graphs of order up to $2n - 5$. In this paper we characterize the classes of all graphs whose sum of paired domination number and chromatic number equals to $2n - 6$, for any $n \geq 4$.

Keywords: Paired domination number, Chromatic number AMS (2010) 05C69

1. Introduction

Throughout this paper, by a graph we mean a finite, simple, connected and undirected graph G(V, E). For notations and terminology, we follow **[11]**. The number of vertices in G is denoted by n. Degree of a vertex v is denoted by deg(v). We denote a cycle on n vertices by C_n, a path of n vertices by P_n, complete graph on n vertices by K_n. If S is a subset of V, then <S> denotes the vertex induced subgraph of G induced by S. A subset S of V is called a dominating set of G if every vertex in V-S is adjacent to at least one vertex in S. The domination number γ(G) of G is the minimum cardinality of all such dominating sets in G. A dominating set S is called a total dominating set ,if the induced subgraph <S> has no isolated vertices. The minimum cardinality taken over all total dominating sets in G is called the total domination number and is denoted by $\gamma_t(G)$. One can get a comprehensive survey of results on various types of domination number of a graph in **[10]**. The chromatic number χ(G) is defined as the minimum number of colors required to color all the vertices such that adjacent vertices receive the same color.

Recently many authors have introduced different types of domination parameters by imposing conditions on the dominating set and/or its complement. Teresa W. Haynes **[9]** introduced the concept of paired domination number of a graph. If we think of each vertex s ∈ S, as the location of a guard capable of protecting each vertex dominated by S, then for domination a guard protects itself, and for total domination each guard must be protected by another guard. For a paired domination the guards location must be selected as adjacent pairs of vertices so that each guard is assigned one other and they are designated as a backup for each other. Thus a paired dominating set S with matching M is a dominating set S = { $v_1, v_2, v_3, \ldots v_{2t-1}, v_{2t}$ } with independent edge set M = { $e_1, e_2, e_3, \ldots e_t$ } where each edge e_i is incident to two vertices of S, that is M is a perfect Matching in <S>. A set S ⊆ V is a paired dominating set if S is a dominating set of G and the induced subgraph <S> has a perfect matching. The paired domination number $\gamma_{pr}(G)$ is the minimum cardinality taken over all paired dominating sets in G

Several authors have studied the problem of obtaining an upper bound for the sum of a domination parameter and a graph theoretic parameter and characterized the corresponding extremal graphs. In **[8]**, Paulraj Joseph J and Arumugam S proved that $\gamma + \kappa \leq p$, where κ denotes the vertex connectivity of the graph. In **[7]**, Paulraj Joseph J and Arumugam S proved that $\gamma_c + \chi \leq p + 1$ and characterized the corresponding extremal graphs. They also proved similar results for γ and γ_t. In **[6]**, Mahadevan G Selvam A, Iravithul Basira A characterized the extremal of graphs for which the sum of the complementary connected domination number and chromatic number. In **[3]**, Mahadevan G proved that $\gamma_{pr} + \chi \leq 2n - 1$, and characterized the corresponding extremal graphs of order up to $2n - 5$. Motivated by the above results, in this paper we characterize all graphs for which $\gamma_{pr}(G) + \chi(G) = 2n - 6$ for any $n \geq 4$.

We use the following preliminary results and notations for our consequent characterization:

Theorem 1.1[9] For any connected graph G of order $n \geq 3$, $\gamma_{pr}(G) \leq n - 1$ and equality holds if and only if G = C_3, C_5 or subdivided star $S^*(K_{1,n})$

Notation 1.2 $C_3(n_1P_{m_1}, n_2P_{m_2}, n_3P_{m_3})$ is a graph obtained from C_3 by attaching n_1 times the pendent vertex of P_{m_1} (Path on m_1 vertices) to a vertex u_i of C_3 and attaching n_2 times the pendent vertex of P_{m_2} (Path on m_2 vertices) to a vertex u_j for $i \neq j$ of C_3 and attaching n_3 times the pendent vertex of P_{m_3} (Path on m_3 vertices) to a vertex u_k for $i \neq j \neq k$ of C_3.

Notation 1.3 $C_3(u(P_{m_1}, P_{m_2}))$ is a graph obtained from C_3 by attaching the pendent vertex of P_{m_1} (Path on m_1 vertices) and the pendent vertex of P_{m_2} (Paths on m_2 vertices) to any vertex u of C_3.

Notation 1.4 $K_5(n_1P_{m_1}, n_2P_{m_2}, n_3P_{m_3}, n_4P_{m_4}, n_5P_{m_5})$ is a graph obtained from K_5 by attaching n_1 times the pendent vertex of P_{m_1} (Paths on m_1 vertices) to a vertex u_i of K_5 and attaching n_2 times the pendent vertex of P_{m_2} (Paths on m_2 vertices) to a vertex u_j for $i \neq j$ of K_5 and attaching n_3 times the pendent vertex of P_{m_3} (Paths on m_3 vertices) to a vertex u_k for $i \neq j \neq k$ of K_5 and attaching n_4 times the pendent vertex of P_{m_4} (Paths on m_4 vertices) to a vertex u_l for $i \neq j \neq k \neq l$ of K_5 and attaching n_5 times the pendent vertex of P_{m_5} (Paths on m_5 vertices) to a vertex u_m for $i \neq j \neq k \neq l \neq m$ of K_5.

Notation 1.5 $C_3(P_n)$ is the graph obtained from C_3 by attaching the pendant edge of P_n to any one vertices of C_3 and $K_n(P_m)$ is the graph obtained from K_n by attaching the pendant edge of P_m to any one vertices of K_n. For $n \leq p$, $K_p(n)$ is the graph obtained from K_p by adding a new vertex and join it with n vertices of K_p.

2. Main Result

Theorem 2.1 For any connected graph G of order n, $n \geq 3$, $\gamma_{pr} + \chi = 2n - 6$ if only if $G \cong K_8$, C_6, P_6, $S^*(K_{1,3})$, $K_{1,4}$, $K_4(P_4)$, $K_4(P_3)$, $K_4(2P_2)$, $K_4(P_3, P_2, 0, 0)$, $K_4(P_2, P_2, 0, 0)$, $P_5(0, P_2, 0, 0, 0)$, $C_4(P_3)$, $C_4(P_2)$, $C_4(P_2, P_2, 0, 0)$, $C_4(P_2, 0, P_2, 0)$, $K_4(, P_2, P_2, P_2, 0)$, $K_6(1)$, $K_6(2)$, $K_6(3)$, $K_6(4)$, $K_6(5)$ or any one of the graphs shown in Figure 2.1.

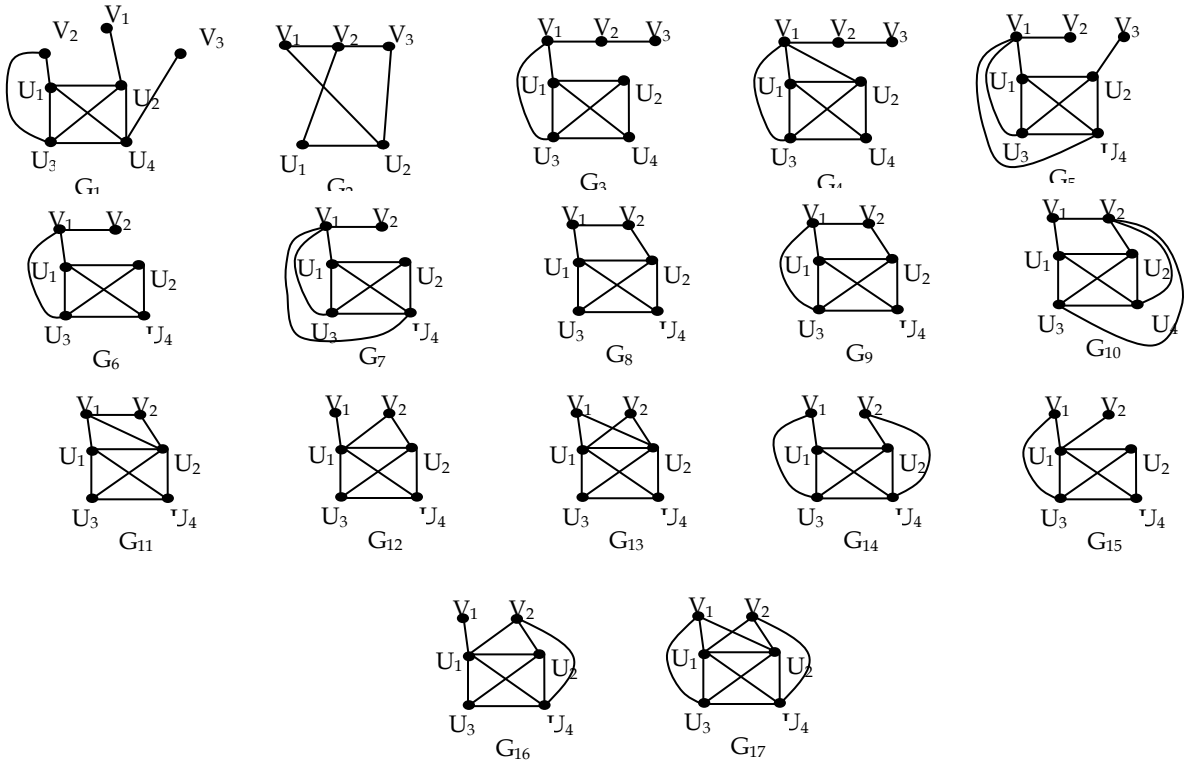

Figure 2.1

Proof: If G is any one the graphs given in the Figure 2.1, then it can be verified that $\gamma_{pr}(G) + \chi(G) = 2n - 6$. Conversely, let $\gamma_{pr}(G) + \chi(G) = 2n - 6$ .Then the various possible cases are (i) $\gamma_{pr}(G) = n - 1$ and $\chi(G) = n - 5$ (ii) $\gamma_{pr}(G) = n - 2$ and $\chi(G) = n - 4$ (iii) $\gamma_{pr}(G) = n - 3$ and $\chi(G) = n - 3$ (iv) $\gamma_{pr}(G) = n - 4$ and $\chi(G) = n - 2$ (v) $\gamma_{pr}(G) = n - 5$ and $\chi(G) = n - 1$ (vi) $\gamma_{pr}(G) = n - 6$ and $\chi(G) = n$.

Case i. $\gamma_{pr}(G) = n - 1$ and $\chi(G) = n - 5$.

Since $\gamma_{pr}(G) = n - 1$, By theorem 1.1, G is isomorphic to C_3, C_5 or subdivided star $S^*(K_{1,n})$. Hence $\chi(G) = 2$ or 3. If $\chi(G) = 3$ we have n = 8, which is a contradiction. If $\chi(G) = 2$ we have n = 7. Hence G is isomorphic to $S^*(K_{1,3})$.

Case ii. $\gamma_{pr}(G) = n - 2$ and $\chi(G) = n - 4$.

Since $\chi(G) = n - 4$, G contains a clique on n - 4 vertices or does not contain clique on n-4 vertices. Let G contains a clique on n - 4 vertices. Let $S = \{v_1, v_2, v_3, v_4\}$. Then the induced subgraph <S> has the following possible cases. <S> = K_4, $\overline{K_4}$, P_4, C_4, $K_{1,3}$, $K_2 \cup K_2$, $K_3 \cup K_1$, $\{K_4 - e\}$,) $C_3(1, 0, 0)$, $P_3 \cup K_1$, $K_2 \cup \overline{K}_2$.

Subcase i. Let <S> = K_4.

Since G is connected, there exists a vertex u_i of K_{n-4} which is adjacent to any one of $\{v_1, v_2, v_3, v_4\}$. Let u_i be adjacent to v_1 for some i in K_{n-4}. Then $\{v_1, u_i\}$ is an γ_{pr} set of G, so that $\gamma_{pr} = 2$ and n = 4, which is a contradiction. Hence no graph exists.

Subcase ii. Let <S> = $\overline{K_4}$.

Let $\{v_1,v_2,v_3,v_4\}$ be the vertices of $\overline{K_4}$. Since G is connected, two vertices of the $\overline{K_4}$ are adjacent to one vertex say u_i and the remaining two vertices of $\overline{K_4}$ are adjacent to one vertex say u_j for $i \neq j$. In this case $\{u_i, u_j\}$ for $i \neq j$ is a γ_{pr} set of G, so that $\gamma_{pr} = 2$ and n = 4, which is a contradiction. Hence no graph exists. Since G is connected, one vertex of $\overline{K_4}$ is adjacent to u_i and the remaining three vertices of $\overline{K_4}$ are adjacent to vertex say u_j for $i \neq j$. In this case $\{u_i, u_j\}$ for $i \neq j$ forms a γ_{pr} set of G, so that $\gamma_{pr} = 2$ and n = 4 , which is a contradiction. Hence no graph exists. Since G is connected, all the vertices of $\overline{K_4}$ are adjacent to one vertex say u_i in the vertices of K_{n-4} . In this case $\{u_i, u_j\}$ for $i \neq j$ is a γ_{pr} set of G, so that $\gamma_{pr} = 2$ and n = 4, which is a contradiction. Hence no graph exists. Since G is connected, two vertices of $\overline{K_4}$ is adjacent to u_i and one vertex is adjacent to u_j for $i \neq j$ and the remaining one vertex is adjancent to a vertex say u_k for $i \neq j \neq k$. In this case γ_{pr} set does not exist. If u_i is adjacent to v_1 and u_j for $i \neq j$ is adjacent to v_2 and u_k for $i \neq j \neq k$ is adjacent to v_3 and u_s for $i \neq j \neq k \neq s$ is adjacent to v_4. In this case $\{u_i, u_j, u_r, u_s\}$ for $i \neq j \neq k \neq s$ is a γ_{pr} set of G, so that $\gamma_{pr} = 4$ and n = 6, which is a contradiction.

Subcase iii. Let <S> = $P_4 = v_1v_2v_3v_4$.

Since G is connected, there exists a vertex u_i in K_{n-4} which is adjacent to v_1(or v_4) or v_2(or v_3). If u_i is adjacent to v_1, then $\{u_i, v_1, v_2, v_3\}$ forms a γ_{pr} set of G, so that $\gamma_{pr} = 4$ and n = 6. Hence $K = K_2 = u_1u_2$. If u_1 is adjacent to v_1. If $\deg(v_1) = 2 = \deg(v_2) = \deg(v_3)$, $\deg(v_4) = 1$, then $G \cong P_6$. Let u_1 be adjacent to v_1 and u_2 be adjacent to v_4. If $\deg(v_1) = 2 = \deg(v_2)$, $\deg(v_3) = 2 = \deg(v_4)$, then $G \cong C_6$. Let u_1 be adjacent to v_1 and u_2 be adjacent to v_2. If $\deg(v_1) = 2 = \deg(v_3)$, $\deg(v_2) = 3$, $\deg(v_4) = 1$, then $G \cong C_4(P_3)$. If u_i is adjacent to v_2, then $\{u_j, u_k, v_2, v_3\}$ forms a γ_{pr} set of G, so that $\gamma_{pr} = 4$ and n = 6 and hence $K = K_2 = u_1u_2$. Let u_1 be adjacent to v_2. If $\deg(v_1) = 1$, $\deg(v_2) = \deg(v_3) = 2$, $\deg(v_4) = 1$, then $G \cong S^*(K_{1,3})$. Let u_1 be adjacent to v_2 and u_2 be adjacent to v_3. If $\deg(v_1) = 1$, $\deg(v_2) = \deg(v_3) = 3$, $\deg(v_4) = 1$, then $G \cong C_4(P_2, P_2, 0, 0)$.

Subcase iv. Let <S> = $K_2 \cup K_2$.

Let v_1, v_2 be the vertices of K_2 and v_3, v_4 be the vertices of K_2. Since G is connected, there exists a vertex u_i in K_{n-4} which is adjacent to any one of $\{v_1, v_2\}$ and any one of $\{v_3, v_4\}$. Let u_i be adjacent to v_1 and v_3. In this case $\{u_i, u_j, v_1, v_3\}$ forms an γ_{pr} set of G so that $\gamma_{pr} = 4$ and n = 6 and hence $K = K_2 = u_1u_2$. Let u_1 be adjacent to v_1 and u_1 be adjacent to v_3, then $G \cong S^*(K_{1,3})$. Let u_1 be adjacent to v_1 and v_3 and u_2 be adjacent to v_4, then $G \cong C_4(P_3)$. Let u_2 be adjacent to v_2 and u_1 be adjacent to v_1 and v_3, then $G \cong S^*(K_{1,3})$. Since G is connected, there exists a vertex u_i in k_{n-4} which is adjacent to v_1 and u_j for $i \neq j$ is adjacent to v_3. In this case $\{u_i, u_j, v_1, v_3\}$ forms an γ_{pr} set of G so that $\gamma_{pr} = 4$ and n = 6 and hence $K = K_2 = u_1u_2$. Let u_1 be adjacent to v_3 and u_2 be adjacent to v_1, then $G \cong P_6$. Let u_1 be adjacent to v_3 and u_2 be adjacent to v_1 and v_4, then $G \cong C_4(P_3)$.

Subcase v. <S> = $K_2 \cup \overline{K}_2$.

Let v_1,v_2 be the vertices of $\overline{K}_2$ and v_3, v_4 be the vertices of K_2. Since G is connected, there exists a vertex u_i in K_{n-4}, which is adjacent to v_1 and v_2 and any one of $\{v_3,v_4\}$. Let u_i be adjacent to v_1, v_2, v_3. In this case $\{u_i,v_3\}$ is a γ_{pr} set of G so that $\gamma_{pr} = 2$ and n = 4, which is a contradiction . Hence no graph exists. Since G is connected, there exists a vertex u_i

in K_{n-4} which is adjacent to v_1 and there exists a vertex u_j for $i \neq j$ in K_{n-4} is adjacent to v_2 and v_3. In this case $\{u_i, u_j, u_k, v_3\}$ forms an γ_{pr} set of G so that $\gamma_{pr} = 4$ and n = 6 and hence $K = K_2 = u_1u_2$. Let u_1 be adjacent to v_1 and u_2 be adjacent to v_2 and v_3, then $G \cong S^*(K_{1,3})$. Since G is connected, there exists a vertex u_i in K_{n-4} which is adjacent v_1 and u_j for $i \neq j$ is adjacent to v_2 and u_k for $i \neq j \neq k$ is adjacent to v_3. In this case $\{u_i, u_j, u_k, v_4\}$ forms a γ_{pr} set of G. So that $\gamma_{pr} = 4$ and hence $K = K_2$, which is a ontradiction. Hence no graph exists.

Subcase vi. $<S> = P_3 \cup K_1$.

Let v_1, v_2, v_3 be the vertices of P_3 and v_4 be the vertex of K_1. Since G is connected, there exists a vertex u_i in K_{n-4} which is adjacent to any one of $\{v_1, v_2, v_3\}$ and v_4. In this case $\{u_i, v_1, v_2, v_4\}$ is a γ_{pr} set of G so that $\gamma_{pr} = 4$ and n = 6. Hence $K = K_2 = u_1u_2$. Let u_1 be adjacent to v_1 and v_4. If $\deg(v_1) = 2 = \deg(v_2)$, $\deg(v_4) = 1 = \deg(v_3)$ then $G \cong P_5(0, P_2, 0, 0, 0)$. Let u_1 be adjacent to v_1 and v_4 and u_2 be adjacent to v_2. If $\deg(v_1) = 2$, $\deg(v_2) = 3$, $\deg(v_3) = 1 = \deg(v_4)$, then $G \cong C_4(P_2, 0, P_2, 0)$. Since G is connected, there exists a vertex u_i in K_{n-4} which is adjacent to v_1 and u_j for $i \neq j$ is adjacent to v_4. In this case $\{u_i, u_j, v_1, v_2\}$ is a γ_{pr} set of G, so that $\gamma_{pr} = 4$ and n = 6 and hence $K = K_2 = u_1u_2$. Let u_1 be adjacent to v_1 and u_2 be adjacent to v_4, then $G \cong P_6$. Let u_1 be adjacent to v_1 and v_3 and u_2 be adjacent to v_4, then $G \cong C_4(P_3)$. Since G is connected, there exists a vertex u_i in K_{n-4}, which is adjacent to v_2 and v_4. In this case $\{u_i, v_2\}$is a γ_{pr} set of G, so that $\gamma_{pr} = 2$ and n = 4, which is a contradiction. Hence no graph exists. Since G is connected, there exists a vertex u_i in K_{n-4} which is adjacent to v_2 and u_j for $i \neq j$ is adjacent to v_4. In this case $\{u_i, u_j, u_k, v_2\}$ is a γ_{pr} set of G, so that $\gamma_{pr} = 4$ and n = 6 and hence $K = K_2 = u_1u_2$. Let u_1 be adjacent to v_2 and u_2 be adjacent to v_4. If $\deg(v_1) = 1$, $\deg(v_2) = 3$, $\deg(v_3) = \deg(v_4) = 1$, then $G \cong P_5(0, P_2, 0, 0, 0)$.

Subcase vii . $<S> = K_3 \cup K_1$.

Let v_1, v_2, v_3 be the vertices of K_3 and v_4 be the vertices of K_1. Since G is connected, there exists a vertex u_i in K_{n-4} is adjacent to any one of $\{v_1, v_2, v_3\}$ and v_4. In this case $\{u_i, v_2\}$ is a γ_{pr} set of G, so that $\gamma_{pr} = 2$ and n = 4, which is a contradiction. Hence no graph exists. Since G is connected, there exists a vertex u_i in K_{n-4} which is adjacent to v_2 and u_j for $i \neq j$ is adjacent to v_4. In this case $\{u_i, u_j, u_k, v_2\}$ for $i \neq j \neq k$ is a γ_{pr} set of G, so that $\gamma_{pr} = 4$ and n = 6 and hence $K = K_2$, which is a contradiction. Hence no graph exists.

Subcase viii. $<S>=K_4-\{e\}$

Let v_1, v_2, v_3, v_4 be the vertices of K_4. Let $\{e\}$ be any one the edge inside the cycle C_4. Since G is connected, there exists a vertex u_i in K_{n-4} which is adjacent to v_1. In this case $\{u_i, v_1\}$ is a γ_{pr} set of G, so that $\gamma_{pr} = 2$ and n = 4, which is a contradiction. Hence no graph exists.

Subcase ix. $<S> = C_3(1, 0, 0)$.

Let v_1, v_2, v_3 be the vertices of C_3 and let v_4 be adjacent to v_1. Since G is connected, there exists a vertex u_i in K_{n-4} which is adjacent to v_2. In this case $\{u_i, u_j, v_1, v_2\}$ is a γ_{pr} set of G, so that $\gamma_{pr} = 4$ and n = 6, which is a contradiction. Hence no graph exists.

Subcase x. $<S> = K_{1,3}$.

Let v_1 be the root vertex and v_2, v_3, v_4 are adjacent to v_1. Since G is connected, there exists a vertex u_i in K_{n-4} which is adjacent to v_1. In this case $\{u_i, v_1\}$ is a γ_{pr} set of G, so that $\gamma_{pr} = 2$ and n = 4, which is a contradiction. Hence no graph exists. Since G is connected, there exists a vertex u_i in K_{n-4} which is adjacent to any one of $\{v_2, v_3, v_4\}$. Let u_i be adjacent to v_2. In this case $\{u_i, u_j, v_2, v_1\}$is a γ_{pr} set of G, so that $\gamma_{pr} = 4$ and n = 6, and hence $K = K_2 = u_1u_2$. Let u_1 be adjacent to v_2. If $\deg(v_1) = 3$, $\deg(v_3) = \deg(v_4) = 1$, $\deg(v_2) = 2$, then $G \cong P_5(0, P_2, 0, 0, 0)$. Let u_1 be adjacent to v_2 and v_3. If $\deg(v_1) = 3$, $\deg(v_2) = 2 = \deg(v_3)$, $\deg(v_4) = 1$, then $G \cong C_4(P_2, 0, P_2, 0)$. Let u_1 be adjacent to v_2 and v_4. If $\deg(v_1) = 3$, $\deg(v_2) = 2 = \deg(v_4)$, $\deg(v_3) = 1$, then $G \cong C_4(P_2, 0, P_2, 0)$.

Subcase xi. $<S> = C_4$.

In this case it can be verified that no new graph exists.

If G does not contain clique on n-4 vertices, then it can be verified that no new graph exists.

Case iii. $\gamma_{pr} = n - 3$ and $\chi = n - 3$.

Since $\chi = n - 3$, G contains a clique K on n - 3 vertices or does not contain a clique K on n - 3 vertices. Let G contains a clique K on n - 3 vertices. Let $S = V(G) - V(K) = \{v_1, v_2, v_3\}$. Then the induced subgraph $<S>$ has the following possible cases. $<S> = K_3$, $\overline{K}_3$, P_3, $K_2 \cup K_1$.

Subcase i. $<S> = K_3$.

Since G is connected, there exists a vertex u_i in K_{n-3} which is adjacent to any one of $\{v_1, v_2, v_3\}$. Let u_i be adjacent to v_1, then $\{u_i, v_1\}$is a γ_{pr} set of G, so that $\gamma_{pr} = 2$ and n = 5, which is a contradiction. Hence no graph exists.

Subcase ii. $<S> = \bar{K}_3$.

Since G is connected, one of the vertices of K_{n-3} say u_i is adjacent to all the vertices of S (or) u_i be adjacent to v_1 ,v_2 and u_j be adjacent to v_3 ($i \neq j$) (or) u_i be adjacent v_1 and u_j be adjacent to v_2 and u_k be adjacent to v_3 ($i \neq j \neq k$). If u_i for some i is adjacent to all the vertices of S, then $\{u_i, v\}$ for some v in K_{n-3} is a γ_{pr} set of G, so that $\gamma_{pr} = 2$ and n = 5 and hence $K = K_2 = u_1u_2$. If u_1 is adjacent to v_1, v_2 and v_3, then $G \cong K_{1,4}$. If u_i is adjacent to v_1 and u_j for $i \neq j$ is adjacent to v_2 and v_3, then $\{u_i,u_j\}$ is an γ_{pr} set of G, so that $\gamma_{pr} = 2$ and n = 5. Hence $K = K_2 = u_1u_2$. If u_1 is adjacent to v_1 and v_2 and u_2 is adjacent to v_3, then $G \cong S^*(K_{1,3})$. Since G is connected, there exists a vertex u_i in K_{n-3} which is adjacent to v_1 and u_j for $i \neq j$ in K_{n-3} is adjacent to v_2 and u_k for $i \neq j \neq k$ in K_{n-3}, which is adjacent to v_3. In this case $\{u_i, u_j, u_k, v\}$ for some v in K_{n-3} is a γ_{pr} set of G, so that $\gamma_{pr} = 4$ and n = 7, and hence $K = K_4 = <u_1, u_2, u_3, u_4>$. Let u_1 be adjacent to v_1 and u_2 be adjacent to v_2 and u_4 be adjacent to v_3. If $\deg(v_1) = \deg(v_2) = \deg(v_3) = 1$, then $G \cong K_4(, P_2, P_2, P_2, 0)$. Let u_1 be adjacent to v_1 and u_2 be adjacent to v_2 and u_3 be adjacent to v_1 and u_4 be adjacent to v_3. If $\deg(v_1) = 2$, $\deg(v_2) = \deg(v_3) = 1$, , then $G \cong G_1$.

Subcase iii. $<P_3> = v_1v_2v_3$.

Since G is connected, there exists a vertex u_i in K_{n-3} which is adjacent to v_1 (or equivalently v_3) or v_2. If u_i is adjacent to v_2, then $\{u_i, v_2\}$ is a γ_{pr} set of G, so that $\gamma_{ip} = 2$ and n = 5. Hence $K = K_2 = u_1u_2$. If u_1 is adjacent to v_2, then $G \cong S^*(K_{1,3})$. If u_1 is adjacent to v_2 and u_2 is adjacent to v_3, then $G \cong C_4(P_2)$. If u_1 is adjacent to v_2 and u_2 is adjacent to v_1 and v_3. If deg $(v_1) = 2$, $\deg(v_2) = 3$, $\deg(v_3) = 2$, then $G \cong G_2$. Since G is connected, there exists a vertex u_i in K_{n-3} which is adjacent to v_1, then $\{u_i,u_j,v_1,v_2\}$ for some $i \neq j$ is a γ_{pr} set of G, so that $\gamma_{pr} = 4$ and n = 7 and hence $K = K_4 = < u_1, u_2, u_3, u_4 >$. Let u_1 be adjacent to v_1, then $G \cong K_4(P_4)$. Let u_1 be adjacent to v_1 and u_3 be adjacent to v_1. If $\deg(v_1) = 3$, $\deg(v_2) = 2$, $\deg(v_3) = 1$, then $G \cong G_3$. Let u_1 be adjacent to v_1 and u_3 be adjacent to v_1 and u_2 be adjacent to v_1. If $\deg(v_1) = 4$, $\deg(v_2) = 2$, $\deg(v_3) = 1$, then $G \cong G_4$.

Subcase iv. $<S> = K_2 \cup K_1$.

Let v_1, v_2 be the vertices of K_2 and v_3 be the isolated vertex. Since G is connected, there exists a vertex u_i in K_{n-3} which is adjacent to any one of $\{v_1, v_2\}$ and $\{v_3\}$ (or) u_i is adjacent to any one of $\{v_1, v_2\}$ and u_j for $i \neq j$ is adjacent to v_3. In this case $\{v_1, v_2, v_3, u_j\}$ is a γ_{pr} set of G, so that $\gamma_{pr} = 4$ and n = 7 and hence $K = K_4 = <u_1,u_2,u_3,u_4>$. Let u_1 be adjacent to v_1 and u_2 be adjacent to v_3. If $\deg(v_1) = 2$, $\deg(v_2) = 1 = \deg(v_3)$, then $G \cong K_4(P_3, P_3, 0, 0)$. Let u_1 be adjacent to v_1 and u_2 be adjacent to v_3 and u_3 be adjacent to v_1 and u_4 be adjacent to v_1. If $\deg(v_1) = 4$, $\deg(v_2) = 1 = \deg(v_3)$, then $G \cong G_5$. If a vertex u_i in K_{n-3} is adjacent to v_1&v_3 then $\{u_i,v_1\}$ is a γ_{pr} set of G, so that $\gamma_{pr}=2$ and n=5 and hence $K = K_2 = <u_1, u_2>$. Let u_1 be adjacent to v_1 and v_3. If $\deg(v_1) = 2$, $\deg(v_2) = 1 = \deg(v_3)$ then $G \cong S^*(K_{1,3})$.

If G does not contain a clique K on n - 3 vertices, then it can be verified that no new graph exists.

Case v. $\gamma_{pr} = n - 4$ and $\chi = n - 2$.

Since $\chi = n - 2$, G contains a clique K on n - 2 vertices or does not contain a clique K on n - 2 vertices. Let G contains a clique K on n - 2 vertices. Let $S = V(G) - V(K) = \{V_1, V_2\}$. Then $<S> = K_2, \bar{K}_2$.

Subcase i. $<S> = K_2$.

Since G is connected, there exists a vertex u_i in K_{n-2} is adjacent to any one of $\{v_1, v_2\}$ then $\{u_i, v_1\}$ is a γ_{pr} set of G, so that $\gamma_{pr} = 2$ and n = 6 and hence $K = K_4 = <u_1, u_2, u_3, u_4>$. Let u_1 be adjacent to v_1. If $\deg(v_1) = 2$, $\deg(v_2) = 1$, then $G \cong K_4(P_3)$. Let u_1 be adjacent to v_1 and u_3 be adjacent to v_1. If $\deg(v_1) = 3$, $\deg(v_2) = 1$, then $G \cong G_6$. Let u_1 be adjacent to v_1 and u_3 be adjacent to v_1 and u_4 be adjacent to v_1. If $\deg(v_1) = 4$, $\deg(v_2) = 1$ then $G \cong G_7$. Let u_1 be adjacent to v_1 and u_2 be adjacent to v_2. If $\deg(v_1) = 2 = \deg(v_2)$, then $G \cong G_8$. Let u_1 be adjacent to v_1 and u_2 be adjacent to v_2 and u_3 be adjacent to v_1. If $\deg(v_1) = 3$, $\deg(v_2) = 2$, then $G \cong G_9$. Let u_1 be adjacent to v_1 and u_2 be adjacent to v_2 and u_3 be adjacent to v_2 and u_4 be adjacent to v_2. If $\deg(v_1) = 2$, $\deg(v_2) = 4$, then $G \cong G_{10}$. Let u_1 be adjacent to v_1 and u_2 be adjacent to v_1 and v_2. If $\deg(v_1) = 3$, $\deg(v_2) = 2$, $G \cong G_{11}$.

Subcase ii. Let $<S> = \bar{K}_2$.

Since G is connected, v_1 and v_2 are adjacent to a common vertex say u_i of K_{n-2} (or) v_1 is adjacent to u_i for some i and v_2 is adjacent to u_j for some $i \neq j$ in K_{n-2}. In both cases $\{u_i, u_j\}$ is a γ_{pr} set of G, so that $\gamma_{pr} = 2$ and n = 6 and hence K = $K_4 = \langle u_1, u_2, u_3, u_4 \rangle$. Let u_1 be adjacent to v_1 and u_2 be adjacent to v_2. If $\deg(v_1) = 1 = \deg(v_2)$, then $G \cong K_4(P_2,P_2,0,0)$. Let u_1 be adjacent to v_1 and v_2. If $\deg(v_1) = 1 = \deg(v_2)$, then $G \cong K_4(2P_2)$. Let u_1 be adjacent to v_1 and v_2 and u_2 be adjacent to v_2. If $\deg(v_2) = 2$, then $G \cong G_{12}$. Let u_1 be adjacent to v_1 and v_2 and u_2 be adjacent to v_1 and v_2. If $\deg(v_1) = 2 = \deg(v_2)$, then $G \cong G_{13}$. Let u_1 be adjacent to v_1 and u_2 be adjacent to v_2 and u_3 be adjacent to v_1 and u_4 be adjacent to v_2. If $\deg(v_1) = 2 = \deg(v_2)$, then $G \cong G_{14}$. Let u_1 be adjacent to v_1 and v_2 and u_3 be adjacent to v_1. If $\deg(v_1) = 2$, $\deg(v_2) = 1$, then $G \cong G_{15}$. Let u_1 be adjacent to v_1 and v_2 and u_2 be adjacent to v_2 and u_4 be adjacent to v_2. If $\deg(v_1) = 1$, $\deg(v_2) = 3$, then $G \cong G_{16}$. Let u_1 be adjacent to v_1 and v_2 and u_2 be adjacent to v_1 and v_2 and u_3 be adjacent to v_1 and u_4 be adjacent to v_2. If $\deg(v_1) = \deg(v_2) = 3$, then $G \cong G_{17}$.

If G does not contain a clique K on n - 2 vertices, then it can be verified that no new graph exits.

Case v. $\gamma_{pr} = n - 5$ and $\chi = n - 1$.

Since $\chi = n - 1$, G contains a clique K on n - 1 vertices. Let v_1 be the vertex not on K_{n-1}. Since G is connected, there exists a vertex v_1 is adjacent to one vertex u_i of K_{n-1}. In this case $\{u_i,v_1\}$ is a γ_{pr} set of G, so that $\gamma_{pr} = 2$ and n = 7 and hence $K = K_6 = \langle u_1,u_2,u_3,u_4,u_5,u_6 \rangle$. Let u_1 be adjacent to v_1. If $\deg(v_1) = 1$, then $G \cong K_6(1)$. Let u_1 be adjacent to v_1 and u_2 be adjacent to v_1. If $\deg(v_1) = 2$, then $G \cong K_6(2)$. Let u_1 be adjacent to v_1 and u_2 be adjacent to v_1 and u_3 be adjacent to v_1. If $\deg(v_1) = 3$, then $G \cong K_6(3)$. Let u_1 be adjacent to v_1 and u_2 be adjacent to v_1 and u_3 be adjacent to v_1 and u_4 be adjacent to v_1. If $\deg(v_1) = 4$, then $G \cong K_6(4)$. Let u_1 be adjacent to v_1 and u_2 be adjacent to v_1 and u_3 be adjacent to v_1 and u_4 be adjacent to v_1 and u_5 be adjacent to v_1. If $\deg(v_1) = 5$, then $G \cong K_6(5)$.

Case vi. $\gamma_{pr} = n - 6$ and $\chi = n$.

Since $\chi = n$, $G = K_n$. But for K_n, $\gamma_{pr} = 2$, so that n = 8. Hence $G \cong K_8$.

References:

[1] Berge C. (1962): Theory of graphs and its applications, Methuen London.

[2] Harary F. (1972) : Graph Theory, Addison Wesley Reading Mass.

[3] Mahadevan G. (2005): On domination theory and related concepts in graphs, Ph.D. thesis, Manonmaniam Sundaranar University, Tirunelveli, India.

[4] Mahadevan G, Selvam Avadayappan and Amra Parveen M. (2008): Graphs whose sum of independent domination number and chromatic number equals to 2n-6 for any n > 3, International Journal of Physical Sciences, (Ultra Science), Vol. 20(3)M, 757-762.

[5] Mahadevan G, Selvam A. and Hajmeral (2008): On connected efficient domination number of a graph, International Journal of Intelligent Information Processing, 2(2), July-December, pp.313-319.

[6] Mahadevan G, Selvam Avadayappan and Iravithual Basira A. (2008): Sum of complementary connected domination number and chromatic number of a graph, International Journal of Computing and Mathematical Applications, Vol. 2, No. 1-2, pp.159-169.

[7] Paulraj Joseph J. and Arumugam. S. (1995): Domination in graphs. International Journal of Management Systems, 11: 177-182.

[8] Paulraj Joseph J. and Arumugam S. (1992): Domination and connectivity in graphs, International Journal of Management and systems, 8 No.3: 233-236.

[9] Teresa W. Haynes (2001): Paired domination in graphs, Congr. Numer 150.

[10] Teresa W. Haynes, Stephen T. Hedetniemi and Peter J. Slater (1998): Domination in graphs, Advanced Topics, Marcel Dekker, New York.

[11] Teresa W. Haynes, Stephen T. Hedetniemi and Peter J.Slater (1998): Fundamentals of domination in graphs, Marcel Dekker, New York.

The Role of Decision Tree Technique for Automating Intrusion Detection System

Neha Jain, Shikha Sharma
Department of Software Engineering, Suresh Gyan Vihar University, Jaipur
Department of Computer Science & Information Technology, ECA, Ajmer

Abstract-Security of computers and the networks that connect them is increasingly becoming of great significance. Intrusion detection is a mechanism of providing security to computer networks. Although there are some existing mechanisms for Intrusion detection, there is need to improve the performance. Data mining techniques, such as decision tree analysis, offers a semi-automated approach to detect threats. In this paper, decision tree technique is applied on a small set of network data. Then build a decision tree model, and incorporates the model's logic into snort signatures or firewall rules.

Keywords: Denial of Service, Data mining, IDS, Network security, decision tree

I. INTRODUCTION

One of the main challenges in the security management of large-scale high-speed networks is the detection of suspicious anomalies in network traffic patterns due to Distributed Denial of Service (DDoS) attacks or worm propagation [1][2] A secure network must provide the following:

1. Data confidentiality: Data that are being transferred through the network should be accessible only to those that have been properly authorized.
2. Data integrity: Data should maintain their integrity from the moment they are transmitted to the moment they are actually received. No corruption or data loss is accepted either from random events or malicious activity.

3. Data availability: The network should be resilient to Denial of Service attacks.

An intrusion detection system (IDS) inspects all inbound and outbound network activity and identifies suspicious patterns that may indicate a network or system attack from someone attempting to break into or compromise a system. When a potential attack is detected the IDS logs the information and sends an alert to the console. IDS try to find data packets that contain any known intrusion-related signatures or anomalies related to Internet protocols.

II IDS TAXONOMY

The goal of IDS is to detect malicious traffic. In order to accomplish this, the IDS monitor all incoming and outgoing traffic. There are several approaches on the implementation of IDS. Among those, two are the most popular [11]:

***A. Anomaly detection*:** This technique is based on the detection of traffic anomalies. The deviation of the monitored traffic from the normal profile is measured. Various different implementations of this technique have been proposed, based on the metrics used for measuring traffic profile deviation.

B. Misuse/Signature detection: This technique looks for patterns and signatures of already known attacks in the network traffic [12]. A constantly updated database is usually used to store the signatures of known attacks. The way this technique deals with intrusion detection resembles the way that anti-virus software operates. [3][4][5][6][7].

III. DRAWBACKS OF IDS

Intrusion Detection Systems (IDS) have become a standard component in security infrastructures as they allow network administrators to detect policy violations.

Current IDS have a number of significant drawbacks:

1. *Current IDS* are usually tuned to detect known service level network attacks. This leaves them vulnerable to original and novel malicious attacks.

2. *Data overload:* Another aspect which does not relate directly to misuse detection but is extremely important is how much data an analyst can efficiently analyze. That amount of data he needs to look at seems to be growing rapidly. Depending on the intrusion detection tools employed by a company and its size there is the possibility for logs to reach millions of records per day.

3. *False positives:* A common complaint is the amount of false positives a IDS will generate. A false positive occurs when normal attack is mistakenly classified as malicious and treated accordingly.

4. *False negatives:* This is the case where an IDS does not generate an alert when an intrusion is actually taking place. (Classification of malicious traffic as normal)

Data mining can help improve intrusion detection by addressing each and every one of the above mentioned problems.

IV. DATA MINING: DEFINITION

Data mining is, at its core, pattern finding. Data miners are experts at using specialized software to find regularities (and irregularities) in large data sets. Here are a few specific things that data mining might contribute to an intrusion detection project:

- Remove normal activity from alarm data to allow analysts to focus on real attacks

- Identify false alarm generators and "bad" sensor signatures
- Find anomalous activity that uncovers a real attack
- Identify long, ongoing patterns (different IP address, same activity)

To accomplish these tasks, data miners use one or more of the following techniques [8][9][10]:

- *Data summarization* with statistics, including finding outliers
- *Visualization*: presenting a graphical summary of the data
- *Clustering* of the data into natural categories
- *Association rule discovery*: defining normal activity and enabling the discovery of anomalies
- *Classification*: predicting the category to which a particular record belongs

V. DECISION TREE: A CLASSIFICATION TECHNIQUE

A decision tree is defined as "a predictive modeling technique from the fields of machine learning and statistics that builds a simple tree-like structure to model the underlying pattern [of data]".

Decision trees are one example of a classification algorithm. Classification is a data mining technique that assigns objects to one of several predefined categories. From an intrusion detection perspective, classification algorithms can characterize network data as malicious, benign, scanning, or any other category of interest using information like source/destination ports, IP addresses, and the number of bytes sent during a connection.

VI. WHY USE DECISION TREE

Decision trees is a viable tool in the intrusion detection toolkit, the technique needs to satisfy a minimum set of requirements. The technique needs to be beneficial to the intrusion analysis mission and produce real results for an organization.

In addition, decision trees must be unique among existing tools. If other tools exist with the same functionality provided by decision trees, then decision trees may be redundant and unnecessary.

VII. USING DECISION TREE FOR INTRUSION DETECTION

Two prerequisites for the analysis are data collection (i.e. identifying and collecting data of interest) and tool acquisition and selection (i.e. identifying and deploying data mining tools). The gathered data requires a pre-processing phase to move it into the form necessary for decision tree algorithms. After the data is processed, decision trees can be trained using the processed data and tools. Running and analyzing the result of this data is an important next step to understand the resulting model and its rule sets. The final step is using the results of the analysis to run the decision rules in real-time.

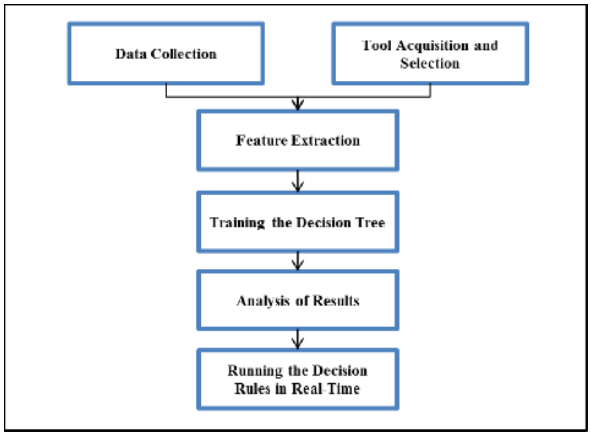

Fig 1: Process to implement decision tree for Intrusion Detection

VIII. IMPLEMENTATION

1. Implementing decision trees can require some network data. Download the following files from http://www.openpacket.org/
   example.com-3.pcap
   example.com-4.pcap
   example.com-5.pcap
   zeus-sample-3.pcap (botnet traffic)
2. Implementing decision trees can require various tools:

- *Feature extraction tools*: used during the data pre-processing phase. For this we use tcptrace tool to perform feature extraction from pcap files.
  Download and install tcptrace from http://www.tcptrace.org/
- *Data mining analysis tool*: Weka is used for this purpose. Of all the open-source tools, Weka has been described as "perhaps the best-known open-source machine learning and data mining environment"
  Download and install Weka from http://www.cs.waikato.ac.nz/ml/weka/

3. Now the Feature Extraction tool is used to collect and structure the features from a dataset in a format that can be used for training the decision tree.

Steps:

i) For each pcap file, run the command:
tcptrace --csv -l filename1.pcap > filename1.csv
(where filename is the name of the pcap file)

ii) From each csv file, remove rows 1-8 (the row before conn #)

iii) From each csv file, delete the following columns EXCEPT

- port_a
- port_b
- total_packets_a2b
- total_packets_b2a
- unique_bytes_sent_a2b
- unique_bytes_sent_b2a

iv) Add new column called "class" to each spreadsheet. Fill in each cell of the new column with either "normal" or "malicious".

v) Copy and paste all cells from the spreadsheets into a single csv file called analysis_of_traffic.csv

4. Run Weka

i) From the Weka GUI Chooser, click on the Explorer button

ii) From the Weka Explorer GUI, click on Open File.

iii) Using the explorer, open the traffic_analysis.csv file

iv) Click on the Classify tab at the top of the Weka Explorer GUI
Click on the "choose" button to select a classifier
From the menu, expand the trees icon
Click on the J48 Tree classifier

v) On the Classify GUI, click on the Start button to start the classifier

5. Weka Output

This decision tree in the output listed above states that connections with port_a <= 1049 and port_b <= 445 are malicious, otherwise the connection is normal.
For reference, tcptrace defines port_a as the port of the machine initiating the connection and port_b as the port of the machine receiving the connection.

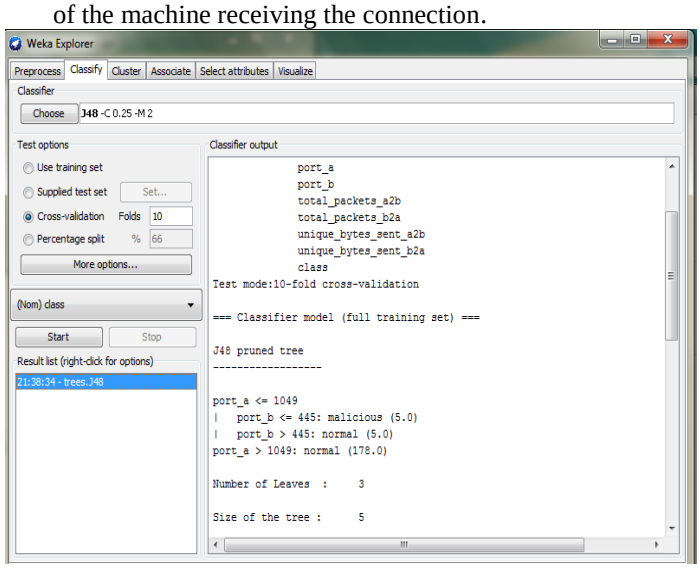

Fig 2: Weka output

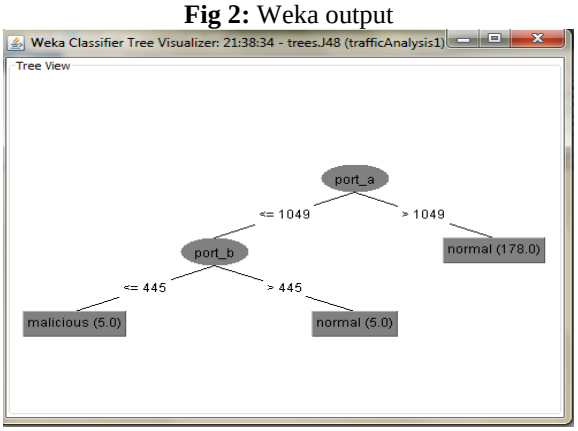

Fig 3: Tree view

IX. CONCLUSIONS

This paper has presented a decision tree technique that categorize new piece of information into a number of predefined categories. Decision tree uses a pre-classified dataset to learn to categorize data based on existing trends and patterns. After the tree is created, the logic from the decision tree can be incorporated into number of intrusion detection technologies including firewalls and IDS signatures.

With the increasing incidents of cyber attacks, building an effective intrusion detection models with good accuracy and real-time performance are essential. Data mining is relatively new approach for intrusion detection. More data mining techniques should be investigated and their efficiency should be evaluated as intrusion detection models.

REFERENCES

[1] Christos Douligeris, Aikaterini Mitrokotsa, "DDoS attacks and defense mechanisms: classification and state-of-the-art" ,Computer Networks: The International Journal of Computer and Telecommunications Networking,Vol. 44, Issue 5 , pp: 643 - 666, 2004.

[2] Z. Chen, L. Gao, K. Kwiat, Modeling the spread of active worms,Twenty- Second Annual Joint Conference of the IEEE Computer and Communications Societies (INFOCOM), Vol. 3, pp. 1890 1900, 2003.

[3] Mithcell Rowton, Introduction to Network SecurityIntrusion Detection,December 2005.

[4] Biswanath Mukherjee, L.Todd Heberlein, Karl N.Levitt, "Network Intrusion Detection",IEEE, June 1994.

[5] Presentation on Intrusion Detection Systems, Arian Mavriqi.

[6] Intrusion Detection Methodologies Demystified, Enterasys Networks TM.

[7] Protocol Analysis VS Pattern matching in Network and Host IDS, 3rd Generation Intrusion Detection Technology from Network ICE

[8] Han, J. and Kamber, M. (2000). Data Mining: Concepts and
Techniques, Morgan Kaufmann Publisher.

[9] Mannila, H., Smyth, P., and Hand, D. J. (2001). Principles of Data Mining. MIT Press. Mannila, H., Toivonen, H., and Verkamo, A. I. (1997)

[10] Berry, M. J. A. and Lino_,G. (1997). Data Mining Techniques. John Wiley and Sons, Inc

[11] Mithcell Rowton, Introduction to Network Security Intrusion
Detection, December 2005.

[12] Mounji, A. (1997). Languages and Tools for Rule-Based Distributed Intrusion Detection. PhD thesis, Faculties Universitaires Notre-Dame dela Paix Namur (Belgium).

Echo Cancellation by Adaptive Combination of Nsafs Adaptedbystocastic Gradient Method

Rekha Saroha [1], Sonia Malik [2], Rohit Anand [3]
[1] [2] Department of Electronics and Communication Engineering, NCCE, Panipat, INDIA
[3] Assistant Professor, Electronics and Communication Engineering, NCCE, Panipat, INDIA

Abstract
In acoustic echo cancellation the highly correlated speech input signal and very large impulse response path of echo signal will slow down the convergence rate of adaptive filters if fullband adaptive filter is used. To solve these problems subband adaptive filters are used. Adaptive combination methods provide an interesting way to improve adaptive filter's performance. A tradeoff between fast convergence rate and small steady state mean square error (MSE) in adaptive combination is achieved by stochastic gradient algorithm. The individual each filter is independently adapted by it's own error signal while combination is adapted by sum of squared subband errors as the cost function. Adaptive combination of normalized sub band adaptive filters is used. In our proposed method, adaptive combination of sub band signals before going to the adaptive filters. Experimental results show that the combination method can obtain both fast convergence rate and small steady state MSE by using less number of adaptive filters.

General Terms: Acoustic Echo Cancellation, subband adaptive filters, echo return loss enhancement.

Keywords: Round Trip Delay (RTD), Acoustic Echo Cancellation (AEC), Normalized Least Mean Square Algorithm (NLMS), Mean Square Error (MSE), Subband Adaptive Filters (SAF), Adaptive Combination Normalized Subband Adaptive Filters (NSAF) ,signal to noise ratio (SNR).

1. Introduction
The history of echo cancellation begins on 10th July 1962.In telephones and teleconferencing; a reflection can occur where there is an impedance mismatch. If the reflected signal reaches the far end subscriber with a RTD of a few milliseconds then it is perceived as reverberator. If RTD exceeds a few tens of milliseconds the reflection is known as distinct echo [1].

Echo suppressor was used to remove echo which introduces a very large transmission loss in return path. A new technique that did not interrupt the echo return path called echo cancellation. The AEC estimates the characteristics of the echo path and generates a replica of the echo. The echo is then subtracted from the received signal. Adaptive filters are used as echo canceller. The normalized least-mean-square (NLMS) algorithm is one of the most popular adaptive filters. Speech input signal of the adaptive filter is highly correlated and the impulse response of the acoustic echo path is very long.These two characteristics will slow down the convergence rate of the acoustic echo canceller. So sub band adaptive filtering is used to solve these problems. In SAFs, each sub band uses an individual adaptive sub filters. Recently, an adaptive combination of fullband adaptive filters has been proposed in [8], and its mean-square performance has been analyzed in [9]. More recently, a combination of SAFs for AEC has been proposed [10], which is based on a conventional sub band structure. In this paper we propose a new scheme for adaptive combination of subband adaptive filters deal with the tradeoff problem encountered in AEC which are implemented by NSAFs. The NSAF can be viewed as a subband generalization of the NLMS based adaptive filter. In the proposed combination, mixing parameter that controls the combination is adapted by means of a stochastic gradient algorithm which employs the sum of squared subband errors as the cost function.

Section II represents the Simulink model for fullband adaptive filter acts as acoustic echo cancellation [2].Section III represents sub band adaptive filter and adaptive combination of normalized sub band adaptive filters. Section IV improved adaptive combination of normalized subband adaptive filters. Section v represents Experiment results.

Notation: Symbols in uppercase letters are used for matrices and in lower cases are used for vectors. Other notations are as follows: (.) T represents transpose,E(.) is expectation, || ·|| represents the Euclidean vector, and *diag*(□) stands for a diagonal matrix.

2. Simulink Model Of Fullband Adaptive Filter Acts As Acoustic Echo Cancellation
A block diagram of AEC is shown in Fig.1 [2].

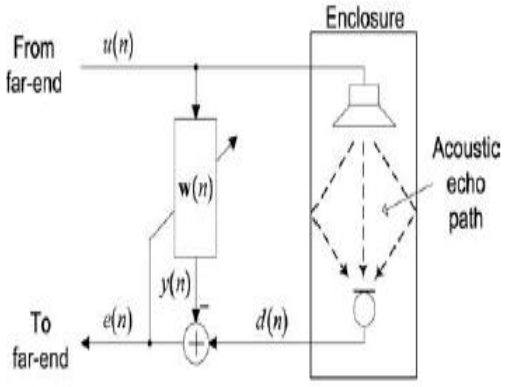

Fig. 1: Block diagram of fullband adaptive filter acts as AEC

Speech signal originating from loudspeaker is received by microphone passing through acoustic echo path. The acoustic echo is removed by adaptive filters. The d (n) signal contains the speech signal and noise signal. The goal of the adaptive filter **w** (n) is to produce a replica of the echo signal *y* (*n*). *y*(*n*) can be used to cancel the echo by subtracting it from the microphone signal *d*(*n*) resulting in error free signal e(n)[3].Algorithm for AEC is as follows [2]:

Adjustable tap weights can be expressed as:

$$w(n) = [w_0(n), w_1(n), \ldots . w_{M-1}(n)]^T = w^T(n)u(n) \quad ..(1)$$

Input signal can be expressed as

$$U(n) = [u(n), u(n-1), \ldots u(n-M+1)]^T \quad \ldots . (2)$$

The output signal y(n) of adaptive filter is the multiplication of w(n) and u(n).

$$Y(n) = \sum_{m=0}^{M-1} w_m(n)u(n-m) = w^T(n)u(n) \ldots . (3)$$

The error signals difference between the desired response d (n) and filter response y (n) is expressed as:

$$e(n) = d(n) - w^T(n)u(n) \quad \ldots\ldots\ldots (4)$$

3. Simulink Model of Nsaf and Its Adaptive Combination

3.1 Simulink Model of NSAF

The block diagram of normalized subband adaptive filter is shown in fig. 2[5,6].

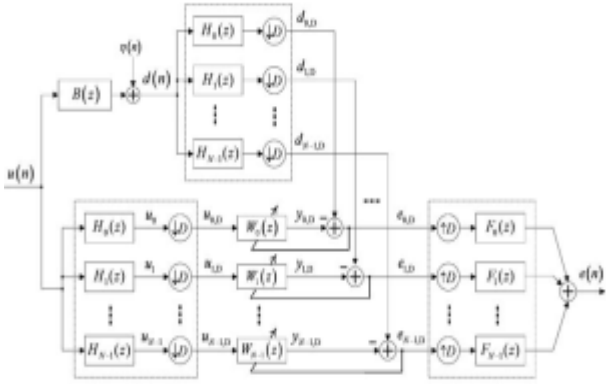

Fig. 2: Block diagram of NSAF

The input speech signal u (n) and desired output d(n) are decomposed into N spectral bands using analysis filters. Analysis filtering is then performed in these sub-bands by a set of independent filters (h0 (n), h1 (n),…, hM-1(n))[2].The sub band signals are further processed by individual adaptive sub filters Wi(z).Each sub band is computing error signal e(n). By updating the tap weights, minimizes the sub band error signal. The full band error signal *e(n)* is finally obtained by interpolating and recombining all the subband error signals using a synthesis filter bank. The updating equation of NSAFs is written as follows [3]:

$w_i(n+1) = w_i(n) + \mu_i \sum_{i=0}^{N-1} \frac{u_i(n)}{\delta + \|u_i(k)\|^2} e_i(n)$…..(5)

Where i=1,2,…N-1. Where $u_i(k) = [u_i(kN), u_i(kN-1) \ldots, u_i(kN-M+1)]^T$,M is the length of the adaptive filter **w**ˆ (*k*) ,μ is the step-size, and δ is the regularization parameter[3].

3.2 Simulink Model of Adaptive Combination of NSAFs

The block diagram of adaptive combination of normalized subband adaptive filters is shown in fig.3[9].

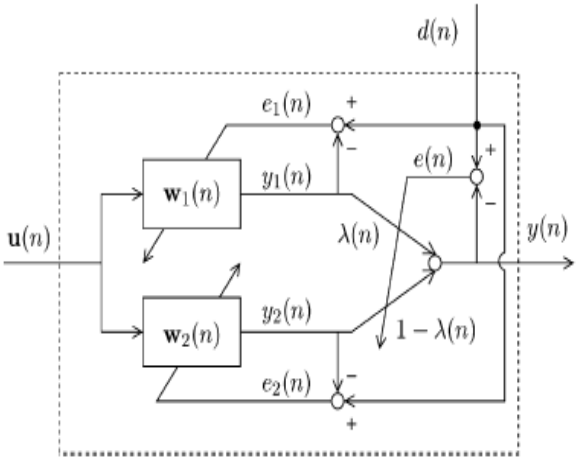

Fig. 3: Adaptive combination of NSAFs

A large step size yields a fast convergence rate but also a large steady state MSE [7].To achieve fast convergence rate and small steady state MSE, adaptive combination of subband adaptive filters is done .So that large step sizes adaptive filters give fast convergence rate and small step sizes adaptive filters give small steady state MSE.So idea becomes to adapt different step sizes filters independently and combination is carried out by using a mixing parameter lambda.

The input signal is U (n)=$[u(n), u(n-1), \ldots u(n-M+1)]^T$, weight vectors are $w(n) = [w_0(n), w_1(n), \ldots, w_{M-1}(n)]^T = w^T(n)u(n)$. So output becomes y(n)=$w^T(n)u(n)$. The update eq. of sub band adaptive filter is given in eq. 5.

$w_i(n+1) = w_i(n) + \mu_i \sum_{i=0}^{N-1} \frac{u_i(n)}{\delta + \|u_i(k)\|^2} e_i(n)$ Where

$e_1(n)$= d(n)-y_1(n) and $e_2(n)$= d(n)-y_2(n) and

$y_1(n) = w_1^T(n)u_n$, $y_2(n) = w_2^T(n)u_n$. Consider $\mu_1 > \mu_2$, then $w_1(n)$ adaptive filter has faster convergence rate and large steady state MSE whereas $w_2(n)$ has slower faster convergence rate but small steady state MSE.So our purpose is to get large convergence rate and small steady state MSE ,So combine both adaptive filters. The output of overall filter is: Y(n)=$\lambda(n)\, y_1$(n)+[1- $\lambda(n)$] y_2(n)…….(6) where **λ** is mixing parameter. The overall filter with tap weight factor of the form is: w(n)=$\lambda(n) w_1$(n)+ [1- $\lambda(n)$] w_2(n).For adaptation of mixing parameter $\lambda(n)$,use stocastic gradient method to minimize error of overall filter $e^2(n) = [d(n) - y(n)]^2$.

However instead of directly adjusting (n), we will adapt a variable $\alpha(n)$ that defines **λ**(n) as a sigmoidal function. (n)=sgm [α(n)]=$\frac{1}{1+e^{-\alpha(n)}}$…….(7)

The update eq. for α(n) is given as:

α(n+1)=α(n)+μ e(n) [y_1(n)- y_2(n)]**λ**(n)[1-**λ**(n)]……..(8)

where μ is the step size for adapting α(n).since the mixing parameter is defined by the sigmoidal function[15],which insists the mixing parameter to lie exactly inside the interval (0,1), this combination is convex combination.[14][3].

4. Improved Adaptive Combination Of Normalized Subband Adaptive Filters

In improved adaptive combination of normalized subband adaptive filters,we take the following assumption.

1) d(n) and u(n) are related by a linear regression model d(n)= w_o^T (n)u(n)+ $\eta(n)$

for some unknown weight vector w_0 of length M and where $\eta(n)$ is an independent distributed noise.

2) The initial condition w_1 (0), w_2 (0) and a(0) are independent of u(n),d(n) or all n.

3) $E\{\mathbf{u}(n)\} = \mathbf{0}, E\{\mathbf{u}(n)\mathbf{u}^T(n)\} = \mathbf{R}, E\{d(n)\} = 0$, and $E\{e_0(n)\} = 0$.[1]

A large convergence rate and small steady state MSE can be greatly achieved by using less amount of adaptive filters as comparison to the previous adaptive combination method. This can be achieved by using the idea of adaptive combination of speech input signal before going to the NSAF.

5. Experimental Results

The full-band and sub-band systems, adaptive combination of subband adaptive filters and its improvement were modeled in Matlab Simulink and many simulations for different inputs and number of sub-bands were performed. For the adaptive algorithm several different algorithms can be used, but the most common one is the normalized least mean squares (NLMS). The order of the NLMS filters was chosen from N=64 to N=2 . The designs were made in Matlab-Simulink environment and the simulations were run for 5000 samples for Gaussian noise and sine wave input, respective 12*104 samples in the case of speech input. A reverberating effect was added to the input by an artificial Schroeder I reverberator which contained four comb filters in parallel and two all-passes filters series connected. The first estimation of a system capability is represented by the (output error-voice input), but in order to measure its potential, Echo Return Loss Enhancement (ERLE) should be computed; it is defined as the ratio of the power of the desired signal over the power of the residual signal. Comparison between full band, sub bands, adaptive combination, and their improvement is done based on SNR and MSE and by using output error- voice input and ERLE.

6. Conclusion

The NSAF is a good candidate for implementing acoustic echo cancellers because of its fast convergence rate. However, it requires a tradeoff between fast convergence rate and small steady-state MSE. This paper presented an adaptive convex combination of two NSAFs to solve this problem. In addition to the conventional coupling update method for component filters, we also proposed a coupling update mechanism which requires less number of adaptive filters as than used in conventional method. To verify the effectiveness of the proposed scheme, simulations using different input signals as well as system noises with different SNRs were performed. The experimental results demonstrated that the proposed scheme can obtain improved performance as compared to the conventional NSAF.

7. Acknowledgments

With a deep sense of gratitude and heartiest honor, I would like to express my immense thanks to Mr. Rohit Anand, Assistant Professor, N.C College of Engineering, Panipat for their valuable and sustained guidance, constant encouragement and careful supervision during the entire course which made the project successful. I proudly acknowledge my sincere and heartfelt thanks to

Ms. Sonia Malik, Department of N.C College of Engineering, Panipat for their valuable help, constant encouragement and careful supervision during the entire course which made the project successful.

References

[1] M. M. Sondhi, "The history of echo cancellation," IEEE Signal Process.Mag., vol. 23, no. 5, pp. 95–98, Sep. 2006.
[2] K. A. Lee, W. S. Gan, and S. M. Kuo, Subband Adaptive Filtering: Theory and Implementation. Hoboken, NJ: Wiley, 2009.
[3] Jingen Ni and Feng Li ,"adaptive combination of subband adaptive filters for acoustic echo cancellation." IEEE Transactions on Consumer Electronics, Vol. 56, No. 3, August 2010
[4] Irina Dornean, Marina Topa, Botond Sandor Kirei, Marius Neag, "Sub-band adaptive filtering for acoustic echo cancellation."2009.
[5] B. Farhang-Boroujeny, Adaptive Filters: Theory and Applications, New York: John Wiley & Sons, Inc., 1998.
[6] J. J. Shynk, 'Frequency domain and multirate adaptive filtering filtering', IEEE Signal Processing Mag., 9, January 1992, 14–37.
[7] N. J. Bershad, J. C. M. Bermudez and J.-Y. Tourneret, "An affine combination of two LMS adaptive filtersTransient mean-square analysis," IEEE Trans. Signal Process., vol. 56, no. 5, pp. 1853–1864, May 2008.
[8] J. Arenas-García, M. Martínez-Ramón, A. Navia-Vázquez, and A. R. Figueiras-Vidal, "Plant identification via adaptive combination of transversal filters," Signal Process., vol. 86, pp. 2430–2438, 2006.
[9] J. Arenas-Garcia, A. R. Figueiras-Vidal, and A. H. Sayed, "Mean-square performance of a convex combination of two adaptive filters," IEEE Trans. Signal Process., vol. 54, no. 3, pp. 1078–1090, Mar. 2006.
[10] L. A. Azpicueta-Ruiz, A. R. Figueiras-Vidal, and J. Arenas-García, "Acoustic echo cancellation in frequency domain using combinations of filters," in 19th Int. Congress on Acoustics (ICA), Madrid, Sep. 2007.
[11] J. Arenas-García, V. Gómez-Verdejo, M. Martínez-Ramón, and A. R. Figueiras-Vidal, "Separate-variable adaptive combination of LMS adaptive filters for plant identification," in Proc. 13th IEEE Int. Workshop Neural Networks Signal Processing, Toulouse, France, 2003, pp. 239–248.
[12] J. Arenas-García, M. Martínez-Ramón, V. Gómez-Verdejo, and A. R. Figueiras-Vidal, "Multiple plant identifier via adaptive LMS convex combination," in Proc. IEEE Int. Symp. Intel. Signal Processing, Budapest, Hungary, 2003, pp. 137–142.
[13] A. H. Sayed, Fundamentals of Adaptive Filtering. New York: Wiley,2003.
[14] N. J. Bershad, J. C. M. Bermudez and J.-Y. Tourneret, "An affine combination of two LMS adaptive filters —Transient mean-square analysis," IEEE Trans. Signal Process., vol. 56, no. 5, pp. 1853–1864, May 2008.
[15] K. A. Lee and W. S. Gan, "Improving convergence of the NLMS algorithm using constrained subband updates," IEEE Signal Process. Lett., vol. 11, no. 9, pp. 736–739 , Sep. 2004.
[16] P. P. Vaidyanathan, Multirate Systems and Filter Banks. Englewood Cliffs, NJ: Prentice-Hall, 1993.
[17] S. Haykin, Adaptive Filter Theory. Upper Saddle River, NJ: Prentice- Hall, 2002.

An Improved Self Cancellation Scheme to Reduce Non-Linearity in OFDM Spectrum

Kunal mann[1], Rakesh kumar[2], Poonam[3]

Abstract-- As the wireless communication system has evolved tremendously, leading to the need for high performance and much higher capacity for the multiuser communication systems but within the constraints of limited spectrum and limited bandwidth. The main function of OFDM is to convert a frequency selective channel into a collection of frequency- Flat sub channels with partially overlapping spectra. The differentiating factor of this scheme is the orthogonality provided to the subcarriers that provided synchronisation and helps in avoiding ISI .An OFDM signal consists of a number of closely spaced modulated carriers.

I. Introduction

Cognitive radio is:" A radio which is capable of sensing its operational environment and can adjust its parameters according to the environment dynamically and behave accordingly."The most significant objectives for which cognitive radio networks were introduced are:

i. To utilise the spectrum efficiently.
ii. To make highly reliable communication networks available wherever and whenever needed

As it is known that there is rapid deployment of wireless devices, as a result the demand of wireless radio spectrum is also increasing rapidly. But fixed spectrum assignment policy is proving a bottleneck in efficient utilisation of spectrum. Cognitive radio networks helps in eliminating inefficient usage of limited spectrum by using various dynamic spectrum access techniques, through which, unlicensed users called *Secondary users*, are allowed to temporarily use the unused portion of licensed spectrum. The licensed users are called *Primary users.* In cognitive radio networks, secondary users dynamically access the spectrum in opportunistic fashion, without interfering with the primary users.

Ii Literature Survey

Technically, Cognitive Radio is a kind of two way radio that can automatically change its transmission or reception parameters in such a way that the entire wireless communication network communicates efficiently, while avoiding interference between licensed or unlicensed users.
The definition of Cognitive radio can be "a cognitive radio is a software radio whose control processes leverage situational knowledge and intelligent processing to work for achieving the goals related to the needs of the user, Application, and/or network". The concept of Cognitive emerges from Software defined Radios as Cognitive radio is a "step ahead" of SDR technology. Cognitive radio can be summarized through following definitions:

Definition 1: A radio or system that senses its operational electromagnetic environment and can dynamically and autonomously adjust its radio operating parameters to modify system operation, such as maximize throughput, mitigate interference, facilitate interoperability, access secondary markets.

Definition 2: A cognitive radio is an adaptive, multi-dimensionally aware, autonomous radio system that learns from its experiences to reason, plan, and decide future actions to meet user needs.

Depending upon the type of parameters taken into consideration while transmission or reception, there can be various types of cognitive radios:

- **Full Cognitive Radio**: In this CR, each and every parameter which is observable by a wireless network is taken into account.
- **Spectrum Sensing Cognitive Radio**: In this CR, only Radio Frequency spectrum is taken into account.
- **Licensed Band Cognitive Radio**: In this, along with unlicensed bands, CR can use bands assigned to licensed users.
- **Unlicensed Band Cognitive Radio:** In this, CR can use only unlicensed bands of radio frequency spectrum.

III Problem Defination

The main aim of this paper is to optimize the Parallel Cooperative sensing technique and to simulate efficient results for better spectrum utilization .For this scheme a spectrum would be generated to analyze the effect of various parameters like noise, throughput etc on the overall efficiency. A parallel scheme would be used for carrying out the signal transmission.

Cognitive Radio System

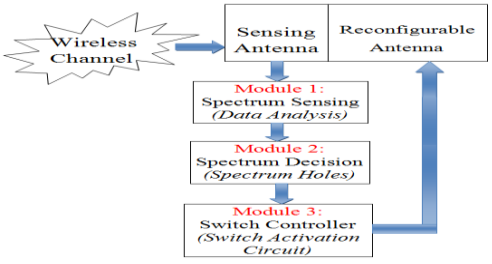

Figure Cognitive Radio System

The RF architecture of a CR system consists of a "sensing antenna" to continuously monitor the wireless channels and to look for unused frequency bands (holes) and a "reconfigurable transmit/receive antenna" to perform the required communication within those unused frequency channels. "Spectrum Sensing" and "Spectrum Decision" modules are required to determine the unused frequency bands and assign the appropriate frequency to the secondary users. Based on the output of these modules the "Switch Controller" will communicate with the switch activation circuit in order to change the physical/electrical structure of the reconfigurable antenna.

Analysis of Inter-Carrier Interference

The main disadvantage of OFDM, however, is its susceptibility to small differences in frequency at the transmitter and receiver, normally referred to as frequency offset. This frequency offset can be caused by Doppler shift due to relative motion between the transmitter and receiver, or by differences between the frequencies of the local oscillators at the transmitter and receiver. In this project, the frequency offset is modeled as a multiplicative factor introduced in the channel, as shown in Figure: shows.

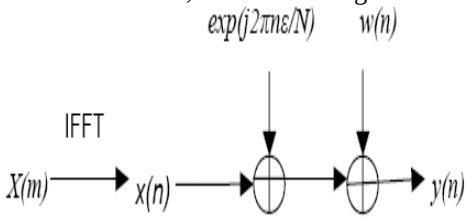

Figure : Frequency Offset Model

The received signal is given by,

$$y(n) = x(n)\ e^{\frac{j2\pi n\varepsilon}{N}} + w(n)$$

Where ε is the normalized frequency offset, and is given by $\Delta f N T_s$. Δf is the frequency difference between the transmitted and received carrier frequencies and T_s is the sub-carrier symbol period. $w(n)$ is the AWGN introduced in the channel. The effect of this frequency offset on the received symbol stream can be understood by considering the received symbol $Y(k)$ on the k^{th} sub-carrier.

$$Y(k) = X(k)S(0) + \sum_{l=0, l\neq k}^{N-1} X(l)S(l-k) + n_k$$

$$k = 0,1.....N-1$$

Where N is the total number of sub-carriers, $X(k)$ is the transmitted symbol (M-ary phase-shift keying (M-PSK), for example) for the k^{th} sub-carrier, is the FFT of $w(n)$, and $S(l-k)$ are the complex coefficients for the ICI components in the received signal. The ICI components are the interfering signals transmitted on sub-carriers other than the k^{th} sub-carrier. The complex coefficients are given by

$$S(l-k) = \frac{\sin(\pi(l+\varepsilon-k))}{N\sin(\pi(l+\varepsilon-k)/N)} \exp\left(j\pi\left(1-\frac{1}{N}\right)(l+\varepsilon-k)\right)$$

To analyze the effect of ICI on the received signal, we consider a system with N=16 carriers. The frequency offset values used are 0.2 and 0.4, and l is taken as 0, that is, we are analyzing the signal received at the sub-carrier with index 0. The complex ICI coefficients $S(l-k)$ are plotted for all sub-carrier indices in figure.

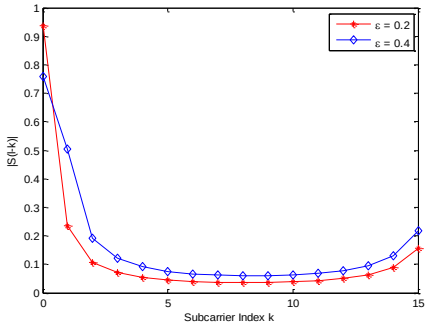

Figure ICI Coefficients for N=16 Carriers

This figure shows that for a larger ε, the weight of the desired signal component, $S(0)$, decreases, while the weights of the ICI components increases. The authors also notice that the adjacent carrier has the maximum contribution to the ICI. This fact is used in the ICI self-cancellation technique described.

IV CONCLUSION

In this project, the performance of OFDM systems in the presence of frequency offset between the transmitter and the receiver has been studied in terms of the Carrier-to-Interference ratio (CIR) and the bit error rate (BER) performance. Inter-carrier interference (ICI), which results from the frequency offset, degrades the performance of the OFDM system.

One method is explored in this project for mitigation of the ICI i.e. ICI self-cancellation (SC). By using this method the BER is improved in comparison to simple OFDM system.

.

References

[1] www.mprg.org/people/gametheory/files/chapter%201.pdf.

[2] Beibei Wang and K. J. Ray Liu , "Advances in Cognitive Radio Networks: A Survey", IEEE JOURNAL OF SELECTED TOPICS IN SIGNAL PROCESSING, VOL. 5, NO. 1, FEBRUARY 2011.

[3] http://en.wikipedia.org/wiki/Cognitive_radio.

[4] Federal Communications Commission, "Notice of proposed rule making and order: Facilitating opportunities for flexible, efficient, and reliable spectrum use employing cognitive radio technologies," ET Docket No. 03-108, Feb. 2005.

[5] www.wirelessinnovation.org/assets/documents/tut-cognitive_radio.pdf.

[6] Sugata Sanyal , Rohit Bhadauria and Chittabrata Ghosh, "Secure Communication in Cognitive RadioNetworks", 2009 International Conference on Computers and Devices for Communication.

[7] Luca Bixio, Marina Ottonello, Mirco Raffetto, Carlo S. Regazzoni ," A comparison between stand-alone and distributed architectures for spectrum hole detection",IEEE,2010.

[8] Q. Zhao and B. M. Sadler, "A survey of dynamic spectrum access,"*IEEE Sig. Proc. Mag.*, vol. 24, pp. 79–89, May 2007.

[9] S. Srinivasa and S. A. Jafar, "The throughput potential of cognitive radio: a theoretical perspective," *IEEE Comm. Mag.*, vol. 45, pp. 73–79, May 2007.

[10] Citeseerx.ist.psu.edu/viewdoc/download?doi=10.1.1.91.567.

[11] Rajni Dubey and Sanjeev Sharma ," Distributed Shared Spectrum Techniques for Cognitive Wireless Radio Networks", 2010 International Conference on Computational Intelligence and Communication Networks.

[12] Ines AISSA, Mounir FRIKHA and Sami TABBANE ," Dynamic Spectrum Hole Management in Cognitive Radio",IEEE,2011.

A Survey on Models and Test strategies for Event-Driven Software

[1]Mr.J.Praveen Kumar [2]Manas Kumar Yogi
Asst.Prof. CSE Dept.
Malla Reddy College of Engineering and Technology

Abstract
A Graphical User Interface (GUI) testing tool is one to test applications user
Interface and to detect the correctness of applications functionality. Event-Driven Software (EDS) can change state based on incoming events; common examples are GUI and web applications.
These EDS pose a challenge to testing because there are a large number of possible event sequences that users can invoke through a user interface. While valuable contributions have been made for testing these two subclasses of EDS, such efforts have been disjoint. This work provides the first single model that is generic enough to study GUI and web applications together. This paper presentsdetail survey of the existing GUI testing tools . This paperalso summarizes various existing automated GUI testing approaches such as PerformanceTesting and Analysis (PTA), Model Based Testing (MBT), CombinatorialInteractionTesting (CIT), (GUI)-based Applications (GAPs). The feasibility of using java GUI captureand replay tools for GUI performance test automation has been studied.
The severelimitations of GUI tools when used for recording and replaying realistic session of the realworld Java applications have been also addressed. Various GUI testing tool are comparedin terms of performance.In this we use the model to define generic prioritization criteria that are applicable to both GUI and web applications. Our ultimate goal is to evolve the model and use it to develop a unified theory of how all EDS should be tested.

Keywords: Graphical User Interface, Performance Testing, event driven software (EDS), *t*-way interaction coverage, test suite prioritization, user-session testing, web-application testing, GUI testing

1. Introduction

The GUI testing is a process to test application's user interface and to detect if application is
functionally correct. GUI testing involves carrying set of tasks and comparing the result of same withthe expected output and ability to repeat same set of tasks multiple times with different data input and same level of accuracy. GUI Testing includes how the application handles keyboard and mouse events, how different GUI components like menubars, toolbars, dialogs, buttons, edit fields, list controls,images etc. reacts to user input and whether or not it performs in the desired manner.

ImplementingGUI testing for your application early in the software development cycle speeds up developmentimproves quality and reduces risks towards the end of the cycle. GUI
Testing can be performed bothmanually with a human tester or could be performed automatically with use of a software program.

Every software organization tests its software's, still the end product always have some issues
left. Testing team tries their best to find all the bugs before release of the software but still there areissues left in the product and they often re-appear as new modules are added to the software. Even thebest of manual testing process struggle to deliver an effective, efficient, accurate and increased testcoverage.

Manual testing is often error prone and there are chances of most of the test scenarios left out.

Automated GUI Testing is a software program which is used to analyze whether the desktop
application is functionally correct. Automated GUI Testing includes automating manual testing taskswhich are mostly time consuming and error prone. Automated GUI Testing is a more accurate,efficient, reliable and cost effective replacement to manual testing. Automated GUI Testing involves carrying set of tasks automatically and comparing the result of same with the expected output andability to repeat same set of tasks multiple times with different data input and same level of accuracy.
Implementing GUI Testing for your application early in the software development cycle speeds updevelopment improves quality and reduces risks towards the end of the cycle .
Automated GUI Testing is a solution to all the issues raised with Manual GUI Testing. An
Automated GUI Testing tool can playback all the recorded set of tasks, compare the results of
execution with the expected behavior and report success or failure to the test engineers. Once the GUItests are created they can easily be repeated for multiple number of times with different data sets andcan be extended to cover additional features at a later time. Most of the software organizations considerGUI Testing as critical to their functional testing process and there are many things which should beconsidered before selecting an Automated GUI Testing tool. A company can make great strides usingfunctional test automation. The

important benefits include, higher test coverage levels, greaterreliability, shorted test cycles, ability to do multi user testing at no extra cost, all resulting in increasedlevels of confidence in the software.

2. Existing models :

Testing for functional correctness of EDS such as stand-alone GUI and web-based applications is critical to many organizations. These applications share several important characteristics. Both are particularly challenging to test because users can invoke many different sequences of events that affect application behavior. Earlier research has shown that existing conventional testing techniques do not apply to either GUIs or web applications, primarily because the number of permutations of input events leads to a large number of states, and for adequate testing, an event may need to be tested in many of these states, thus requiring a large number of test cases (each represented as an event sequence). Researchers have developed several models for automated GUI testing and web application testing.

2.1. Performance Testing and Analysis (PTA)

It is practical to automatically test the performance of interactive rich-client Java applications when thefollowing two issues are addressed.

1) A metric need a measurement approach to quantify the performance of an interactive
application, and

2) A way to automatically perform realistic interactive sessions on an application, without
perturbing the measured performance .

This kind of GUI performance test automation has two key requirements that go beyond
traditional GUI test automation: (a) the need to replay realistically complex interactive sessions and (b)the minimal perturbation of the measured performance by the tool [1].

To find performance problemsin real applications, the length of the event sequences played during testing is important. Sequencesrepresenting only one or two events are often used for functional testing. They represent a form of unittest. Slightly longer sequences could be considered integration tests, as they often cover someinteractions between components. To find performance problems, however, event sequences need to besignificantly longer, so that the underlying system can reach the steady-state behavior that is normal inreal world usage. Using the GUI testing tools for performance testing is their use of harnesses andmock objects. Those artifacts represent deviations from the real-world setup and thus can affect theobserved performance [1].

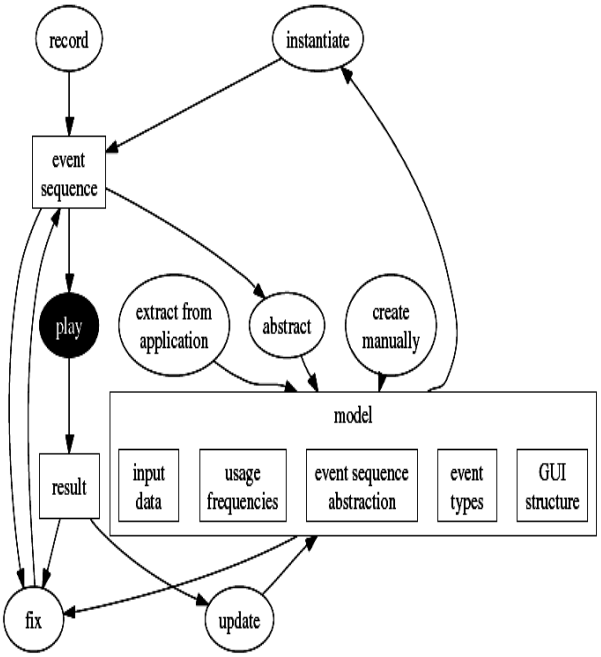

2.2. Model Based Testing (MBT)

The new feedback-based technique has been used in a fully automatic end-to-end process for a specific type of GUI testing. The seed test suite (in this case, the smoke tests) is generated automatically using an existing event interaction graph model of the GUI, which represents all possible sequences of events that may be executed on the GUI.[2]. It utilizes runtime information as feedback for model-based GUI test case generation. However, runtime information has previously been employed for various aspects of test automation, and model-based testing has been applied to conventional software as well as *event driven software (EDS)*.It presents an overview of related research in the areas of model-based and EDS testing, GUI testing, and the use of runtime information as feedback for test generation.

Model-based testing automates some aspect of software testing by employing a model of the
software. The model is an abstraction of the software's behavior from a particular perspective (e.g.,software states, configuration, values of variables, etc.); it may be at different levels of abstraction,such as abstract states, GUI states, internal variable states, or path predicates, State machine models.

The most popular models used for software testing are state machine models. They model the
software's behavior in terms of its abstract or concrete states; they are typically represented as state transition diagrams. Several types of state machine models have been used for software testing .

The main inclusions in this test are:

- extension of work on automated, model-based ,systematic GUI test case generation.

- definition of new relationships among GUI events based on their execution.
- utilization of runtime state to explore a larger input space and improve fault detection.
- Immersion of the feedback-based technique into a fully automatic end-to-end GUI
- testing process and demonstration of its effectiveness on fielded and fault-seeded
- applications.
- Empirical evidence tying fault characteristics to types of test suites.
- Demonstration that certain faults require well crafted combinations of test cases and

oracles.

2.3. Combinatorial Interaction Testing (CIT)

Combinatorial Interaction Testing is a method which focuses on test prioritization techniques for GUI. The specific contributions of this work include: the first single model for testing stand-alone GUI and Web-based applications, a shared prioritization function based on the abstract model, and shared prioritization criteria. We validate the usefulness of these artifacts through an empirical study. The results show that GUI and Web-based applications, when recast using the model, showed similar behavior, reinforcing our belief that these classes of applications should be modeled and studied together. Other results show that GUI and Web applications behave differently, which has created opportunities for evolving the model and further experimentation.The generalize the model by evaluating its applicability and usefulness for other software testing activities, such as test generation.

It also makes contributions toward test prioritization research. Many of our prioritization criteria

improve the rate of fault detection of the test cases over random orderings of tests. We also develop hybrid prioritization criteria that combine several criteria that work well individually and evaluate whether the hybrid criteria result in more effective test orders.

3. Proposed model:

3.1. Modeling Test Cases

A test case is modeled as a sequence of actions. For eachaction, a user sets a value for one or more parameters.We provide examples of test cases for both GUI and webapplications next.

(a) Example GUI application window

Parameter, Value
1. <"Find what" drop-box, settext>
2. <"Find what" drop-box, leftclick dropdown>
3. <"Match case" checkbox, leftclick select>
4. <"Match case" checkbox, leftclick unselect>
5. <"Find whole words only" checkbox, leftclick select>
6. <"Find whole words only" checkbox, leftclick unselect>
7. <"Find Next" button, leftclick>
8. <"Close" button, leftclick>
9. <"Replace" button, leftclick>

(b) Nine parameter-values on the GUI window

(c) Example web application window

Parameter and value descriptions for Login.jsp
1. < Login text field, guest >
2. < Password text field, guest >
3. < FormAction, Login >
4. < FormName, Login >

(d) Four parameter-values in the Web Application window

Start of TC No. of Actions	<Testcase> <Length>4</Length>
Action 1	<Menu> <Window>TerpWord</Window> <Nonterminal>File</Nonterminal> </Menu> <Menu> <Window>TerpWord</Window> <Nonterminal>Save</Nonterminal> </Menu>
Action 2	<Component> <Window>Save</Window> <Nonterminal>File Name text field</Nonterminal <Eventtype>SETTEXT</Eventtype> <Eventvalue>exampleFile</Eventvalue> </Component> <Component> <Window>Save</Window> <Nonterminal>Files of Type drop-down box</Nonterminal> <Eventtype>LEFTCLICK SELECT</Eventtype> <Eventvalue>Plain Text File (*.txt)</Eventvalue> </Component> <Component> <Window>SAVE</Window> <Nonterminal>OK button</Nonterminal> <Eventtype>LEFTCLICK</Eventtype> </Component>
Action 3	<Menu> <Window>TerpWord</Window> <Nonterminal>Edit</Nonterminal> </Menu> <Menu> <Window>TerpWord</Window> <Nonterminal>Find...</Nonterminal> </Menu>
Action 4	<Component> <Window>Find</Window> <Nonterminal>Find what drop-box</Nonterminal <Eventtype>SETTEXT</Eventtype> <Eventvalue>software defect</Eventvalue> </Component> <Component> <Window>Find</Window> <Nonterminal>FindNext button</Nonterminal> <Eventtype>LEFTCLICK</Eventtype> </Component>
End of TC	</Testcase>

(a) Sample GUI test case

Window name	P-V No.	P-V description (<parameter,value>)
TerpWord	PV.1	<File,null>
	PV.2	<Save,null>
Save	PV.3	<File name text field, SETTEXT="exampleFile">
	PV.4	<Files of Type drop-down box, LEFTCLICK SELECT="Plain Text File (*.txt)">
	PV.5	<OK button, LEFTCLICK>
TerpWord	PV.6	<Edit, null>
	PV.7	<Find..., null>
Find	PV.8	<Find what drop-box, SETTEXT="software defect">
	PV.9	<FindNext button, LEFTCLICK>

(b) Windows and User Interactions in test case

TABLE 2: Example GUI test case

No. of actions in Test	Action
Action 1	GET Default.jsp
Action 2	GET Login.jsp
Action 3	POST Login.jsp?Password=guest &FormName=Login& FormAction=login&Login=guest
Action 4	GET BookDetail.jsp?item_id=22

(a) Sample user-session-based web test case

Window name	Parameter-value No.	PV Description (<parameter,value>)
GET Default.jsp	PV.1	<null,null>
GET Login.jsp	PV.2	<null, null>
POST Login.jsp	PV.3	<Password,guest>
	PV.4	<FormName,Login>
	PV.5	<FormAction,login>
	PV.6	<Login,guest>
GET BookDetail.jsp	PV.7	<item_id,22>

(b) Windows and Parameter-Values in test case

TABLE 3: Example Web test case

Previous work treats stand-alone GUI and web-based applications as separate areas of research. However, these types of applications have many similarities that allow us to create a single model for testing such event driven systems. This model may promote future research to more broadly focus on stand-alone GUI and web-based applications instead of addressing them as disjoint topics. Within the context of this model, we develop and empirically evaluate several prioritization criteria and apply them to four stand-alone GUI and three web-based applications and their existing test suites. Our empirical study evaluates the prioritization criteria. We present our threats to validity in this section because several opportunities for future research are created by the threats to validity of the results of our empirical study. Threats to construct validity are factors in the study
design that may cause us to inadequately measure concepts of interest.

	Calc	Paint	SSheet	Word	Book	CPM	Masplas
Windows	2	11	9	12	9	65	18
Parameter-values	85	247	188	156	415	4166	646
LOC	9916	18376	12791	4893	7615	9401	999
Classes	141	219	125	104	11	75	9
Methods	446	644	579	236	319	173	22
Branches	1306	1277	1521	452	1720	1260	108
Total no. of tests	300	300	300	250	125	890	169
Largest count of actions in a test case	47	51	50	50	160	585	69
Average count of actions in a test case	14.5	19.7	19	27.8	29	14	7
2-way parameter-value inter-actions covered in test suite	99.34%	46.34%	50.75%	64.58%	92.50%	97.80%	96.20%
No. of seeded faults	175	182	79	96	40	135	29
Fault Detection Density (FDD)	.05	.02	.02	.29	.59	.056	.19
Min. no. faults found by a test	0	0	0	0	6	0	1
Avg. no. faults found by a test	9.4	1.6	4	24	21.43	4.67	4.62
Max. no. faults found by a test	48	64	71	87	32	33	15

Test suit

3.2. Test suites

Models of the TerpOffice applications, called event-flow graphs [1], were used to generate test cases. The test-case generation algorithm has also been described earlier [1]; in summary, the algorithm is based on graph traversal;
starting in one of the events in the application's main window,the event-flow graphs were traversed, outputting the encountered event sequences as test cases. In all, 300 test cases were generated for each application.
The suites for web applications are based on usage of the application, also referred to as user-session-based testsuites.
A total of 125 test cases were collected for Book, by asking for volunteer users by sending emails to local newsgroups and posting advertisements in the University of Delaware's classifieds. For CPM, 890 test cases were collected from instructors, teaching assistants, and students using CPM during the 2004-05 and
2005-06 academic years at the University of Delaware. A total of 169 test cases were collected when our third subject application, Masplas, was deployed for the Mid-Atlantic Symposium on Programming Languages .
Table shows the characteristics of the test casesused in our study, such as the total number of testcases for each application, and statistics on the lengths
of the test cases. We also report the total numberof unique parameter-values and the percentage of 2-way parameter-value interactions covered in the test suites. We compute the percentage of 2-way parametervalueinteractions by counting the number of uniqueparameter-values on each window that can be selectedin combination with unique parameter-values on otherwindows within the application.

4. Conclusion

stand-alone GUI and web-based applications as separate areas of research. However, these types of applications have many similarities that allow us to create a single model for testing such eventdriven systems. This model may promote future research to more broadly focus on stand-alone GUI and webbased applications instead of addressing them as disjoint topics. Other researchers can use our common model to apply testing techniques more broadly. their existing test suites. Our empirical study evaluates the prioritization criteria. Our ability to develop prioritization
criteria for two types of event-driven software indicates the usefulness of our combined model for the
problem of test prioritization. Our results are promising as many of the prioritization criteria that we use improve
the rate of fault detection over random ordering of test cases. We learn that prioritization by 2-way and PV-LtoS
generally result in the best improvement for the rate of fault detection in our GUI applications and one of our
web applications. However, for our web applications ,frequency-based techniques provide the best rate of fault
detection in 2 out of the 3 subjects. We attribute this to the source of the test cases. The test suites for the
web applications come from real user-sessions, whereas the GUI test cases were automatically generated without
influence from users.

REFERENCES

[1] A. M. Memon and Q. Xie, "Studying the fault-detection effectiveness of GUI test cases for rapidly evolving software," *IEEE Trans. Softw. Eng.*, vol. 31, no. 10, pp. 884–896, Oct. 2005.

[2] A. Andrews, J. Offutt, and R. Alexander, "Testing web applications by modeling with FSMs," *Software and Systems Modeling*, vol. 4, no. 3, pp. 326–345, Jul. 2005.

[3] G. D. Lucca, A. Fasolino, F. Faralli, and U. D. Carlini, "Testing web applications," in *the IEEE Intl. Conf. on Software Maintenance*. Montreal, Canada: IEEE Computer Society, Oct. 2002, pp. 310–319.

[4] F. Ricca and P. Tonella, "Analysis and testing of web applications," in*the Intl. Conf. on Software Engineering*. Toronto, Ontario, Canada: IEEE Computer Society, May 2001, pp. 25–34.

[5] R. C. Bryce and A. M. Memon, "Test suite prioritization by interactioncoverage," in *Proceedings of The Workshop on Domain-Specific Approaches to Software Test Automation (DoSTA 2007); co-located with The 6th joint meeting of the European Software Engineering Conference and the ACM SIGSOFT Symposium on the Foundations of Software Engineering*. Dubrovnik, Croatia: ACM, Sep. 2007, pp. 1–7.

[6] S. Sampath, R. Bryce, G. Viswanath, V. Kandimalla, and A. G. Koru, "Prioritizing user-session-based test cases for web application testing," in *the International Conference on Software Testing, Verification and Validation*. Lillehammer, Norway: IEEE Computer Society, Apr. 2008, pp. 141–150. IEEE TRANSACTIONS ON SOFTWARE ENGINEERING, VOL. 37, NO. 1, JAN/FEB 2011 IEEE TRANSACTIONS ON SOFTWARE ENGINEERING, VOL. X, NO. X, JANUARY 2010 18

[7] P. Brooks, B. Robinson, and A. M. Memon, "An initial characterization of industrial graphical user interface systems," in *Proceedings of the International Conference on Software Testing, Verification and Validation*, 2009, pp. 11–20.

[8] L. White, "Regression testing of GUI event interactions," in *Proceedings of the International Conference on Software Maintenance*. IEEE Computer Society, Nov. 1996, pp. 350–358.

[9] "Web site test tools and site management tools," accessed on <http://www.softwareqatest.com/qatweb1.html>, accessed on Apr. 5, 2009.

[10] D. C. Kung, C.-H. Liu, and P. Hsia, "An object-oriented web test model for testing web applications," in *The First Asia-Pacific Conf. on Quality Software*. Singapore: IEEE Computer Society, Oct. 2000, pp. 111–120.

Authors Description

Manas Kumar Yogi
Pursuing Mtech.(CSE Dept.)
Malla Reddy College of Engineering and Technology, Hyderabad.

Mr.J.Praveen Kumar
Asst.Prof. CSE Dept.
Malla Reddy College of Engineering and Technology, Hyderabad.

Comparison of Power Consumption and Strict Avalanche Criteria at Encryption/Decryption Side of Different AES Standards

Navraj Khatri [1], Rajeev Dhanda [2], Jagtar Singh [3]
[1] [2] Department of Electronics and Communication Engineering, NCCE, Israna, Panipat, INDIA
[3] Senior Lecturer, Electronics and Communication engineering, NCCE, Israna, Panipat, INDIA

Abstract:
The selective application of technological and related procedural safeguards is an important responsibility of every organization in providing adequate security to its electronic data systems. Now as the world is moving towards high speed of communication (larger data rate),more secure and fast algorithms are required to keep the information secret. In the present work, a new model is proposed and implemented, which is very similar to the conventional AES. The fundamental difference in the AES and proposed model is in block size which has been increased from 128 bits in conventional AES to 200 bits in proposed algorithm[1-4].The proposed algorithm is giving very good randomness and hence enhances the security in comparison to conventional AES. The performance is measured based upon Power Consumption at Encryption/Decryption time, and Strict Avalanche Criteria of various AES Standards. In this paper, we showed the effect in security increment through AES methodology.

Keywords: Plain text, cipher text, stream cipher, Symmetric Encryption, Computer Security.

1. Introduction:

The introduction of wireless data communication at the beginning of 20th century resulted in an increasing interest in cryptography due to insecure nature of Wireless medium.In this paper,symmetric block cipher algorithm is proposed likewise Advance Encryption Standard (AES).The proposed algorithm differs from AES as it has 200 bits block size and key size both. Number of rounds is constant and equal to ten in this algorithm.The key expansion and substitution box generation are done in the same way as in conventional AES block cipher.AES has 10 rounds for 128-bit keys,12 rounds for 192-bit keys, and 14 rounds for 256-bit keys[5].Section 2 describes the Our Proposed Algorithm properly.Section 3 gives the Comparison of Power Consumption at Encryption and Decryption side and Strict Avalanche Criteria of different AES Standards. Section 4 gives the Advantages and Disadvantages of AES.Section 5 and Section 6 gives us the Conclusion and Acknowledgement..

2. Proposed Algorithm

2.1 General Definitions

Block size and key size are the important parameters of any encryption algorithm because the level of security provided by a cipher completely depends upon these two parameters.In our proposed encryption algorithm,we are using 200 bits block and key size instead of 128 bit used in conventional Rijndael'salgorithm.[6-8].This increased block and key size will improve the security level of the cipher with a negligible loss in efficiency.The original data which needs to be encrypted will be termed as plaintext.Our encryption algorithm is a symmetric block cipher algorithm.This algorithm will operate on fixed size blocks of plaintext to generate ciphertext.In the process of encryption, the first step is formation of data blocks from the original plaintext.Our basic block length is 200 bits which can be shown by a 5 by 5 matrix of byte. The data bytes are filled first in the column then in the rows.Once the data block is formed, different rounds take place to modify data to the cipher text.

$$\begin{vmatrix} a_{0,0} & a_{0,1} & a_{0,2} & a_{0,3} & a_{0,4} \\ a_{1,0} & a_{1,1} & a_{1,2} & a_{1,3} & a_{1,4} \\ a_{2,0} & a_{2,1} & a_{2,2} & a_{2,3} & a_{2,4} \\ a_{3,0} & a_{3,1} & a_{3,2} & a_{3,3} & a_{3,4} \\ a_{4,0} & a_{4,1} & a_{4,2} & a_{4,3} & a_{4,4} \end{vmatrix}$$

Figure 1. Making of data block from stream

2.2 The Round Transformation

There are ten rounds, and in each of the round there are series of transformations takes place except the final round.A pseudo algorithm for each of the common round is given below and later the final round transformation algorithm is given.The state is referred as the output of the previous transformation. Each function in the round is explained later.The final round is equal to others when mix-column transformation is removed from general one.

Algorithm 1: (For Common Rounds)
Round(state, Round Key)

{
ByteSub(state);
ShiftRow(state);
MixColumn(state);
AddRoundKey(state, Round Key);
}
Algorithm 2: (For Final Round)
FinalRound(state, Round Key)
{
ByteSub(state);
ShiftRow(state);
AddRoundKey(state, Round Key);
}

2.3 The Byte Sub Transform

The ByteSub transformation is a non linear byte substitution that acts on every byte of the state in isolation to produce a new byte value using an S-box substitution table.In this transformation, each of the byte in the state matrix is replaced with another byte as per the S-box (Substitution Box).The S-box is generated by calculating the respective reciprocal of that byte in GF (2^8) and then affine transform is applied.Similarly,Inverse S-Matrix can be formed during the decryption of the cipher text.For increasing the efficiency,we use Rijndael S-box.

Table 1. S-Box

	x0	x1	x2	x3	x4	x5	x6	x7	x8	x9	xa	xb	xc	xd	xe	xf
0x	63	7c	77	7b	f2	6b	6f	c5	30	01	67	2b	fe	d7	ab	76
1x	ca	82	c9	7d	fa	59	47	f0	ad	d4	a2	af	9c	a4	72	c0
2x	b7	fd	93	26	36	3f	f7	cc	34	a5	e5	f1	71	d8	31	15
3x	04	c7	23	c3	18	96	05	9a	07	12	80	e2	eb	27	b2	75
4x	09	83	2c	1a	1b	6e	5a	a0	52	3b	d6	b3	29	e3	2f	84
5x	53	d1	00	ed	20	fc	b1	5b	6a	cb	be	39	4a	4c	58	cf
6x	d0	ef	aa	fb	43	4d	33	85	45	f9	02	7f	50	3c	9f	a8
7x	51	a3	40	8f	92	9d	38	f5	bc	b6	da	21	10	ff	f3	d2
8x	cd	0c	13	ec	5f	97	44	17	c4	a7	7e	3d	64	5d	19	73
9x	60	81	4f	dc	22	2a	90	88	46	ee	b8	14	de	5e	0b	db
ax	e0	32	3a	0a	49	06	24	5c	c2	d3	ac	62	91	95	e4	79
bx	e7	c8	37	6d	8d	d5	4e	a9	6c	56	f4	ea	65	7a	ae	08
cx	ba	78	25	2e	1c	a6	b4	c6	e8	dd	74	1f	4b	bd	8b	8a
dx	70	3e	b5	66	48	03	f6	0e	61	35	57	b9	86	c1	1d	9e
ex	e1	f8	98	11	69	d9	8e	94	9b	1e	87	e9	ce	55	28	df
fx	8c	a1	89	0d	bf	e6	42	68	41	99	2d	0f	b0	54	bb	16

2.4 The Shift Row Transform

For encryption, the 1st row remain unchanged, 2nd row is shifted 1 byte to the left, 3rd is 2 byte to the left, 4th is 3 byte to the left and 5th row is shifted 4 byte to the left.For decryption the operation is similar to that for encryption but in reverse direction.

2.5 The Mix Column Transform

$$\begin{vmatrix} 02 & 04 & 03 & 01 & 01 \\ 01 & 02 & 04 & 03 & 01 \\ 01 & 01 & 02 & 04 & 03 \\ 03 & 01 & 01 & 02 & 04 \\ 04 & 03 & 01 & 01 & 02 \end{vmatrix} \qquad \begin{vmatrix} E0 & 7D & 09 & 8A & 4C \\ 4C & E0 & 7D & 09 & 8A \\ 8A & 4C & E0 & 7D & 09 \\ 09 & 8A & 4C & E0 & 7D \\ 7D & 09 & 8A & 4C & E0 \end{vmatrix}$$

(a) (b)

Figure 2. (a) Polynomial Matrix (b) Inverse Polynomial Matrix for Mix column transformation.

This is a complex procedure as it involves severely the byte multiplication under GF (2^8). The whole state is to be multiplied with pre-defined matrix called polynomial matrix. It completely changes the scenario of the cipher even if the all bytes look very similar. The Inverse Polynomial Matrix does exist in order to reverse the mix column transformation. Each Column is replaced by the multiplicative value such as b(x)=c(x)*a(x), where, '*' refers to multiplication under GF (2^8).

2.6 The AddRoundKey Transform

During this, the round key is simply bitwise XORed with the state came from above.The round keys are generated similarly as in the Rijndael Algorithm of 128 bits.To inverse this state, one need to again XOR the Round Key in the state.

2.7 Key Schedule

The Round Keys are derived from the Cipher Key by means of the key schedule.This consists of two components: the Key Expansion and the Round Key Selection.The basic principle is the following.

- The total number of Round Key bits is equal to the block length multiplied by the number of rounds plus 1.
- The Cipher Key is expanded into an Expanded Key.

3. Experiment and Result

3.1 Power Consumed

The consumed power during any encryption and decryption is also one of the parameter to check their hardware efficiency. And hence, the consumed power is calculated for all mentioned algorithms in the following manner:

$$P_C = N_C . V_i . I_{avg}$$

Where,P_C represents consumed power,N_C denotes number of CPU cycles consumed during process, V_i denotes the input voltage for processor,equal to 3.3V and I_{avg}represents the average current drawn at processor per cycle which is approximately 48 Na.

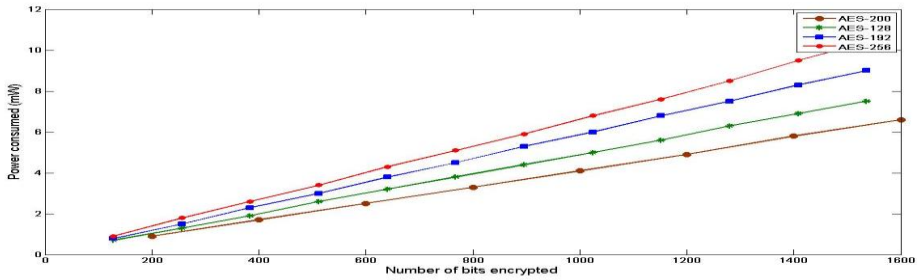

Figure 3. Comparison of power Consumption at encryption side

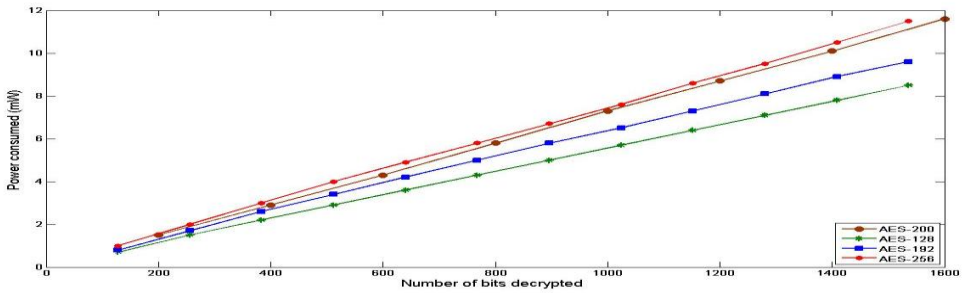

Figure 4. Comparison of power Consumption at decryption side

Since the consumed power directly depends on the number of CPU cycles taken for the process, so power during encryption and decryption is proportional to the CPU cycles, and varies in accordance. From the graph, it is observed that number of CPU cycles taken to encrypt the block is up to 30% lesser than other conventional algorithms.However, number of CPU cycles needed during decryption is higher and above 20% from the conventional AES algorithms.

3.2 Strict Avalanche Criteria

The strict avalanche criterion (SAC) is a generalization of the avalanche effect. It is satisfied if, whenever a single input bit is complemented, each of the output bits changes with a 50% probability [18]. The SAC builds on the concepts of completeness and avalanche.

$$K_{SAC}(i,j) = \frac{1}{2^n} W(a_j^{ei}) = \frac{1}{2}$$

where, $K_{SAC}(i,j)$can take values in the range [0,1], it should be interpreted as the probability of change of the j^{th} output bit when the i^{th} bit in the input string is changed.

$W(a_j^{gi})$ is input word to the system and here less than 256 always.

The Security of the proposed model is examined by performing the test: Strict Avalanche Criterion and Bit Independence Criterion. SAC tells about the probability of the bit change while the BIC states the correlation that output bit possess. Both of the criteria are analyzed and the proposed algorithm falls within the desired level of security.

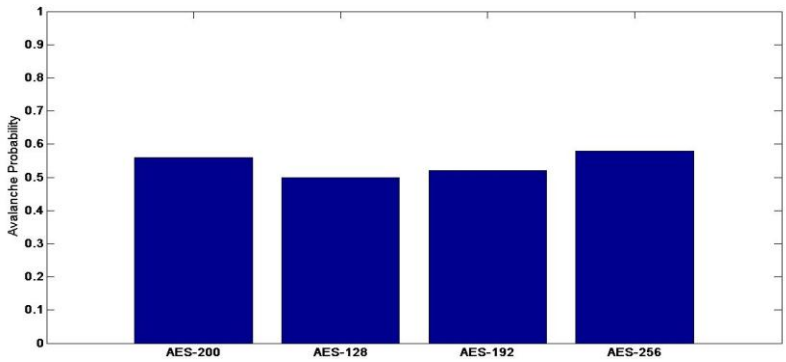

Fig Figure 5. Avalanche probability for various algorithms

From the plot, it can be seen that probability to get a bit changed for a highly correlated input, in proposed work, is very similar to the conventional AES, which results this in a secure algorithm and validates it to be used in communication.

4. Advantages and Disadvantages

Advantages

- Resistance against all known attacks.
- Speed and code compactness on a wide range of platforms.
- Design simplicity.
- Our proposed algorithm can be implemented to run at speeds unusually fast for a block cipher on a Pentium (Pro).There is a trade-off between table size / performance.
- The round transformation is parallel by design, an important advantage in future processors and dedicated hardware.

Limitations

- The inverse cipher is less suited to be implemented on a smart card than the cipher itself: it takes more code and cycles.
- In software, the cipher and its inverse make use of different code and/or tables.
- In hardware, the inverse cipher can only partially re-use the circuitry that implements the cipher.

5. Conclusion

The announcement of AES attracted concentration of cryptanalysts to measure its level of security.As mentioned earlier, there is always a trade-off between the security and performance of wireless network. AES provides a very high level of security in an efficient way, but it also has some flaws in terms of security and the performance[11-14].The improvement AES must possess similar level of security as in conventional AES.The proposed model has bigger block size which is 200 bits rather than conventional 128 bits. Also, the block is made by 5 rows and 5 columns unlike the AES's 4 rows and 4 columns.As the size of the matrix has increased, all the transformations of the AES don't need to change except the mixcolumn transformation. During mixcolumn transformation, the diffusion takes place in form of matrix multiplication under finite field. Having a bigger block, hence, requires a new matrix of size 5 X 5, to enable matrix multiplication.Here number of CPU cycles taken to encrypt the block is up to 30% lesser than other conventional algorithms.However, number of CPU cycles needed during decryption is higher and above 20% from the conventional AES algorithms.Hence, it can be said that the proposed model is secure and can be considered for communication where high data rate is required[20-24].

6. Acknowledgement

I proudly acknowledge my sincere and heartfelt thanks to Mr. Jagtar Singh, Senior Lecturer, N.C College of Engineering, Panipat for their valuable and sustained guidance, constant encouragement and careful supervision during the entire course which made the project successful.I would like to express my immense thanks to my friend Mr. Rajeev Dhanda,Associate Professor,ECE Dept,RVIT,U.P for providing me all the help to pursue my dessirtation to its successful accomplishment.

Reference:

[1] C.Shannon,Communication theory of secrecy systems,Bell Systems Technical Journal,vol.28,1949.
[2] Schneier B. and Whiting D.,Performance Comparison of AES Finalist,2000.
[3] "National Policy on the Use of the AES to Protect National Security Systems and National Security Information",Lynn Hathnway(June 2003),Retrieved 2011-02-15.
[4] "Performance Comparison of the AES submissions",1999-02-01.Retrieved 2010-12-28.
[5] "An Efficient Approach For Increasing Security to Symmetric Data Encryption",International Journal of Computer Science and Network Security,Vol.8 No.4,April,2008.
[6] J.Daemen and V.Raemen,The Design of Rijndael:AES-The Advanced Encryption Standards.Springer-Verlag,2002.
[7] J. Daemen, V. Rijmen, The block cipher Rijindael, Proceedings of the Third International Conference on smart card Research and Applications, CARDIS'98, Lecture Notes in computer Science, vol.1820, Springer, Berlin, 2000, pp.277_284.
[8] Federal Information Processing Standards Publications (FIPS 197), Advanced Encryption Standard (AES) ,26 Nov. 2001.
[9] Shivkumar S, Umamaheswari G., Performance Comparison of Advanced Encryption Standard(AES) and AES key dependent S-box - Simulation using MATLAB, International Journal of Computer Theory , 2011.
[10] Fahmy A., Shaarawy M., El-Hadad K., Salama G. and Hassanain K., A Proposal For A Key-Dependent AES, SETIT, Tunisia, 2005.
[11] Schneier B., Applied Cryptography: Protocols, Algorithms and Source Code in *C.* John Wiley and Sons, 1996.
[12] Stallings W., Cryptography and Network Security, Third Edition, Pearson Education, 2003.
[13] Anne Canteaut, Ongoing Research Areas in Symmetric Cryptography, 1999.
[14] Heys H. M., A Tutorial on Linear and Differential Cryptanalysis, St. John's, NF, Canada, 2008.
[15] Chandrashekharan, J., et al. A chao Based Approach for Improving Non-linearity in the S-box Design of Symmetric Key Cryptosystem, Advances in Networks and communication, First International Conference on Computer Science and Information Technology (CSIT), Springer Bangalore, p. 516, ISBN- 978-3-642-17877-1, India, 2011.
[16] Nyberg K., Perfect Nonlinear S-boxes, Advances in Cryptography, Brioghtenpp 378-386, 1991.
[17] IBM Corporation MARS, A Candidate of AES cipher, http://www.research.ibm.com/security/mars.html, 1999.
[18] Burwick, C., Coppersmith, D., D.Avignon, E., Gennaro, R., Halevi, S., Jutla, C., Matyas,S., O.Connor, L., Peyravian, M., Safford, D., Zunic, N.: MARS- a candidate cipher for AES. Proceedings of the First AES Conference (1999). Revised September 22, 1999.
[19] Parker G. M., Generalised S-Box Nonlinearity, SBoxLin.tex, 11.02.03, IST -1999-12324, 2003.
[20] Keliher, L., Substitution permutation network cryptosystem using S-boxes.
[21] Stoianov N., One Software Tool for Testing Square S-boxes, Technical University of Sofia (TUS), Bulgaria 2008.
[22] Ahmed N., Testing an S-Box for Cryptographic Use, International Journal of Computer and Electrical Engineering.
[23] Adams, C. M.: Designing S-Boxes For Ciphers Resistant To Differential Cryptanalysis (Extended Abstract), Feb 2010.
[24] M. Dawson, S. Tavares, An Expanded Set of S-box Design Criteria Based on Information Theory and its Relation to Differential-like Attacks, Advances in Cryptology, Springer-Verlag, 1991.

A SIMPLE ALGORITHM FOR REDUCTION OF BLOCKING ARTIFACTS USING SAWS TECHNIQUE BASED ON FUZZY LOGIC

Sonia Malik [1], Rekha Saroha [2], Rohit Anand [3]
[1] [2] Department of Electronics and Communication Engineering, NCCE, Panipat, INDIA
[3] Assistant Professor, Electronics and Communication Engineering, NCCE, Panipat, INDIA

ABSTRACT
Reducing blocking artifacts encountered in highly compressed images is a very active research area in image processing. Coding artifacts are very annoying in these highly compressed images. Most of the artifact reduction techniques blur the details of the images while removing coding artifacts. In this paper , we propose a novel and explicit approach for reducing coding artifacts in an image by using the combination of SAWS equation and Fuzzy Rules. We use FIDRM for the detection of noisy pixel and NAFSM filter for correction. Experimental results demonstrate that the proposed approach achieves excellent visual quality and PSNR as compared to a number of deblocking methods in the literature.

Keywords: Block Based Discrete Cosine Transform (BDCT), Deblocking Block (DB), Fuzzy Impulse Artifact Detection and Reduction Method (FIDRM), Noise Adaptive Fuzzy Switching Median Filter (NAFSM), Signal Adaptive Weighted Sum Technique (SAWS).

I. Introduction
Image compression is a very important issue in both image and video coding applications. The main purpose of image compression is to reduce storage and transmission costs while maintaining image quality.
It is known that blocking artifacts are introduced by coarse quantization of transform coefficients at low bit rates and independent quantization of each block [2]. There are three types of blocking artifacts in BDCT coded images. One is staircase noise along the image edges, another is grid noise in monotone area, and the other one is corner outliers in corner point of 8 x 8 DCT block.[1] To remove blocking artifacts, many deblocking techniques have been proposed in last decade, but they often introduce excessive blurring, ringing and in many cases they produce poor deblocking results at certain areas of image. So to reduce excessive blurring and removing artifacts a algorithm is proposed for BDCT- coded images, based on Signal Adaptive Weighted Sum Technique. In this method the center pixel is calculated as the weighted sum of the boundary pixels. Therefore SAWS technique is applied to center pixel and boundary pixels. We adjust the weights according to directional correlation and block activities [3]. In this paper, we propose a blocking artifact removal algorithm for BDCT-coded images using SAWS technique based on combination of FIDRM And NAFSM. FIDRM is a two step filter: the detection phase and the filtering phase. The detection phase uses fuzzy rule to determine whether a pixel is corrupted or not. Then we try to indicate the values of detected pixels p_k ($k \in \{1,..., n\}$ with $1 \leq n < 255$). After this detection fuzzy filtering focuses on only p_k values [4]. The NAFSM filter uses a square filtering window with odd dimensions which is used to satisfy the criterion of choosing only a noise free pixel as the median pixel [5]. The rest of the paper is organised as follows. Section II introduces SAWS technique. Section III represents the proposed method of reducing artifacts using SAWS technique along with NAFSM and FIDRM filters. Experimental results and Conclusion are presented in Sections IV and V.

II. Saws Equation
A Deblocking block and its subblocks are shown in the Fig. 1. A pixel in Deblocking Block (DB) is modified by using three pixels at block boundaries, to remove block discontinuities in this SAWS technique. And these three pixels belongs to three SubBlocks except for the SubBlock containing the to-be-modified pixel.
Let $p'_{i,j}$ be the modified pixel of $p_{i,j}$ in the DB, and the weighted sum equation is given by

$$p'_{i,j} = \frac{p_{i,j} + \alpha_{i,j} p_{i,n} + \beta_{i,j} p_{m,j} + \gamma_{i,j} p_{m,n}}{1 + \alpha_{i,j} + \beta_{i,j} + \gamma_{i,j}} \quad (1)$$

Where m is N/2 if I is less than N/2; otherwise, (N/2)-1, and n is N/2 if j is less than N/2 otherwise, (N/2)-1. In the above equation $p_{i,n}$ and $p_{m,j}$ are the boundary pixels lying on the $p_{i,j}$'s row and column, respectively, and $p_{m,n}$ is a boundary pixel lying on diagonal position.

The weights a, b and c are functions of distance between $p_{i,j}$ and its boundary pixel.

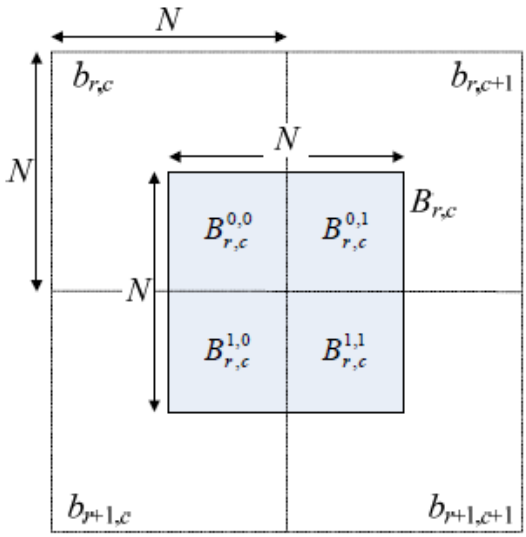

Fig. 1. A Deblocking Block (DB) and its SubBlocks.

III. PROPOSED METHOD

In our proposed method instead of using only above saws equation we are using the combination of SAWS technique, fuzzy gradient values as introduced with GOA filter [6],[7] and median filter[5].

3.1 Fuzzy Gradient Values

For each pixel (i,j) of the image, not a border pixel, we use a 3x3 neighborhood window as shown in Fig. 2

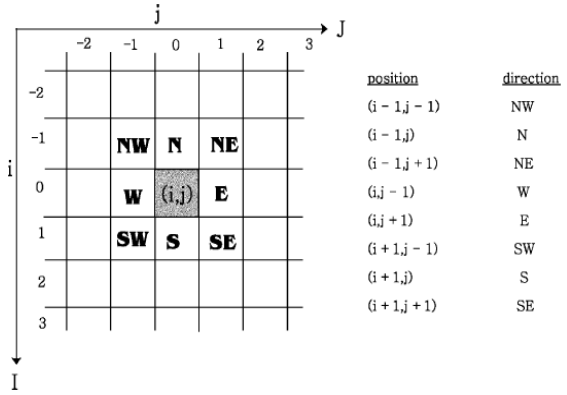

position	direction
(i − 1,j − 1)	NW
(i − 1,j)	N
(i − 1,j + 1)	NE
(i,j − 1)	W
(i,j + 1)	E
(i + 1,j − 1)	SW
(i + 1,j)	S
(i + 1,j + 1)	SE

Fig. 2. Neighborhood of a central pixel.

Each neighbor with respect to (i,j) corresponds to one direction {NW= north west, N= north, NE= north east, W= west, E= east, S= south, SE= south east, SW= south West}.

If A denotes input image then the gradient is defined as the difference

$$Del(k,l)A(i,j) = A(i+k, j+l) - A(i,j) \text{ with } k,l \in \{-1,0,1\} \quad (2)$$

where the pair (k,l) corresponds to one of the eight directions and (i,j) is called center of gradient. The eight gradient values are called the basic gradient values. One such gradient value can be used to determine if a central pixel is corrupted or not because if gradient is large it indicates that some artifacts are present in the central pixel (i,j), but this conclusion is wrong in two cases.

1) If the central pixel is not noisy, but one of the neighbors is then this can also cause large gradient values.
2) An edge in an image causes some kind of natural large gradient values.

To solve first case, only only one gradient value is used, and to solve the second case one basic and two related gradient values for each direction. The two related gradient values are determined by the centers making a right angle with the direction of the basic gradient.

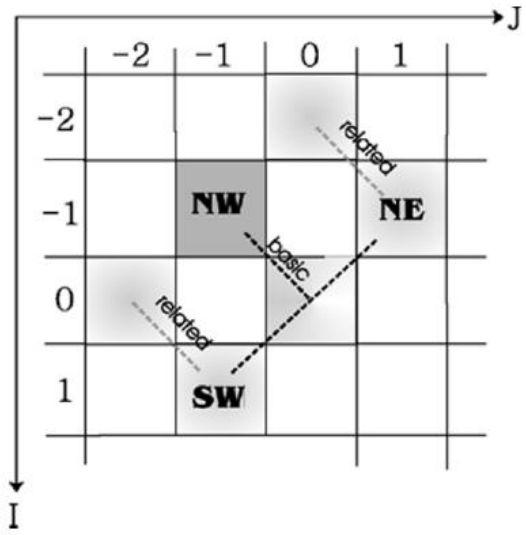

Fig. 3. Involved centers for the calculation of the related gradient values in the NW-direction.

Table1. Involved gradient values to calculate fuzzy gradient

R	basic gradient	related gradients
NW	$\nabla_{NW}A(i,j)$	$\nabla_{NW}A(i+1,j-1), \nabla_{NW}A(i-1,j+1)$
N	$\nabla_{N}A(i,j)$	$\nabla_{N}A(i,j-1), \nabla_{N}A(i,j+1)$
NE	$\nabla_{NE}A(i,j)$	$\nabla_{NE}A(i-1,j-1), \nabla_{NE}A(i+1,j+1)$
E	$\nabla_{E}A(i,j)$	$\nabla_{E}A(i-1,j), \nabla_{E}A(i+1,j)$
SE	$\nabla_{SE}A(i,j)$	$\nabla_{SE}A(i-1,j+1), \nabla_{SE}A(i+1,j-1)$
S	$\nabla_{S}A(i,j)$	$\nabla_{S}A(i,j-1), \nabla_{S}A(i,j+1)$
SW	$\nabla_{SW}A(i,j)$	$\nabla_{SW}A(i-1,j-1), \nabla_{SW}A(i+1,j+1)$
W	$\nabla_{W}A(i,j)$	$\nabla_{W}A(i-1,j), \nabla_{W}A(i+1,j)$

Table 1 gives an overview of the involved gradient values. First column gives the direction corresponds to a position with respect to central position. Column two gives basic gradient values and column three gives the two related gradients. Eight fuzzy gradient values are defined for each of the eight directions. The fuzzy gradient value for direction R(R€ {NW, N, NE, E, SE, S, SW, W}), is calculated by the fuzzy rule.

IF $|delR\ A(i,j)|$ *is large AND* $|del'R\ A(i,j)|$ *is small*
OR
$|$delR A(i,j)$|$ is large AND $|$del''R A(i,j)$|$ is small
OR
delR A(i,j) is big positive AND del'R A(i,j) AND del''R A(i,j) are big negative
OR
delR A(i,j) is big negative AND del'R A(i,j) AND del'' A(i,j) are big positive

THEN fuzzy gradient value is large.

Where delR A(i,j) is basic gradient value and del'R A(i,j) and del''R A(i,j) are two related gradient values for direction R. Large, small, big positive and big negative are nondeterministic features, therefore these can be represented as fuzzy sets [8].

Fuzzy set can be represented by membership functions, as the membership function large represents fuzzy set large, small represents fuzzy set small, big positive represents fuzzy set big positive and big negative represents fuzzy set big negative as shown in fig.4.

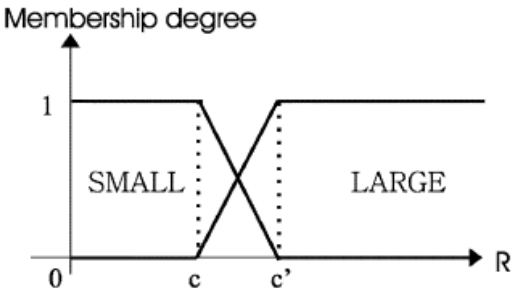

(a)

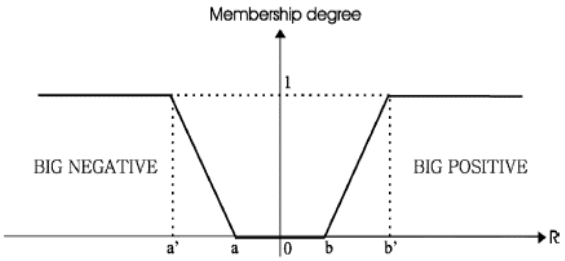

(b)

Fig. 4 . Membership functions (a) SMALL, respectively, LARGE; (b) BIG NEGATIVE, respectively, BIG POSITIVE.

A. Detection stage

To decide whether the central pixel contains block discontinuity or not, we use the following fuzzy rule:

IF most of the eight gradient values are large THEN the central pixel A(i,j) is an block discontinuous pixel.

We translate this rule by: if for a certain central pixel (i,j) more than half of the fuzzy gradient values are part of the support of the fuzzy set large[8], then we can conclude that pixel as a block discontinued pixel.

B. Filtering stage

The NAFSM filter uses a square filtering window W(i,j) with odd (2s+1) x (2s+1) dimensions. The noise free pixels are used for selecting median pixel, given by

$$M(i,j) = \text{median}\{X(i+m, j+n)\} \quad \text{with } N(i+m, j+n) = 1 \tag{3}$$

After median pixel M(i,j) is found, the local information in a 3x3 window is extracted by first computing the absolute luminous difference d(i,j) as given by

$$D(i+k, j+l) = \left| X(i+k, j+l) - X(i,j) \right| \quad \text{with } (i+k, j+l) \neq (i,j) \tag{4}$$

Then the local information is defined as the maximum absolute luminance difference in the 3x3 filtering window

$$D(i,j) = \max\{d(i+k, j+l)\} \tag{5}$$

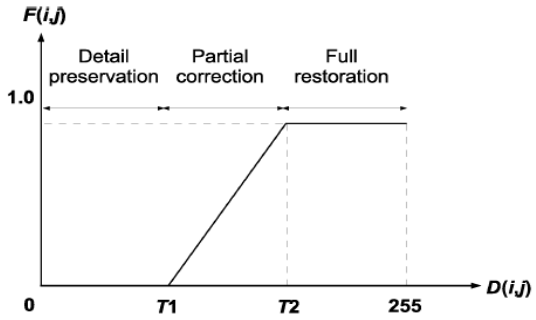

Fig.5 Fuzzy set adopted by NAFSM filter

In NAFSM filter, fuzzy reasoning is applied to the extracted local information D(i,j). The fuzzy set adopted is shown in fig.5 and defined by the fuzzy membership function F(i,j)

$$F(i,j) = \begin{cases} 0, & : \quad D(i,j) < T_1 \\ \frac{D(i,j)-T_1}{T_2-T_1}, & : \quad T_1 \leq D(i,j) < T_2 \\ 1, & : \quad D(i,j) \geq T_2 \end{cases} \tag{6}$$

where the local information D(i,j) is used as fuzzy input variable and the two predefined thresholds T1 and T2 are set to 10 and 30, respectively, for optimal performance[9][10].
Finally, the correction term to restore a detected 'noise pixel' is a linear combination between the processing pixel X(i,j) and median pixel M(i,j). the restoration term Y(i,j) is given as

$$Y(i,j) = [1- F(i,j)] \, . \, X(i,j) + F(i,j) \, . \, M(i,j) \tag{7}$$

where the fuzzy membership value F(i,j) lends a weight on whether more of pixel X(i,j) or M(i,j) is to be used.

4. Experimental Results

To demonstrate the performance of the proposed algorithm, we conduct comprehensive experiments with a number of 512x512 grayscale images, Lena, Peppers, and Goldhill. These images are compressed at various bit rates. Initially, we provide the objective performance in PSNR by proposed algorithm, and compare them with some of the existing deblocking methods. Experimental results shows that the proposed algorithm gives improved PSNR then the other debloking methods in the literature.

5. Conclusion

In this paper a new approach for reducing artifact is presented which is based on two types of filter i.e FIDRM and NAFSM filters. These filters are based on fuzzy rules. The main feature of FIDRM filter is that it leaves the noise free pixels unchanged. Experimental results show the feasibility of the new algorithm. A numerical measure, such as PSNR, and visual quality show convincing results for grayscale images . The proposed approach can be used in many mobile devices that have limted storage and bandwidth and therefore suffer from blocking artifacts.

6. Acknowledgments

With a deep sense of gratitude and heartiest honour, I would like to express my immense thanks to Dr. Vijay Nehra, Associate Professor, ECE Dept, BPSMV Khanpur, Sonipat for providing me all the facilities to pursue my dessertation to its successful accomplishment. I proudly acknowledge my sincere and heartfelt thanks to Mr. Rohit Anand, Assistant Professor, N.C College of Engineering, Panipat for his valuable and sustained guidance, constant encouragement and careful supervision during the entire course which made the project successful.

References

[1] Y. Lee, H. Kim, and H. Park, "Blocking effect reduction of JPEG images by signal adaptive filtering," *IEEE Trans. Image Process.*, vol. 7, no. 2, pp. 229-234, Feb. 1998.
[2] T. Chen, H. R. Wu, and B. Qiu, "Adaptive postfiltering of transform coefficients for the reduction of blocking artifacts," *IEEE Trans. Circuits Syst. Video Technol.*, vol. 11, no. 5, pp. 594-602, May 2001.
[3] Jongho Kim and Chun Bo Sim, "Compression artifacts removal by signal adaptive weighted sum technique," *IEEE Transactions on Consumer Electronics*, Vol. 57, No. 4, November 2011.
[4] Stefan Schulte, Mike Nachtegael, Valérie De Witte, Dietrich Van der Weken, and Etienne E. Kerre, "A Fuzzy Impulse Noise Detection and Reduction Method*," IEEE Transactions On Image Processing*, Vol. 15, No. 5, May 2006.
[5] Kenny Kal Vin Toh, *Student Member, IEEE*, and Nor Ashidi Mat Isa*, Member, IEEE, "*Noise adaptive fuzzy switching median filter for salt-and-pepper noise reduction" *IEEE Signal Processing Letters*, Vol. 17, No. 3, March 2010.
[6] D. Van De Ville, M. Nachtegael, D. Van derWeken, E. E. Kerre, and W. Philips, "Noise reduction by fuzzy image filtering," *IEEE Trans. Fuzzy Syst.*, vol. 11, no. 4, pp. 429–436, Aug. 2001.
[7] M. Nachtegael, D. Van der Weken, and E. E. Kerre, "Fuzzy techniques in image processing: three case studies," *Int. J. Comput. Anticipatory Syst.*, vol. 12, pp. 89–104, Aug. 2002.
[8] E. E. Kerre, *Fuzzy Sets and Approximate Reasoning* . Xian, China: Xian Jiaotong Univ. Press, 1998.
[9] K. K. V. Toh, H. Ibrahim, and M. N. Mahyuddin, "Salt-and-pepper noise detection and reduction using fuzzy switching median filter," *IEEE Trans. Consumer Electron.*, vol. 54, no. 4, pp. 1956–1961, Nov. 2008.
[10] W. Luo, "Eficient removal of impulse noise from digital images," *IEEE Trans. Consumer Electron.*, vol. 52, no. 2, pp. 523–527, May 2006.

A Study on Strength Characteristics of Flyash, Lime and Sodium Silicate Mixtures at Their Free Pouring Conditions

[1]P.V.V.Satayanarayana [2]Ganapati Naidu. P [3]S .Adiseshu
[4]P.Padmanabha Reddy
[1]Professor [2, 4] M.E [3] Associate Professor
Department of Civil Engineering
Andhra University, Visakhapatnam

Abstract:
For the utilization of flyash in improving the strength of problematic soils a detail experimental study on the behavior of flyash stabilized with various percentages of lime and sodium silicate and the strength characteristics at their free pouring (30%, 35% & 40% of water by weight of flyash)consistencies have been studied. Different percentages of lime and sodium silicate (gel) were added to flyash and tested for UCS and split tensile strength for different curing periods like 3 days, 7 days and 28 days to obtain optimum dosage of lime and sodium silicate. From the test data it was found that 10 to 15 % of lime and 3 to 5 % of sodium silicate have been identified as optimum dosages. These mixes can be used for bricks and grouting techniques in civil engineering sector.

Keywords– flyash, sodium silicate (gel), unconfined compressive strength (UCS), split tensile strength.

Introduction:

To meet the demands of industrialization and urbanization high volume of road a network is required. Performance of road depends on the structural components such as subgrade, sub base, and base course etc. when roads are running on problematic subgrade such as expansive, soft, collapsible sub grades. Partial or complete failure of pavements takes place; repeated failures require lot of maintenance cost. This can be reduced by ground improvement techniques like full replacement, partial by stabilized material and grouting etc can be used.

Lot of researches has been conducted on flyashes with admixtures, some of these are Yudbhir and Honjo (1991) considered unconfined compressive strength of flyashes as a measure of self hardening property of flyashes. They explain free lime content of flyash contributes to pronounced self hardening. Sherwood and Ryley (1966); and Raymond(1961)v reported that the fraction of lime, present as free lime in the form of calcium hydroxide controls self hardening characteristics of flyashes. Syngh (1996a) studied the unconfined compressive strength of flyashes as a function of free lime present in them and found that flyashes having higher free lime content shows higher strength. In addition to these flyash columns and flyash admixture columns can also be used. In this study NTPC fly ash is stabilized with lime and sodium silicate and performed tests like Unconfined compressive strength, Split tensile strength to identify optimum dosage of lime and sodium silicate for bulk utilization of fly ash.

2.0 Material used

The materials used in this investigation are Flyash (NTPC), Lime and sodium silicate.
Flyash is collected from NTPC Paravada in Visakhapatnam and laboratory study was carried out for salient geotechnical characteristics of such as grading, Atterberg limits, compaction and strength. The physical properties of flyash shown in table 2 and chemical composition of flyash shown in table : 1.

Table: 1

Compound	Formula	Percentage (%)
Magnesium oxide	MgO	0.86
Aluminum trioxide	Al2O3	30.48
Silica dioxide	SiO2	59.83
Calcium oxide	CaO	1.74
Titanium oxide	TiO2	6.91
Zinc oxide	ZnO	0.09

Property	Values
Sand (%)	28
Fines (%)	72
a. Silt(%)	72
b. Clay(%)	0
Liquid Limit (%)	24
Plastic Limit (%)	NP
Specific gravity	2.1
OMC (IS heavy Compaction)	
Optimum moisture content (%)	21.0
Maximum dry density (g/cc)	1.28
California bearing ratio	3

Table : 2

3.0 Experimental programme:

In this study dry flyash has mixed with lime (5%, 10% and 15%) and Sodium silicate gel (1, 2, 3, 4 and 5%) by percentage weight of dry flyash and added water of 30%, 35% and 40% by their weight and thoroughly mixed to get the required consistency and poured these samples into given sizes(38mm X 76mm) of samplers and kept cured for 1 day , 3 days, 7 days and 28 days respectively by maintaining 100% humidity and without loss of moisture from the samples.

4.0 Results and Discussions:

4.1 Unconfined Compressive strength (kg/ cm^2):

The samples of sizes 38 mm diameter and height of 76 mm were prepared as said above by free pouring in the UCS moulds. All the prepared samples were cured for 1 day, 3 days, 7 days and 28 days by maintaining 100% humidity. Compressive strength test were conducted after completion of their curing period at a strain rate of 1.25 mm/min.

Unconfined Compressive strength of flyash with 5% lime and sodium silicate (free pouring consistency):

Curing period	Water content	sodium silicate %					
		1	2	3	4	5	6
1	30	0.569	0.823	0.84	0.9	1.12	
	35	0.52	0.8	0.84	0.88	1	1.19
	40	0.5	0.75	0.8	0.84	0.86	1.12
3	35	0.84	2.06	1.96	1.86	1.52	
	40	1.19	2.12	2.89	3.34	2.85	2.62
	30	3.88	5.52	8.89	7.46	7.02	6.84
7	40	2.32	4.26	3.28	2.89	2.65	
	30	3.02	3.68	5.74	5.12	4.06	
	35	5.08	9.06	14.4	13.2	12.5	12
28	30	3.42	5.24	8.78	8.24	7.58	
	35	5.72	8.62	10.32	9.24	8.84	.
	40	8.06	11.42	18.35	17.04	16.17	

Table: 3

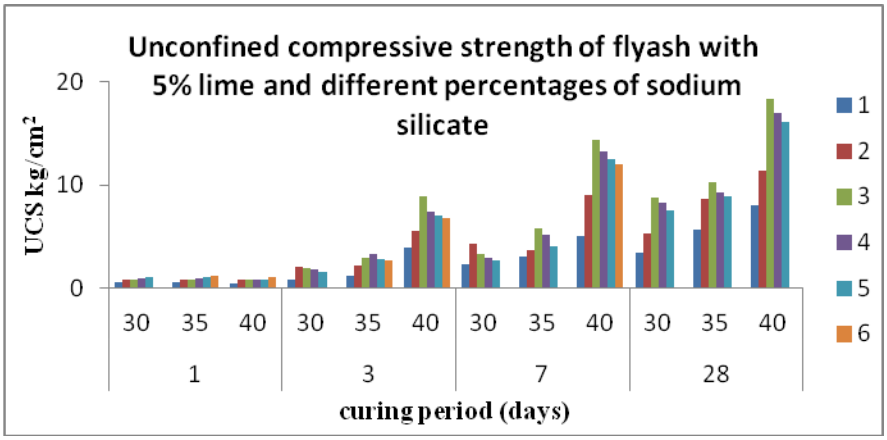

Fig: 1

For 5% lime, at different percentage of water content 3% sodium silicate gives good strength of flyash at all curing periods and the maximum strength observed at 40% water content and 28 days curing period is 18.35kg/cm^2.

Unconfined Compressive strength of flyash with 5% lime and sodium silicate (free pouring consistency):

Curing period	Water content	sodium silicate %					
		1	2	3	4	5	6
1	30	1.232	1.454	1.982	2.539	2.394	2.094
	35	1.14	1.69	2.07	2.842	2.53	2.21
	40	1.42	1.962	2.48	3.02	2.69	2.34
3	35	2.49	4.07	6.12	6.69	5.49	5.02
	40	4.18	6.39	8.12	10.68	9.12	8.24
	30	6.56	10.19	13.56	15.75	14.25	13.82
7	40	5.704	8.81	10.28	11.95	11.21	10.86
	30	8.78	12.45	14.8	15.32	14.24	13.63
	35	11.56	16.1	18.74	21.97	20.54	20.02
28	30	8.38	14.95	16.59	21.7	19.24	18.65
	35	10.82	14.95	17.62	21.71	19.23	18.12
	40	15.89	21.4	26.89	30.62	28.8	26.7

Table: 4

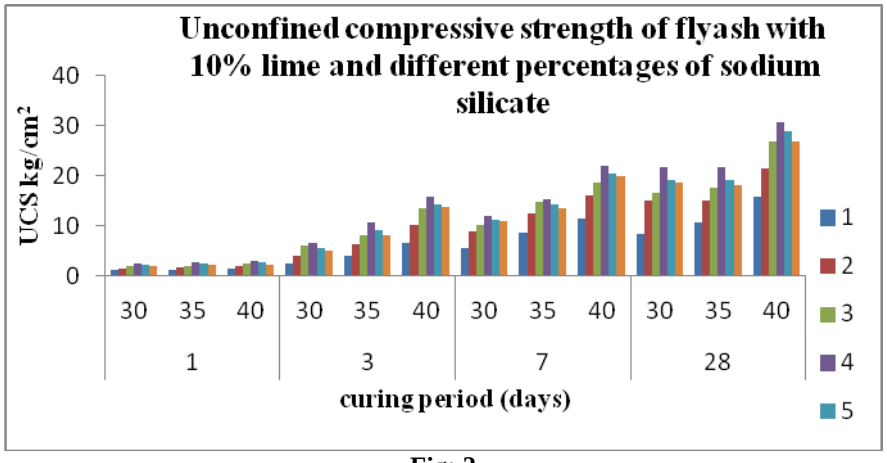

Fig: 2

For 10% lime, at different percentage of water content 4% sodium silicate gives good strength of flyash at all curing periods and the maximum strength observed at 40% water content and 28 days curing period is 30.62kg/cm^2.

Unconfined Compressive strength of flyash with 5% lime and sodium silicate (free pouring consistency):

Curing period	Water content	sodium silicate %					
		1	2	3	4	5	6
1	30	1.43	1.619	2.04	2.14	2.19	2.11
	35	1.85	2.12	2.36	2.58	2.91	2.46
	40	2	2.38	2.84	3.26	3.82	3.24
3	35	2.65	5.58	7.46	8.18	8.65	8.04
	40	4.95	7.68	9.65	11.72	12.86	11.24
	30	7.82	14.89	17.66	20.65	23.2	21.2
7	40	6.88	10.12	12.56	14.41	16.29	15.24
	30	9.66	13.89	16.2	17.54	18	17.12
	35	13.24	18.4	22.24	24.6	25.1	23.2
28	30	10.32	16.82	20.75	23.42	25.21	23.43
	35	11.64	18.35	22.89	24.85	26.39	25.21
	40	17.69	23.6	29.2	32.64	34.35	32.6

Table: 5

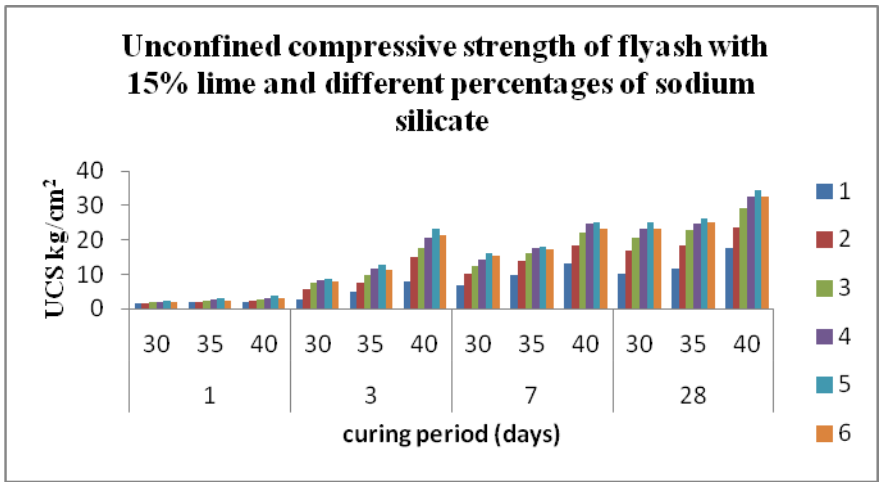

Fig: 3

For 15% lime, at different percentage of water content 5% sodium silicate gives good strength of flyash at all curing periods and the maximum strength observed at 40% water content and 28 days curing period is 34.35kg/cm^2.

4.4 Split Tensile Strength (kg/cm^2):

The samples of sizes 38 mm diameter and height of 76 mm were prepared by static compaction method to achieve maximum dry density at their optimum moisture contents OMC. All the prepared samples were cured for 1 day, 3days, 7 days and 28 days by maintaining 100% humidity. The sample is loaded until splitting / failure load takes after completion of their curing period at a strain rate of 1.25 mm/min.

Tensile strength, $S_t = 2P_u/ \pi Dt$

Where, P_u = ultimate load at which failure of sample.

D = diameter of specimen, mm. t = length of specimen, mm

Split tensile strength of flyash with 5% lime and sodium silicate (free pouring consistency):

Curing period	Water content	sodium silicate %				
		2	3	4	5	6
3	35	0.21	0.18	0.17	0.16	0.15
	40	0.26	0.36	0.41	0.38	0.34
	45	0.71	1.15	0.94	0.88	0.82
7	35	0.36	0.41	0.33	0.31	0.29
	40	0.48	0.73	0.68	0.59	0.53
	45	1.3	2.12	1.9	1.76	1.72
28	35	0.63	1.14	1.07	1.02	0.96
	40	1.22	1.49	1.33	1.29	1.27
	45	1.64	2.66	2.45	2.32	2.29

Table: 6

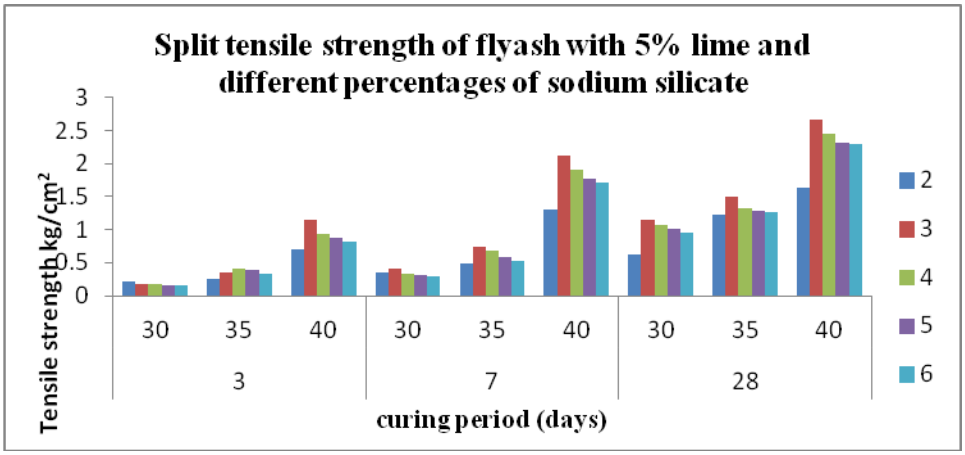

Fig: 4

For 5% lime, at different percentage of water content 3% sodium silicate gives good strength of flyash at all curing periods and the maximum strength observed at 40% water content and 28 days curing period is 2.66kg/cm^2.

Split tensile strength of flyash with 5% lime and sodium silicate (free pouring consistency):

Curing period	Water content	sodium silicate %				
		2	3	4	5	6
3	35	0.42	0.63	0.74	0.72	0.7
	40	0.81	1.04	1.35	1.31	1.29
	45	1.3	1.75	2.02	1.93	1.87
7	35	1.05	1.26	1.43	1.39	1.37
	40	1.68	1.75	1.86	1.82	1.78
	45	2.32	2.68	2.83	2.69	2.64
28	35	1.98	2.26	2.85	2.79	2.76
	40	2.12	2.62	3.09	2.95	2.89
	45	3.04	3.84	4.38	4.23	4.19

Table: 7

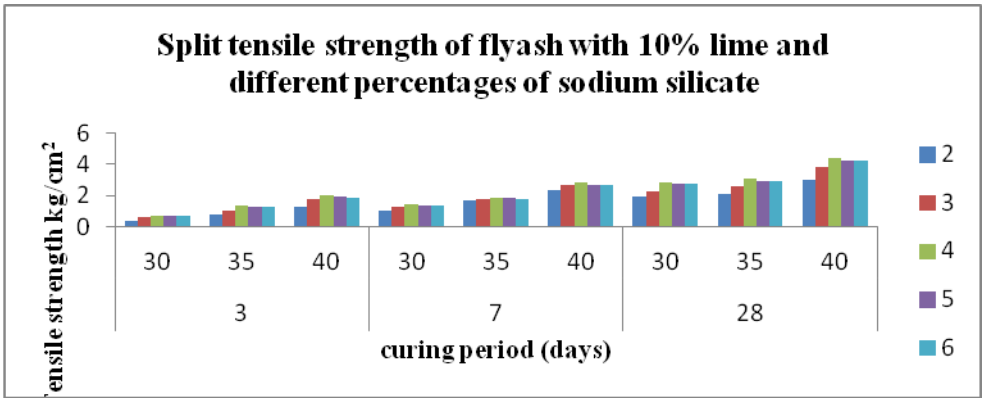

Fig: 5

For 10% lime, at different percentage of water content 4% sodium silicate gives good strength of flyash at all curing periods and the maximum strength observed at 40% water content and 28 days curing period is 4.38kg/cm^2.

Split tensile strength of flyash with 5% lime and sodium silicate (free pouring consistency):

Curing period	Water content	sodium silicate %				
		2	3	4	5	6
3	35	0.61	0.84	0.92	1.15	1.06
	40	1.02	1.26	1.52	1.89	1.76
	45	1.88	2.28	2.65	3	2.91
7	35	1.16	1.46	1.65	1.89	1.76
	40	1.68	1.98	2.1	2.51	2.43
	45	2.62	3.22	3.5	3.86	3.68
28	35	2.24	2.78	3.16	3.54	3.45
	40	2.68	3.32	3.58	4.01	3.89
	45	3.38	4.16	4.66	5.02	4.81

Table: 8

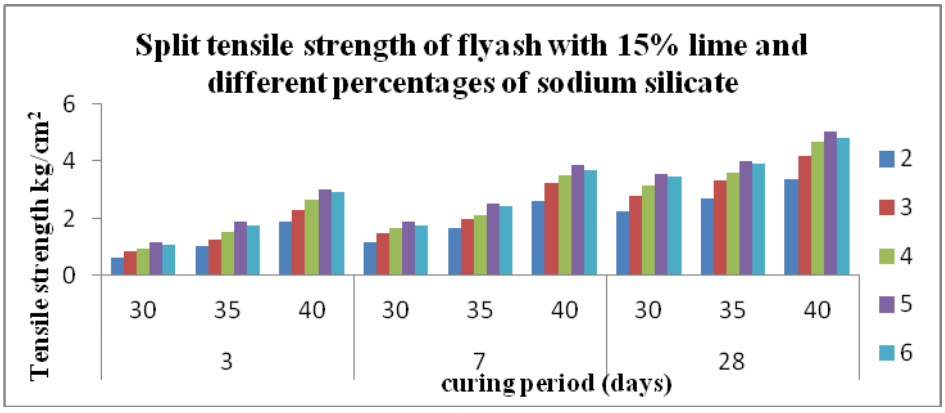

Fig: 6

For 15% lime, at different percentage of water content 5% sodium silicate gives good strength of flyash at all curing periods and the maximum strength observed at 40% water content and 28 days curing period is 5.02kg/cm^2.

Discussions:

For a given percentage of lime strengths increases with increase in sodium silicate content for all consistencies at higher dosages of lime for getting high strengths more dosages of sodium silicate is needed.

At lower consistency, at lower percentage of lime less dosage of sodium silicate was needed. To achieve high strengths at higher percentage of lime high dosage of sodium silicate was needed. At higher dosages a remarkable increase in strengths were observed at higher curing periods (7 days & 28 days).

The increases in strengths are due to interaction between lime and sodium silicate and flyash. This interaction leads to formation of calcium silicate and aluminate hydrated gels for getting high strengths. This gel formation combines particles together and make permanent because of the pozzolanic interaction between flyash, lime and silicate particles over a period of time i.e., at higher curing periods (7 days & 28 days).

Conclusions:

- With increase in percentage of lime and sodium silicate the mix has shown higher values. This is due to pozzolanic action between the particles of flyash and lime.
- For higher percentage of lime more amount of sodium silicate is required.
- As the percentage of lime increases the requirement of water is more for stabilization.
- It is observed that at 28 days curing periods, the strength values are maximum at all percentages of mixes.

References:

- Bowders, J.J, Jr., Usmen, M.A. and Gidluy, J.S. (1987). Stabilized flyash for use as low permeability barriers, proceedings of American society of civil engineers specialty conference.
- Chu.T.Y, Davidson, D.T Goecker, W.L. Moh, Z.C. (1955), *Soil stabilization with lime flyash mixes:* preliminary studies with silty and clayey soils, Highway research Bulletin, 102-112.
- Das, S.C. and Pakrasha, S. (1990).Behaviour of lime stabilized Tit garh PFA through Laboratory tests, IE (1) journal-CV,vol. 70, PP. 181-186.
- Herrin, M. and Mitchell, H. (1961), Lime soil mixtures, highway research board Bulletin, 304, 99-138.
- Mehra, S.R. and Chadda, L.R. (1955), Use of lime in Soil stabilization, Journal of Indian road congress, 19: 3,483.
- Thompson, M.R. (1965), Split tensile strength of lime stabilized soils, Highway research record, 92, 69-82.
- Ghosh RK, Pant, C.S. and Sharma RK. (1979), Stabilization of alluvial soil with lime and flyash. Journal of IRC, New Delhi, vol.35-3, nov.1973.

Performance Analysis of Epileptic Seizure Detection Using DWT & ICA with Neural Networks

M. Stella Mercy
Assistant Professor
Kamaraj college of Engineering and Technology, Virudhunager,
Tamilnadu, India.

Abstract

The electroencephalogram (EEG) signal plays an important role in the detection of epilepsy. The EEG recordings of the ambulatory recording systems generate very lengthy data and the detection of the epileptic activity requires a time- consuming analysis of the entire length of the EEG data by an expert. The aim of this work is compare the automatic detection of EEG patterns using Discrete wavelet Transform (DWT) and Independent Component Analysis (ICA). Our method consists of EEG data collection, feature extraction and classification stages. DWT & ICA methods are used for feature extraction in the principle of time – frequency domain analysis. In classification stage we implement SVM & NN to detect epileptic seizure. Nural Network provides binary classification between preictal/ictal and interictal states. The study is carried out on EEG recordings of two epileptic patients; two classification models are derived from each patient. The models are then tested on the same patient and the other patient, comparing the specificity**,** sensitivity and accuracy of each of the models.

Index terms — Discrete Wavelet Transform (DWT), Independent Component Analysis (ICA), Support Vector Machines (SVM), Electroencephalogram (EEG).

I. INTRODUCTION

Epilepsy is a chronic disorder characterized by recurrent seizures which may vary from muscle jerks to several convolutions. Estimated 1% of world population suffers from epilepsy [1], while 85% of them live in the developing countries. Epileptic detection is done from EEG signal as epilepsy is a condition related to the brain's electrical activity. EEG is routinely used clinically to diagnose, monitor and localize epileptogenic zone.

Occurrence of recurrent seizures in the EEG signal is characteristics of epilepsy. In majority of the cases, the onset of the seizures cannot be predicted in a short period, a continuous recording of the EEG is required to detect epilepsy. The entire length of the EEG recordings is analyzed by expert to detect the traces of epilepsy.

Several approaches have been adopted for automatic detection of epileptiform activities [2]-[6]. A majority of these methods fail to take into account the

Morphological variability of the epileptiform activities and provide little information about the temporal and spatial distributions of the epileptiform activities [7]. And most of these researches focus on the detection of spike and spike-slow complex wave. Since the EEG is non-stationary in general, it is most appropriate to use the time-frequency domain methods.

Wavelet transform provides both time and frequency information of a signal which makes it possible to accurately get and localize features in the data like the epileptiform activities. This paper discusses an automated epileptic EEG detection system using Support Vector Machines (SNM) using a time-frequency domain feature of the EEG signal called Discrete Wavelet Transform (DWT). EEG data is first digitized. The digital EEG data is fed as an input to an automated seizure detection system in order to detect the seizures present in the EEG data.

II. PROPOSED METHODOLOGY

A. Dataset Description

The data used in this research are a subset of the EEG data for both healthy and epileptic subjects made available online by Dr. Ralph Andrzejak of the Epilepsy Centre at the University of Bonn, Germany (http:// www. meb. unibonn.de/epileptologie/science/physik/eeg data.html) [1]. EEGs from two different groups: group H (healthy subjects) and group S (epileptic subjects during seizure) are analyzed. The type of epilepsy was diagnosed as temporal lobe epilepsy with the epileptogenic focus being the hippocampal formation. Each group contains 100 single channel EEG segments of 23.6 sec duration each sampled at 173.61 Hz. As such, each data segment contains N=4097 data points collected at intervals of 1/173.61th of 1s. Each EEG segment is considered as a separate EEG signal resulting in a total of 200 EEG signals or EEGs. As an example, the first 6s of two EEGs (signal numbers in parentheses) for groups H (H029) and S (S001) are magnified and displayed in Fig. 1.

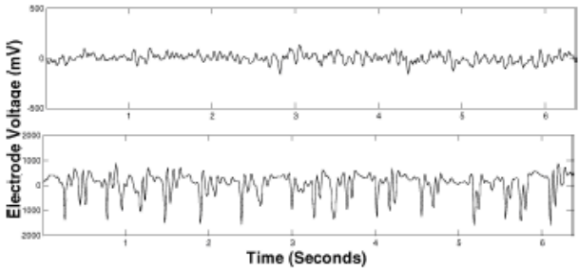

Fig. 1 Sample unfiltered EEGs (0–6 s) for (from top to bottom) Group H (H029) and Group S (S001)

B. Wavelet Transformation

As in traditional pattern recognition systems, the epileptic seizure detection consists of main modules such as a feature extractor that generates a wavelet based feature from the EEG signals, feature selection that composes composite features, and a feature classifier (SVM) that outputs the class based on the composite features. The data flow of the proposed approach is illustrated in Fig. 2.

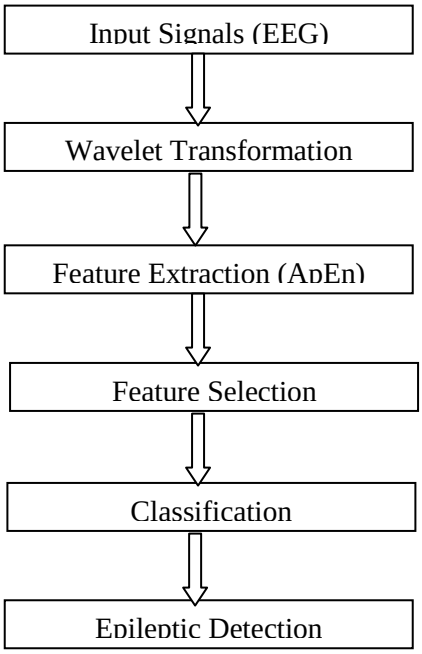

Fig. 2 Data flow diagram of the Proposed system

Wavelet transform is a spectral estimation technique in which any general function can be expressed as an infinite series of wavelets.

The basic idea underlying wavelet analysis consists of expressing a signal as a linear combination of particular set of functions (wavelet transform, WT), obtained by shifting and dilating one single function called a mother wavelet.

The decomposition of the signal leads to a set of coefficients called wavelet coefficients. Therefore the signal can be reconstructed as a linear combination of the wavelet functions weighted by the wavelet coefficients. The key feature of wavelets is the time-frequency localization. It means that most of the energy of the wavelet is restricted to a finite time interval.

The wavelet technique applied to the EEG signal will reveal features related to the transient nature of the signal, which is not made obvious by the Fourier transform. Adeli et al. [7] gave an overview of the discrete wavelet transform (DWT) developed for recognizing and quantifying spikes, sharp waves and spike-waves. In general, it must be said that no time-frequency regions but rather time-scale regions are defined. All wavelet transforms can be specified in terms of a low-pass filter, which satisfies the standard quadrature mirror filter condition. One area in which the wavelet transformation has been particularly successful is the epileptic seizure detection because it captures transient features and localizes them in both time and frequency content accurately.

The wavelet transformation analyses the signal at different frequency bands, with different resolutions by decomposing the signal into a coarse approximation and detail information [8]. The decomposition of the signal into the different frequency bands is merely obtained by consecutive high-pass and low-pass filtering of the time domain signal.

The procedure of multi-resolution decomposition of a signal x[n] is schematically shown in Fig. 3. Each stage of this scheme consists of two digital filters and two down-samplers by 2. The first filter, h[n] is the discrete mother wavelet, high pass in nature, and the second, g[n] is its mirror version, low-pass
in nature. The down-sampled outputs of first high-pass and low-pass filters provide the detail, D1 and the approximation, A1, respectively. The first approximation, A1 is further decomposed and this process is continued as shown in Fig. 3. The EEG sub bands of a2, d2 and d1are shown in fig. 4.

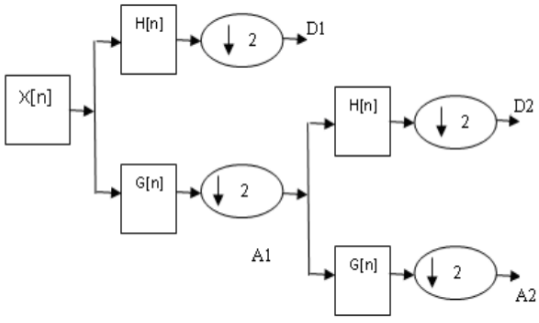

Fig. 3 Two level wavelet decomposition

Selection of suitable wavelet and the number of decomposition levels is very important in analysis of signals

using the wavelet transformation. The number of decomposition levels is chosen based on the dominant frequency components of the signal. In the present study, since the EEG signals do not have any useful frequency components above 30 Hz, the number of decomposition levels was chosen to be 2. Thus, the EEG signals were decomposed into details D1–D2 and one final approximation, A2. Usually, tests are performed with different types of wavelets and the one, which gives maximum efficiency, is selected for the particular application. The smoothing feature of the
Daubechies wavelet of order 4 (db4) made it more appropriate to detect changes of EEG signals. Hence, the wavelet coefficients were computed using the db4 in the present study. The proposed method was applied on both data set of EEG data (Sets H and S).

In the discrete wavelet analysis, a signal can be represented by its approximations and details. The detail at level j is defined as

$$D_j = \sum_{k \in Z} a_{j,k}\, \psi_{j,k}(t) \quad \ldots\ldots\ldots\ldots\ldots (1)$$

and the approximation at level J is defined as

$$A_j = \sum_{j>J} D_j \quad \ldots\ldots\ldots\ldots (2)$$

It becomes obvious that

$$A_{j-1} = A_j + D_j \quad \ldots\ldots\ldots\ldots\ldots (3)$$

And,

$$f(t) = A_j + \sum_{j \le J} D_j \quad \ldots\ldots\ldots\ldots (4)$$

Wavelet has several advantages, which can simultaneously possess compact support, orthogonality, symmetry, and short support, and high order approximation. We experimentally found that time-frequency domain feature provides superior performance over time domain feature in the detection of epileptic EEG signals.

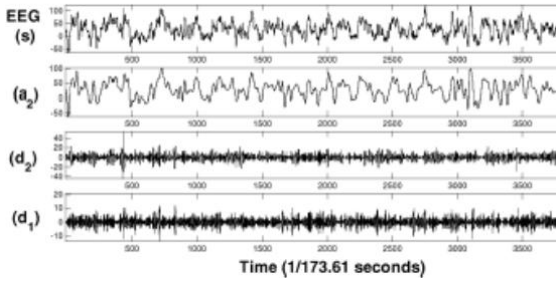

Fig. 4 Level 2 decomposition of the band-limited EEG into three EEG sub bands using fourth-order Daubechies wavelet (s=a2+d2+d1)

C. Classification

The idea of using a hyper plane to separate the feature vectors into two groups works well when there are only two target categories, but how does SVM handle the case where the target variable has more than two categories? Several approaches have been suggested, but two are the most popular:

(1) "One against many" where each category is split out and all of the other categories are merged.

(2) "One against one" where $k(k\text{-}1)/2$ models are constructed where k is the number of categories.

The SVM classify function uses results from SVM train to classify vectors x according to the following equation:

$$c = \sum_i \alpha_i k(s_i, x) + b \quad \ldots\ldots\ldots (5)$$

Where s_i are the support vectors, α_i are the weights, b is the bias, and k is a kernel function. In the case of a linear kernel, k is the dot product. If $c \geq 0$, then x is classified as a member of the first group, otherwise it is classified as a member of the second group.

Where C is the capacity constant, w is the vector of coefficients, b a constant and ξ_i are parameters for handling non separable data (inputs). The index i labels the N training cases.

Note that $y \in \pm 1$ is the class labels and xi is the independent variables. The kernel ϕ is used to transform data from the input (independent) to the feature space.

It should be noted that the larger the C, the more the error is penalized. Thus, C should be chosen with care to avoid over fitting.

For classification tasks, most likely use C-classification with the RBF kernel(default), because of its good general performance and the few number of parameters (only two: C and γ). Libsvm suggest to try small and large values for C— like 1to1000— first, then to decide which are better for the data by cross validation, and finally to try several γ's for the better C's.

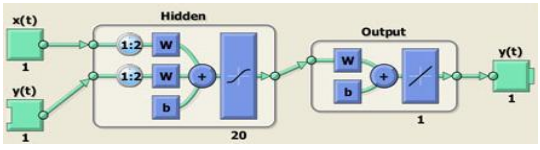

Fig.5 The classification between normal and ictal stages

D. Fast ICA

Fast Independent Component Analysis FastICA) algorithm separates the independent sources from their mixtures by measuring non-Gaussian. FastICA is a common offline ethod to identify artifact and interference from their mixtures such as Electroencephalogram (EEG), Magneto encephalography (MEG), and Electrocardiogram (ECG). FastICA has been compared with neural-based adaptive algorithms and principal component analysis (PCA), and most ICA algorithms were found to outperform. Its popularity has been justified on the grounds of satisfactory performance offered by the method in several applications, as well as its simplicity.

Other advantages of FastICA algorithm are: it can be used to perform projection pursuit and in addition it is used both in an exploratory fashion and also for estimating the independent components (or sources). FastICA maximizes the non-Guassianity mixtures of the detected signals
at different frequencies and thereby tries to separate the different independent components under a number of assumptions.

Once the epileptic seizure is separated from the EEG signals with the aid of Fast Independent Component Analysis, the training process will have to be carried out.

Artificial Neural Networks (ANN) comes in handy for the training purposes and so it is utilized here. Literally speaking, the Artificial Neural Networks (ANN) is the elemental electronic delineation of the neural framework of the brain. An Artificial Neural Network is an adaptive, most often nonlinear system that learns to carry out a function (an input/output map) from data.

The effect of the transformation is determined by the characteristics of the elements and the weights associated with the interconnections among them. By modifying the connections between the nodes the network is able to adapt to the desired outputs.

By employing FastICA to the input signal (EEG), the proposed approach extracts the independent subcomponents corresponding to epileptic seizure from the mixture of EEG signals. This is followed by the training of the ascertained independent subcomponents, applying ANN (Artificial Neural Networks). Fig. 6 depicts the block diagram of epileptic seizure detection process from EEG signal using FastICA and BackPropagation Neural Network (BPNN).

The seizure affected parts of the brain can be identified once the Artificial Neural Networks are trained with the recorded EEG signals. In ANN, there are several techniques for training the input data. In the proposed approach, we use Back propagation algorithm for training the components obtained from the input (EEG) signals Fig. 7).

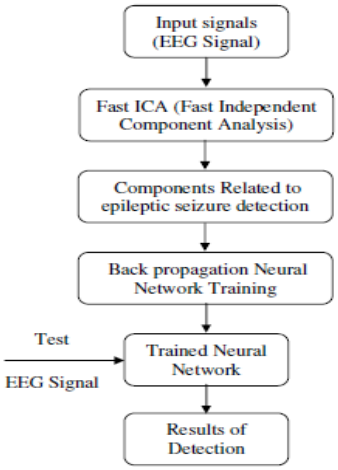

Fig. 6 Block diagram of the epileptic seizure detection by ICA approach

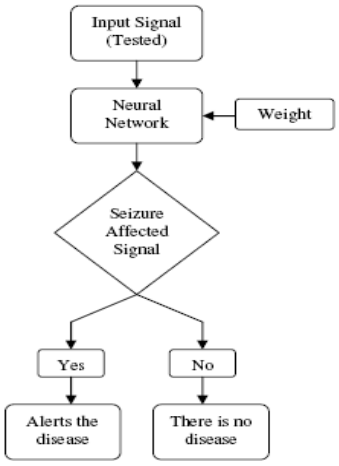

Fig. 7. Block diagram of Neural Network Detection

III. Results And Discussion

The test performance of the classifiers can be determined by the computation of specificity, sensitivity and total classification accuracy. The specificity, sensitivity and total classification accuracy are defined as:

$$Specificity = \frac{Number\ of\ true\ negative\ decisions}{Number\ of\ actually\ negative\ cases}$$

$$Sensitivity = \frac{Number\ of\ true\ positive\ decisions}{Number\ of\ actually\ positive\ cases}$$

$$Accuracy = \frac{Number\ of\ correct\ decisions}{Total\ number\ of\ cases}$$

EEG Signals are obtained from the various hospitals such as Rubi Hall Pune, India as shown below. These signals are in .eeg format which are not supported by the MATLAB software. The original EEG signal is shown below. We have used EEG recording software provided by the doctors and widely used all over the India to convert EEG signal in .eeg format to .xls format supported by MATLAB.

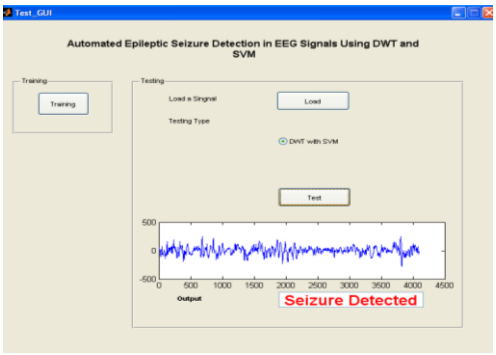

Fig. Seizure detection by DWT & Nural Network

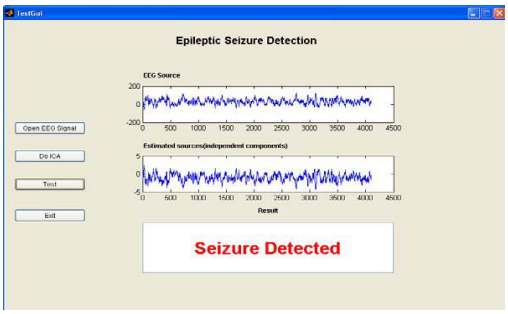

Fig.9 Seizure detection by ICA & Nural Network

TABLE 1- PERFORMANCE ANALYSIS

Performance	ICA	DWT
Sensitivity	**0.35**	**1**
Specificity	**0.62**	**0.95**
Accuracy	**0.49**	**0.98**

IV. CONCLUSION

A method for the analysis of EEG for seizure detection using wavelet based features & ICA have been presented here. As EEG is a non stationary signal the wavelet transform gives good results. After wavelet decomposition at level 4 using Daubechies wavelet of order 2, four statistical features minimum, maximum, mean and standard deviation were computed over the wavelet coefficients at each level. Classification was done using the simple linear classifier. By using the wavelet based features for classification between normal and seizure signals the accuracy obtained was 99.5%. It is greater than ICA method.

In future, apply this same dataset to other epileptic detection methods and compare all their performance.

REFERENCES

[1] Automated Epileptic Seizure Detection in EEG Signals Using Fast ICA and Neural Network **(***Zhongyu Pang, Student Member, IEEE, and Derong Liu, Fellow, IEEE)*

[2] Neural Network Classification Of EEG Signals By Using AR With MLE Preprocessing For Epileptic Seizure Detection. *Abdulhamit Subasia, M. Kemal Kiymika*, Ahmet Alkana, Etem Koklukayab*

[3] Real-Time Epileptic Seizure Prediction Using AR Models and Support Vector Machines. *Luigi Chisci, Antonio Mavino, Guido Perferi, Marco Sciandrone∗, Carmelo Anile, Gabriella Colicchio,and Filomena Fuggetta*

[4] Guler, I., Kiymik, M. K., Akin, M., & Alkan, A. AR spectral analysis of EEG signals by using maximum likelihood estimation. Computers in Biology and Medicine, 31, 441–450, 2001.

[5] A.A. Dingle, R.D. Jones, G.J. Carroll, W.R. Fright, "A multi-stage system to detect epileptiform activity in the EEG," IEEE Trans. Biomed.Eng.40 (12) (1993) 1260-1268.

[6] M. Unser, A. Aldroubi, "A review of wavelets in biomedical applications," Proc. IEEE 84 (1996) 626-638.

[7] S. Mukhopadhyay, G.C. Ray, "A new interpretation of nonlinear energy operator and its efficiency in spike detection," IEEE Trans.Biomed.Eng.45 (2) (1998) 180-187.

[8] F. Sartoretto, M. Ermani, "Automatic detection of epileptiform activity by single level analysis," Clin. Neurophysiol. 110 (1999) 239-249.

[9] G. Calvagno, M. Ermani, R. Rinaldo, F Sartoretto, "A multi-resolution approach to spike detection in EEG," in: IEEE International

[10] Folkers, A., Mosch, F., Malina, T., & Hofmann, U. G. Realtime bioelectrical data acquisition and processing from 128 channels utilizing the wavelet-transformation. Neurocomputing, 52–54, 247– 254, 2003.

[11] Guler I, Ubeyli ED. Application of adaptive neuro-fuzzy inference system for detection of electrocardiographic changes in patientswith partial epilepsy using feature extraction. Expert Syst Appl;27(3):323– 30, 2004.

[12] Subasi, A. Automatic recognition of alertness level from EEG byusing neural network and wavelet coefficients. Expert Systems with Applications, 28, 701–711,2005.

Self-Timed SAPTL using the Bundled Data Protocol

K.V.V.Satyanarayana[1] T.Govinda Rao[2] J.Sathish Kumar[3]

[1]Associate Professor
K.L. University
[2, 3]Assistant Professor
Usha Rama college of Engg and technology

Abstract

This paper presents the design and implementation of a low-energy asynchronous logic topology using sense amplifier- based pass transistor logic (SAPTL). The SAPTL structure can realize very low energy computation by using low-leakage pass transistor networks at low supply voltages. The introduction of asynchronous operation in SAPTL further improves energy-delay performance without a significant increase in hardware complexity. We show two different self-timed approaches: 1) the bundled data and 2) the dual-rail handshaking protocol. The proposed self-timed SAPTL architectures provide robust and efficient asynchronous computation using a glitch-free protocol to avoid possible dynamic timing hazards. Simulation and measurement results show that the self-timed SAPTL with dual-rail protocol exhibits energy-delay characteristics better than synchronous and bundled data self-timed approaches in 180-nm, 120-nm CMOS.

Keywords: pass transistor, self-timing, sense amplifier-based pass transistor logic (SAPTL)

I. Introduction

A CMOS technology continues to scale, both supply Voltage and device threshold voltage must scale down Together to achieve the required performance. Lowering the supply voltage effectively reduces dynamic energy consumption but is accompanied by a dramatic increase in leakage energy due to the lower device threshold voltage needed to maintain performance [1].As a result, for low-energy applications, the leakage energy that the system can tolerate ultimately limits the minimum device threshold voltage. Speed, therefore, benefits little from technology scaling. The sense amplifier-based pass transistor logic (SAPTL) [2] is a novel circuit topology that breaks this tradeoff in order to achieve very low energy without sacrificing speed. The initial SAPTL circuits were designed to operate synchronously [2] but with the intent of being able to Operate asynchronously with some minor modifications.

As the effects of process variations continue to increase dramatically with technology scaling, it is becoming harder to design variation-tolerant timing schemes using the traditional synchronous methodologies. To meet a certain timing requirement, the synchronous approach must use a very conservative "worst case" design that is slow enough for the needs of the statistically slowest circuit elements and, thus, will fail to exercise the whole capacity of statistically faster parts of the circuit. The asynchronous approach, on the other hand, can exploit local timing information to achieve "average-case" performance. An asynchronous design can get the best performance out of all components independent of statistical variations in local speed while guaranteeing correct circuit operation.

Asynchronous operation is also attractive to the low-power designer. The absence of a clock distribution network can significantly reduce the power overhead needed to generate timing information. Furthermore, an idle asynchronous system avoids consuming any active power. Despite the advantages of asynchronous operation, the circuit complexity and performance overhead required to implement the needed handshaking protocol may not be trivial. The overhead cost might offset all benefits and make the asynchronous approach impractical. The SAPTL, however, offers a relatively easy way to realize asynchronous operation. Because of the differential signaling used, it is easy to determine when a logical operation completes. Therefore, the self-timed SAPTL topology is a promising candidate for reducing power consumption and improving speed in extremely low energy applications.

II. Saptl Architecture

The basic architecture of the SAPTL circuit is shown in Fig. 1. It is composed of a pass transistor stack, a driver, and a sense amplifier [2]. The SAPTL achieves low energy operation 1) by decoupling sub threshold leakage current from the stack threshold voltage, allowing for increased performance without an increase in leakage energy, and 2) by confining sub threshold leakage to well-defined and controllable paths found only in the drivers and sense amplifiers.
Note that the total energy consumed by the SAPTL is composed of the following: 1) the energy used by the driver to energize the stack; 2) the energy used by the sense amplifier to resolve the correct logical levels and drive the inputs of the fan-out stacks; and (3) the energy needed to generate the appropriate timing information, either globally, such as clock distribution networks, or locally, as in handshaking circuits.

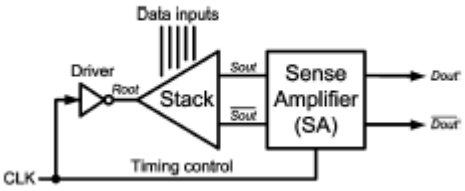

Fig.1 Architecture of SAPTL module with synchronous timing control.

A. Stack and Driver

The stack consists of an NMOS-only pass transistor tree with full-swing inputs and low-swing pseudo differential outputs to perform the required logic function, as shown in Fig. 2. The stack can implement any Boolean expression by connecting the min term branches of the tree to one output and the max term branches to the other as illustrated by the programming switches in the diagram. In our current implementation, the logic function of an SAPTL stack is determined and permanently fixed at fabrication by replacing the programming switches with hardwired connections. Because the stack has no supply rail connections, it does not contribute sub threshold leakage current, and it also has no gain.

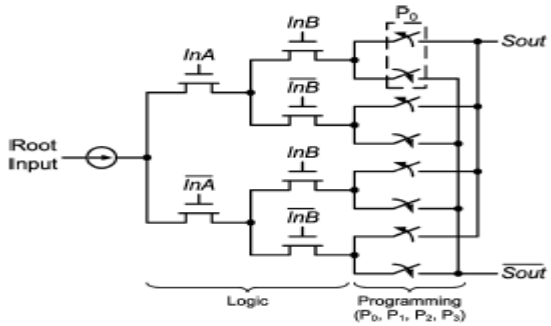

Fig.2 Schematic of a two-input stack with Nstack =2.

A driver, which is a simple inverter in this case, injects an evaluation current into the root of the stack. In operation, either Sout or Sout bar , but not both, is charged toward the supply rail when the driver energizes the selected path through the stack. After each computation and before every evaluation, both differential outputs are reset to ground (logical "0") to initialize the stack to a known state. This initialization is done by turning on all the transistors in the stack and draining the charges out through the root of the stack when the driver output is zero. The alternate charging and resetting of Sout or Sout bar realizes a standard dual-rail encoding scheme [3].

The speed of the SAPTL module depends strongly on the depth of the stack Nstack, which is defined as the number of transistors in series from the root node to the differential outputs. Because the stack contributes no sub threshold leakage current, the stack transistors can have a very low threshold voltage and still operate in the super threshold region even with a very low supply voltage. Therefore, SAPTL is a promising candidate to realize ultralow energy computation without entering the sub threshold region of operation [2].

B. Sense Amplifier

The sense amplifier, shown in Fig. 3, serves three purposes: 1) it amplifies the low-voltage stack output, restoring the signal to full voltage; 2) it serves as a buffer stage at the output of the stack, so as to improve overall speed; and 3) it pre charges both its outputs to Vdd (logical "1"), allowing the reset of the driven fan-out stacks. The sense amplifier consists of two stages. The first stage acts as a preamplifier to reduce the impact of mismatch in the actual technology environment, and the second stage acts as a cross-coupled latch which retains the processed data even after the stack is reset. The sense amplifier is designed to detect input voltages that are less than $(V_{dd} - V_{th})$, thus reducing the performance degradation due to the low stack voltage swings and the absence of gain in the pass transistor network. By turning off the driver as soon as the sense amplifier makes a decision, the stack voltage swings are kept to a minimum, reducing the energy required to perform the desired logical operation.

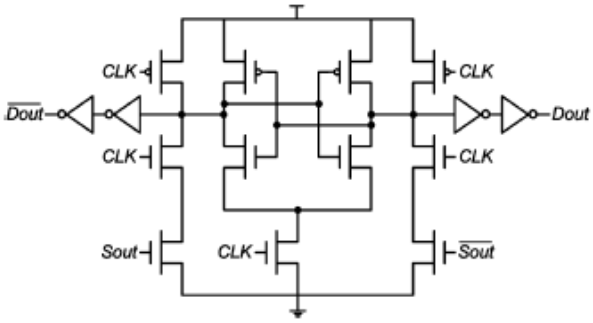

Fig.3 Sense amplifier circuit.

The leakage of the sense amplifier accounts for most of the leakage energy of the SAPTL module. It can be directly traded off against the input sensitivity of the sense amplifier to size and threshold voltage mismatch as shown in Fig. 4. Using a supply voltage of 300 mV and a minimum input voltage of 100 mV, 55% of the sense amplifier leakage is due to the four output buffers (inverters). Thus, an increase in sense amplifier performance can be achieved 1) by reducing the minimum input voltage or 2) by increasing the output drive of the sense amplifier, either of which would result in an increase in leakage current.

III. Bundled Data Self-Timed Saptl Design

The circuit implementation of the self-timed SAPTL module using the bundled data protocol [7] is shown in Fig. 4. The main data path, composed of a driver and stack, evaluates data or resets after receiving the request signal Rqein and data input signals Din and Din bar from the previous SAPTL stage. The control path, which consists of a delay line and a C-element, produces the local clock signal Enable to trigger the sense amplifier.

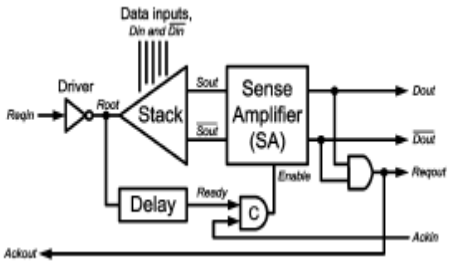

Fig.4 Architecture of self-timed SAPTL module with bundled data protocol.

The delay line mimics the delay of the stack to generate the control signal Ready indicating that the stack has finished an operation. The C-element then produces Enable by collecting Ready and the acknowledge signal Ackin from the next SAPTL stage. In multiple fan-in and fan-out situations, additional C-element can be employed to reconverge multiple request and acknowledge events from the different fan-in and fan-out stages. When triggered by Enable , the sense amplifier latches the stack output data or resets depending on the logical state of Enable. The full-swing data output signals Dout and Dout bar are made available at the outputs of the sense amplifier. The AND gate serves

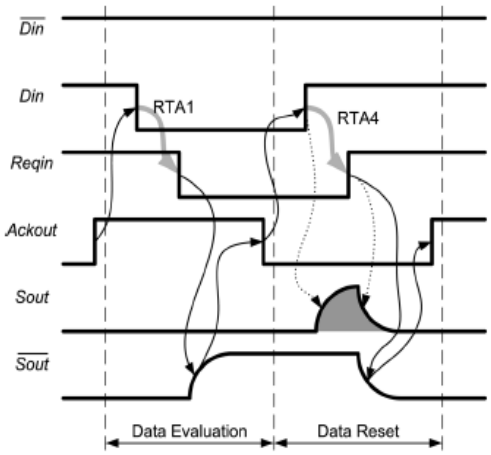

Fig.5 Timing diagram of self-timed SAPTL**.**

As a completion detection circuit, generating the handshake signals Ackout and Requot that indicate the completion of the current operation. We can summarize the relationship between the input and output signals of the th SAPTL stage as

$$\begin{aligned} \mathrm{Dout}_i, \overline{\mathrm{Dout}_i} &= f\left(Enable_i, \mathrm{Sout}_i, \overline{\mathrm{Sout}_i}\right) \\ &= ff\left(Reqin_i, Ackin_i, Din_i, \overline{Din_i}\right) \quad (1) \\ Ackout_i &= Reqout_i \\ &= g\left(\mathrm{Dout}_i, \overline{\mathrm{Dout}_i}\right) \quad (2) \\ Enable_i &= h\left(Reqin_i, Ackin_i\right) \quad (3) \end{aligned}$$

where for the subsequent $(i+1)$th SAPTL stage

$$\begin{aligned} Din_{i+1} &= \mathrm{Dout}_i \\ \overline{Din_{i+1}} &= \overline{\mathrm{Dout}_i} \\ Reqin_{i+1} &= Reqout_i \\ Ackout_{i+1} &= Ackin_i. \end{aligned}$$

IV. Dual-Railself-Timed Saptl Design

In a self-timed SAPTL structure using the bundled data protocol, RTA2 is the most critical design constraint. In order to guarantee correct operation under process, voltage, and temperature variations, the latency of the delay line can become very large and can severely limit the overall performance. Because the SAPTL uses dual-rail coding to represent data, we can use the output signals of the stack and, instead of from the delay line, to trigger the C-element. As a result, we can 1) eliminate the delay line and 2) design the C-element to respond immediately after the stack finishes operation, without being limited by RTA2.

Furthermore, we can combine the sense amplifier and C-element circuits into a composite block through gate-level optimization, yielding a more energy-efficient architecture, as shown in Fig.7. The optimized architecture with dual-rail protocol [7] eliminates the traditional

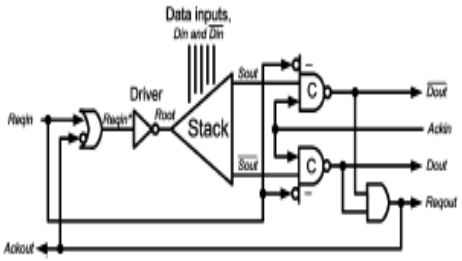

Fig.6 Architecture of glitch-free self-timed SAPTL module with dual-rail protocol.

Sense amplifier circuit and directly employs two C-element circuits as a complex gain stage at the outputs of the stack. The overall conversion speed, however, may be slower than the design with a sense amplifier due to the absence of a differential amplification and

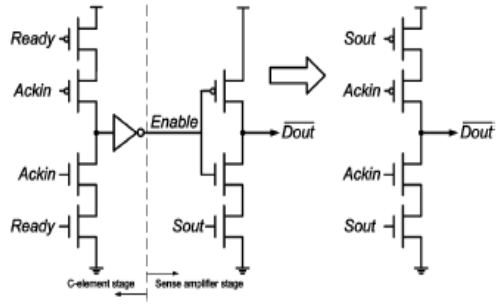

Fig.7 Logic combination of two-input C element and sense amplifier circuits.

The loss the loss of a positive-feedback mechanism between the two data paths Fig.6 shows the implementation of a glitch-free self-timed SAPTL architecture without the delay line.

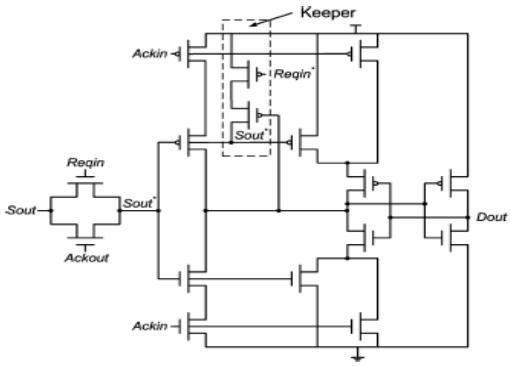

Fig.7: Two-input C-element circuit with additional decision-making logic for glitch-free self-timed SAPTL.

The design and performance of the C-element circuits are particularly important in this architecture because the C-element not only plays the role of the gain stage but also serves as the handshaking element. The self-timed SAPTL with dual-rail protocol has latency and cycle time expressions similar to (4)–(8). Note that the speed enhancement discussed in Section IV-C does not apply to the dual-rail design in Fig.6, because of the absence of the internal signal. However, the single self-timed SAPTL stage is now elastic and able to achieve the best performance across process, voltage, and temperature variations and different input characteristics. The self-timed SAPTL can thus exercise the full potential of asynchronous computation without the limitations of the delay line. It is interesting tonote that the optimized self-timed SAPTL architecture in Fig.6.

Has almost the same hardware complexity as the original synchronous SAPTL design in Fig. 1. This means that, with almost "zero cost," SAPTL is able to achieve both better performance and better robustness in the presence of variability by operating asynchronously.

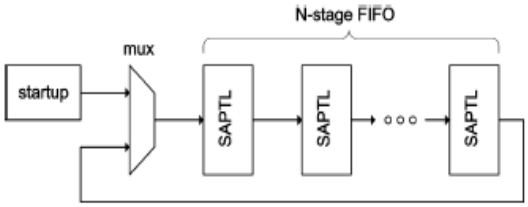

Fig.8 Test setup for energy and delay measurements.

The energy and delay of the various SAPTL5
Implementations were measured using N=8**.**

V. Performance Evaluation And Comparison

We evaluated and compared the performance of the self-timed and synchronous SAPTL circuits using the Spectre circuit simulator. We also performed Monte Carlo simulations to ensure the correct operation of the SAPTL circuits even with 6σ process variations. In addition, we implemented the self-timed SAPTL circuits in a 120-nm CMOS test chip and compared the actual measurement results to the simulated data. This section presents the energy-delay and leakage comparisons of synchronous versus self-timed SAPTL. The simulations exclude the parasitic contributions from the interconnect wires and the clock network. However, the effect of global parameters, such as clocks and long interconnect wires, should be done at the system level, in the context of an actual application. Comparisons between the synchronous SAPTL and other logic styles can be found in [2].

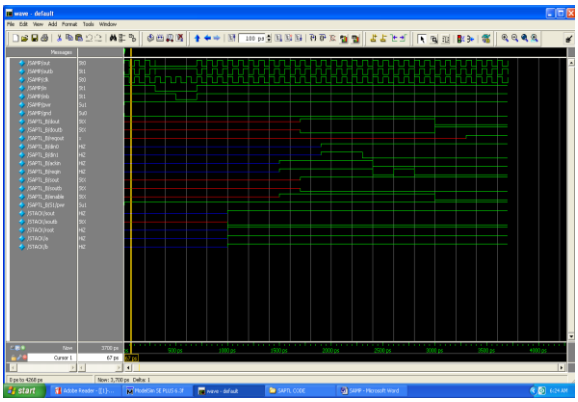

Fig .9.1 Simulation results

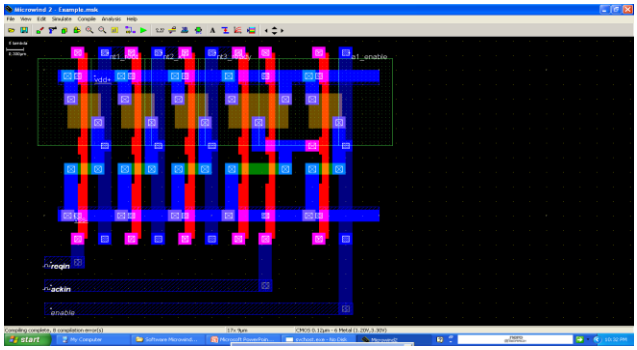

Fig .9.2 Layout design for Bundled –Data Self-Timed SAPTL

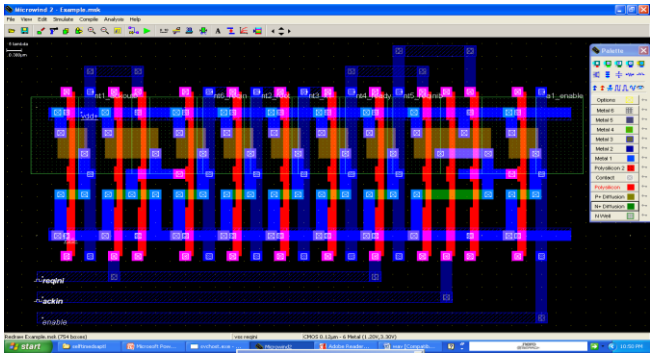

Fig .9.3 Layout design for Dual-rail-self timed SAPTL

Energy-Delay Characteristics

The pre-layout simulated energy and delay behavior of the synchronous SAPTL5 and both versions of the self-timed SAPTL5 is shown in Fig.9.4.

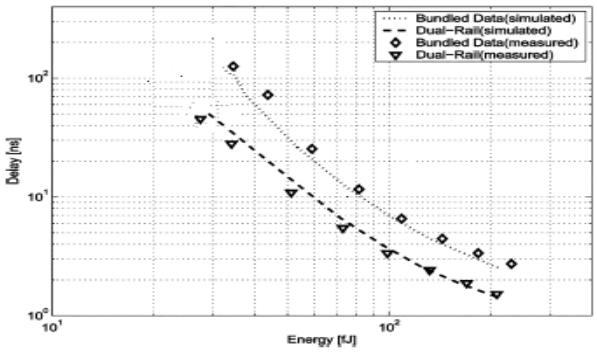

Fig.9.4 Measured versus simulated energy-delay plots for The 120-nm CMOS Self-timed SAPTL5, as the supply Voltage is varied from 300 mV to 1.2 V

echnology	**ower 80 nm Technology)**	**Power 20 nm echnology)**
ynchronous	6.87µW	6.58µW
undled-data	6.35µW	6.64µW
ual-rail	6.64µW	99µW

Table .1 Comparisons of different Methodologies

V. Conclusion

The asynchronous operation of the SAPTL provides robustness in the presence of variability as well as performance advantages over synchronous operation. While the self-timed SAPTL using the bundled data protocol can potentially achieve higher speed performance by overlapping the data evaluation and reset cycle, the self-timed design based on the dual-rail protocol has less rigid relative timing constraints, which leads to better energy and speed performance in technologies with increased process variations. The early reset operation ofself-timed SAPTL not only prevents dynamic timing hazards from glitches but also improves both energy and speed performance. We evaluated and compared the performance of the self-timed and synchronous SAPTL circuits using the Spectre circuit simulator. We also performed Monte Carlo simulations to ensure the correct operation of the SAPTL circuits even with process variations. In addition, we implemented the self-timed SAPTL circuits a 120-nm CMOS test chip and compared the actual measurement results is less than the simulated data. And also 180-nm CMOS is less than the simulated data This section presents the energy-delay and leakage comparisons of synchronous versus self-timed SAPTL. The simulations exclude the parasitic contributions from the interconnect wires and the clock network. However, as pointed out earlier in Section II-D, the effect of global parameters, such as clocks and long interconnect wires, should be done at the system level, in the context of an actual application. Comparisons between the synchronous SAPTL and other logic styles can be found in [2].

REFERENCES

[1] T. Sakurai, “Perspectives on power-awar electronics,” in ISSCC Dig. Te ch. Papers, 2003, vol.1, pp. 26–29.

[2] L. Alarcón, T.-T. Liu, M. Pierson, and J. Rabaey, “Exploring very lowenergy logic: A case study,” J. Low Power Electron., vol. 3, no. 3, pp. 223–233, Dec. 2007.

[3] J. Sparsø and S. Furber, Principles of Asynchronous Circuit Design.Norwell, MA: Kluwer, 2001.

[4] J. Rabaey, A. Chandrakasan, and B. Nikolic, Digital Integrated Circuits:A Design Perspective, 2nd ed . Englewood Cliffs, NJ: Prentice-Hall, 2003.

[5] H. Li, S. Bhunia, Y. Chen, K. Roy, and T. Vijaykumar, “DCG: deterministic clock-gating for low-power microprocessor design,” IEEE Trans. Very Large Scale Integr. (VLSI) Syst., vol. 12, no. 3, pp. 245–254,Mar. 2004.

[6] N. Banerjee, K. Roy, H. Mahmoodi, and S. Bhunia, "Low power synthesis of dynamic logic circuits using fine-grained clock gating," in Proc. DATE, Mar.2006, vol. 1, pp. 1–6.

[7] T.-T. Liu, L. Alarcón, M. Pierson, and J. Rabaey, "Asynchronous computing in sense amplifier-based pass transistor logic," in Proc. 14th IEEE Int. Symp. ASYNC, Apr. 2008, pp. 105–115.

[8] T. Williams, "Performance of iterative computation in self-timed rings," J. VLSI Signal Process., vol. 7, no. 1/2, pp. 17–31, Feb. 1994.

[9] K. Stevens, R. Ginosar, and S. Rotem, "Relative timing," IEEE Trans. Very Large Scale Integr. (VLSI) Syst., vol. 11, no. 1, pp. 129–140, Feb. 2003.

[10] I. Sutherland, "Micropipelines," Commun. ACM, vol. 32, no. 6, pp.720–738, Jun.1989.

[11] S. Narendra, "Scaling of stack effect and its application for leakage reduction," in Proc. ISLPED, Aug. 2001, pp. 195–200.

[12] K. Yano, Y. Sasaki, K. Rikino, and K. Seki, Top- down pass-transistor logic design. IEEE Journal of Solid-State Circuits 31, 792 (1996).

13] R. Shelar and S. Sapatnekar, BDD decomposition for delay oriented pass transistor logic synthesis. IEEE Transactions on Very Large Scale Integration (VLSI) Systems 13, 957 (2005).

[14] P. Buch, A. Narayan, A. Newton, and A. Sangiovanni-Vincentelli, Logic synthesis for large pass transistor circuits. IEEE/ACM International Conference on Computer-Aided Design, November (1997), pp. 663–670.

[15] W. C. Elmore, The transient analysis of damped linear networks with particular regard to wideband amplifiers. J. Appl. Phys. 19, 55 (1948).

[16] V. Kheterpal, V. Rovner, T. Hersan, D. Motiani, Y. Takegawa, A. Strojwas, and L. Pileggi, Design methodology for IC manufacturability based on regular logic-bricks. Proceedings of the 42nd Design Automation Conference, June (2005), pp. 353–358.

K. V. V. Satyanarayana received the M.Tech degree from Jawaharlal Nehru Technological University, Kakinada in 2008 in Electronics and Communication engineering. He is an Associate Professor in the Department of Electronics and Communication engineering, K.L.University,Vaddeswaram. His current research interests include the area of Communications, video coding techniques, and Architectures design.

T. GOVINDA RAO received the M.Tech (VLSISD) degree from Jawaharlal Nehru Technological University, Kakinada in 2011 in Electronics and Communication engineering. he is an Assistant Professor in the Department of Electronics and Communication engineering, Usha Rama College Of Engineering and Technology, Vijayawada. His current research interests include the areas of very large scale integration (VLSI) testing and fault-tolerant computing, video coding techniques, and Architectures design.

J. SATHISH KUMAR received the M.Tech degree from Jawaharlal Nehru Technological University, Hyderabad in 2011 in Electronics and Communication Engineering. He is an Assistant Professor in the Department of Electronics and Communication Engineering, Usha Rama College of Engineering and Technology, Vijayawada. His current research interests include the areas of very large scale integration (VLSI) testing and fault-tolerant computing, video coding techniques and Architectures design.

A survey on retrieving Contextual User Profiles from Search Engine Repository

[1]G.Ravi, [2]JELLA SANTHOSH
[1]Asst.Prof. CSE Dept.
[2] Mtech. (CSE Dept.)
Malla Reddy College of Engineering and Technology, Hyderabad.

Abstract
Personalized search is an important research area that aims to resolve the ambiguity of query terms. Therefore a Personalized Search engine return the most appropriate search results related to users interest. For example, a query "apple" a farmer would be interested in the apple fruits plants, farm etc. a technician would be interested in apple OS, Mac, Macintosh where as a gadget freak would be interested in latest apple products like ipad, iphone, iPod etc.

Here we focus on search engine personalization and develop several concept-based user profiling methods that are based on both positive and negative preferences. We evaluate the proposed methods against our proposed personalized query clustering method.

Experimental results show that profiles which capture and utilize both of the user's positive and negative preferences perform the best. An important result from the experiments is that profiles with negative preferences can increase the separation between similar and dissimilar queries. The separation provides a clear threshold for an agglomerative clustering algorithm to terminate and improve the overall quality of the resulting query clusters.

Keywords-Negative Preferences, Personalization, Positive Preferences, User Profiling.

1.Introduction
A web search engine is designed to search for information on the World Wide Web and FTP servers. The search results are generally presented in a list of results and are often called hits. The information may consist of web pages, images, information and other types of files.A Query is the content the text that the user submits to the search engine. Most commercial search engines return roughly the same results for the same query, regardless of the user's real interest. Since queries submitted to search engines tend to be short and ambiguous, they are not likely to be able to express the user's precise needs.

User profiling is a fundamental component of any personalization applications. Most existing user profiling strategies are based on objects that users are interested in (i.e. positive preferences), but not the objects that users dislike (i.e. negative preferences).Is personalisation for every organisation? Probably not. If your website does not have enough content to personalise then there is little point in trying to fragment it into profiles or tracked experiences - but if your site is large and you are struggling to ensure users get presented with appropriate content - then it would be one very powerful way to improve the user experience.

Recommended systems technologies have been introduced to help people deal with these vast amounts of information, and they have been widely used in research as well as e-commerce applications, such as the ones used by Amazon and Netflix. The most common formulation of the recommendation problem relies on the notion of ratings, i.e., recommender systems estimate ratings of items (or products) that are yet to be consumed by users, based on the ratings of items already consumed. Recommender systems typically try to predict the ratings of unknown items for each user, often using other users' ratings, and recommend top *N* items with the highest predicted ratings. Accordingly, there have been many studies on developing new algorithms that can improve the predictive accuracy of recommendations. However, the quality of recommendations can be evaluated along a number of dimensions, and relying on the accuracy of recommendations alone may not be enough to find the most relevant items for each user. In particular, the importance of *diverse* recommendations has been previously emphasized in several studies. These studies argue that one of the goals of recommender systems is to provide a user with highly idiosyncratic or personalized items, and more diverse recommendations result in more opportunities for users to get recommended such items. With this motivation, some studies proposed new recommendation methods that can increase the diversity of recommendation sets for a given *individual* user, often measured by an average dissimilarity between all pairs of recommended items, while maintaining an acceptable level of accuracy. These studies measure recommendation diversity from an individual user's perspective (i.e., *individual diversity*).

As a model for knowledge description and formalization, ontology's are widely used to represent user profiles in personalized web information gathering. However, user profiles, many models have utilized only knowledge from either a global knowledge base or user local information.

By this survey we conclude that

- Most of the present search engines are not personalized.
- Users queries that is what the user is interested in searching are not anticipated correctly.
- Users interested search results are not appropriately received.
- Users previous search record is not maintained. Whatever interested or his clicked are done by the user are not recorded.
- Few personalized search engine exists, but ask user to fill a detailed form of his personal information based on that information these search engines generate a near about personalized search results.
- Most of the users refrain from providing their detailed information to unknown website.

2.Proposed System

Architecture:

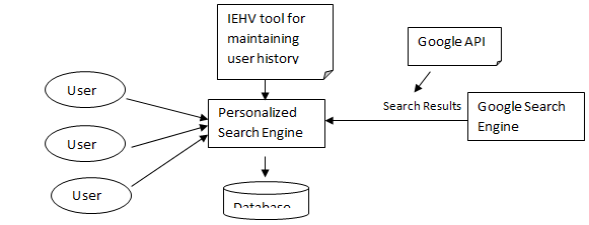

- User past search history is recorded.
- User is given a login account.
- User profile is created based on the previous searches done by the user.
- User positive and negative preferences are calculated. Positive preferences are the concepts or the topics in which a user is interested and negative preferences are the concepts in which the user is not interested at all.
- A track is maintained on what user clicked.
- Next time when a user login to his personalized search engine account he receives his most interested hits.
- Next time when he fires the same previous query he gets the results with his interested concept appended to the query.
- To extract users' positive preferences PClick algorithm is used and to extract users positives and negative preferences PmJoachims_C algorithm is used.
- Concept clustering is done using Personalized Agglomerative Clustering algorithm.

2. 1. CONSTRUCTING A USER PROFILE

Any personal documents such as browsing history and emails on a user's computer could be the data source for user profiles. This focus on frequent terms limits the dimensionality of the document set, which further provides a clear description of users' interest. This approach proposes to build a hierarchical user profile based on frequent terms. In the hierarchy, general terms with higher frequency are placed at higher levels, and specific terms with lower frequency are placed at lower levels.

2.2. PRIVACY VS SEARCH QUALITY

In this experiment, users are required to try different privacy thresholds to explore the relationship between privacy preservation and search quality. For each query, all parameters are fixed. A group of search results is presented to show how search quality is affected by the amount of private information that is exposed. These include general interest terms like "research", "search", "sports" and websites frequently visited such as "Google" and "NYTimes". Experiments showed that these general terms are especially helpful in identifying ambiguous queries like "conference" and "IT news". At the opposite extreme, over 100 terms are exposed. Most of these terms indicate specific events that happened recently, such as "websites that are occasionally visited (such as friends' blogs) which are too detailed to help refine the search.

2.3. QUERY CLUSTERING

User's queries can be classified into different query clusters. Concept-based user profiles are employed in the clustering process to achieve personalization effect. The personalized clustering algorithm iteratively merges the most similar pair of query nodes, and then, the most similar pair of concept nodes, and then, merge the most similar pair of query nodes, and so on. Each individual query submitted by each user is treated as an individual node and each query with a user identifier.

2.4. CLICK THROUGHS

when the user searches for the query "apple," the concept space derived from our concept extraction method contains the concepts "macintosh," "iPod," and "fruit." If the user is indeed interested in "apple" as a fruit and clicks on pages containing the concept "fruit," the user profile represented as a weighted concept vector should record the user interest on the concept "apple" and its neighborhood (i.e., concepts which having similar meaning as "fruit"),

Concept Preference Pairs Obtained Using Joachims-C Methods

Concept Preference Pairs for d_1	Concept Preference Pairs for d_5	Concept Preference Pairs for d_8
Empty Set	apple store $<_{r'}$ product macintosh $<_{r'}$ product	macintosh $<_{r'}$ product catalog $<_{r'}$ product
	apple store $<_{r'}$ mac os macintosh $<_{r'}$ mac os	macintosh $<_{r'}$ mac os catalog $<_{r'}$ mac os
	macintosh $<_{r'}$ apple store apple store $<_{r'}$ iPod macintosh $<_{r'}$ iPod	macintosh $<_{r'}$ apple store catalog $<_{r'}$ apple store macintosh $<_{r'}$ iPod catalog $<_{r'}$ iPod
		macintosh $<_{r'}$ fruit catalog $<_{r'}$ fruit macintosh $<_{r'}$ apple hill catalog $<_{r'}$ apple hill
		macintosh $<_{r'}$ fruit catalog $<_{r'}$ fruit

while downgrading unrelated concepts such as"macintosh," "ipod," and their neighborhood. The click-based profile PClick in which the user is interested in information about "macintosh." Hence, the concept "macintosh" receives the highest weight among all of the concepts extracted for the query "apple." The weights of the concepts "mac os," "software," "apple store," "iPod," "iPhone," and "hardware" are increased based on method we used, because they are related to the concept "macintosh." The weights for concepts "fruit," "apple farm," "juice," and "apple grower" remain zero, showing that the user is not interested in information about "apple fruit."

3.Conclusion

An accurate user profile can greatly improve a search engine's performance by identifying the information needs for individual users. In this paper, we proposed and evaluated several user profiling strategies. The techniques make use of click through data to extract from Web-snippets to build concept-based user profiles automatically. We Applied preference mining rules to infer not only users' positive preferences but also their negative preferences, and Utilized both kinds of preferences in deriving users profiles.

The user profiling strategies were evaluated and compared with the personalized query clustering method that we proposed previously. Our experimental results show that profiles capturing both of the user's positive and negative preferences perform the best among the user profiling strategies studied. Apart from improving the quality of the resulting clusters, the negative preferences in the proposed user profiles also help to separate similar and dissimilar queries into distant clusters, which helps to determine near optimal terminating points for our clustering algorithm. We plan to take on the following two directions forfuture work. First, relationships between users can be mined from the concept-based user profiles to perform collaborative filtering. This allows users with th same interests to share their profiles. Second, the existing user profiles can be used to predict the intent of unseen queries,such that when a user submits a new query, personalization can benefit the unseen query. Finally, the concept-based user profiles can be integrated into the ranking algorithms of a search engine so that search results can be ranked according to individual users' interests.

References

[1] E. Agichtein, E. Brill, and S. Dumais, "Improving Web Search Ranking by Incorporating User Behavior Information," Proc. ACM SIGIR, 2006.

[2] E. Agichtein, E. Brill, S. Dumais, and R. Ragno, "Learning User Interaction Models for Predicting Web Search Result Preferences," Proc. ACM SIGIR, 2006.

[3] Appendix: 500 Test Queries, http://www.cse.ust.hk/~dlee/ tkde09/Appendix.pdf, 2009.

[4] R. Baeza-yates, C. Hurtado, and M. Mendoza, "Query Recommendation Using Query Logs in Search Engines," Proc. Int'l Workshop Current Trends in Database Technology, pp. 588-596, 2004.

[5] D. Beeferman and A. Berger, "Agglomerative Clustering of a Search Engine Query Log," Proc. ACM SIGKDD, 2000.

[6] C. Burges, T. Shaked, E. Renshaw, A. Lazier, M. Deeds, N. Hamilton, and G. Hullender, "Learning to Rank Using Gradient Descent," Proc. Int'l Conf. Machine learning (ICML), 2005.

[7] K.W. Church, W. Gale, P. Hanks, and D. Hindle, "Using Statistics in Lexical Analysis," Lexical Acquisition: Exploiting On-Line Resources to Build a Lexicon, Lawrence Erlbaum, 1991.

[8] Z. Dou, R. Song, and J.-R. Wen, "A Largescale Evaluation and Analysis of Personalized Search Strategies," Proc. World Wide Web (WWW) Conf., 2007.

[9] S. Gauch, J. Chaffee, and A. Pretschner, "Ontology-Based Personalized Search and Browsing," ACM Web Intelligence and Agent System, vol. 1, nos. 3/4, pp. 219-234, 2003.

[10] T. Joachims, "Optimizing Search Engines Using Clickthrough Data," Proc. ACM SIGKDD, 2002.

[11] K.W.-T. Leung, W. Ng, and D.L. Lee, "Personalized Concept- Based Clustering of Search Engine Queries," IEEE Trans. Knowledge and Data Eng., vol. 20, no. 11, pp. 1505-1518, Nov. 2008.

[12] B. Liu, W.S. Lee, P.S. Yu, and X. Li, "Partially Supervised Classification of Text Documents," Proc. Int'l Conf. Machine Learning (ICML), 2002.

Jella Santhosh

Pursuing Mtech. (CSE Dept.) Malla Reddy College of Engineering and Technology, Hyderabad.

Mr. G.Ravi

Asst.Prof. CSE Dept. Malla Reddy College of Engineering and Technology, Hyderabad.

Optimized solutions for mobile Cloud Computing

[1]Mr.J.Praveen Kumar,[2] Rajesh Badam
[1]Asst.Prof.CSE Dept.
[2]Mtech.(CSE Dept.)
Malla Reddy College of Engineering and Technology

Abstract: As mobile device popularity grows, end-user demands to run heavier applications are equally increasing. Mobile cloud computing integrates the cloud computing into the mobile environment and overcomes obstacles related to the performance environment and security discussed in mobile computing. This paper gives an idea of MCC, which helps general readers have an overview of the MCC including the architecture, applications and solutions. The issues, existing solutions and approaches are presented. In addition, the future research directions of MCC are discussed

Keywords- Mobile cloud computing, offloading, Mobile services.

Introduction

Mobile devices are becoming an important part of human life as the most effective and convenient communication tools not bounded by time and place. The rapid progress of mobile computing becomes a powerful trend in the development of IT technology as well as commerce and industry fields.

The mobile devices are facing many challenges in their resources(e.g., battery life, storage, and bandwidth) and communications (e.g., mobility and security) . The limited resources significantly impede the improvement of service qualities.

"Mobile Cloud Computing at its simplest, refers to an infrastructure where both the data storage and the data processing happen outside of the mobile device. Mobile cloud applications move the computing power and data storage away from mobile phones and into the cloud, bringing applications and mobilecomputing to not just smartphone users but a much broader range of mobile subscribers".

The term "mobile cloud computing" was introduced not long after the concept of "cloud computing" launched in mid-2007. It has been attracting the attentions of entrepreneurs as a profitable business option that reduces the development and running cost of mobile applications, of mobile users as a new technology to achieve rich experience of a variety of mobile services at low cost, and of researchers as a promising solution for green IT . This section provides an overview of MCC including definition, architecture, and advantages of MCC.

MCC as a new paradigm for mobile applications whereby the data processing and storage are moved from the mobile device to powerful and centralized computing platforms located in clouds. These centralized applications are then accessed over the wireless connection based on a thin native client or web browser on the mobile devices.

CC offers some advantages by allowing users to use infrastructure, platforms and software .

Existing approaches/solutions:

- Mobile phones preserve the advantages of weight, size and device independence but will always impose basic limits on processing power, storage capacity, battery lifetime and display size.
- Conventional desktop applications are redesigned to operate on mobile hardware platforms, thereby often losing functionality.
- Demanding applications typically require specific hardware resources that are not available on mobile devices.
- To get the display users connect over a wired local area network to the central company server executing typical office applications.

Proposed solutions for mobile challenges:

- The principle of mobile cloud computing physically separates the user interface from the application logic.
- Here, a Viewer component is executed on the mobile device, which is operating as a remote display for the applications running on distant servers in the cloud.
- Remote display framework is composed of three components: a server side component that intercepts encodes and transmits the application graphics to the client, a viewer component on the client and a remote display protocol that transfers display updates and user events between both endpoints.
- In a mobile cloud computing environment, the remote display protocol deliver complex multimedia graphics over wireless links and render these graphics on a resource constrained mobile device. Offloading applications to the cloud is a straight forward way to

save on energy consumption because the amount of local processing is reduced.

- Efficient compression techniques to reduce the amount of exchanged data are done using compression techniques and versatile graphics encoding, downstream data peak reduction and Optimization of upstream packetization overhead.

Mobile cloud computing architecture

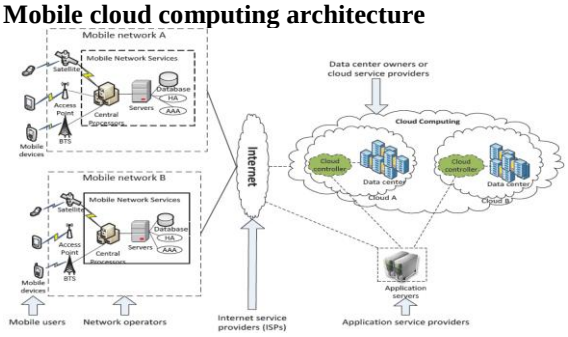

Cross-layer identification of WNIC sleep intervals

To develop strategies that optimize the energy balance,it is important to study WNIC energy consumption, which is the product of the number of bytes exchanged over the wireless interface and the energy cost per byte. The average energy cost per byte is determined by the distribution of time over the four possible WNIC states: send, receive, idle, and sleep. Because a specific set of WNIC components are activated in each state, power consumption varies widely between the states.

Although the send and receive modes consume the most power, energy-saving approaches should focus on the large idle times observed in remote display scenarios. These idle times are a consequence of the limited frequency of user interactions imposed by the network round-trip time. After some interaction, users must wait until the results become visible on the screen before continuing their work. furthermore, interactive applications will only update their display when instructed by the user—for example, by entering a URL or clicking on a hyperlink.

A proposed cross-layer power-saving approach operates between the MAC layer and the remote display protocol layer (see Figure 2).8 Because the MAC layer operates on binary data and cannot discriminate between, for example, transmitted user input and Transmission Control Protocol (TCP) acknowledgments, it is unaware of the arrival of the next display update. The appropriate sleep intervals must therefore be determined at the remote display protocol layer, where the display update schedule is established—for example, via a push approach in which the server sends display updates with fixed intervals or a pull approach in which the client sends an explicit request.

Correlating the transmission of user input to the network round-trip time predicts the arrival of the next display update. In between two display updates, the WNIC enters sleep mode. This sleep mode is interrupted at regular intervals to transmit user events. Researchers have used cross-layer optimization to reduce WNIC energy consumption By up to 52 percent.8

Wireless Bandwidth Availability

Compared to fixed access networks, modern broadband mobile and wireless technologies offer limited and variable bandwidth availability. Universal Mobile Telecommunications System (UMTS) users typically receive up to 384 kilobits per second, while Krishna Balachandran and colleagues9 reported practical throughputs of 347 Kbps for Long Term Evolution (LTE) and up to 6.1 Mbps for WiMAX. Actual throughput depends on user mobility, interference, and fading effects.

Versatile graphics encoding

The choice of codec to compress the intercepted application graphics at the server is a tradeoff between visual quality, compression efficiency, and decoding complexity.

Conventional remote display architectures including RDP, ICA, and VNC typically virtualize a layer of the graphic rendering stack at the server and forward intercepted drawing primitives to the client, such as instructions to draw a rectangle, display a bitmap, or put some text on the screen.

This approach is optimal for applications, such as typical office applications, that only update small regions of the display or have a slow refresh rate with respect to the network round-trip time. Bandwidth requirements to remotely display this type of graphics do not exceed 200 Kbps and can be adequately served over wireless links.

On the other hand, encoding multimedia graphics applications would require numerous drawing primitives because they update large parts of the screen at high refresh rates and they often contain fine-grained and complex color patterns. This kind of graphics can be more efficiently encoded using a video codec, such as H.264 or MPEG-4. Using video codecs for remote display purposes is referred to as interactive live streaming because the graphics are mainly the result of user interaction, in contrast to regular video streaming, which requires only limited user interaction—for example, to start and stop the video. Even when only a single application is used, the characteristics of the graphics on the user display might significantly differ when a user is accessing mobile cloud computing services. For example, a user browsing a Wikipedia page might click on a link that opens a YouTube video in the same browser window. Remote display frameworks must therefore be able to switch seamlessly between multiple encoding modes based on an analysis of graphics at the server.

Downstream data peak reduction

Interactive applications only update their display when instructed by the user. These display updates usually involve sending a large amount of data to the client in a short interval, which requires an instantaneous bandwidth much higher than the average bandwidth requirement. Furthermore, this bursty traffic pattern is unfavorable in wireless network environments, as it might induce additional collisions on the wireless channel.

Optimization of upstream Packetization overhead

User events are the principal source of upstream remote display traffic from client to server. Individually, each user event embodies only a small amount of information: a key or button ID, one bit to discriminate between the press and release actions, and possibly the current pointer coordinates. Nevertheless, user events induce important upstream traffic because they are often generated shortly after each other. Entering a single character results in two user events to indicate the press and release actions, whereas moving the mouse results in a sequence of pointer position updates.

Usually, the system transmits user events as they occur to minimize interaction latency. Because data packets sent upstream often contain a single user event, headers added at the TCP, IP, and wireless link layer cause large Packetization overhead. Table 3 quantifies the Packetization overhead of TCP/IP headers of three commonly used remote display protocols—the VNC Remote Framebuffer (RFB) Protocol, RDP, and ICA—when sending a single keystroke to the server. Optional headers and the wireless link layer header further increase total overhead.

Interaction Latency

While technological advances are likely to overcome bandwidth limitations, interaction latency—the delay users experience between generating some input and seeing the result on their display—is an intrinsic challenge of mobile cloud computing because the device must communicate even the most trivial user operations to the server.

Solutions to mitigate interaction latency try to either reduce the number of hops on the end-to-end path by moving the application closer to the client or provide better synchronization mechanisms between client and server

Computing display updates in advance

Given the current application state, the application server can predict potential display updates and stream them in advance to the client. Contrary to video streaming, in which the frame order is known in advance, in mobile cloud computing, the next display update depends on user input. For example, when a user opens an application menu, the server can precompute all dialog windows that can be opened by selecting one of the menu items.

Image buffering for virtual environment streaming

Due to limitations in mobile bandwidth and mobile device memory resources, in most cases, streaming all possible next display updates in advance is unfeasible. Furthermore, the gains of this precomputing technique are highly dependent on prediction accuracy. A better
strategy might be to buffer some key display updates, for which the server only needs to provide a differential update.

Scene object caching

For more static applications, such as office applications, the potential next updates can be more accurately predicted as, for example, a menu layout will rarely change. Consequently, the number of corrective server updates will be more limited. A typical example would be the list of recently opened files in a text editor's File menu. Scene description languages such as MPEG-4 BiFS are particularly suited to support this client-side handling of user input.13 The client not only receives graphic updates, but also is informed about the structure of the displayed scene and its composing objects, as well as how the user can manipulate these objects.

By physically separating the user interface from the application logic, mobile cloud computing allows access to even the most demanding applications from intrinsically resource-constrained mobile devices. Developers tailor contemporary remote display optimization techniques to mobile devices' short battery lifetime, the varying and limited bandwidth availability on wireless links, and interaction latency. Although each of these solutions adequately addresses specific mobile cloud computing challenges, an overall approach is currently lacking.

Because of user mobility, the wide diversity of applications, and the varying wireless channel status, the mobile cloud computing context is highly dynamic. Future research should therefore focus on the design of a comprehensive framework that integrates the existing solutions and activates the most appropriate one depending on the current device, network, and cloud server status.

Conclusion

Mobile cloud computing is one of mobile technology trends in the future since it combines the advantages of both mobile computing and cloud computing, thereby providing optimal services for mobile users. This article has provided an overview of mobile cloud computing in which its definitions, architecture, and optimized solutions have been presented. The applications supported by mobile cloud computing including mobile commerce, mobile learning, and mobile healthcare have been discussed which clearly show the applicability of the mobile cloud computing to a wide range of mobile services. Then, the issues and related approaches for mobile cloud computing have been discussed. Finally, the future research directions have been outlined.

References

[1.] C. Albanesius, "Smartphone Shipments Surpass PC Shipments for First Time. What's Next?" *PC Magazine*, 8 Feb. 2011; www.pcmag.com/article 2/0,2817,2379665,00.asp.

[2.] V.S. Pendyala and S.S.Y. Shim, "The Web as the Ubiquitous Computer," *Computer*, Sept. 2009, pp. 90-92.

[3.] F. Lamberti and A. Sanna, "A Streaming-Based Solution for Remote Visualization of 3D Graphics on Mobile Devices," *IEEE Trans. Visualization and Computer Graphics*, Mar./Apr. 2007, pp. 247-260.

[4.] H. Kawashima et al., "Virtual PC-Type Thin Client System," *NEC Technical J.*, Sept. 2007, pp. 42-47.

[5.] K. Pentikousis, "In Search of Energy-Efficient Mobile Networking," *IEEE Comm. Magazine*, Jan. 2010, pp. 95-103.

[6.] K. Kumar and Y.-H. Lu, "Cloud Computing for Mobile Users: Can Offloading Computation Save Energy?" *Computer*, Apr. 2010, pp. 51-56.

[7.] T. Kim et al., "An Energy-Aware Transmission Mechanism for WiFi-Based Mobile Devices Handling Upload TCP Traffic," *Int'l J. Comm. Systems*, May 2009, pp. 625-640.

[8.] P. Simoens et al., "Cross-Layer Optimization of Radio Sleep Intervals to Increase Thin Client Energy Efficiency," *IEEE Comm. Letters*, Dec. 2010, pp. 1095-1097.

[9.] K. Balachandran et al., "Performance Assessment of Next-Generation Wireless Mobile Systems," *Bell Labs Technical J.*, Feb. 2009, pp. 35-58.

[10.] http://onlinelibrary.wiley.com/doi/10.1002/wcm.1203/abstract,

[11.] I. Nave et al., "Games@Large Graphics Streaming Architecture," *Proc. IEEE Int'l Symp. Consumer Electronics* (ICSE 08), IEEE Press, 2008, pp. 205-208.

[12.] K.-J. Tan et al., "A Remote Thin Client System for Real-Time Multimedia Streaming over VNC," *Proc. IEEE Int'l Conf. Multimedia and Expo* (ICME 10), IEEE Press, 2010, pp. 992-997.

Author's profile

Rajesh Badam: Pursuing Mtech. (CSE Dept.) Malla Reddy College of Engineering and Technology, Hyderabad.

Mr. J.Praveen Kumar
Asst.Prof. CSE Dept.
Malla Reddy College of Engineering and Technology, Hyderabad.

Effect of dyke structure on ground water in between Sangamner and Sinnar area: A Case study of Bhokani Dyke.

[1.] P. D. Sabale, [2] S. A. Meshram
[1] Associate Professor, Deccan College (Deemed University), Pune.
[2.] Associate Professor in Geology, College Of Engg, Pune (COEP.)

Abstract
In semi-arid regions, particularly in hard rock areas, shallow aquifers are a major source of potable groundwater. These aquifers are indiscriminately exploited to meet the growing demand of water for domestic, irrigation as well as industrial uses. Therefore, peoples in this area are continuously pumping ground water from the well and in most of the days they found empty. Due to the over pumping through tube wells and dug wells, the ground water level is goes down below day to day. Therefore, due to such situation, people move to search the water from one place to another. In this situation, presence of a dyke is gives a new avenue to recharge the wells in the concern area.

Dykes in the Deccan Trap areas are to a great extent, known to control the movement of groundwater, and success or otherwise of the well in the field area depends very much upon its location. The Bhokani dyke area has opened the door of excellent irrigation. Those wells which are taken on dyke are giving good yield and therefore farmers are pumping water continuously.

In short, in areas of harsh Ground water situation, presence of dyke is an good as avenue for the ground water in the said region. This avenue acts as a source for the supply for irrigation and drinking water needs of the study area. Therefore this is an important factor in deciding the socio-economical conditions of the farmers in this area. This paper deals with study of such dyke which occurs near Sangamner area.

Introduction:

Failure of open dug wells and tube wells in most of parts of the hard rock areas in Deccan Traps is a common phenomenon. This problem usually arises, either because of the over exploitation / pumping of water from the existing wells or due to missing of the exact water potential zones in this terrain. As on the hard rock region water mainly exists in fracture and joints, locating such zones and predicting the flow processes is a difficult process.

Draught in the semiarid areas of hard rock is mainly due to low rate of precipitation and results into low irrigation in dry regions. Therefore, in this region, there is a growing demand for ground water resource as the surface water resources are not available adequately.

In semi-arid regions where groundwater occurs in shallow weathered zones, the rise in groundwater level is a direct consequence of precipitation, particularly in the monsoon season, when the groundwater withdrawal is minimum (Mondal et al., 2011).

India is seventeenth largest country in the world with diverse climate, topography, geology; soil types, land cover and land use pattern (National Institute of Hydrology, Report, 1998-99). The water resources of India are enormous but they are unevenly distributed in several terms. Seasonally, regionally, basin wise cultivator cross wise and crop wise.

In general, the ground water potential of hard rock's is poor, though relatively high yields may be obtained from in restricted locations under favorable circumstances of topography and rainfall. The size and the frequency of opening s in the fractured rocks are normally restricted to shallow depth resulting in low void ratio and hydraulic conductivity.

Draught in the semiarid area of hard rock is due to low rainfall and low irrigation in dry regions. Therefore, during summer groundwater from the basaltic aquifers is the prime source of water (Kale and Kulkarni, 1992).

Failure of tube well and open well in many parts of the hard rock regions are common phenomenon. This problem usually arises, either because of the over abstraction in existing wells or due to the missing of the exact water potential zone. As on the hard rock region water mainly exists in fracture and joints, locating such zones and predicting the flow processes are a difficult process.

The geometry of the joint and fracture set is determined by the types of rock and the stress to which they have been subjected, besides the effect of weathering and relief which makes the void space constituting the system progressively larger and approaching the surface. The study area is also parts of hard rock terrain and the same situation is observed in this area. The population in the rural area is mainly dependent on the ground water as a source of drinking and irrigation (Srikanth, 2009). But, successful wells in study area are also become dry because of the over pumping practices.

In hard rock region, there is a growing demand for ground water resource as the surface water resources are not available adequately (National Institute of Hydrology, Report, 1998-99).

Study Area:
Study area is southern boundaries of Sinnar and northern boundaries of Sangamner and is belongs to a severe part of draught prone regions of Ahmednagar and Nasik district respectively of Maharashtra (Fig. 1). This area lies between latitude 19° 40' 04" N to 19°51'05' and longitude 74° 04'11"E to 74°14'10"E on Survey of India (SOI) toposheet No. 47I/1 and 2. This region is located 10 miles from east of Sinnar (Nasik) and 16 miles from Sangamner (Ahmednagar district).

Geomorphology of the area:
Geomorphologically the terrain shows plain to undulating topography. The highest elevation in this area is 2824 mts. at east of Chas i.e. southern end while lowest elevation is 1836 mts. at north of Panchale i.e. northern boundary of study area.

The main drain in this area is Deo river, which is right side tributary of Godavari, confluences at Somathane village, NW of Kopargaon. In this study area, the locations of the tributaries of Deo River are shows good network of drainage. Along the channel of this river, the surface shows moderate to stiff slope.

Geology of the area:
The study area is a part of Deccan Volcanic Province (DVP). This region consists of alternate flows of compact and amygdaloidal basalt. Compact basalt flows are thick, tabular and shows more lateral extent while amygdaloidal basalt flows are thin, irregular and shows less extent than compact basalt flows.

Study area is a part of Deccan Volcanic Province (DVP) which generally shows (i) pipe amygdale flows shows irregular vesicles, weak tabular, glassy and sub horizontal sheet joints at the bottom (ii) compact, absence of vesicles, joints and fractures, and (iii) sub horizontal sheet joints with spheroidal amygdales (unfilled with vesicles) at the top (Kale and Kulkarni, 1992). The relative thickness in between these three layers is varying place to place.

These flows are characterized by variable thickness, irregularity, local dips, small extent , and lateral variation (Chaubey, 1973, Sukheswala and Polder Vaart, 1958; West, 1958, Gupte, 2007). In addition to the above predominant flows, at places some pocket deposit or cluster of volcanic breccias observed which might be outpoured in the volcanic activity during post – Deccan Trap period (Gupte et al., 1984).

Weathering and Erosion in Deccan Trap:
Due to the effect of physical weathering agents, rock found degraded condition and micro cracks are developed. Therefore, due to such continuous disintegration on the exposure of the rock, resulting depth of weathering goes deep and deep. Resulting, up to this weathered portion, surface water is penetrating down and ground water is formed. Here the trough shaped upper portion of the dyke is filled and surrounded by thick or thin blanket of black cotton soil, followed by deeply weathered, moderately weathered and finally fresh rock at the bottom. A typical stratigraphical section in study area is shown in (Fig. 2). Amygdaloidal basalt gives better response than compact to such kind of activity (Sabale, 2005). And the study area is more dominant region of Amygdaloidal basalt than compact.

Water bearing characters of Deccan Trap:
As stated above, in the Deccan Trap, water table conditions occurs under in weathered and jointed traps, and under confined conditions in weathered and jointed traps, and under confined conditions in the zeolitic and vesicular traps. Wells in valleys nearer to nallas and zeolotic traps yielded better than those located on elevated areas. The saturated fractures and joints found in the relatively unweathered bed rock are capable of yielding a substantial quantity of water at greater depth. The fractures and joints are mostly sheet type, sometimes are having good lateral extent and interconnected with each other. Therefore, groundwater level in this zonesis not readily affected by seasonal changes.

In dry draught prone areas, in harsh situation, presence of dyke is get as a avenue for the ground water Supply for drinking situation. This paper deals with study of such dyke which occur Deccan Volcanic Province (DVP) of draught prone region near Sangamner – Shirdi area.

The groundwater possibilities in the three groups viz.1.Numerous dolerite dykes in Deccan Traps of Dhulia district (2) Areally extensive trap flows resulting from slow and quiescent type of flood eruption occupying the gently undulating terrain, of Sholapur and Osmanabad districts and (3) the traps characterised by intertrappean sediments, dolerite dykes and volcanic ash beds, indicative of violent outbursts resulting in the Sahyadri geomorphologic unit of Kolaba, Thana and Bombay-Poona regions, are to a great extent governed by the nature and constitution of the individual flows. This character is given by Adyalkar and Mani(1971), based on their mode of emplacement, geomorphic setting and hydro geological of the Deccan Traps of western Maharashtra.

Single Unit of Deccan Trap Groundwater Province into 3 Sub-Provinces, based on geomorphological, geological and geohydrological setting in the region of western Maharashtra of the present investigation.

The dolerite dykes most of the time control the movement of groundwater, and success or otherwise of the well field area depends very much upon its location with reference to adjacent dykes, found in the Dhulia district.Thick vesicular, extensive traps with their gentle dips towards east have to be explored for possible artesian conditions in the down dip directions of the trappean units to be tapped, in Sholapur district (GSDA & CGWB Report, 2007-08).

The Bhokani Dyke Areas:

Bhokani dyke is doleritic type, width ranging from 7 ft. to 16 ft and 28.50 kilometers in length. This dyke is having N07°E strike and showing N-NE to S-SW trend. Dyke rock is black colored doleritic rock with well prismatic joints. The local people used term 'KAR' in Marathi for dyke in this area. It is move through Dodi, Khambale, Bhokani, Tamaswadi, Dambra, Chauri, Mendi villages etc. from S-SW to N-NE trend. At the beginning at S-SW portion, it is crossing Mhaladevi river and at the N-NE side it confluence in the Godavari river.

As per as the dug well and tube wells are concern, the maximum number of wells are present on the dyke alignment. Most of the wells (of about 95%) are yielding good amount of water. Therefore, the green zone is observe along the whole alignment of dyke, while rest of the area is found dry and partly green (only rainy and autumn season) due to the less irrigation. Because most of the wells in this area are dry of seasonal. Therefore, farmers are pumping day-night water from these wells with one or at some places two pumps of 5 or 10 HP are set up on the well.

Well Inventory:

In India, ground water has been exploited substantially during the past few decaded for irrigation. Most of the ground water utilization in India is from shallow depth aquifer zones at depth less than 100 m (Khepar and Chaturvedi, 1982, Rangnath, 1982). But the dykes which are constructed on dyke are yielding good amount of ground water. Therefore, to know the ground water conditions of such wells, a detailed well inventory survey was carried out in central part of the study area i.e. especially at Bhokani and Khambale area. In this survey well inventory work for 22 wells were carried out. To know the exact water carrying capacity and ground water situation, for this study the wells are selected in middle reaches or central zone out of total extension in this area of dyke.

During this survey well number, name of owner, whether it is lined or unlined (i.e. whether it is constructed or non-constructed) is reported. If it is lined the type and nature of material, cement or mortar, with the help of dressed stone, which are available in the surrounding area. In addition to this, the important ground water information such as depth of ground water from ground level and pumping hours for respective well in summer etc. is given in the following table.

Trend	Well No.	Name of owner / farmer	Constructed / Non-constructed	Well dimension Width (ft.)	Depth (ft.)	Water level From bottom (ft.)	Width of dyke (ft.)
S-SW	1.	Kisan S. Sabale	Masonry constructed	17	47	4	14-16
	2.	Trimbak G. Sabale	Masonry constructed	16	45	6	17-19
	3.	Chandrakant	Masonry	12	34	2	10-12

		Domaji Ranshivre	constructed				
	4.	Chandrakant D. Ranshivre	Masonry constructed	12	46	4	8-10
	5.	Eknath Ranshivre	Masonry constructed	10	42	5	8-10
	6.	Dr. Ranshivre	Masonry constructed	10	40	5	6-8
	7.	Ranshivre	Masonry constructed	12	42		7-10
Centre							
	1.	Mahadu Y. Sirsat	Masonry constructed	14	42	5	10-12
	2.	Chandrabhan S. Shirole	Masonry constructed	15	44	6	12-14
	3.	ChandrabhanP. Walekar	Masonry constructed	14	36	4	10-12
	4.	Chandrabhan P. Walekar	Masonry constructed	16	46	5	10-12
	5.	NamdeoMalhariWalekar	Masonry constructed	11	34	2.5	8-10
	6.	Trimbak N. Shirole	Masonry constructed	18	47	4.5	10-12
	7.	Bibhishen N. Walekar	Masonry constructed	17	42	6	14-16
	8.	Rahadu A. Shirole	Masonry constructed	12	35	2	12-14
	9.	Navnath K. Shirole	Masonry constructed	16	44	4	10-12
	10.	Ramchandra Shirole	Masonry constructed	16	44	4.5	10-12
	11.	Ramchandra Shirole	Masonry constructed	17	45	3.5	11-12
	12.	Bhima K. Kale	Masonry constructed	17	46	5	15-16
	13.	Datta S. Kale	unconstructed	14	37	2.5	10-12
	14.	Narayan B. Shirole	Masonry constructed	12	48	4	8-10
	15.	Bhaskar B. Shirole	Masonry constructed	14	44	5	7-8
	16.	Pandurang K. Shirole	Masonry constructed	12	36	4.5	8-10

Ground water condition in the well along the dyke:

As we know, dyke is having prismatic joints, which acts as an avenue for ground water flows, just like is leaky pipe. The water carrying capacity of a dyke is depend upon a. nature of joints (whether it is tight or open) b. presence of type of joints c. Dimension of the dyke. Slope of the area e. Water body in the path of the dyke. As describe above, the of Bhokani dyke is from Northern region of Akola and south of Sinnar from Ahmednagar and Nasik district respectively. In this area, at the beginning, the dyke is crossing a percolation tank. Therefore, this dyke is become recharge and it carries water from south to north part.

Crop Yield / Production of crop in the study area:

During the well inventory survey, type of crops, their yield and production of crop in the zone of dyke and outside the dike area for one acre area is collected from the local farmers. Then this crop wise production data is compared to each other in the study area.

Season	Sr. No.	Name of the crop	Production in the zone of dyke area (Ton/acre).	Production outside of the dyke area (Ton/acre).
Rainy	1	Legume / ground nut	20	16
	2	onion	30	16
	3	Bajar	25	17
	4	Maize	20	10
Summer	1	Wheat	27	15

The table data reveals that, crop production (in ton/acre) in the zone of dyke area is roughly double than production outside of the dyke area. This excess production in the zone of dyke area is only due to the good recharge of the well.

Improvement in the standard of living of peoples:
Ground water recharging conditions in the wells of the study areas farmers could able to good practice of irrigation. The production of food in the zone is high as compare to the peripheral areas. Therefore, standards of living of the farmers are increasing day to day in this area. In addition to this, very important change observed here is in the 'Standard of living' of the people. The main reason for the up gradation of these peoples in this area because i. wells are constructed up to deeper level and therefore they store large amount of water can store. ii. Water level in the wells which are located on dyke is rise due to good recharge conditions due to the presence prismatic joints of dyke.iii. Due to the presence of dyke the wells in the villages have enough of water. iv. Farmers have sufficient work on the farm and they are fully involved in taking more crops. v. The fodder is enough available for their cattle. vi. Milk production has increased drastically. vii.Resulting, women do not have to go to long distance for drinking water and viii. Due to good irrigation practices, milk production, and scheme for women development the economical condition of the people is increased and standard of living has also increased.

Results and discussion:
According to Bondre et al. (2006), numerous large dimensional mafic dyke outcrops are generally shows NE-SW to E-W trending in outcrop around Sangamner in the Western Deccan Volcanic Province. He also argued that, this area is a part of broader region of postulated to be a shield like feature and major eruption centre. But as per as the Bhokani dyke is concern, whether it is concern with the same dyke swarm, that has to check. Because, as per as the distribution of dykes identified and given by Bondre et al. (2006), northern extension of his Fig. 2, is up to Dapur (North of Akole), while southern extension of this dyke is up to Godavari river. These dykes are compositionally similar to the south western Deccan formations, although most of them can be best related to either Poladpur formation or Khandala formation. While geochemical composition is not necessarily correlated with location, in this area (Bondre, et al., 2006).

While much of the previous work pertains to lava flows, a few workers (e.g. Deshmukh and Sehgal, 1988, Bhattacharji et al. 1996; Mellusco et al.1999; Subbarao et al. 1999) have also studied the two principal dike swarm in this province, where the dike occur with high frequency. The West Coast Dike Swarm (WCDS) trending N-S to NNW –SSE, consist of tholeitic and alkaline compositions. The Narmada-Tapi Dike Swarm (NTDS) also contains tholeitic as well as alkaline dikes has predominant ENE-WSW trend (Sheth, 1998; Molluso et al. 1999).

Beane et al. (1986) observed that their compositions are similar to those of the associated flows. Bhattacharji et al. (1996) considered the random orientation to the result of stress regime dictated by large crustal magma chambers. Sheth (2000) argued that true feeder dikes in central volcanoes usually have a radial arrangement, not random arrangement.

Conclusion:
The dolerite dykes most of the time control the movement of groundwater, and success or otherwise of the well field area depends very much upon its location with reference to adjacent dykes, found in the Dhulia district.

Bhokani dyke is doleritic type, with sufficient dimensions and extensions. Due to the presence of prismatic joints, those wells which are found on the dyke and side of the dyke yielding good amount of ground water. Therefore, this dyke throughout his length giving recharge to the connecting and adjacent wells along its N-NE to S-SW trend. Resulting, the farmers are able to take more crops with good yield. Therefore, the green zone is observe along the whole alignment of dyke, while rest of the area is found dry and partly green (only rainy and autumn season) due to the less irrigation. Good irrigation practices, milk production, etc. activities are responsible for improvement of the economiccondition of people in this area. Many social changes took place and especially the women's groups became independent in decision making and their involvement has

increased in day to day activities. Due to education, the number of students has increased. Awareness tendency has been generated in the minds of illiterate village people.

This results into the improvement of the economic condition of the peoples in this area.

References:

[1.] Adyalkar, P. G. and Mani, V. S. (1971) Paleogeography, geomorphological setting and groundwater possibilities in the Deccan Traps. *Bulletin Volcanologique, 35 (3), pp.696-708.*

[2.] Beane J E, Turner C A, Hooper P R, Subbarao K V and Walsh J N 1986 Stratigraphy, composition and form of the Deccan basalts,Western Ghats, India; *Bull. Volcanol*. **48,** pp.61-83

[3.] Bhattacharji S, Chatterjee N, Wampler J M and Gazi M 1994 Ma_c dikes in Deccan volcanics - indicator of India intraplate rifting, crustal extension and Deccan flood basalt volcanism. In: *Volcanism*, ed. K V Subbarao *Geol.Soc. India*, 253, pp.27.

[4.] Bondre, N. R., Hart, W. K., Sheth, H. C. (2006) Geology and geochemistry of the Sangamner mafic dike swarm, western Deccan volcanic province, India: Implications for regional stratigraphy. J. Geol., v. 114, pp. 155-170.

[5.] Chaubey,V.D.(1973). Long Distance Correlation of Deccan Flow, Central India, Geological Society of America, Bulletin 84, pp.2785-2790.

[6.] Khepar, S. D. and Chaturvedi, M. C.: 1982, 'Optimum cropping and groundwater management', Water Resources Bulletin 18 (4), 655–660.

[7.] Deshmukh, S. S., Sehgal, M. N. (1988) Mafic dyke swarms in Deccan Volcanic Province of Madhya Pradesh and Maharashtra. In: Subbarao, K. V. (Ed.), Deccan Flood Basalts. Geol. Soc. Ind. Mem., v. 10, pp. 323-340.

[8.] DYNAMIC GROUNDWATER RESOURCES OF MAHARASHTRA ABRIDGED REPORT (AS ON 2007-08) .Prepared by -Groundwater Surveys and Development Agency, GoM & Central Ground Water Board, Central Region, Nagpur, GoI.

[9.] Gupte, R.B. (2008). Indian Geology. A Text of Engineering Geology. Third Edition (Revised), Pune Vidyarthi Griha Publication, Pune. pp.105-148.

[10.] Gupte, R.B., Kulkarni, S.R. and Marathe, S.S. (1984). Post –Deccan Trap Volcanic Activity in Western Maharashtra. Indian Mineralogist. pp. 69-74.

[11.] Kale, V. S. and Kulkarni, H. (1992) IRS-1A and LANDSAT data in mapping Deccan Trap flows around Pune, India: Implications in hydrogeological modeling. *Archives Int. Soc. Photogramm. and Rem. Sensing, 29(B-7): 429-435.*

[12.] Melluso, L., Sethna, S. F., Morra, V., Khateeb, A., Javeri, P. (1999) Petrology of the mafic dyke swarm of the Tapti River in the Nandurbar area (Deccan Volcanic Province). In: Subbarao, K. V.

[13.] (Ed.), Deccan Volcanic Province. Geol. Soc. Ind. Mem., v. 43, pp. 735-755.

[14.] Mondal, Nepal C, Singh, Vijay P. and Somayaji Sankaran (2011). Demarcation of prospective groundwater recharge zones in hard rock area from Southern India. Scientific Research and Essays Vol. 6(16), pp. 3539-3552.

[15.] National Institute of Hydrology, Report, (1998-99). Hydrological Problems of Hard Rock Region- State of Art Report. National Institute of Hydrology. Roorki.

[16.] Peshwa A, V. and Kale, V. S. (1988). Role of remote sensing in the detection of potential sites for landslides / rockfalls in the Deccan Trap lava terrain of western India. Environmental Geotechnics and Problematic Soils and Rocks; Balkema, Rotterdam;, pp.367 - 374.

[17.] Sabale, P.D. (2005). "Watershed Development and Management in Siddheshwarwadi: A Review". ICEM, Vol.5, Editor-Anji Reddy, B.S.Publ., J.N.T.U., H'bad. Pp. 318-325.

[18.] Rangnath, 1982

[19.] Sheth, 1998. Geochemistry, petrogenesis,Stratigraphy and structure of Deccanflood basalts of the western Satpura-Tapi region,india. Ph.D dissertation, Indian Institute of Technology, Bomboy.

[20.] Subbarao et al. 1999 Narmada dyke. In Subbarao, K.V., ed. Deccan Volcanic Province. Geol. Soc. India Mem. 43, pp.891-902.

[21.] Srikanth, R. (2009). Challenges of sustainable water quality management in rural india Current Science, Vol.97, No.3, pp.317-325.

[22.] Sukheswala R N and Poldervaart A 1958 Deccan basalts of the Bombay area, India: *Bull. Geol. Soc. Am.* 69, pp.1475-1494.

[23.] West W D 1958 The petrography and petrogenesis of forty- eight flows of Deccan Traps penetrated by borings in western India; *Trans. Nat. Inst. Sci. India* 4**,** pp.1-56.

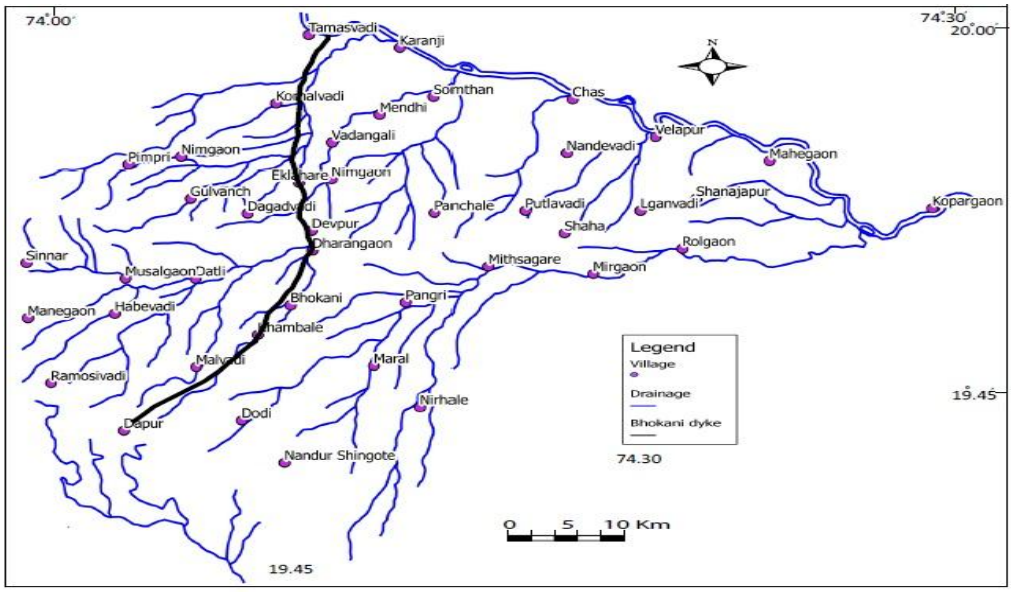

Fig. 1 Location map of the study area.

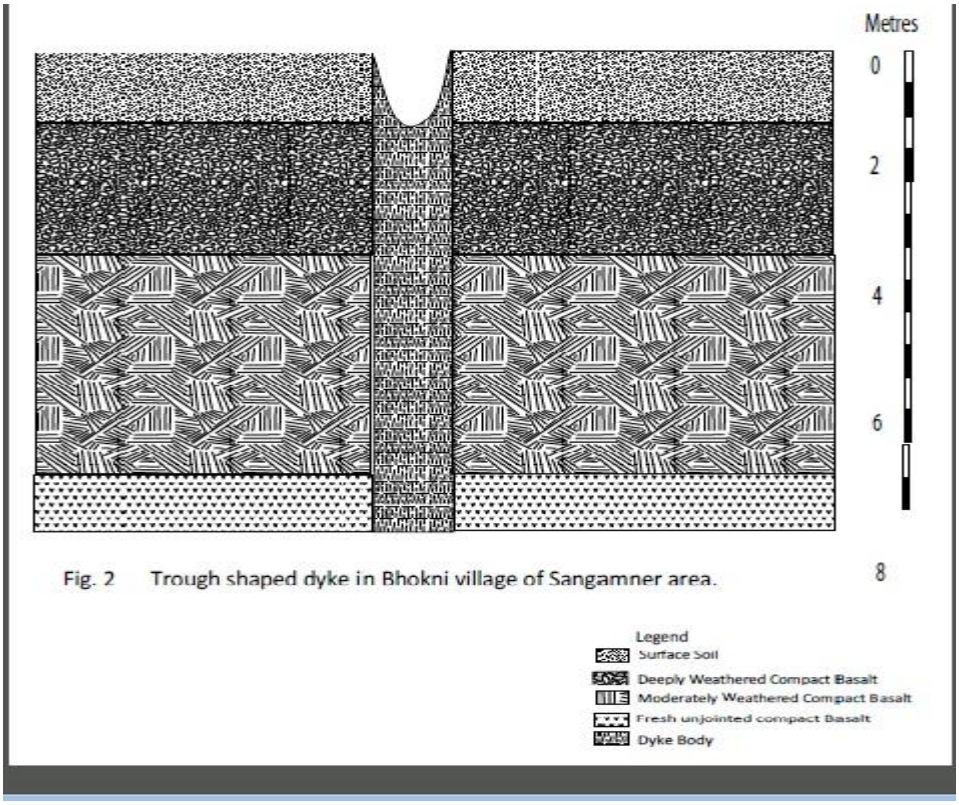

Fig. 2 Trough shaped dyke in Bhokni village of Sangamner area.

Algorithm for Merging Search Interfaces over Hidden Web

Harish Saini[1], Kirti Nagpal[2]
[1]Assistant Professor N.C.College of Engineering Israna, Panipat
[2]Research Scholar, N.C.College of Engineering Israna, Panipat

Abstract: This is the world of information. The size of world wide web [4,5] is growing at an exponential rate day by day. The information on the web is accessed through search engine. These search engines [8] uses web crawlers to prepare the repository and update that index at an regular interval. These web crawlers [3, 6] are the heart of search engines. Web crawlers continuously keep on crawling the web and find any new web pages that have been added to the web, pages that have been removed from the web and reflect all these changes in the repository of the search engine so that the search engines produce the most up to date results.

Keywords: Hidden Web, Web Crawler, Ranking, Merging

I. INTRODUCTION

This is the world of information. The size of world wide web [4,5] is growing at an exponential rate day by day. The information on the web is accessed through search engine. These search engines [8] uses web crawlers to prepare the repository and update that index at an regular interval. Web crawlers continuously keep on crawling the web and find any new web pages that have been added to the web, pages that have been removed from the web and reflect all these changes in the repository of the search engine so that the search engines produce the most up to date results. There is some data on the web that is hidden behind some query interfaces and that data can't be accessed by these search engines. These kind of data is called hidden web [41] or deep web. These days the contents on the hidden web are of higher interests to the users because the contents of hidden web are of higher quality and greater relevance. The contents on hidden web can be accessed by filling some search forms which are also called sometimes search interfaces. Search interfaces [37] are the entry points to the hidden web and make it possible to access the contents on the hidden web. These search interfaces are simply like filling any forms like forms for creating e-mail ids etc. Each search interface has number of input controls like text boxes, selection lists, radio buttons etc.. To access hidden web one needs to fill these search interfaces for which a crawler is required which finds for forms on the web known as form crawler. There can be multiple search interfaces for the same information domain on the web. In that case all those search interfaces are required to be merged or integrated so that crawler[3] finds all data relevant to the user input despite of existence of multiple search interfaces for the same domain. Hidden web crawler is the crawler which continuously crawls hidden web so that it could be indexed by search engines. The major functions which are to be performed by hidden web crawler are getting form filled, finding search query, submitting query and indexing the results. The challenge of the hidden web crawlers are the huge and dynamic nature of the hidden web. The merging[46] or integration of search interfaces over hidden web is required to response queries so that it answers queries at its best. For the integration of search interfaces over hidden web two steps are required

- Finding semantic mapping over the different search interfaces to be merged.
- Merging search interfaces on the basis of semantic mappings found earlier.

A *Ranking the Web Pages by Search Engine*

Search for anything using our favorite crawler-based search engine will sort through the millions of pages it knows about and present you with ones that match your topic. The matches will even be ranked, so that the most relevant ones come first. Of course, the search engines don't always get it right. So, how do crawler-based search engines go about determining relevancy, when confronted with hundreds of millions of web pages to sort through? They follow a set of rules, known as an algorithm. Exactly how a particular search engine's algorithm works is a closely kept trade secret.

One of the main rules in a ranking algorithm involves the location and frequency of keywords on a web page. Call it the location/frequency method. Pages with the search terms appearing in the HTML title tag are often assumed to be more relevant than others to the topic. Search engines will also check to see if the search keywords appear near the top of a web page, such as in the headline or in the first few paragraphs of text. They assume that any page relevant to the topic will mention those words right from the beginning. Frequency is the other major factor in how search engines determine relevancy. A search engine will analyze how often keywords appear in relation to other words in a web page. Those with a higher frequency are often deemed more relevant than other web pages.

B. *Web Crawler*

A crawler [14,20] is a program that are typically programmed to visit sites that have been submitted by their owners as new or updated. The contents of the Entire sites or specific pages is selectively visited and indexed. The key reason of using web crawlers is to visit web pages and add them to the repository so that a database can be prepared which in turn serves applications like search engines.

Crawlers use graph structure of the web to move from pages to pages. The simplest architecture of web crawler is to start from a seed web page and traverse all hyperlinks encountered in this web pages then all encountered hyperlinks are added to the queue which in turn are traversed. The process is repeated until a sufficient number of pages are identified...

The main goal of the web crawler is to keep the coverage and freshness of the search engine index as high as possible which is not informed by user interaction. For this task the crawler and other parts of the search engine have no communication between them. Because web is a purely dynamic collection of web pages there is a need for crawling cycles frequently to refresh the web repository so that all new pages that have been added to the web are included in the repository similarly the web pages that have been removed from web are deleted from web repository

C *Hidden Web Crawler*

Current day crawlers crawls only publicly indexable web (PIW) i.e set of pages which are accessible by following hyperlinks ignoring search pages and forms which require authorization or prior registration. In reality they may ignore huge amount of high quality data which is hidden behind search forms. Pages in hidden web are dynamically generated in response to the queries submitted via search forms. Crawling the hidden web is highly challenging task because of scale and the need for crawlers to handle search interfaces designed primarily for human beings. The other challenges of hidden web data are:

- Ordinary web crawlers can't be used for hidden web
- The data in hidden web can be accessed only through a search interface
- Usually the underlying structure of the database is unknown.

The size of hidden web is continuously increasing as more and more organizations are putting their high quality data online hidden behind search forms. Because there are no static links to hidden web pages therefore search engines can't discover and index these web pages.

Because the only entry point to hidden web is search interface the main challenge is how to generate meaningful queries to issue to the site. Hidden web crawler is the one which automatically crawls hidden web so that it can be indexed by search engines. Hidden web crawler is able to allow an average use to explore the amount of information, which is mostly hidden behind search interfaces. The other motive for hidden web crawler is to make hidden web pages searchable at a central location so that the significant amount of time and effort wasted in searching the hidden web can be reduced. One more motive for hidden web crawlers is that due to heavy reliance of web users on search engines for locating information, search engine influence how the users perceive the web..

There are two core challenges while implementing an effective hidden web crawler

- The crawler has to be able to understand and model a query interface.
- The crawler has to come up with meaningful queries to issue to the query interface.

The first of the two challenges was addressed by a method for learning search interfaces. For the latter challenge if the search interface is able to list all possible values for a query with help of some selection list or drop down list in that case solution is straight forward. possible so all of the possible queries can't be exhaustively listed.

D *Search Interfaces*

While accessing hidden web [49] search query is submitted to the search interface of the hidden web crawler. The selection of web pages and the relevance of results produced from hidden web is determined by the effectiveness of search interfaces [42,43]. The different actions performed by search interfaces are getting input from user, selection of query, submitting query to the hidden web and merging of results produced by hidden web crawlers.

The most important activity of search interface is selection of query which may be implemented in variety of ways. One method is random method in which random keywords are selected from the English dictionary and are submitted to the database. Random approach generates a reasonable number of relevant pages. The other technique is using generic frequency. In this method we find a document and obtain general distribution frequency of each word in the document. Based on this *frequency* distribution we find the most frequent keyword, issue it to the hidden web database and retrieve the result. The same process is repeated with the second most frequent word and so on till the downloaded resources are exhausted. After that it analyses the returned web pages that whether they contain results or not. Another method is adaptive in this method the documents returned from the previous queries issued to the Hidden-Web database is analysed and it is estimated which keyword is most likely to

return the most documents. Based on this analysis, the process is repeated with the most promising queries.

E *Problems in Integration of Hidden Web*

Recently keen interest has been developed in the retrieval and integration of hidden web with the intention of having high quality data for the databases. As the size of information in hidden web is growing, search forms or search interfaces are needed to be located which serves as an entry point to hidden web database. But there exists crawlers which focus search on specific database domains and retrieve invariable diversified set of forms like login form, quote request forms and searchable forms from multiple domains. The process of grouping these search interfaces or search forms over the same database domain is called integration of search interfaces.

These search form are input to algorithm which finds correspondences among attributes of different forms. This task is not so easy because of dynamic nature of the web the new information is added to web and new information is being modified or even removed. Therefore a scalable solution suitable for large scale integration is required for the purpose of large scale integration. In addition in a well defined domain there may be variation in both structure and vocabulary of search forms. So in order to obtain information that covers the whole domain it is required to find correspondences among attributes of forms and for that a broad search is needed to be performed.

For this either full crawl is needed to be performed but this is really inefficient approach as it can take weeks for the exhaustive crawling process. Another alternative can be focus crawling in which only pages relevant to a specific topic are crawled. This has a better quality index as compared to exhaustive crawling. In this case focused crawler that focus solely on the contents of retrieved web pages may not be a very good alternative also because forms are sparsely distributed and thus the number of forms retrieved per total number of pages retrieved may be very low. For tackling this problem a focused crawler has been developed which used reinforcement learning to build a focus crawler that is effective for sparse concepts.

The kind of web crawler which crawl web pages which contain search forms are called form crawlers. Since form crawler find thousand of forms for the same domain. Those different forms even for the same domain may be different in the structure and vocabulary they use. For that semantic mappings are required to be found among all attributes of those forms and after finding semantic mappings those are integrated so that queries involving that domain can be answered suppressing the existence of multiple search forms using different structures and vocabulary. There exist multiple integration techniques which integrates these search forms over the hidden web. Most of those are semiautomatic.

F. Need For Merging Search Interfaces

It seems that there will always be more then one search interfaces even for the same domain. Therefore, coordination(i.e. mapping, alignment, merging) of search interfaces is a major challenge for bridging the gaps between agents with different conceptualizations.

Two approaches are possible:

(1) merging the search interfaces to create a single coherent search interface

(2) aligning the search interfaces by establishing links between them and allowing them to reuse information from one another.

Here we propose a new method for search interface merging.

Whenever multiple search forms are to be integrated the task can be divided into two major steps

- Finding semantic mapping among search forms or interfaces
- Merging search interfaces on the basis of mapping

The first step in merging [46] of search forms or interfaces are finding semantic mapping and correspondences among attributes of those forms so that on the basis of that mapping search interfaces or forms could be merged. This semantic mapping serves as the domain specific knowledge base for the process of merging [47] of search interfaces. The proposed algorithm is semi automatic. It finds similar terms from a look-up table which stores all similar terms in the different search interfaces to be merged along with the relationship between those similar terms so that it may be decided which term will be appearing in the merged search interface. The algorithm makes use of search interfaces in form of a taxonomy tree to cluster the concepts in the search interfaces on the basis of level

II Merging of Search Interfaces

More and more applications are in need to utilize multiple heterogeneous search interfaces across various domains. To facilitate such applications it is urgent to reuse and interoperate heterogeneous search interfaces. Both merge and integration produces a static search interface based on the existing search interfaces. The resulting search interface is relatively hard to evolve with the change of existing search interfaces.

The search interface merge module takes source search interfaces as input and a table that lists all similar terms coming from different search interfaces along with the relationship between those similar terms. The similar terms can have relationship like meronym, hyper name and synonym. The search interface merge process is divided into **several steps.**

Step 1. Find set of similar terms

Step 2. Children of similar terms are merged and point to the same parent.

Table 1.1 Domain specific knowledge base

Concept	Concept	Relation
Optical_drive	OpticalDisk	Synonym
HardDrive	HardDisk	Synonym
DVD	DVD-Rom	Synonym
CDRW	CD-RW	Synonym
CDRom	CD-ROM	Synonym
Computer	Personal Computer	Synonym

A *Merging Observations and Results*

Let us consider two source search interfaces and apply the above stated algorithm to merge those search interfaces as a case study. The source search interfaces under consideration are given along with the domain specific knowledge base.

The taxonomy trees of search interfaces A and B respectively are as following

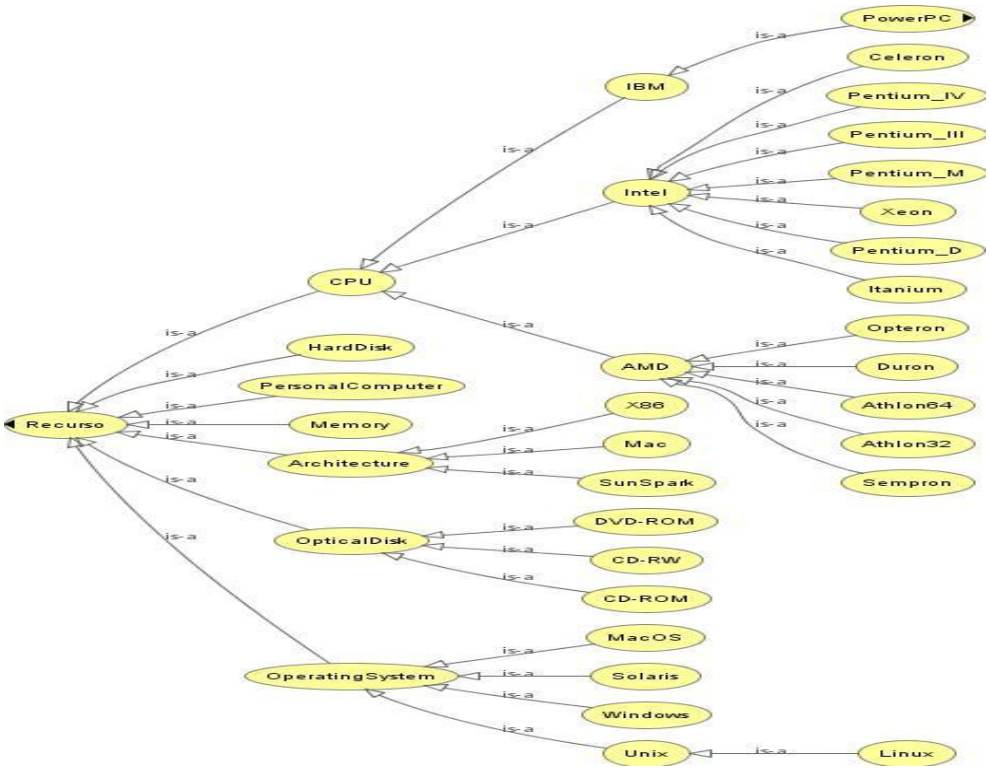

Fig1.1TaxonomytreeforSearchInterfaceS1

The codes assigned to the terms in the source search interface are as follows. Let us consider search interface a first and see the codes assigned

Table 1.2 Codes of terms in search interface A

Term	**Code**
Recurso	A
CPU	A01
Hard Disk	A02
Personal computer	A03
Memory	A04
Architecture	A05
Optical disk	A06
Operating System	A07
IBM	A0101
Intel	A0102

AMD	A0103
X86	A0501
MAC	A0502
Sunsparc	A0503
DVD-Rom	A0601
CD-RW	A0602
CD-Rom	A0603
Macos	A0701
Solaris	A0702
Windows	A0703
Unix	A0704
PowerPC	A010101
Celeron	A010201

PIV	A010202
PIII	A010203
PM	A010204
Xeon	A010205
Pentium_D	A010206
Itanium	A010207
Opetron	A010301
Duron	A010302
Athlen 64	A010303
Athlen 32	A010304
Semaron	A010305
Linux	A070401

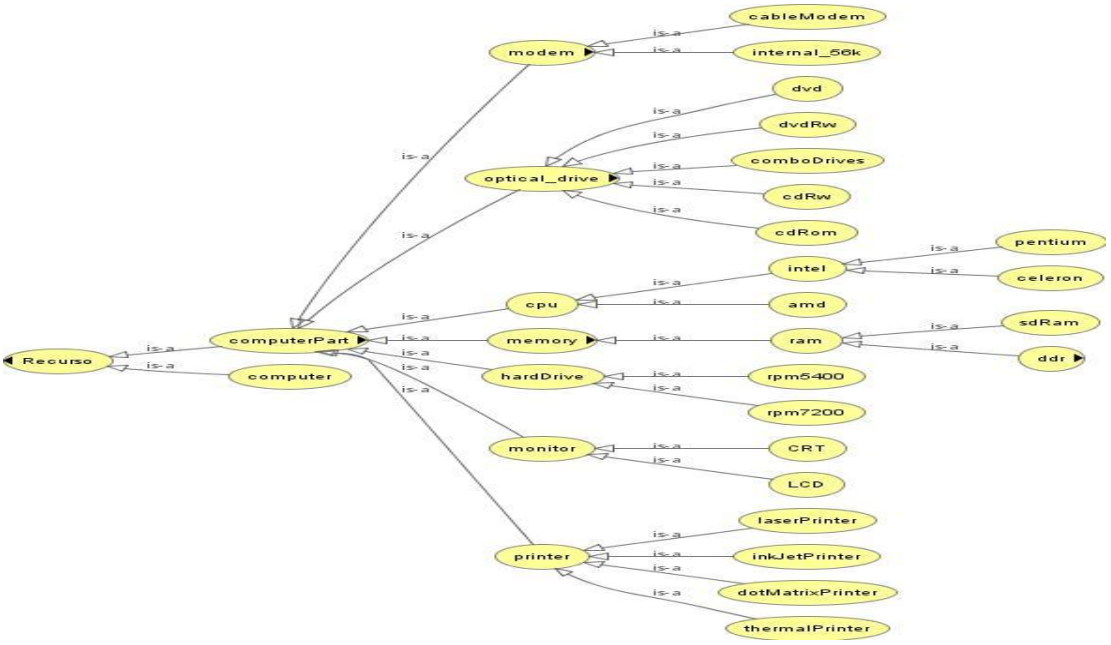

Fig 1.2 Taxonomy tree for Search Interface S2

Similarly the second search interface O2 under consideration becomes as follows

Table 1.3 Codes of terms in search interface B

Term	Code
Recurso	B
Computer part	B01
Computer	B02
Modem	B0101
Optical_drive	B0102
CPU	B0103
Memory	B0104
Hard Drive	B0105
Monitor	B0106
Printer	B0107
Cable Modem	B010101
Internal 56K	B010102
DVD	B010201
DVD RW	B010202

Combo-drive	B010203
CDRW	B010204
CDROM	B010205
Intel	B010301
Amd	B010302
RAM	B010401
Rpm5400	B010501
Rpm7200	B010502
CRT	B010601
LCD	B010602
Laser	B010701
Inkjet	B010702
Dotmatrix	B010703
Thermal	B010704
Pentium	B01030101
Celeron	B01030102
Sdram	B01040101
DDRam	B01040102

Now depending upon the length of codes assigned to each term search interface can be divided into clusters so that all terms having codes of same length reside in the same cluster. The methodology used for clustering has been defined earlier. The clusters becomes as follows for each search interface.

The algorithm suggested above makes use of recursive calls so that all children of the terms under consideration are also checked for the similarity. We take example of term Intel in search interface o1 and the same term Intel in search interface O2. Then we try to combine the children of both terms. This term has been selected for the purpose of clarity and simplicity only so that it doesn't become too complex.

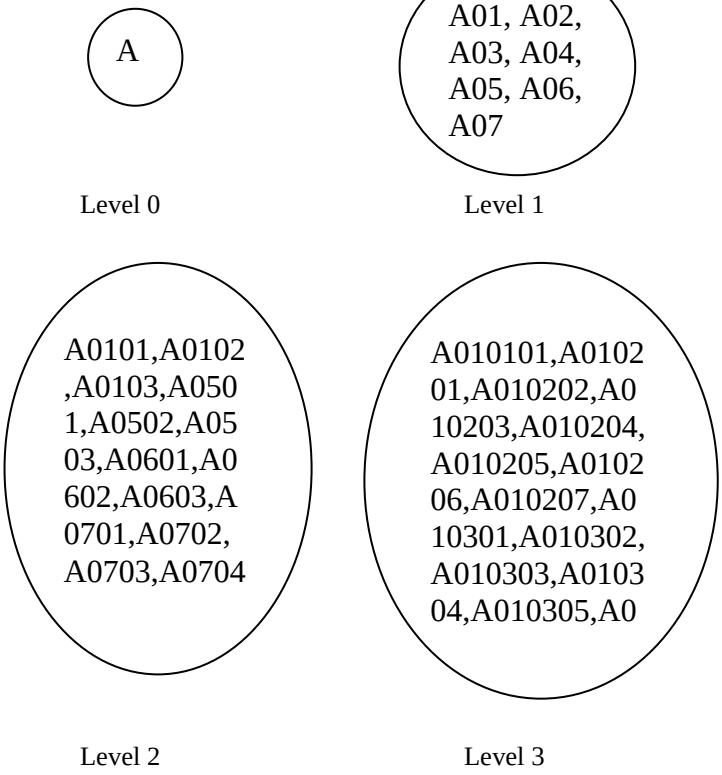

Fig 1.3 Clusters for Search Interface S1

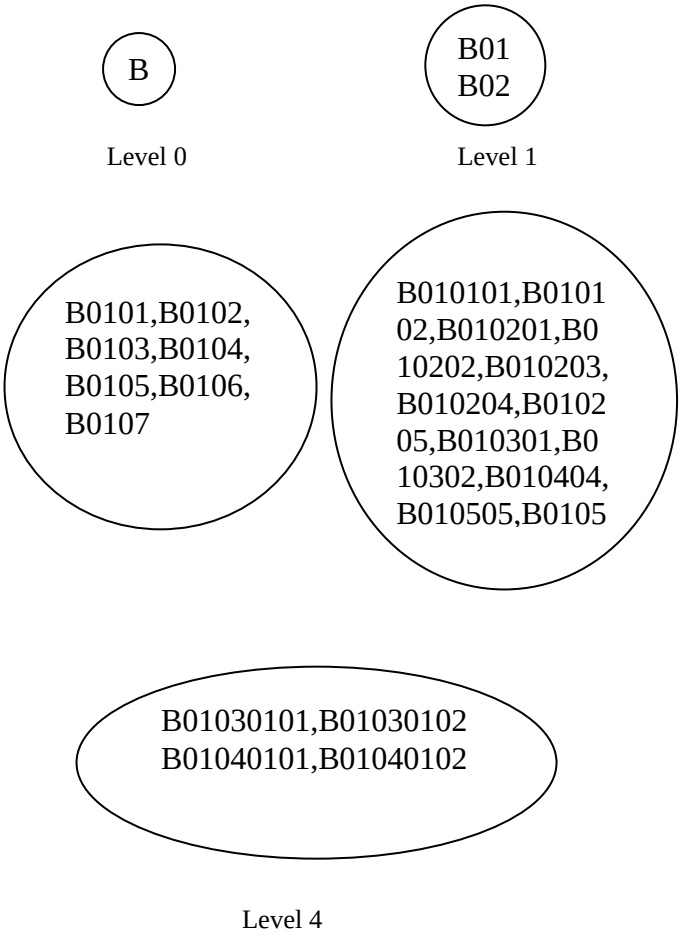

Fig 1.4Clusters for Search Interface S2

To see how the process of merging of search interfaces will take place we consider example of term **CPU** which appears in both search interfaces. The process of merging will be followed as per the algorithm suggested above.First of all both search interfaces O1 and O2 will be passed to function Integrate. The two tables table 1 and table 2 are already available with us as given above. While scanning through these tables as given in the algorithm it will be detected that cpu appearing in table 1 is same as cpu appearing in table 2 and whenever two same or similar terms are encountered the codes of both terms are fetched. From tables the fetched codes of both terms in different search interfaces are A01 and B0103 in search interface 1 and 2 respectively. These two codes A01 and B0103 will be passed to function merge. Function merge will make two queues from these two codes one for each code having all its descendants upto any level. So that those queues can be passed to function combine and queues can be merged. In function merge q1 and q2 will be created having code A01 and B0103 in q1 and q2 respectively. The color will be assigned to each term in the queue just to check whether immediate children of the term have been added to the queue or not. Initially term will be of white color and the color will be changed to black when its children has been added to the queue. The process will be repeated until all terms in the queue are black which represents that children of each term has been added to the queue.

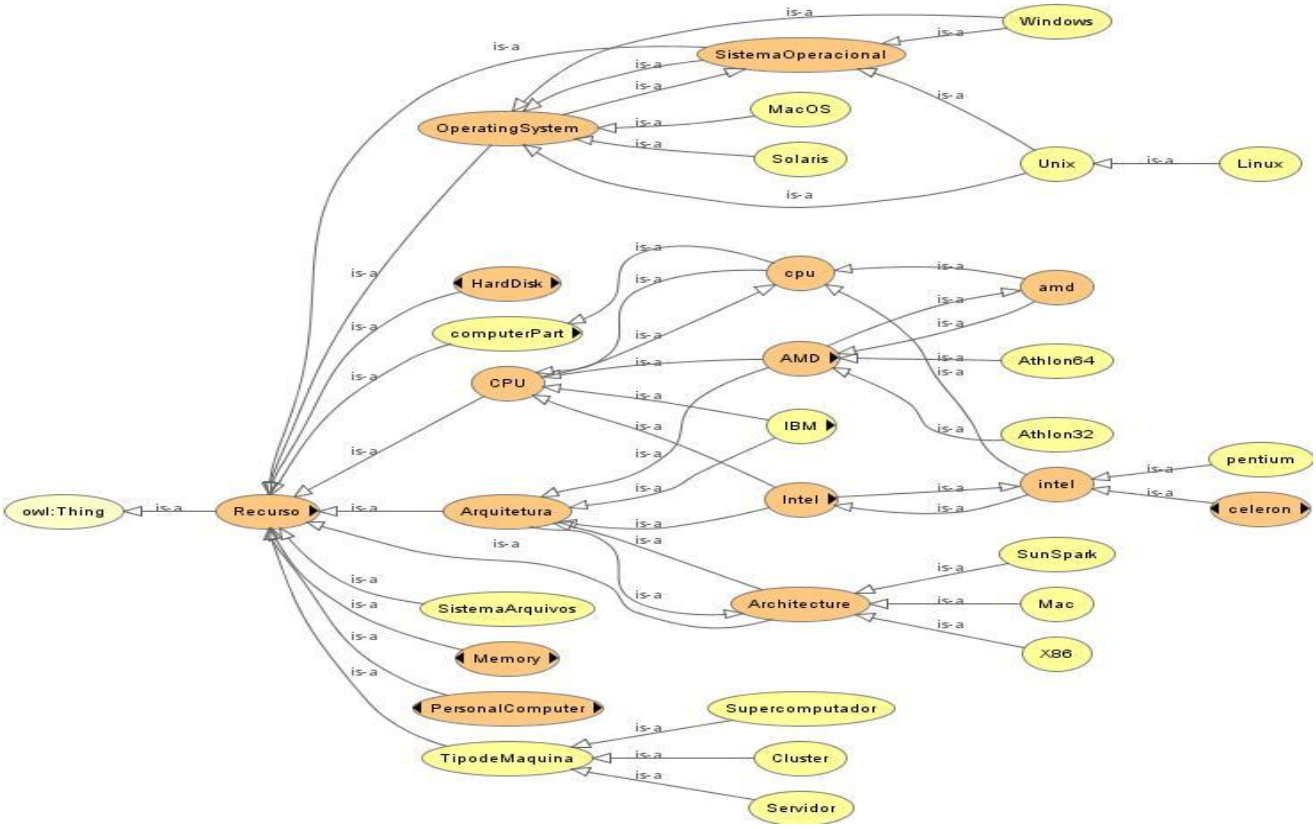

Fig 1.5 Taxonomy tree for Search Interface after merging S1 and S2

This way merging process proceeds in the algorithm. The same process will be repeated for any term in the search interface. And after merging two search interfaces result will be stored in form of a queue only. The result obtained after merging the two search interfaces above the resulting search interface becomes as follows. The case study has shown that how the proposed algorithm is implemented for merging search interfaces. It is seen from the Fig 3.6 that all similar terms appear only once in the resulting search interface and none of the concept is left. The same algorithm can be implemented for merging more than two search interfaces.

REFERENCES

[1] Brian Pinkerton, "*Finding what people want: Experiences with the web crawler*." Proceedings Of WWW conf., 1994.

[2] Alexandros Ntoulas, Junghoo Cho, Christopher Olston "*What's New on the Web? The Evolution of the Web from a Search Engine Perspective.*" In Proceedings of the World-Wide Web Conference (WWW), May 2004.

[3] Vladislav Shkapenyuk and Torsten Suel, "*Design and Implementation of a High performance Distributed Web Crawler*", Technical Report, Department of Computer and Information Science, Polytechnic University, Brooklyn, July 2001.

[4] Junghoo Cho, Narayanan Shivakumar, Hector Garcia-Molina *"Finding replicated Web collections." In Proceedings of 2000 ACM International Conference on Management of Data (SIGMOD)*, May 2000.

[5] Douglas E. Comer, "*The Internet Book*", Prentice Hall of India, New Delhi, 2001.

[6] A. K. Sharma, J. P. Gupta, D. P. Agarwal, "*A novel approach towards efficient Volatile Information Management*", Proc. Of National Conference on Quantum Computing, 5-6 Oct.' 2002, Gwalior.

[7] AltaVista, "*AltaVista Search Engine*," WWW, http://www.altavista.com.

[8] Shaw Green, Leon Hurst , Brenda Nangle , Dr. Pádraig Cunningham, Fergal Somers, Dr. Richard Evans, "*Sofware Agents* : A Review", May 1997.

[9] Cho, J., Garcia-Molina, H., Page, L., "*Efficient Crawling Through URL Ordering*," Computer Science Department, Stanford University, Stanford, CA, USA, 1997.

[10] O. Kaljuvee, O. Buyukkokten, H. Garcia-Molina, and A. Paepcke. "Efficient web form entry on pdas". Proc. of the 10th Intl. WWW Conf., May 2001.

[11] Ching-yao wang, ying-chieh lei, pei-chi chang and shian- shyong tsen National chiao-tung university, *"A level wise clustering algorithm on structured documents"*

[12] Benjamin Chin Ming Fung**,** *"Hierarchical document clustering using frequent itemsets"*

[13] Francis Crimmins, "*Web Crawler Review*".

[14] A.K.Sharma, J.P.Gupta, D.P.Agarwal, "*An Alternative Scheme for Generating Fingerprints of Static Documents*", accepted for publication in Journal of CSI..

[15] Allan Heydon, Marc Najork, 1999," Mercator: "*A Scalable, Extensible Web Crawler*", Proceedings of the Eighth International World Wide Web Conference, 219-229, Toronto, Canada, 1999.

[16] F.C. Cheong, "*Internet Agents: Spiders, Wanderers, Brokers and Bots* ", New Riders Publishing, Indianapolis, Indiana, USA, 1996.

[17] Frank M. Shipman III, Haowei Hsieh, J. Michael Moore, Anna Zacchi , "Supporting Personal Collections across Digital Libraries in Spatial Hypertext"

[18] Stephen Davies, Serdar Badem, Michael D. Williams, Roger King, *"Google by Reformulation": Modeling Search as Successive Refinement*

[19] Gautam Pant, Padmini Srinivasan1, and Filippo Menczer, "*Crawling the Web"*

[20] Monica Peshave ,"How Search engines work *and a web crawler application"*

[21] Ben Shneiderman ," *A Framework for Search Interfaces"*

[22] Danny C.C. POO Teck Kang TOH, " Search *Interface for Z39.50 Compliant Online Catalogs Over The Internet"*

[23] David Hawking CSIRO ICT Centre, "*Web Search Engines: Part 1"*

[24] M.D. Lee, G.M. Roberts, F. Sollich, and C.J. Woodru, "*Towards Intelligent Search Interfaces"*

[25] Sriram Raghavan Hector Garcia-Molina, "*Crawling the Hidden Web"*

[26] Jared Cope, "*Automated Discovery of Search Interfaces on the Web"*

[27] IVataru Sunayama' Yukio Osan-a? and Iviasahiko Yachida', "*Search Interface for Query Restructuring with Discovering User Interest"*

[28] Stephen W. Liddle, Sai Ho Yau, and David W. Embley, "*On the automatic Extraction of Data from the Hidden Web"*

[29] Gualglei song, Yu Qian, Ying Liu and Kang Zhang, *"Oasis: a Mapping and Integrated framework for Biomedical ontologies"*

[30] Miyoung cho, Hanil Kim and Pankoo Kim, " *A new method for ontology merging based on the concept using wordnet"*

[31] Pascal Hitzler, Markus Krotzsch, Marc Ehrig and York Sure, " *What is ontology merging"*

[32] Natalya Fridman Noy and Mark A. Musen, "*PROMPT: Algorithm and tool for automated ontology merging and alignment"*

[33] Dinesh Sharma, Komal Kumar Bhatia, A.K Sharma, "*Crawling the Hidden web resources", NCIT-07 , Delhi*

[34] Dinesh Sharma, *"Crawling the hidden web resources using agent" ETCC-07. NIT- Hamirpur*

Performance Evaluation in Wireless Network

Harish Saini[1], Renu Ghanghs[2]
[1]Assistant Professor N.C.College of Engineering Israna, Panipat
[2]Research Scholar, N.C.College of Engineering Israna, Panipat

Abstract: An ad hoc network is a self –configuring network of wireless links connecting mobile nodes. These nodes may be routers and/or hosts. Each node or mobile device is equipped with a transmitter and receiver. They are said to be purpose-specific, autonomous and dynamic. Ad hoc networking is a concept in computer communications, which means that users wanting to communicate with each other from a temporary network, without any form of central administration. Term ad hoc means a network, which can take different forms in terms of topologies and in term of devices used. Ad hoc devices can be mobile, standalone or networked. A Mobile Ad hoc Network (MANET) is an autonomous system of mobile hosts, which are free to move around randomly and organize themselves arbitrarily. MANET is viewed as suitable systems which can support some specific applications as virtual classrooms, military communications, emergency search and rescue operations, data acquisition in hostile environments, communications set up in exhibitions, conferences and meetings, in battle field among soldiers to coordinate defense or attack, at airport terminals for workers to share files etc. In ad hoc networks nodes can change position quite frequently. The nodes in an ad-hoc network can be laptops, PDA (Personal Digital Assistant) or palm tops etc. These are often limited in resources such as CPU capacity, storage capacity, battery power, and bandwidth. Each node participating in the network acts both as a router and as a host and must therefore be willing to transfer packets to other nodes. For this purpose routing protocol is needed and the new protocol should try to minimize control traffic. An ad hoc network has certain characteristics, which impose new demands on routing protocols. The most important characteristic is dynamic topology, which is a consequence of node mobility. It should be reactive i.e. calculates routes only upon receiving a specific request.

I. INTRODUCTION

Wireless and mobile environments bring different challenges to users and service providers when compared to fixed, wired networks. Physical constraints become much more important, such as device weight, battery power, screen size, portability, quality of radio transmission, error rates. Mobility brings additional uncertainties, as well as opportunities to provide new services and supplementary information to users in the locations where they find themselves. If a user, application or company wishes to make data portable, mobile and accessible then wireless network is the answer. A wireless networking system would rid of the downtime normally have in a wired network due to cable problems. It will also save time and money due to the fact that it would square the expenses of installing a lot of cables. Wireless networking can prove to be very useful in public places, libraries, guesthouses, and hotels where one might find wireless access to Internet. In general, most application software, operating systems and network infrastructures are intended for more conventional environments, and so the mobile wireless user has great difficulty exploiting the computational infrastructure as fully as he or she might. There is an emerging consensus among researchers that a new architecture and dynamic infrastructure is inappropriate way to address this problem.

As the Internet becomes ever more pervasive, and wireless access to it becomes more common, there will be a growing need for middleware that can mediate among several parties involved. Infrastructure providers can provide location-based information to the subscribers and service-providers; they can also exploit aggregate and individual location information to better manage their own communication infrastructure. Mobile ISPs can provide value added services that enhance the user's awareness of services in the environment, and provide means of interacting with those services. Users perceive a rich, adaptive electronic infrastructure that presents the entire Internet to them in a convenient, controllable, dynamic way.

A *Objective*

The objective of this M.Tech(IT) thesis is to differentiate between various Ad hoc routing protocols by comparing all protocols with the help of simulator. To compare some factors like number of packets delivered, numbers of packets sent, pause time, congestion, efficiency, total number of nodes in network, number of connections between nodes, size of packets etc.

B. *Research Method Used*

In this thesis empirical research method is followed to compare the different Ad hoc routing algorithms. It is part of the scientific method, but is often mistakenly assumed to be synonymous with the experimental method. In this research the following steps have been tried to follow. Though step order may vary depending on the subject matter and researcher, the following steps are usually part of most formal research, both basic and applied:

- Formation of the topic
- Hypothesis
- Conceptual definitions
- Operational definitions
- Gathering of data
- Analysis of data
- Test, revising of hypothesis
- Conclusion

11. LITERATURE REVIEW

A. *Mobile Ad-hoc Network (MANET)*

An Ad hoc wireless network is a collection of two or more devices equipped with wireless communications and networking capability. Such devices can communicate with another node that is immediately within their range or one that is outside their radio range. For the latter scenario, an intermediate node is used to rely or forward the packet from the source to destination. An ad hoc wireless network is self-organizing and adaptive. This means that a formed network can be de formed on the fly without the need of system administration. The term Ad hoc tends to imply "can take different forms" and "can be mobile, stand alone, or networked." Ad hoc nodes or devices should be able to detect the presence of other such devices and to perform the necessary handshaking to allow the sharing of information and services.

B. *Applications*

A mobile Ad hoc network includes several advantages over traditional wireless networks, including: ease of deployment, speed of deployment, and decreased dependence on a fixed infrastructure. MANET is attractive because it provides an instant network formation without the presence of fixed base stations and system administrations. MANET is being viewed as suitable systems for some specific applications including:

- Personal communications like cell phones, laptops.
- Group communication such as communication set up in exhibitions, conference, presentation, meeting, and lectures.
- Military, emergency, discovery and civil communication.

C. *Characteristics of Manet*

A MANET consists of mobile platforms (e.g. a router with multiple hosts and wireless communication devices), herein simply referred to as "nodes", which are free to move about arbitrarily. The nodes may be located in or on airplanes, ships, trucks, cars, perhaps, even on people or very small devices, and there may be multiple hosts per router. A MANET is an autonomous system of mobile nodes. The system may operate in isolation, or may have gateways to and interface with a fixed network. In the latter operational mode, it is typically envisioned to operate as a stub network connecting to a fixed network. Stub networks carry traffic originating at and/or destined for internal nodes, but do not permit exogenous traffic to transit through the stub network.

MANET nodes are equipped with wireless transmitter and receivers using antennas, which may be Omni directional (broadcast), highly directional (point to point), possibly steer able, or some combination thereof. At a given point in time, depending on node position and their transmitter and receiver coverage pattern, transmission power levels and co-channel interfaces levels, a wireless connectivity in the form of random, multi hop graph or ad-hoc network exists between the nodes. This Ad hoc topology may changes with time as nodes move or adjusts their transmission and reception parameters.

MANETs have several salient characteristics that have to be taken into account when considering their design and deployment.

1. Dynamic Topologies: Nodes are free to move arbitrarily: thus, the network topology, which is typically multihop, may change randomly and rapidly at unpredictable times, and may consist of both bi-directional and unidirectional links.
2. Bandwidth-constrained, variable capacity links: wireless links will continue to face significantly lower capacity than their hardwired counterparts. In addition, the realized throughput of wireless communications, after accounting for the effects of multiple access, fading, noise and interference conditions, etc, is often much less than a radio's maximum transmission rate. As the mobile network is often simply an extension of the fixed network infrastructure, mobile ad-hoc users will demand similar services. These demands will continue to increase multimedia computing and collaborative network applications rise.
3. Energy-constrained operation: some or all of the nodes in a MANET may rely on batteries or other exhaustible means for their energy. For these nodes, the most important system design criteria for optimization may be energy conservation.
4. Limited Physical Security: Mobile wireless networks are generally more prone to physical security threats than are fixed cable nets. The increased possibility of eavesdropping, spoofing, and denial-of-service attacks should be carefully considered. Existing link security techniques are often applied within wireless network to reduce security threats. As a benefit, the additional robustness against the single points of failure of more centralized approaches.

111. ROUTING APPROACHES

A. *Classification of routing protocols*

Routing is the process of selecting paths in a network along which to send network traffic. Routing is performed for many kinds of networks, including the telephone network, electronic data networks (such as the Internet), and transportation (transport) networks. Different Routing approaches are as following:

Proactive (Table Driven) Protocols

These protocols are based on distance vector/ link state algorithms. These algorithms attempt to monitor the current status of network topology by maintaining routing tables. The information in tables may be updated periodically at regular time intervals. Alternatively, the information in table may be updated when an event occur independent of traffic demand. An event may be a predefined distance traveled by a node, or a predefined number of links formed or broken by the movement of a node.

The advantage of such protocols is that route information for each destination is available whenever required. On the other hand these protocols waste network capacity to keep routing information current, even though most of information becomes stale even before it is used, due to node mobility. The communication overhead involved in maintaining global information about the networks is not acceptable for networks whose bandwidth and battery power are severely limited. These

protocols work well for small size of networks with low mobility rate of nodes.

Reactive (On Demand) Protocols

These protocols discover the routes when they are required. These algorithms minimize the communication overheads and are adaptive to sleep period operation since inactive nodes do not participate at the time when route is established. On-demand protocols typically have the following components:

- Route discovery (destination search): When the source node S needs to send a message to destination D, it issues a destination search request if route to destination D is not available.
  Flooding a short message performs the destination search, so that each node in the network is reached. Path to destination is memorized in the process.
- Route reply: When the destination node D receives the first short search message, D will send a route reply message to the source through the path obtained by reversing the path followed by the route request received by D. The route reply message may contain exact location, time, speed, etc of destination.
- Routing data message: After receiving route reply, the source node S then sends a data message ('long' message) towards the exact location of destination through the route obtained from the route reply message. The efficiency of destination search depends on the corresponding location update scheme.
- Route maintenance: The routes discovered are stored in the route table temporarily while it is in use or for some limited time to avoid frequent route discovery. A source restarts a route discovery procedure whenever it detects that a previously discovered route is obsolete.
- Route erasure: Obsolete route information or non-active routes are removed from routing tables to check the table size.

These protocols reduce redundant routing information in the network, do not waste network capacity on updates, and allow nodes to save power by going into sleep modes. On the other side, these protocols may suffer from high route latency. Also, the routes discovered using flooding, may cause large overheads, nullify the savings on updates.

C. Routing protocols for ad hoc Network

A number of routing algorithms have been developed to operate efficiently in mobile networking context. These algorithms can be classified into different categories based on the following qualitative and quantitative properties.

- Demand based routing
- Distributed Routing
- Position based Routing.
- Flat Routing
- Hierarchical Routing

B. Ad hoc Wireless Network

Operating Principles

To illustrate the general operating principles of a mobile ad hoc network, consider figure 3.1, which depicts the peer-level, multi-hop representation of a sample ad hoc network. Here, mobile node A communicates directly (single-hop) with another such node B whenever a radio channel with adequate propagation characteristics is available between them. Otherwise, multi-hop communication is necessary where one or more intermediate nodes must act as a relay (router) between the communicating nodes. For example, there is no direct radio channel (shown by the lines) between A and C or between A and E as shown in figure 3.1. Nodes B and D must serve as intermediate routers for communication between A and C, and between A and E, respectively. Thus, a distinguishing feature of ad hoc networks is that all nodes must be able to function as routers on demand along with acting as source and destination for packets. To prevent packets from traversing infinitely long paths, an obvious essential requirement for choosing a path is

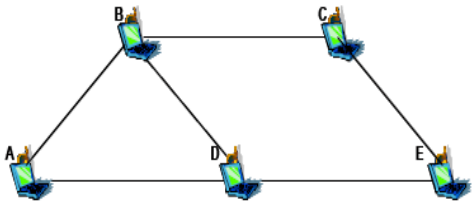

that it must be loop-free. And this loop- free path between a pair of nodes is called a route.

Figure: Ad hoc Networks

An ad hoc network begins with at least two nodes, broadcasting their presence (beaconing) with their respective address information. If node A is able to establish direct communication with node B as in figure 3.1, verified by exchanging suitable control messages between them, they both update their routing tables. When a third node C joins the network with its beacon signal, two scenarios are possible. The first is where both A and B determine that single-hop communication with C is feasible. The second is where only one of the nodes, say B, recognizes the beacon signal from C and establishes direct communication with C. The distinct topology updates, consisting of both address and route updates, are made available in all three nodes immediately afterwards. In the first case, all routes are direct. For the other, the route update first happens between B and C, then between B and A, and then again between B and C, confirming the mutual reach ability between A and C via B. As the node moves, it may cause the reach ability relations to change in time, requiring route updates. Assume that, for some reason, the link between B and C is no longer available as shown in figure 3.2 Nodes A and C are still reachable from each other, although this time only via nodes D and E. Equivalently, the original loop- free route A□B□C is now replaced by the new loop- free route A□D□E□C. All five nodes in the network are required to update their routing tables appropriately to reflect this topology change, which will be first detected by nodes B and C, then communicated to A, E, and D.

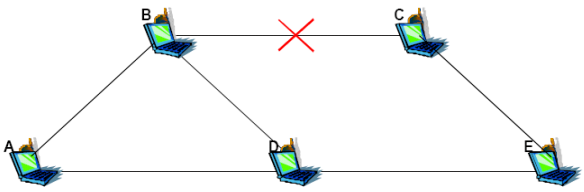

Figure: Changing Topology

This reach ability relation among the nodes may also change for various reasons. For example, a node may wander too far out of range, its battery may be depleted, or it may just suffer from software or hardware failure. As more nodes join the network, or some of the existing nodes leave, the topology updates become more numerous, complex, and usually, more frequent, thus diminishing the network resources available for exchanging user information (i.e., data). Finding a loop-free path between a source-destination pair may therefore become impossible if the changes in network topology occur too frequently. Too frequently here means that there may not be enough time to propagate to all the pertinent nodes the changes arising from the last change in network topology. Thus the ability to communicate degrades with increasing mobility and as a result the knowledge of the network topology becomes increasingly inconsistent. A network is combinatorial stable if, and only if, the topology changes occur slowly enough to allow successful propagation of all topology updates as necessary or if the routing algorithm is efficient enough to propagate the changes in the network before the next change occurs. Clearly, combinatorial stability is determined not only by the connectivity properties of the networks, but also by the efficiency of the routing protocol in use and the instantaneous computational capacity of the nodes, among others. Combinatorial stability thus forms an essential consideration for attaining efficient routing objectives in an ad hoc network.

1V. ROUTING PROTOCOLS

A. *Mobile Routing Protocols*

The Mobile Routing Protocols can be of two types.
Table Driven Routing Protocols (Proactive Protocols)
On Demand Routing Protocols (Reactive Protocols)

B. *Table Driven Routing Protocols in Ad hoc Networks*

In table driven routing protocols, consistent and up-to-date routing information to all nodes is maintained at each node. Following are the mainly used Table Driven Routing Protocols in ad hoc Networks: -

- DBF
- GSR
- DSDV
- WRP
- STAR

On Demand Routing Protocols

In On-Demand routing protocols, the routes are created as and when required. When a source wants to send to a destination, it invokes the route discovery mechanisms to find the path to the destination. Following are the mainly use On Demand Routing Protocols:-

- DDR
- DSR
- AODV
- RDMAR
- TORA

Bellman Ford Algorithm (DBF)

Shortest path routing algorithm based on distributed technique. According to DBF, a routing node knows the length of the shortest path from each neighbor to every network destination and this information is used to compute the shortest path successor in the path to each destination. It is table driven protocol, supports a flat architecture. Performance of this algorithm is as follows:

(a) Shortest path routing
(b) Simple in use
(c) Better computation efficiency due to distributed characteristic.
(d) It is available for both wire line and wireless networks.

Distance Sequenced Distance Vector Routing (DSDV)

Distance Sequenced Distance Vector (DSDV) routing protocol is a variant of distance vector routing method by which mobile nodes cooperate among themselves to form an ad hoc network. DSDV is based on RIP (Routing Information Protocol), which is used for Intra-Domain routing in Internet. DSDV requires each node in the network to maintain complete list of distance information to reach each node in the ad hoc network. In DSDV, each node uses a Sequence Number, which is a counter that can be incremented only by that node. Each node increments the Sequence Number every time it sends an update message and this Sequence Number uniquely identifies the update messages sent from a particular node. Routing information is propagated using broadcast or multicasting the messages periodically or triggered upon a change in the topology. DSDV uses only bi-directional links for routing as it is based on Distance Vector Routing. So in DSDV, each node does not insert information into its Routing table received from other neighbors unless the node is sure that the other node can listen to its advertisements.

Wireless Routing Protocol (WRP)

WRP is another protocol based on distributed Bellman-Ford algorithm (DBF). It substantially reduces the number of cases in which routing loops (count-to-infinity problem) can occur. It utilizes information regarding the length and second to last hop (predecessor) of the shortest path to each destination. Each node maintains a distance table, a routing table, a link-cost table and a message retransmission list. The distance table of a node contains tuples <destination, next hop, distance, predecessor (as reported by next hop)> for each destination and each neighbor. The routing table of a node contains tuples <destination, next hop, distance, predecessor, and marker> for each known destination where marker specifies whether the entry corresponds to a simple path, a loop or a destination that has not been marked. The link-cost table contains the cost of the link to each neighbor and the number of periodic update periods elapsed since the node received any error-free message from it. The message transmission list (MRL) contains sequence number of update message, retransmission counter, and acknowledgement required flag vector with one entry per neighbor, and a list of updates sent in the update message. It records which updates of an update message have to be transmitted and which neighbors should be requested to acknowledge such retransmission.

GLOBAL STATE ROUTING (GSR) PROTOCOL

This protocol is based on Link State routing, which has the advantage of routing accuracy, and dissemination method used in DBF, to avoid inefficient flooding in LS routing. Each node

maintains a neighbor list, a topology table, a next hop table and a distance table. The neighbor list contains the list of nodes adjacent to the node. The topology table contains the link state information reported by a destination and a timestamp indicating the time at which this is generated. The next hop table and the distance table contain the next hop and the distance of the shortest path for each destination respectively. Initially, each node learns about its neighbors and the distance of the link to it (generally hop count equals one) by examining each packet in its inbound queue and broadcasts this information to its neighbors. Upon receiving the link state message from its neighbors, each node updates the link state information corresponding to that neighbor in the topology table to the most up to date information using timestamps. Then, the node rebuilds the routing table based on newly computed topology table and broadcasts it to its neighbors. The routing table information is exchanged periodically with the neighbors only.

Fisheye State Routing (FSR) Protocol

FSR protocol is an extension of GSR protocol. It attempts to reduce the size of update messages in GSR without seriously affecting the routing accuracy. The reduction in routing size is obtained by using different exchange periods for different entries in the routing table. Entries corresponding to nodes within the smaller scope are propagated to the neighbors with the highest frequency.

Temporally Ordered Routing Algorithm (TORA)

TORA is designed to work below Internet Protocol (IP). It does not have properties of link state or distance-vector algorithms, but link-reversal. The protocol is adaptive, and highly scalable. It is designed to minimize reaction to topological changes. TORA control messages are localized to a very small set of nodes near the occurrence of a topological change. To achieve this, nodes maintain routing information about adjacent nodes. TORA quickly discovers multiple routes on demand. Route does not have to be optimal, but it guarantees that all routes are loop-free. TORA only does the routing job, and heavily depends on Internet MANET Encapsulation Protocol (IMEP). A good analogy would be water flowing down the hill through pipes. Hilltop is the source, pipes are links, and pipe connections are nodes. TORA assigns level numbers to each node down the hill. When two intermediate nodes cannot communicate, the last node raises its level higher than any of its neighbors, so that water, which is data, flows back out of it.

Dynamic Source Routing (DSR)

Dynamic source routing is a Source routed On-Demand routing protocol in ad hoc networks. It uses Source Routing, which is a technique in which the sender of a packet determines the complete sequence of nodes through which the node has travel. The sender of the packet explicitly mentions the list of all nodes in the packet's header, identifying each forwarding 'hop' by the address of the next node to which to transmit the packet on its way to destination host. In this protocol the nodes don't need to exchange the Routing table information periodically and thus reduces the bandwidth overhead in the network. Each Mobile node participating in the protocol maintains a 'routing cache', which contains the list of routes that the node has learnt. Whenever the node finds a new route it adds the new route in its 'routing cache'. Each mobile node also maintains a sequence counter 'request id' to uniquely identify the requests generated by a mobile host. The pair < source address, request id > uniquely identifies any request in the ad hoc network. The protocol does not need transmissions between hosts to work in bi-direction. The main phases in the protocol are Route Discovery process and Route Maintenance process.

Ad hoc On-Demand Distance Vector (AODV)

The ad hoc On Demand Distance Vector (AODV) routing protocol is intended for use by the mobile nodes for routing data in Ad Hoc networks. AODV is an extension of Distance Sequenced Distance Vector (DSDV) routing protocol, a Table Driven routing protocol for Ad hoc networks that is discussed in the previous section. AODV is designed to improve upon the performance characteristics of DSDV in the creation and maintenance of routes.

Relative Distance Micro Discovery Ad hoc Routing Protocol (RDMAR)

RDMAR is a loop free routing protocol for ad hoc mobile networks. The protocol is highly adaptive, efficient and scaleable and is well suited in large mobile networks. The protocol is called Relative Distance Micro Discovery Ad hoc Routing Protocol (RDMAR). It uses the mechanism for route discovery, called Relative Distance Micro discovery (RDM). The concept is that query flood can be localized by knowing the relative distance between two terminals. RDMAR does not use a route cache. Each node has a routing table that lists all available destinations and number of hops to each. It is on demand routing with hybrid architecture.

Summary of the Routing Protocols:

DSDV was the only proactive protocol discussed. AODV is reactive, an on-demand version of DSDV. Authors of AODV, who were also authors of DSDV added multicast capability to AODV. Reactive approach of AODV is similar to DSR's. They both have a route discovery mode, which uses messaging to find new routes. DSR uses source routing; the route is in each packet. Thus, DSR learns more routes than AODV. DSR supports unidirectional links due to its vast knowledge on the topology. TORA runs on top of IMEP, and suffers for its internal instability and IMEP's too frequent HELLO messages generating too much control overhead in the network. DSDV and GSR are table-driven protocols that use destination sequence numbers to keep routes loop-free and up-to-date. HSR is a hierarchical routing protocol derived from FSR. FSR reduces the size of tables to be exchanged by maintaining less accurate information about nodes farther away. CGSR is a cluster-based routing protocol where nodes are grouped into clusters of transmission size ranges.

TABLE: Comparison of Major ad-hoc Routing Protocols

Protocol Property	DSDV	AODV	DSR	ZRP	TORA
Loop free	Yes	Yes	Yes	Yes	Yes
Multiple routes	No	No	Yes	No	Yes
Distributed	Yes	Yes	Yes	Yes	Yes
Reactive	No	Yes	Yes	Variable	Yes
Unidirectional	No	No	Yes	No	Yes

link support					
QoS support	No	No	No	No	No
Multicast	No	Yes	No	No	No
Security	No	No	No	No	Possible
Power efficiency	No	No	No	No	No
Periodic broadcasts	Yes	Yes	No	Yes	Yes

Comparison between On-Demand and Table Driven Protocols

These two types of protocols have their own working areas. At some places one type is suitable and in others the second category is used. Choice of protocol depends on the type of network in operation and working requirements.

V. RESULTS AND DISCUSSION

Successful Packet Delivery

The fraction of successfully received packets, which survive while finding their destination is called packet delivery ratio. This performance measure also determines the completeness and correctness of the routing protocol. Successful packet delivery is calculated such that, all data packets with unique identifier leaving the source MAC are counted and defined as originating packets. Received packet IDs are compared to collected transmission database and each unique packet are counted once to ensure prevention of counting excess receptions

Simulation Results

Parameters chosen for all protocols have been same, sending 4 packets per second of size 512 bytes and using 15-20 connections with 50 nodes. Protocols have been evaluated in 750*750 meters environment for 700 seconds of simulated time at a speed of 10 meter per second. Pause time used is 0, 25, 50, 100, 200, 300, 400, 500, 600 and 700. Pause time 0 means continuous motion while 700 corresponds to no motion. When each data packet is originated, simulator calculates the shortest path between packet's sender and its destination. Traffic type used has been CBR (Constant Bit Rate) using both TCP and UDP packets. It has been observed that simulations were more stable with TCP packets than UDP; in particular DSR has some problems dealing with UDP packets.

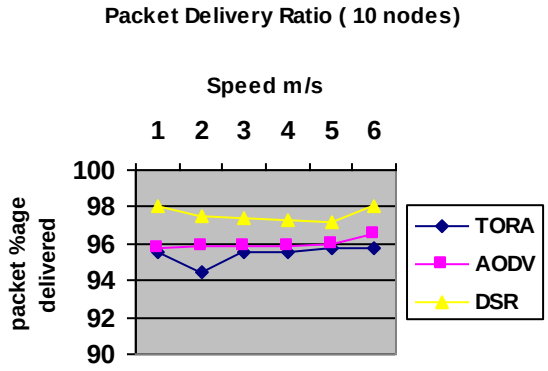

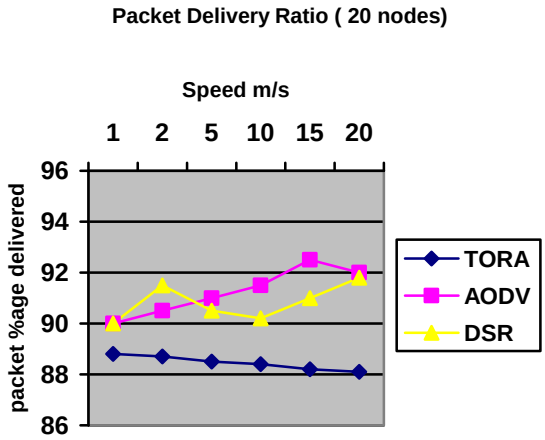

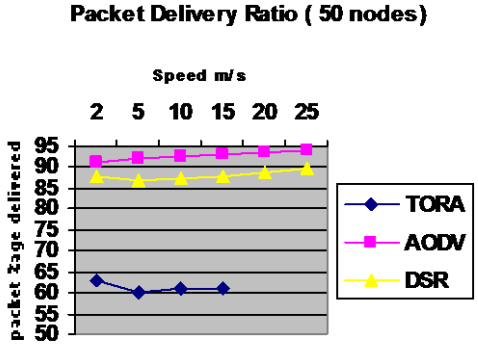

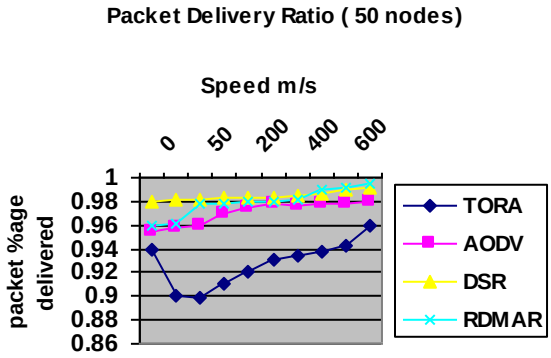

The Graphs show packet delivery ratio of 50 nodes at speed 10 meters per second. It shows that all the protocols deliver more than 98% of their packets at this speed. DSR and AODV deliver almost 97 to 100 % of packet in all cases. TORA does well. RDMAR behaves better than TORA and AODV. It was seen that if sources are increased DSR and AODV behave nicely but TORA has problems in initially, below 250ms. It may be because of increased congestion. It was seen that if sources are increased then DSR, AODV and RDMAR behaves same with only very slight changes but TORA drops in packet deliver ratio. It is because of increased congestion in case of TORA.

In order to explore the change in the behavior of the protocols with varying speed, we performed the experiments with speed change from 10 meter per second to 1 meter per second. Figure shows results at 1 meter per second speed sending 4 packets per second of size 512 bytes and using 20 sources.

It was observed that with change in speed, all protocols deliver above 98% of the packets with slight drops in case of TORA and RDMAR DSR and AODV were excellent in performances at all speeds. Overhead also have less effect for DSR and AODV. DSR caching is effective at faster speeds, but works much better at slower speeds also. Some simulation studies for protocols have been done earlier also, although those simulations used different parameters and sources with varying results. No study involving RDMAR comparisons have been published earlier. In this study, several existing routing protocols for ad hoc wireless networks have been described. Results based on the simulations have been analyzed and presented with the advantages and disadvantages of each protocol. It is not simple to determine which of the four protocols under comparison is the best for Ad hoc network environment. No Protocol is ideal for all scenarios. A good criterion to choose a protocol might be the size and expected traffic load in the target network. The simulations presented here clearly show that there is a need for routing protocols specifically tuned to the characteristics of ad-hoc networks. Overall, the proactive protocols (AODV and DSR) behaved similar in terms of delivery and throughput. On the basis of this study both should be considered suitable for mobile ad-hoc networks. However, a number of differences among the protocols do exist. The source routes used by DSR give increased byte over-head compared to AODV when routes have many hops and packet rates are high. DSR is, on the other hand, efficient in finding (learning) routes in terms of the number of control packets used, and does not use periodic control messages. Data packets in AODV carry the destination address only. Therefore, the byte overhead for AODV is the lowest of the examined protocols. The overhead is high in terms of packets since AODV broadcasts periodic Hello messages to its neighbors. DSR behaves better in this case.

Each of the routing protocol generated different amount of overhead. DSR has the least overhead, TORA has maximum overhead. DSR, TORA and AODV are all on demand protocols and their overhead drops as mobility rate drops. It has been found from Graph that

(a) DSR performance is very good at all mobility rates and movement speeds with all the metrics of comparison.
(b) TORA is the worst performer in all the experiments the network was unable to handle all the routing traffic and lots of packets were dropped.
(c) AODV has performed as well as DSR and accomplishes its goal of eliminating source routing overhead and
(d) RDMAR has performed well.

V1. CONCLUSION AND FUTURE STUDY

The performance of the protocol has been evaluated with other common ad-hoc network routing protocols like DSR, AODV and TORA using a detailed packet level simulator NS. The traffic schemes assigned are TCP and UDP. Simulations have been carried out in an area as large as 1km x 1km with many sources connected to each other. More sources lead to more network load. Results have shown that quick management of route maintenance is an important factor that affects all the performance measures, especially the successful delivery rate at high workloads and increased speed.

It is found that the AODV has highest packet delivery ratio for all speeds and pause times. In other protocols, for very high-speed networks, AODV performs much better in successful packet delivery. The packet delivery rate of DSR, which is a source routing protocol, is directly related to the generation of control messages. Therefore it is related to the frequency of data packet transmissions. At very high speeds DSR cache transmission suffers and a loss in packet delivery occurs. TORA has the lowest throughput and generates a large amount of control messages to manage DAGs, and its control messages encapsulated in IP are dropped because of collisions, which lead to much more decrease in performance. AODV have used much less control messages, limited to the hosts involved in routing process, therefore they have the highest standard division. This means that they distribute the load over the network in least efficient way.

Results have been derived from a series of experiments conducted on simulated network. The following observations can be made:

- Best packet delivery ratio: AODV is the best in terms of packet transmission. More packets are transmitted than any of the studied protocols. This is true even in case of changing scenario and fast moving nodes. So it is able to achieve one of the most important objectives of ad-hoc networks as successful packet delivery.
- Simple: AODV can easily be implemented and executed. The simulation studies have been conducted on Pentium-IV with standard configurations. Though it is best performing under LINUX environment but can be easily implemented on Windows platform also. Efficiency is particularly important when the software implementing the routing algorithm must run on a computer with limited physical resources.
- Route Repair: The route phase of the protocol is unique as compared to other such protocols and outperform all in its category. It describes the maintenance process, which can be done as fast as possible. It describes the level of self-organization in the network. The protocol uses local route repair of routing process.

Future Work

Some of the objectives remained untouched due to the limited time available. On the other hand, outcome of the current research has exhibited the possibilities of further extensions. List of the work that can be carried out in future as an extension of current work is given below:

(a) There is limitation of Battery Life in an ad hoc environment. Battery is most commonly used; none of the protocols discussed the concept of Power as one of the deciding factor in route selection
(b) The existing strategies use fixed scenarios for carrying out simulations. It means before start of the simulation process, position of the nodes is known and also total sources used are fixed, but real life situations demand random scenes and varying sources.
(c) If a link breaks in the route process due to any reason, repair starts and it involves reconstruction of new path.

Reconstruction phase requires better approach in all protocols for fast selection of new routes.

References

1. A. Kush, P. Gupta, R. Chauhan, C.J. Hwang and A. Pandey(2004), "*Power Aware Virtual Node Routing Scheme In Mobile Ad hoc Networks*", Proceedings of International Conference On Mobile Computing IASTED 2004, Banff , CANADA, pp 698-702, July 2004.
2. P. Bose, P. Morin , I. Stojmenovic and J. Urrutia(1999) "*Routing with Guaranteed Delivery in Ad hoc Wireless Networks*", Proceedings of the 3rd International Workshop on Discrete Algorithms and Methods for Mobile Computing and Communications, Seattle, WA USA, August 20, 1999 pp 47-53.
3. Ajay R. Mishra(2004) "*Fundamentals of Cellular Network Planning and Optimisation: 2G/2.5G/3G ... Evolution to 4G*" John Wiley and Sons,pp 213-215, 2004.
4. A. TanenBaum, "*Computer Networks*", Prentice Hall of India, 2002.
5. C.K. Toh(2005), "*Ad hoc mobile wireless Networks*", Prentice Hall New Jersey, pp 121-128, 2005.
6. Y. Lin, I. Chlamtac(2005), "*Wireless and Mobile Architectures*", Wiley Computer Publications, USA, pp 171-177, 2005.
7. A. Nasipuri, R. Castaneda, and R. SamirDas(1999), "*Performance of Multi path Routing for On Demand Protocols in Mobile Ad hoc Networks*", ACM/Baltzer Journal of Mobile Networks(MONET) pp 377-381,1999.
8. National Science foundation, "*Research Priorities in Wireless and Mobile networking*", available at www.cise.nsf.gov.
9. J.B. Evans, G.J. Minden, K.S. Shanmugan , G. Prescott , V.S. Frost , B. Ewy, R. Sanchez, C. Sparks, K. Malinimohan, J. Roberts, R. Plumb and D. Petr(1999), "*The Rapidly Deployable Radio Network*", IEEE Communications, Vol. 17, No. 4, pp. 689-702 , 1999.
10. Fasbender et al, "*Any Network, Any Terminal, Anywhere*", IEEE Personal communications, Volume 6(2), pp 22-30, 1999.
11. J. Schiller(2004), "*Mobile Communication* ", Addison Wesley, PHI New Jersey USA, pp 412-414, 2004.
12. GSM (Global System for Mobile Communication) Data, Intel Corporation Draft EN (04.60) V 6.0.0 available at www.gsmdata.com, 1998.
13. F. Halsall(2003), "*Data Communication, Computer Networks and Open System*", Addison Wesley, Prentice Hall New Jersey USA, pp 342-351, 2003.
14. TIA/EIA/IS-702-A.2, "*TDMA Cellular Radio Mobile Station Base Structure Compatibility*", 136 A, pp 283-287,March 1999.
15. S. Keshov, "*An Engineering Approach to Computer Networks*", Addison Wesley, Prentice Hall New Jersey USA, pp 189-198, 1997.
16. W.R. Young, "*Advanced Mobile Phone Service (AMPS)*", Bell systems technical journal, Volume 58, pp 234-237,1979.
17. B. D. Johnson, A.M. Davis, "*Dynamic Source Routing in Ad hoc Networks*", Mobile Computing (T. Imielinski and H. Korth, Editions), Dordrecht, The Netherlands: Kluwer Academic Publishers, Chap 5, pp. 152-81, February 1996.
18. N. Nikaein and B. Christina, "*Dynamic Routing Algorithm*", available at Institute Eurecom, Navid.Nikaein@eurocom.frm.
19. V.D. Park and M.S. Corson, "*A Highly Adaptive Distributed Routing Algorithm for Mobile Wireless Networks*", Proceedings of INFOCOM'97, pp 9-12, April 1997.
20. C. Parkins and M.R. Elizabeth(1999), "*Ad hoc On Demand Distance Vector Routing*", Proceedings of IEEE WMCSA'99, New Orleans, LA, pp. 90-100, February 1999.
21. C.E. Perkins and P. Bhagwat, "*Highly Dynamic Destination-Sequenced Distance Vector Routing (DSDV) for Mobile Computers*", ACM SIGCOMM'94 Computer Communication Review, pp. 234–244, October 1994.
22. NS notes and documentation available at www.isi.edu/vint.
23. Lee, S.-J. and M. Gerla, "*A Simulation Study of Table-Driven and On-Demand Routing Protocols for Mobile Ad hoc Networks*", IEEE Network, pp. 48-54, August 1999.
24. Z.J. Hass and M. R. Pearlman, "*The Zone Routing Protocol (ZRP) for Ad hoc Networks*" lnternet Draft available at draft-ietf-manet-zone-zrp.txt, 2000.
25. P. Merlin and A. Segall, "*A Failsafe Distributed Routing Protocol*", IEEE Communications, September 1979.
26. V. Garg and J. Wilkes, "*Principals and Applications of GSM*", Prentice Hall, New Jersey, pp 134-141,1999.
27. D.C. Cox, "*Wireless Personal Communications*", IEEE communications, pp 117-156, April 1995.
28. D. Bertsekas and R. Gallager, "*Data Networks – 2nd Edition*", Prentice Hall, New Jersy, ISBN 0-13-200916-1.
29. T. Wei, L. Chen and M. Gerla, "*Global State Routing: A New Routing Scheme for Ad-hoc Wireless Networks*", Proceedings of IEEE ICC' 98, pp 23-28, 1998.
30. MohammedTarique, Kemal E.Tepe "*Minimum energy hierarchical dynamic source routing for MANET*" in ScienceDirect pp 1125-1135, August 2009.
31. Michael Q. Rieck, Sukesh Pai, Subhankar Dhar *Computer Networks*, Volume 47, Issue 6, Pages 785-799,22 April 2005.
32. Tom Goff, NaelAbu-Ghazaleh, Dhananjay Phatak,Ridvan Kahvecioglu *"Journal of Parallel and Distributed Computing"*, Volume 63, Issue 2, pp 12-14February 2003.

A survey on anonymous ip address blocking

[1.] Prof. P.Pradeepkumar [2.]Amer Ahmed khan [3.]B. Kiran Kumar

ABSTRACT
These days, the Internet is full of suspicious actions and people. We always advise to not take a chance in protecting your IP Address information online.

TheIP was being shown everywhere! To advertisersandother places ,even from SPAM who compromised usersidentity. No more I said, and developed software that would hide ip address.we outline a security protocol that uses resource constrained trusted hardware to facilitate anonymous IP-address blocking in anonym zing networks such as Tor.
Tor allows users to access Internet services privately by using a series of Tor routers to obfuscate the route from the client to the server, thereby hiding the client's IP address from the server. The success of Tor, however, has been limited because of malicious users who misuse the network. administrators block all known exit nodes of anonymizing networks, denying nonymous access to misbehaving and behaving users alike.

To address this problem, we present Nymble, a system in which servers can "blacklist" misbehaving users, thereby blocking users without compromising their anonymity. Our system is thus agnostic to different servers' definitions of misbehavior servers can blacklist users for whatever reason, and the privacy of blacklisted users is maintained.
The IP-address anonymity provided by Tor, however, makes it difficult for administrators to deny access to such

offenders .As a result, administrators resort to blocking all Tor exit nodes, effectively denying
anonymous access for all Tor's users. Our solution makes use of trusted hardware and allows services like Tor to provide anonymous blocking of IP addresses while requiring only a modest amount of storage at the trusted node.

Key terms: IP , pockets, NYMBLE,Anonymizing networks, privacy.

Introduction

Anonymizing networks such as re-route a user's traffic between several nodes in different domains. Since these nodes are operated independently, users are able to trust the anonymizing network to provide anonymity. Real-world deployments of anonymizing networks, however, have had limited success because of their misuse

Administrators of websites are unable to blacklist malicious users' IP addresses because of their anonymity. Left with no other choice, these administrators opt to blacklist the entire anonymizing network. This approach eliminates malicious activity through such networks, but at the cost of the anonymity of honest users. In other words, a few "bad apples" can spoil the fun for everybody else using the anonymizing network. (In fact, this has happened repeatedly with To solve this problem, we present a secure protocol based on trusted hardware that allows servers to block anonymous users without knowledge of their actual IP addresses. Although this work applies to anonymizing networks in general, we consider Tor for purposes of exhibition. Building and prototyping a system based on our proposed solution is ongoingwork. In this paper we present our proposed solution and protocol.

Anonymizing networks such as Tor allow users to access Internet services privately by using a series of routers to hide the client's IP address from the server. The success of such networks, however, has been limited by users employing this anonymity for abusive purposes such as defacing popular websites.
Website administrators routinely rely on IP-address blocking for disabling access to misbehaving users, but blocking IP addresses is not practical if the abuser routes through an anonymizing network. As a result,

2 An Overview To Nymble

We now present a high-level overview of the Nymblesystem, and defer the entire protocol description and security analysis to subsequent sections.

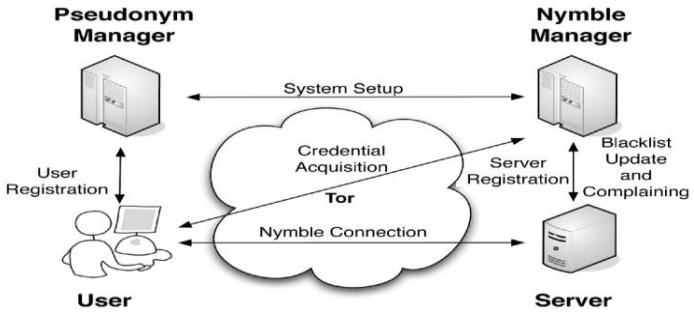

To limit the number of identities a user can obtain (called the Sybil attack), the Nymble system binds nymbles to resources that are sufficiently difficult to obtain in great numbers. For example, we have used IP addresses as the resource in our implementation, but our scheme generalizes to other resources such as email addresses, identity certificates, and trusted hardware. We address the practical issues related with resource-based blocking in Section 8, and suggest other alternatives for resources.

Wedonotclaimto solvethe Sybi lattack.
Thisproblemisfacedbyanycredentialsystem],andwesuggestsomepromisingapproachesbasedonresource-based blocking since we aim to create a real-world deployment.

2.2 The Pseudonym Manager

The user must first contact the Pseudonym Manager (PM) and demonstrate control over a resource;for ip-address blocking the user must connect to the PM directly (i.e., not through a known anonymizing network), We assume the PM has knowledge about Tor routers, for example, and can ensure that users are communicating with it directly.[6] Pseudonyms are deterministically chosen based on the controlled resource, ensuring that the same pseudo-nym is always issued for the same resource.

Note that the user does not disclose what server he or she intends to connect to, and the PM's duties are limited to mapping IP addresses (or other resources) to pseudonyms. As we will explain, the user contacts the PM only once per linkability
window (e.g., once a day).

2.3 The Nymble Manager

After obtaining a pseudonym from the PM, the user connects to the Nymble Manager (NM) through the anonymizing network, and requests nymbles for access to a particular server (such as Wikipedia). A user's requests to the NM are therefore pseudonymous, and nymbles are generated using the user's pseudonym and the server's identity. These nymbles are thus specific to a particular user-serverpair. Nevertheless, as long as the PM and the NM do not collude, the Nymble system cannot identify which user is connecting to what server; the NM knows only the pseudonym-server pair, and the PM knows only the user identity-pseudonym pair.

To provide the requisite cryptographic protection and security properties, the NM encapsulates nymbles within nymble tickets. Servers wrap seeds into linking tokens, and therefore, we will speak of linking tokens being used to link future nymble tickets. The importance of these constructs will become apparent as we proceed. Nymble tickets are bound to specific time periods, time is divided into linkability windows of durationW, each of which is split into L time periods of duration T (i.e., W ¼ L T). We will refer to time periods and linkability windows chronologically as t_1; t_2; . . . ; t_L and w_1;w_2;..., respectively. While a user's access within a time period is tied to a single nymble ticket, the use of different nymble tickets across time periods grants the user anonymity between time periods. Smaller time periods provide users with higher rates of anonymous authentication, while longer time periods allow servers to rate-limit the number
of misbehaviors from a particular user before he or she is blocked. For example, T could be set to five minutes, and W to one day (and thus, L ¼ 288). The linkability window allows for dynamism since resources such as IP addresses can get reassigned and it is undesirable to blacklist such resources indefinitely, and it ensures

forgiveness of misbehavior after a certain period of time. We assume all entities are time synchronized (for example, with time.nist.gov via the Network Time Protocol (NTP)), and can thus calculate the current linkability window and time period.Summary of Updates to the Nymble Protocol We highlight the changes to Nymble since our onferencepaper [24]. Previously, we had proved only the privacy properties associated with nymbles as part of a two-tiered hash chain. Here, we prove security at the protocol level. This process gave us insights into possible (subtle) attacks against privacy, leading us to redesign our protocols and refine our definitions of privacy. For example, users are now either legitimate or illegitimate, and are anonymous within these sets. This redefinition affects how a user establishes a "Nymble connection" , and now prevents the server from distinguishing between users who have already connected in the same time period and those who are blacklisted, resulting in larger anonymity sets.A thorough protocol redesign has also resulted in several optimizations.

We have eliminated blacklist version numbers and users do not need to repeatedly obtain the current version number from the NM. Instead servers obtain proofs of freshness every time period, and users directly verify the freshness of blacklists upon download. Based on a hash chain approach, the NM issues lightweightdaisiestoservers as proof of a blacklist's freshness, thus making blacklist updates highly efficient. Also, instead of embedding seeds, on which users must perform computation to verify their blacklist status, the NM now embeds a unique identifier nymble , which the user can directly recognize. Finally, we have compacted several data structures, especially the servers' blacklists, which are downloaded by each user.

Our Nymble Construction

System Setup

During setup, the NM and the PM interact as follows:

1. The NM executes NMInitStateðÞ (see Algorithm 10) and initializes its state nmState to the algorithm's output.
2. The NM extracts $macKey_{NP}$ from nmState and sends it to the PM over a type-Auth channel. $macKey_{NP}$ is a shared secret between the NM and the PM, so that the NM can verify the authenticity of pseudonyms issued by the .
3. The PM generates $nymKey_P$ by running Mac.Key-Gen() and initializes its state pmState to the pair $ðnymKey_P ; macKey_{NP} Þ$.
4. The NM publishes $verKey_N$ innmState in a way that the users in Nymble can obtain it and verify its integrity at any time (e.g., during registration).

Server Registration

To participate in the Nymble system, a server with identity sid initiates a type-Auth channel to the NM, and registers with the NM according to the Server Registration protocol below. Each server may register at most once in any linkability window.

User Registration

In this procedure, user Alice interacts with the PM in order to register herself to the NYMBLE system for linkability window k. Alice obtains a pseudonym from the PM upon a successful termination of such an interaction. The communication channel between them is confidential and PM-authenticated.

To register, Alice authenticates herself as a user with identity id to the PM by demonstrating her control over some resource(s) as discussed, after which the PM computes pnymHkhkP (id, k) and macPNHMAChmkNP (pnym, k), and returns hpnym, macPNi to Alice, who stores it privately.

Acquisition of Nymble Tickets In order for Alice to authenticate to any server Sj during any linkability window Wk, she must present a nymble ticket to the server. The following describes how she can obtain a credential from the NM containing such tickets. The communication channel is anonymous

(e.g., through Tor), confidential and NM-authenticated.

Alice sends her hpnym, macPNi to the NM, after which the NM:

1. asserts that macPN = HMAChmkNP (pnym, k),
2. computesnymbleTKT` NymbleTktGennmsk (pnym, j, k, `), for ` = 1 to L, and
3. returns cred as hseed, nymbleTKT1, nymbleTKT2, . . . , nymbleTKTLi, where seed =

HkhkN (pnym, j, k) is the seed used within NymbleTktGen.

Alice may acquire credentials for different servers and different linkability windows at any time. She stores these credentials locally before she needs them.

Efficiency. This protocol has a timing complexity of O(L).6 All the computations are quick symmetric operations—there are two cryptographic hashes, two HMACs and one symmetric encryption per loop-iteration A credential is of size O(L).
Request for Services
At a high level, a user Alice presents to server Bob the nymble ticket for the current time period. As nymble tickets are unlinkable until servers complain against them (and thereby blacklisting the corresponding user or IP address), Alice must check whether she is on Bob's blacklist, and verify its integrity and freshness. If Alice decides to proceed, she presents her nymble ticket to Bob, and Bob verifies that the nymble ticket is not on his blacklist. Bob also retains the ticket in case he wants to later complain against the current access. For example,Wikipedia might detect a fraudulent posting several hours after it has been made. The nymble ticket associated with that request can be used to blacklist future accesses by that user.

Ticket Examination

1. The user sets ticketDisclosed in usrEntries½sid inusrState to true. She then sends hticketi to the server, where ticket is ticket½t^{now} in cred in usrEntries½sid in usrState.Note that the user discloses ticket for time period t^{now}after verifying blist's freshness for t^{now}. This procedure avoids the situation in which the user verifies the current blacklist just before a time period ends, and then presents a newer ticket for the next time period.

2. On receiving hticketi, the server reads the currenttime period and linkability window as t^{now} and^{wnow},returns false, the NM terminates with failure; it proceeds otherwise.
3.The NM runsNMCreateCredential$_{nmState}$ðpnym; sid; w_{now}Þ;which returns a credential. The NM sends cred to the user and terminates with success.
4.The user, on receiving cred, creates usrEntry:¼ðsid; cred;falseÞ.

Nymble Connection establishment

To establish a connection to a server sid, the user initiates a type-Anon channel to the server, followed by the Nymbleconnection establishment protocol described below.

5.5.1 Blacklist Validation

1. The server sends hblist; certi to the user, where blist is its blacklist for the current time period and cert is the certificate on blist. (We will describe how the server can update its blacklist soon.)
2. The user reads the current time period and linkability window as t^{now} and^{wnow} andassumes these values to be current for the rest of the protocol.
3. For freshness and integrity, the user checks if VerifyBL$_{usrState}$sid; t^{now}; wnow; blist; cert ¼ true:If not, she terminates the protocol with failure.

5.5.2 Privacy Check

Since multiple connection establishment attempts by a user to the same server within the same time period can be linkable, the user keeps track of whether she has alreadyrespectively. The server then checks that:ticket isfresh,i.e.,ticket
2slistinserver's state. ticket is valid, i.e., on input ðt^{now}; w^{now}; ticketÞ'ServerVerifyTicket returns true. Ticket is not linked ServerLinkTicket$_{svrState}$ðticketÞ ¼ false:
If any of the checks above fails, the server sendshgoodbyei to the user and terminates with failure. Otherwise, it adds ticket to slist in its state, sends hokayi to the user, and terminates with success.On receiving hokayi, the user terminates with success.
Algorithm:.ServerLinkTicketInput: ticket 2 T
Persistent state: svrState 2 S_S

Output: b 2 ftrue; falseg

1: Extract lnkng-tokens from svrState2: ð ;nymble; Þ :¼ ticket
3: for all i ¼ 1 to jlnkng-tokensj do
4: if ð ;nymbleÞ ¼ lnkng-tokens½i then
5: return true 6: return false

Conclusions

We have proposed and built a comprehensive credential system called Nymble, which can be used to add a layer of accountability to any publicly known anonymizing network. Servers can blacklist misbehaving users while maintaining their privacy, and we show how these properties can be attained in a way that is practical, efficient, and sensitive to the needs of both users and services.
We hope that our work will increase the mainstream acceptance of anonymizing networks such as Tor, which has, thus far, been completely blocked by several services because of users who abuse their anonymity.

References

1. Giuseppe Ateniese, Jan Camenisch, Marc Joye, and Gene Tsudik. A practical and provably secure coalition-resistant group signature scheme. In MihirBellare, editor, CRYPTO, volume 1880 of LNCS, pages 255–270.Springer, 2000.

2. MihirBellare, Daniele Micciancio, and BogdanWarinschi. Foundations of group signatures: Formal definitions, simplified requirements, and a construction based on general assumptions. In Eli Biham, editor, EUROCRYPT, volume 2656 of LNCS, pages 614–629. Springer, 2003.

3. MihirBellare, Haixia Shi, and Chong Zhang. Foundations of group signatures: The case of dynamic groups. In Alfred Menezes, editor, CT-RSA, volume 3376 of LNCS, pages 136–153. Springer, 2005.

4. Stefan Brands. Untraceable off-line cash in wallets with observers (extended abstract). In Douglas R. Stinson, editor, CRYPTO, volume 773 of LNCS, pages 302–318. Springer, 1993.

5. Jan Camenisch, Susan Hohenberger, MarkulfKohlweiss, Anna Lysyanskaya, and Mira Meyerovich. How to win the clonewars: efficient periodic n-times anonymous authentication. In Ari Juels, Rebecca N. Wright, and Sabrina De Capitani di Vimercati, editors, ACM Conference on Computer and Communications Security, pages 201–210. ACM, 2006.

6. Jan Camenisch, Susan Hohenberger, and Anna Lysyanskaya.Compact e-cash. In Ronald Cramer, editor, EUROCRYPT, volume 3494 of LNCS, pages 302–321. Springer, 2005.

7. Jan Camenisch and Anna Lysyanskaya. An efficient system for non-transferable anonymous credentials with optional anonymity revocation. In Birgit Pfitzmann, editor, EUROCRYPT, volume 2045 of LNCS, pages 93–118.Springer, 2001.

8. Jan Camenisch and Anna Lysyanskaya. Signature schemes and anonymous credentials from bilinear maps. In Matthew K. Franklin, editor, CRYPTO, volume 3152 of LNCS, pages 56–72. Springer, 2004.

9. David Chaum. Untraceable electronic mail, return addresses, and digital pseudonyms. Communications of the ACM, 4(2), February 1981.

10. David Chaum. Blind signatures for untraceable payments. In CRYPTO, pages 199–203, 1982.

11. David Chaum. Showing credentials without identification transfeering signatures between unconditionallyunlinkable pseudonyms. In Jennifer Seberry and Josef Pieprzyk, editors, AUSCRYPT, volume 453 of LNCS, pages 246–264. Springer, 1990.

12. David Chaum and Eug`ene van Heyst. Group signatures. In EUROCRYPT, pages 257–265, 1991.

13. Lidong Chen. Access with pseudonyms. In Ed Dawson and Jovan Dj. Golic, editors, Cryptography: Policy and Algorithms, volume 1029 of LNCS, pages 232–243.Springer, 1995
.
14. Ivan Damg°ard. Payment systems and credential mechanisms with provable security against abuse by individuals. In ShafiGoldwasser, editor, CRYPTO, volume 403 of LNCS, pages 328–335. Springer, 1988.

15. Roger Dingledine, Nick Mathewson, and Paul Syverson. Tor: The Second-Generation Onion Router. In Usenix Security Symposium, pages 303–320, August 2004.

16. John R. Douceur. The sybil attack. In Peter Druschel, M. FransKaashoek, and Antony I. T. Rowstron, editors, IPTPS, volume 2429 of LNCS, pages 251–260. Springer, 2002.
17
17. Jason E. Holt and Kent E. Seamons.Nym: Practical pseudonymity for anonymous networks. Internet Security Research Lab Technical Report 2006-4, Brigham Young University, June 2006.

18. AggelosKiayias, YiannisTsiounis, and Moti Yung.Traceable signatures. In Christian Cachin and Jan Camenisch, editors, EUROCRYPT, volume 3027 of LNCS, pages 571–589. Springer, 2004.
19. Anna Lysyanskaya, Ronald L. Rivest, AmitSahai, and Stefan Wolf. Pseudonym systems. In Howard M. Heys and Carlisle M. Adams, editors, Selected Areas in Cryptography, volume 1758 of LNCS, pages 184–199. Springer, 1999
.
20. NIST. FIPS 186-2: Digital signature standard (dss). Technical report, National Institute of Standards and Technology (NIST), 2000. http://csrc.nist.gov/publications/ fips/fips186-2/fips186-2-change1.pdf.

AUTHORS PROFILE

Prof Pradeep Kumar Puram
B.E M.Tech(Ph.D) having several
years of experience inAcademic & Industry.
Currently he is the Professor & Head of
Department Of Computer Science & Engineering At Vivekananda Institute of
Technology & Science, Karimnagar, he has guided many UG & PG students. His research areas of interest are Software Engineering, Data mining &Data Warehousing, Information Security, Web
Technologies

2. ——————|
Amer Ahmed khan pursuing M.TechCS
fromVivekananda Institute of Technology &Science, Karimnagar,. His

Research areas include Programming
In JAVA,Security, Cryptography &
Web Technologies currently focusing on Information estimation on Wireless Networks.

3. 

KiranKumar B

Assistant Professor,
Dept of CSE,
VITS Karimnagar.

He received M .Tech from JNTUH .
He has the sound knowledge in computer networks and assembly language programming ,expertised in C with real time application development.

A Technique for Importing Shapefile to Mobile Device in a Distributed System Environment.

[1]Manish Srivastava, [2]Atul Verma, [3]Kanika Gupta
[1]Academy of Business Engineering and Sciences,Ghaziabad, 201001,India
[2]Indian Institute of Information Technology Allahabad, Devghat Jhalwa ,IIITA,Allahabad, 211012, India
[3]Academy of Business Engineering and Sciences,Ghaziabad,201001, India

Abstract
Mobile GIS emerged in the 1990s, with integration of GPS is one of the leading technique. It is a Location Based Services which can be defined as any application that extends spatial information processing or GIS capabilities to end users (based on their geographic location) (ESRI 2000 & 2001d). In other words it can be used to gather information from any place, and in no time. It's where wireless and GIS technologies meet on the Web and it is changing the way businesses and individuals operate"(ESRI 2001a). The technology of mobile devices has been improving since 2000.The various improvements has resulted in developing a high promising technology by taking into account issues like

- Portability
- 'Ruggedness' and
- All-day battery life.

Presently we are designing a mobile application for importing shapefile to a mobile device which on other hand support geospatial vector data format of geographic information systems software. It was firstly developed and regulated by ESRI A "shapefile" commonly refers to a collection of files with ".shp", ".shx", ".dbf". To import a shapefile we need to use an open source software known as geoserver which helps to fetch the desired vector image.
With the help of wireless technology like Bluetooth we can import shapefile to mobile even if the shapefile is located on different system. This will help in fetching information associated within the shapefile ,thus helping to obtained important information without considering its place of storage and location. In this work we have taken MNNIT Allahabad as area of research.

Keywords: Shape file, geoserver, personnel digital assistant (pda) and wireless technology

Introduction
Mobile GIS is the expansion of GIS technology from the office into the field. A mobile GIS enables field-based personnel to capture, store, update, manipulate, analyze, and display geographic information. Mobile GIS integrates one or more of the following technologies:
Mobile Devices,

- Global Positioning Systems, and
- Wireless Communications for Internet GIS access
- GIS applications are software applications that process large amounts of geospatial data, involving heavy computations. Traditionally, these applications have resided on high performance workstations and servers equipped with the necessary resources: large amounts of primary and secondary memory, fast CPUs and graphics processors, and large screens for displaying the data. The recent decade, however, has seen a move of GIS applications onto smaller platforms, including mobile platforms such as personal digital assistants (PDAs). These platforms offer a number of attractive features, primary among which are their extreme mobility: because of its small size, a PDA can be carried and used practically anywhere[1].

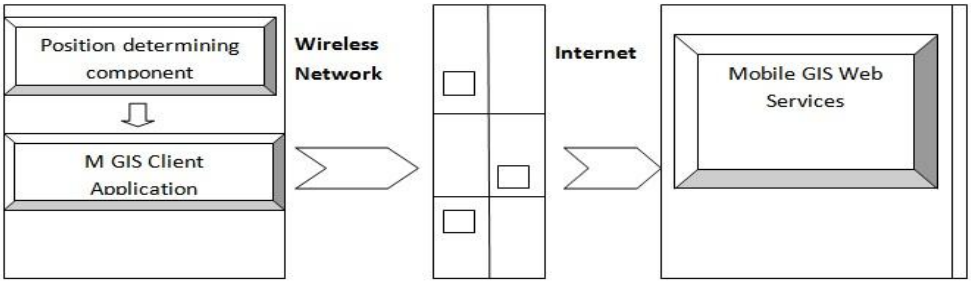

Figure 1: Overall Architecture of Mobile GIS (Ali Monsourian *et.al* 2008)

M-GIS Components

A Mobile Geographic Information System (M-GIS) project consists of several components which represent individual technological fields conceptual to the architectural design of the project (Sarjakoski & Lehto 2003). Client components consist of all the physical mobile devices that are compatible with the front-end requirements of an M-GIS application; in other words, they are the mobile devices that the application can run on. The communication technologies and infrastructure components ("middleware") allow for the transmission of requests and responses between the client and server components. The server components are all the hardware and software involved in serving the client-side of the M-GIS project on the web server and the map server.

Importing Shapefile in Mobile

Basic Aspect of Shapefile

The ESRI Shape file or simply a shape file is a popular geospatial vector data format for geographic information systems software. It is developed and regulated by ESRI as a (mostly) open specification for data interoperability among ESRI and other software products. A "shape file" commonly refers to a collection of files with ".shp", ".shx", ".dbf"[2].

The Shape file Format

ESRI (Environmental Systems Research Institute) is a leading developer of GIS software and the Shape file format used by their products is one of the most popular mediums for storing vector map data. An ESRI shape file is actually composed of three separate files: a main file with a .SHP extension, an index file with a .SHX extension, and a dBase file with a .DBF extension that contains the associated attribute data. The three files must have the same base name and follow 8.3 naming conventions as shown in the figure below

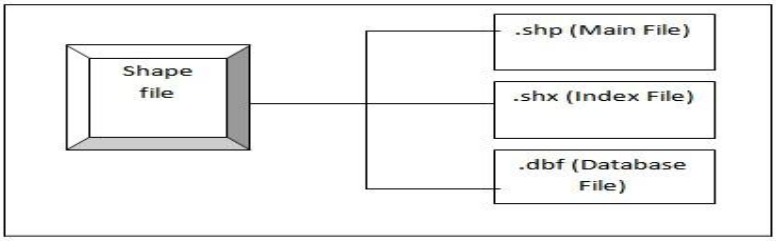

Figure 2: Component of Shape file.

The main file (with a .SHP extension) is the primary component and its structure begins with a fixed-length, 100-byte header containing information about the total length of the file, the file version, and the type of shapes it contains. This file header is then followed by a list of variable-length records, with each record defining the geometry for a single ESRI shape[3]. An ESRI shape might be a polygon that represents the political boundary of a country, a polyline that represents the path of a city street, or a point object that indicates the location of a city. The figure below illustrates the format of a .SHP file. It contain record file, header file with a header name constituting 100 byte. The other supporting file which are required are to collect information about File number, File version, File code, File length and Shape type. We use class ShapeFileHeader to read the content of the shape file which usually contain the address of 100 byte header file.

Reading Database Attributes

The dBase file associated with a shape file contains the attribute data and essentially represents a single database table. There is a one-to-one correspondence between the rows in this table and the shape records in the .SHP file. A typical attribute field that you may find in a dBase table is a field that identifies the name of the corresponding shape (such as a state or province name).

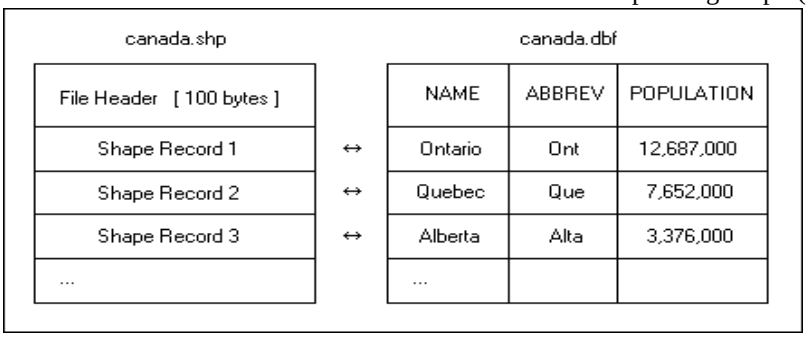

Figure 3: Mapping between shape file and data base file

Methodology

The methodology adopted for the present work has been shown with the help of a flow diagram in Figure.

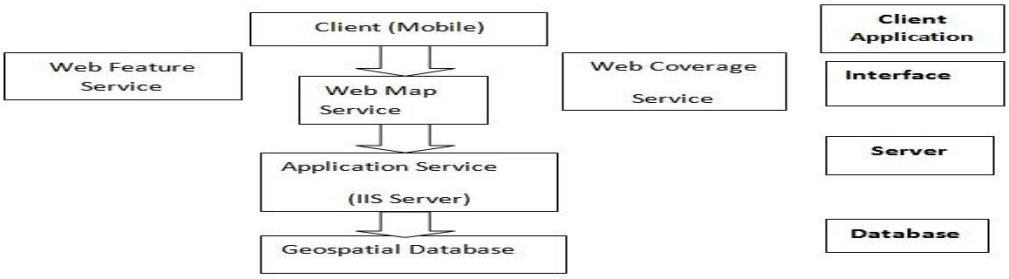

Figure 4: Designing Mobile Web Services

Detailed Planning

The methodology adopted for the thesis work is based on the following factors:

- Availability of the maps of MNNIT Allahabad with respect to the different functionality to be analyzed for the establishment of a mapping application.
- Preparation of the mapping application for the purpose of designing the required functionality.
- Preparing Shape file using ARC GIS. The different layer that are prepared using this software are

a. Road Layer,
b. Railway Layer, and
c. Mnnit Poly Layer.

- Developing a Mobile Device Application and,
- Deploying the overall application on the client side that is on Mobile.

The approach is defined by the above flowchart in section. This flowchart indicates the process of work been carried out. Basis for the work comprises of the literature review which is done to develop a methodology. This literature review helps to find out the objectives of the work and further far. The Web Feature Service defines interface for describing data manipulation operations of geographic features. Data Manipulation operations include the ability to

- Query feature based on spatial and non spatial constraints.
- Create a new feature instance.
- Delete a new feature instance.
- Update a new feature instance.

A Web Map Service (WMS) is a standard protocol for serving georeferenced map images over the Internet that are generated by a map server using data from a GIS database WMS specifies a number of different request types, two of which are required by any WMS server:

After identifying the prime objectives the next was to carry out the detail analysis of the work to be carried out. The individual parameters are identified.

Prepration Of Geo Spatial Database

The following aspect has been considered for the design of the Geospatial databases for the present work: Firstly, the map for MNNIT campus is scanned. Then, this has been used as the base map and its coordinate system has been adopted for integrating other maps with this map. The image to image registration has been carried out to geo reference institute map. From this scanned map, digitization of the institute campus, hostels and staff colony were carried out.After the completion of registration, the on screen digitization process was followed for creation of various thematic layers. This is an important part of project as different layers can then be derived as per the requirement of the study. This will help in populating the database of the project. The various layers prepared in the present work are:-

Institute Campus Block,
Staff Colony Block,
Hostel Block, and

Road Map.

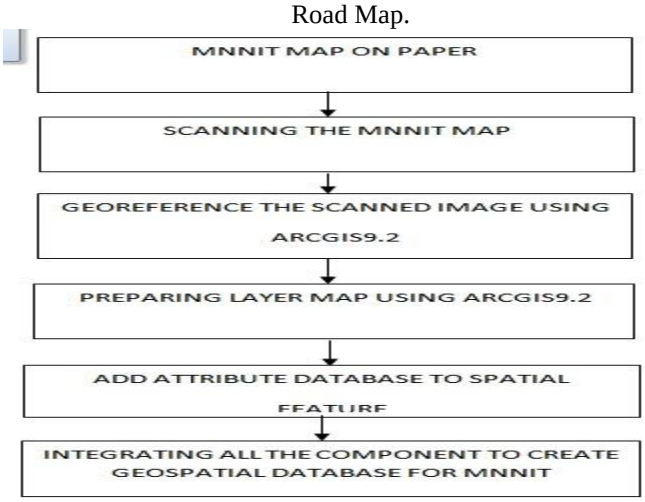

Figure 5 : Creation of Geospatial Database

Integrating Geospatial and Mobile Gis

The application runs on the user mobile phone and gets the required data from a database server on the wireless toolkit. In this case, we keep the data that is the shape file on one computer (172.31.100.62). The application resides on the second computer and we use Wireless Connection to access the data that resides on first computer.

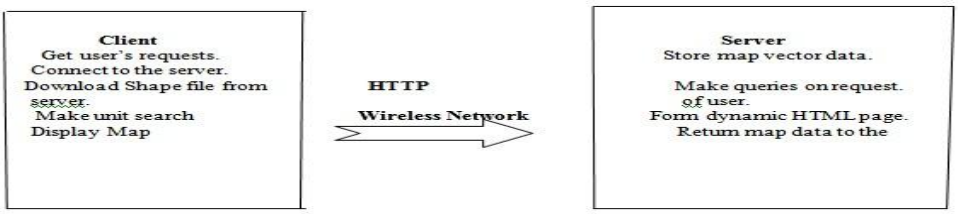

Figure 6: Client Server Functions

Hyper Text Transfer Protocol (HTTP) is assumed to be as the underlying protocol for communication between the client and the server. The graphical user interface of the client contains a canvas for displaying the map. We have used the vector data format in this application because vector graphics are better than bitmap images for querying, manipulating the data. The WAP Gateway can optimize the communication process and may offer mobile service enhancements, such as location, privacy, and presence based services. The WAP Gateway communicates with the client (WAP micro browser) using the WAP protocols and it communicates with the Web Server using the standard Internet protocols such as HTTP/HTTPS.

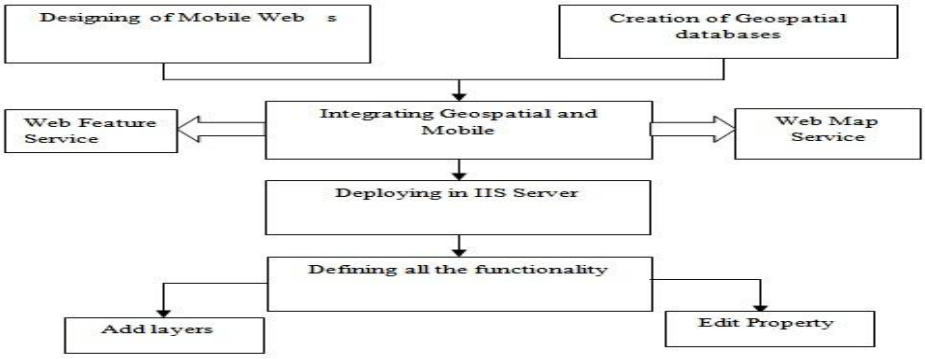

Figure 7: The Overall Methodology adopted in this study.

RESULT

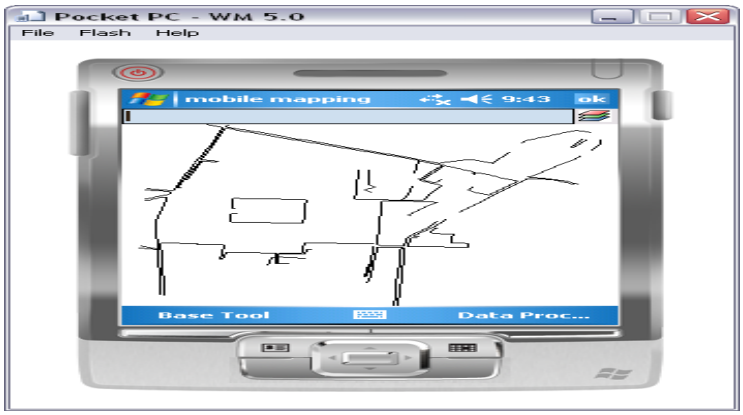

Figure 8: Road Layer: MNNIT

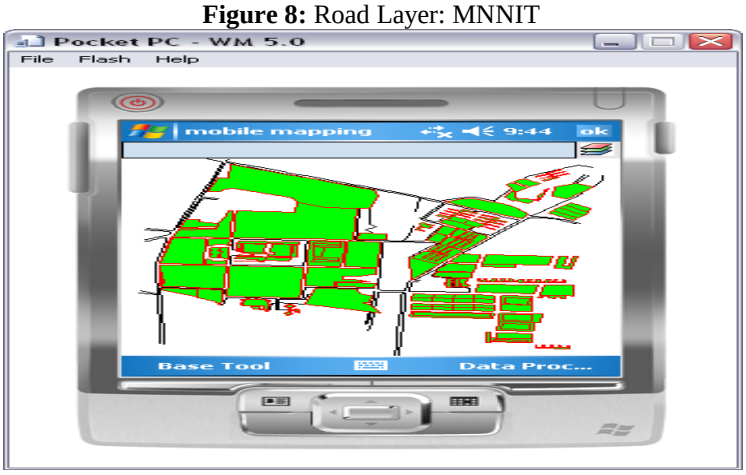

Figure 9: MNNIT POLY NETWORK

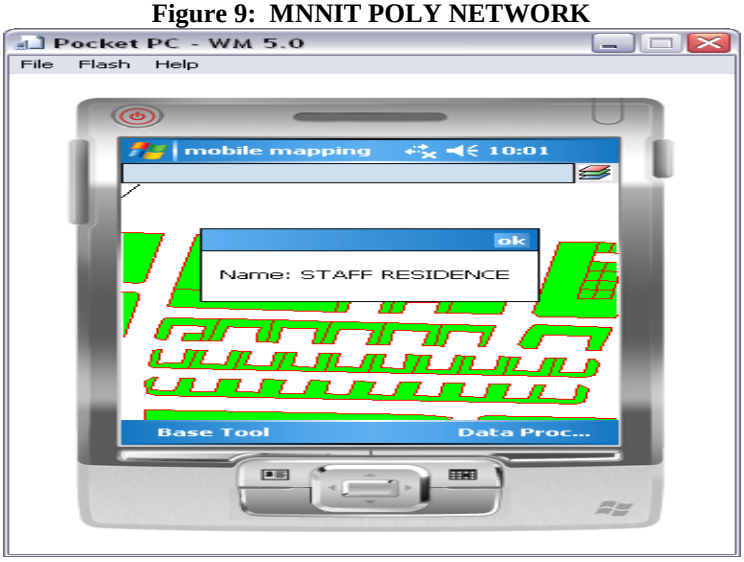

Figure 10: Deriving Information

Conclusion Drawn

Maps or Shape file have a definite role to play in a Mobile GIS environment. In their interactive and dynamic appearance they will guide and assist the user in solving geospatial analysis problems. This can be proved with the help of this work that with the increased availability of mobile devices, proper software and abundant data, maps can play these various roles anywhere and at any time. It uses wireless network and communication network and communication protocol by getting the mapping data from the server and displays shape file on the phone along with many functionality.

In traditional GIS, spatial object were primary focus while in Mobile GIS, the focus has been changed to a particular scene or of a particular location

Future Recommendations

The future recommendation for this work can be in implementing:

- A dynamic Database Application for Mobile GIS.
- It may take a long time to establish a connection between a client and the server on a wireless network. So, the latency time should kept minimum.

References

[1] Maruto Masserie Sardadi, "Quadtree Spatial Indexing Use to Make Faster Showing Geographical Map in Mobile Geographical Information System Technology Using an Oracle 10g Application Server and Map Viewer Applications,", IJCSNS International Journal of Computer Science and Network Security, 2008.

[2] E.Poorazizi, "Developing a Mobile GIS for Field Geospatial data Acquisition,". A.A.Alesheikh and S.Behzadi, Ed. Asian Network for Scientific Information: Journal of Applied Sciences, 2008.

[3] E. Mensah, "Designing a Prototype Mobile GIS to Support Cadastral Data Collection in Ghana," 2007.

[4] A. Vckovski, "Interoperability and spacial information theory. Interoperating Geographic Information Systems." 1999.

[5] M. J. Kraak,"Current trends in visualization of geographic data with special reference to cartography. Invited paper: In Proceedings of the XXIIth INCA Congress Indian National Cartographic Association:" *Convergence of Imagery Information and Maps*, vol. 22, pp. 319-324, 2002.

Experimental Evaluation of Mechanical Properties of 3d Carbon Fiber/Sic Composites Prepared By LSI

Dr. S. Khadar Vali[1*] Dr. P. Ravinder Reddy[2] Dr. P. Ram Reddy[3]

1. Professor and Head, MED, M. J. College of Engineering and Technology, Banjara Hills, Hyderabad, India.
2. Professor and Head, MED, Chaitanya Bharati Institute of Technology, Hyderabad, India.
3. Former Registrar, JNTU Hyderabad, Presently Director, Malla Reddy Institute of Engg. & Technology, Hyderabad, India

Abstract

The structural engineer needs to be familiar with the property of the composite material structures. The behavior of ceramic composite material under impact load plays a pivotal role in designing such structures. An impact test is a test for determining the energy absorbed in fracturing a test piece at high velocity. The impact resistance of a part is, in many applications, a critical measure of service life. In the current work, an attempt is made to present the dynamic behavior of the advanced ceramic composite material, i.e., 3 Dimensional Carbon-Silicon Carbide (3D C-SiC) under the impact, tensile and flexure loads and the mechanical properties, viz., Impact Strength, Tensile Strength and Flexural Strength are determined. 3D C-SiC composite specimens with a fiber volume fraction of 40% are prepared by Liquid Silicon Infiltration (LSI) process to conduct the required experiments for evaluating the mechanical properties. The experimental results of impact, tensile, flexure and shear strengths recorded during the tests are 26.82 kJ/m^2, 70.2 MPa, 230.3 MPa and 30.5 MPa respectively.

Keywords: Carbon Silicon Carbide (C-SiC), Impact strength, Liquid Silicon Infiltration (LSI)

1. Introduction

The minimum knowledge required about a material to characterize fracture properties comes from a force-time (or force-displacement) diagram. When performing a test with an instrumented falling weight, it is possible to record the force acting on the specimen throughout the impact. Silicon carbide matrix based composites exhibit promising mechanical properties at high temperatures and offer very good oxidation and thermal shock resistance. They are finding increasing applications in aerospace, defense and industries. Carbon fiber-reinforced SiC matrix composites are preferred to C-C composites for oxidizing and highly erosive environment. C-SiC composites are used up to 1500^0 C for long durations and up to 2000^{0}C for short durations. The mechanical properties of the fiber-reinforced composites can be tailored by adjusting fiber volume fraction and fiber orientation to meet the needs of the application. C-SiC composites retain mechanical strength up to 1700^{0}C. There are several methods to fabricate C-SiC composites, such as chemical vapor infiltration (CVI), slurry infiltration combined with hot pressing, polymer-infiltration-pyrolysis (PIP), etc. Among these methods, Liquid Silicon Infiltration (LSI) process offers many potential advantages such as single step process, low processing temperature, and near-net-shape processing. Continuous fiber reinforced ceramic matrix composites (CFCCs) are very interesting structural materials because of their higher performance and higher fracture toughness. For this reason, CFCCs are considered as the most potential to be used in advanced aero engines. Among the CFCCs, carbon fiber reinforced silicon carbide matrix composites (C-SiC) are most promising and have been receiving considerable interest. Many investigations have been conducted on two dimensional woven C-SiC composite materials. Recently, attention has been focused on three dimensional woven or braided ceramic matrix composite materials in order to meet mechanical property requirements along the thickness of the composites.

2. The LSI Process

The LSI (Liquid Silicon Infiltration) process consists of 3 stages. Beginning with a carbon fiber reinforced ceramic (CFRC) made of a coal tar pitch with high carbon content, a green-body preform is manufactured. This preform is then pyrolised under inert atmosphere at temperatures greater than 900^{0}C, converting the CFRC into a higher porous carbon-carbon (C-C) composite. In a final step, the porous material is infiltrated with liquid silicon under vacuum to manufacture the final C-SiC ceramic. The quality of the C-SiC materials is influenced by each individual processing stage.

3. Experimental Investigations

3D stitched preform is the simplest case of the 3D composites development; several layers of 8 H satin carbon fabric layers are stitched together with 6000 Carbon fibers to impart third direction reinforcement (Fig.1). The fiber volume fraction is worked out, taking into consideration the infiltration abilities of molten silicon vis-à-vis the thermo mechanical properties.

Fig. 1 The fixture of carbon fiber perform

4. Specimen Preparation And Test Methods

The instrument used to perform impact test is quite similar to drop weight machines. It is usually equipped with a piezoelectric or strain gauge load cell. The standard specimens are prepared with composition shown in Table 1.

Table 1 Composition of Carbon Silicon Carbide (C-SiC)

After preparing the C-SiC

S. No.	Constituents	Percentage (% Vol.)
1.	Carbon (Fibre)	40%
2	SiC	45%
3	Si	10%
4	C	5%

specimens as per the required composition, they are cut into required sizes according to ASTM D256 standards (Fig. 2). The Izod impact tests are conducted using Fractovis drop weight instrumented impact tester acquired with a DAS 8000 WIN data acquisition system as shown in Fig. 3.

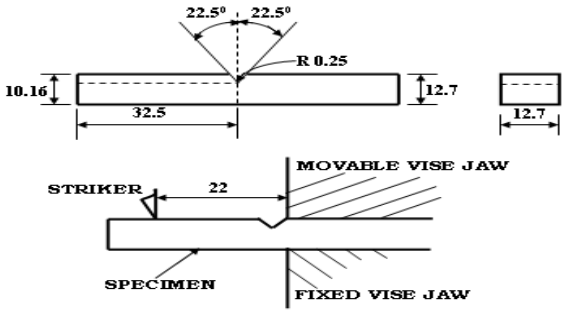

Fig. 2 Izod Test specimen geometry according to ASTM D 256 standards

(a) (b)

Fig. 3 Two Views of the Fractovis Instrumented Impact Tester

5.1 Measurement of Mechanical Properties- Impact Test

Mechanical properties of the C-SiC composite materials are characterized under impact loading to get the reliable design properties at room temperature. Instrumented impact tests on notched Izod samples are conducted as per ASTM D 256 standards to determine the energy absorbing capability and dynamic fracture behavior of the composite materials. The sample sizes are 10.16 x 12.7 x 32.5 mm and the impact velocity of 3 m/s is chosen. The dynamic fracture toughness (α_k) is calculated using equation:

$$\alpha_k = \Delta W / bh$$

where ΔW is the absorbing energy of materials during impact processing, b and h are thickness and width of specimen respectively.

5.2 Flexural Test

This test method covers the determination of flexural properties of continuous fiber reinforced ceramic composites in the form of rectangular bars formed directly or cut from sheets, plates or molded shapes. According to ASTM C1341 standards, a three point loading system utilizing centre loading on a simply supported beam is chosen. The specimen geometry is shown in Fig. 4. The siliconised 3D C-SiC composite specimens shown in Fig. 5 are cut into sizes 6mm x15mm x100mm with support span length of 100mm along principal material direction and tested for three point bend test at room temperature to get flexural strengths.

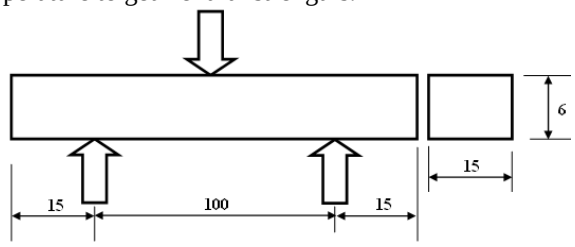

Fig.4 Specimen geometry for flexural test as per ASTM C1341 standards

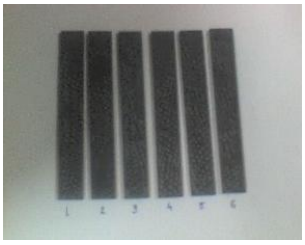

Fig.5 Specimens for Flexural and Shear tests

This test method applies primarily to all advanced ceramic matrix composites with continuous fiber reinforcement: one dimensional (1D), two dimensional (2D), and three dimensional (3D) continuous fiber architectures. In addition, this test method may also be used with glass matrix composites with continuous fiber reinforcement. However, flexural strength can not be determined for those materials that do not break or fail by tension or compression in the outer fibers. Test can be performed at ambient temperatures or at elevated temperatures. At elevated temperatures, a suitable furnace is necessary for heating and holding the specimens at the desired testing temperatures. In this test method, the flexural stress is computed from elastic beam theory with the simplifying assumptions that the material is homogenous and linearly elastic. This is valid for composites where the principal fiber direction is coincident or transverse with the axis of the beam. These assumptions are necessary to calculate a flexural strength value, but limit the application to comparative type testing such as used for material development, quality control and flexure specifications. Such comparative testing requires consistent and standardized test conditions, i.e., specimen geometry (thickness), strain rates, atmospheric test conditions. Flexure tests provide information on the strength and deformation of materials under complex flexural stress conditions. The geometry of the specimen must be chosen so that shear stresses are kept low relative to tension and compression stresses. This is done by maintaining a high ratio between the support span (L) and the thickness or depth (d) of the specimen. This L/d ratio is generally kept at the values of grater than or equal to 16 for 3- point flexure testing following the ASTM C1341 standards. If the span to depth ratio is too low, the specimen may fail in shear. The flexural specimens are tested in a properly calibrated universal testing machine (UTM) shown in Fig. 6 that can be operated at the constant rates of cross head motion over the range required. The system is equipped with a means for retaining the readout of the maximum load as well as the record of load verses deformation.

Fig. 6 Universal Testing Machine (UTM) to conduct Tensile, Flexure and Shear tests

The outer loading span and the desired test geometry determine the dimensions and geometry of the loading fixture. The fixture geometry, i.e., 3- point is selected. The thickness of the specimen to be tested determines the critical out span dimension of the loading fixture. The over all dimension of the specimen and required loading span are selected based on the specimen thickness, the desired test geometry, and the required span to depth ratio following ASTM C1341 standards. An autographic record of the applied load and the centre point deflection is obtained for the specified cross head rate. Either analog chart recorders or digital data acquisition systems may be used for this purpose, although a digital record is recommended for ease of subsequent data analysis. Ideally an analog chart recorder or plotter should be used in conjunction with digital data acquisition system to provide an immediate record of the test as a supplement to the digital record. Specimen width shall not exceed ¼*th* of the support span for specimens greater than 3mm in depth. The specimen shall be long enough to allow for overhang passed the outer supports of at least 5% of the support span, but in no case, less then 5mm on each end. Overhang shall be sufficient to minimize shear failures in the specimen ends and to prevent the specimen from the slipping through the supports at large centre point deflections. The test temperature is determined and recorded. The data acquisition is initiated and the load application is started. The test is continued until

the specimen breaks into two pieces. The maximum load is recorded. After completing the test, the action of the test machine and the data acquisition system is disabled. In addition to the location, carefully the mode of the fracture initiation and crack extension is noted. Fracture may initiate on the tensile (lower) face, on the compression (upper) face of the bar or by shear failure. The bar may fail by a sequential combination of modes. The tensile fracture crack may extend towards the neutral axis directly or may be deflected along low strength planes such as inter laminar regions.

Flexural Stress (σ):

When tested in flexure, a simple beam experiences maximum tensile stresses in the outer fibers and maximum compressive stresses in the inner fibers. The location of the maximum stress along the length of the beam is at the centre point for 3- point testing. Equation for calculating the flexural stress for the 3-point test is give as: Flexure Stress, $\sigma = 3PL/2bd^2$

Where, P = Load at given point in the test (N)
L = Support span (mm)
b = Specimen width (mm)
d = Specimen depth or thickness (mm)

Flexural Strength (σ_f):

The flexural strength is equal to the maximum stress in the outer fibers at the point of maximum load. It is calculated using the equation:

Flexural Strength, $\sigma_f = 3P_UL/ 2bd^2$

Where, P_U = Maximum load in flexural test (N)
L = Support span (mm)
b = Specimen width (mm)
d = Specimen depth or thickness (mm)

5. 3 SHEAR TEST

Shear strength of 3D C-SiC composites is measured by conducting a three point bend test in the same UTM. The shear strength is calculated by the following equation.

$\square = 3P/4bh$

Where P is the fracture load (N), b and h are width and thickness of the specimen respectively.

5. 4 TENSILE TEST

The test specimens cut into sizes 3mm x 6mm x 100mm length according to ASTM C 1275 standards (Fig. 7) are shown in Fig. 8. They are fixed in the universal testing machine (UTM) to conduct tensile test by choosing the tensile fixture and properly adjusting the movable jaw so as to keep the gauge length of 25mm. The tensile load (P) is gradually applied along principal material direction. When the applied load reaches ultimate value, the specimen breaks catastrophically and the load falls to zero.

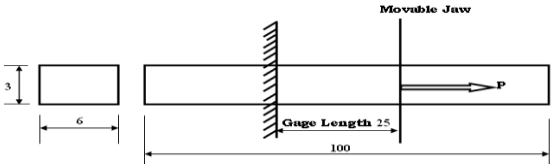

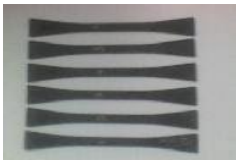

Fig. 7 Tensile test specimen geometry as per ASTM C1275 standards Fig.8 Tensile test specimens

The equation for calculating longitudinal strength in tension is expressed as:

$\sigma_t = P_U/A$

where P_U = Ultimate load (kN)

A = Area of cross-section perpendicular to the direction of applied load

6. Results And Discussions

A typical Force-deformation curve recorded in the impact test is shown in Fig. 9. The test data for 7 sample specimens out of total 31 specimens tested is also shown in Table 2. First of all, when the striker touches the specimen the impact point is immediately accelerated from zero velocity to the initial velocity of the striker. This instantaneous acceleration, for the Newton's second law, causes a first peak of force named inertial peak (because of the inertial nature of this phenomenon). After this, strong oscillation force increases linearly. At low displacements, in fact any material can be considered elastic so that force is proportional to displacement (and therefore to time, if impact energy is high). When the specimen is affected by a great deflection, however, plastic deformation occurs: the load deformation curve deviates from linearity showing the characteristic yield region. Since the materiel chosen for test is C-SiC which is very hard and brittle, there is no noticeable yield region. When the material approaches its maximum deflection, fracture occurs and the measured force falls to zero. From the load displacement curve the evaluation is made on fracture toughness, i.e., the energy absorbed by the specimen during the fracture. The absorbed energy is a measure of material strength and the

ductility can be graphically represented as the area beneath the load-displacement curve. Further the impact strength is obtained by calculating the energy absorbed during fracture per unit cross sectional area of the specimen. The experimental values of fracture toughness and impact strength obtained during impact testing of the specimens with corresponding measured fiber volume fractions is given in Table 3. Fig. 10 and Fig. 11 clearly indicate the increase in fracture toughness and impact strength with the increase of fiber volume fraction in 3D C-SiC specimens. In the specimens tested, a considerable fiber pullout is observed (Fig. 12) indicating the increase of fracture toughness. It is obvious that 3D C-SiC composite materials exhibit an excellent impact damage tolerance because of Z-direction fibers. The measured properties of 3D C – SiC composites are compared with the properties of 2D C-SiC (available from literature) fabricated by different routes as shown in Table 4. The experimental results of impact strength of various specimens with 40 % fiber volume fraction are shown in Table 5. The flexural strengths calculated and maximum load recorded in the test for various specimens having fiber volume fractions 40 % is given in the Table 6. The broken specimen after conducting flexural test (Fig.13) shows lot of fibers being pulled out. This may be the reason for increase in flexural strength. The tensile strengths calculated for the ultimate loads recorded in the test for various specimens having fiber volume fraction of 40 % is shown in Table 7. Fig.14 shows the broken specimen after conducting tensile test. More or less a brittle failure can be observed from this figure which may be attributed to the fact of less tensile strength. The load deflection curves obtained in 3- point bend test for the specimens is shown in Fig.15. The load deformation curves obtained in the tensile test for the specimens are shown in Fig.16.The experimental results of shear strength is shown in Table 8.

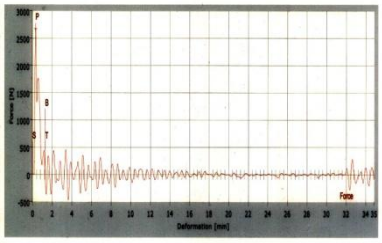

Fig. 9 Force-Deformation curves obtained in impact test up to failure

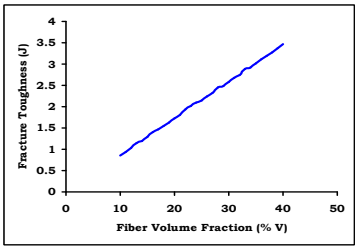

Fig.10 Fracture Toughness Vs Fiber VolumeFraction

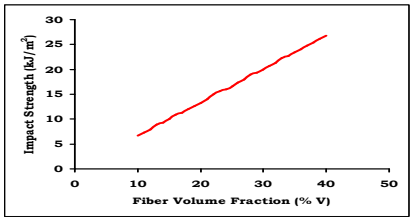

Fig. 11 Variation of Impact strength with fiber volume fraction

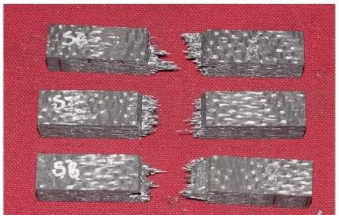

Fig.12 Fiber pull out in impact test

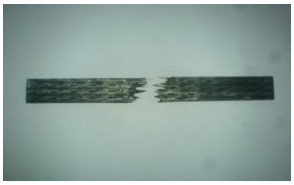

Fig. 13 Broken specimens in Flexural Test

Fig. 14 Broken specimen in Tensile Test

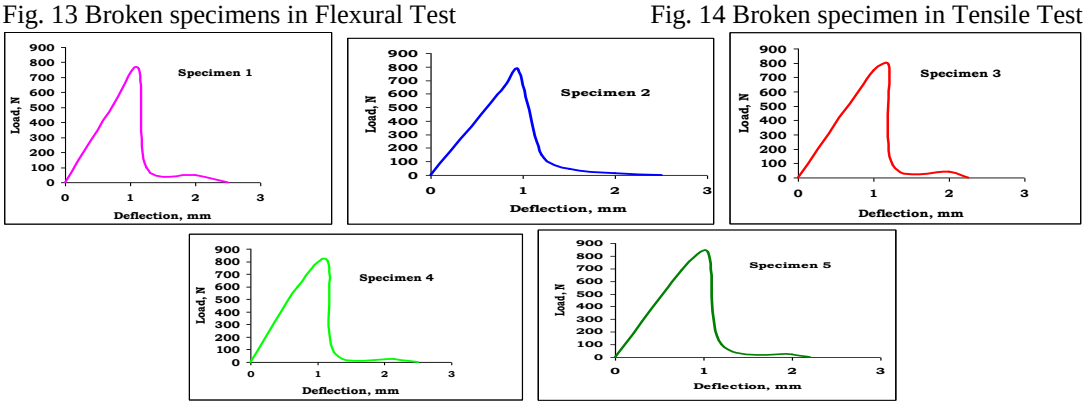

Fig.15 Load-Deflection curves of specimens obtained in Flexural Test

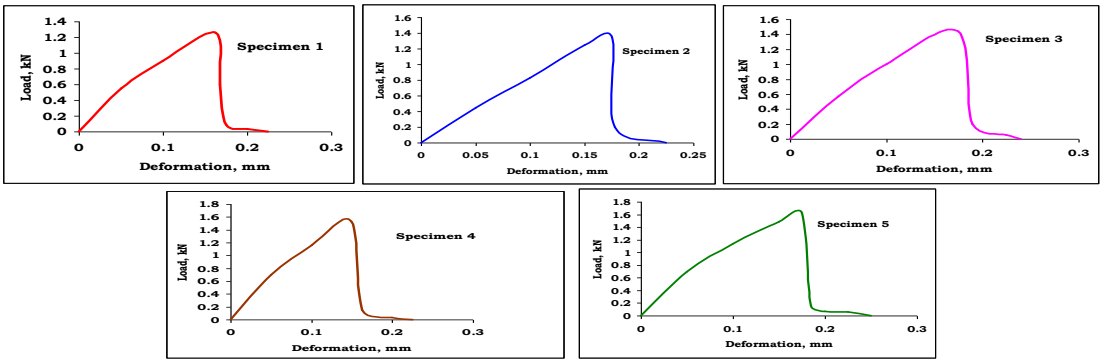

Fig. 16 Load-Deformation curves of specimens obtained in Tensile Test

Table 2 Impact Test Data of 3D C – SiC specimens

	Sample data for Specimen No. 4			Sample data for Specimen No.7			Sample data for Specimen No.13			Sample data for Specimen No.14			Sample data for Specimen No.19			Sample data for Specimen No.24			Sample data for Specimen No.31		
	Start	Peak	Total	Start	Peak	Total	Start	Peak	Total	Start	Peak	Total	Start	Peak	Total	Start	Peak	Total	Start	Peak	Total
Deformation, d (mm)	0.00	0.31	1.27	0.00	0.38	1.53	0.00	0.59	2.19	0.00	0.64	2.24	0.00	0.76	2.78	0.00	0.88	3.27	0.00	1.09	3.95
Velocity, v (m/s)	3.49	3.48	3.44	3.49	3.47	3.43	3.46	3.43	3.37	3.42	3.39	3.33	3.43	3.37	3.31	3.42	3.39	3.26	3.42	3.27	3.16
Fracture Toughness (J)	0.00	0.22	1.15	0.00	0.27	1.41	0.00	0.37	1.93	0.00	0.38	2.02	0.00	0.47	2.45	0.00	0.56	2.88	0.00	0.67	3.46
Force (N)	0.00	2683.51	0.00	0.00	2541.93	0.81	0.00	2370.06	0.00	0.00	2352.44	0.00	0.00	2224.96	0.55	0.00	2134.83	0.68	0.00	1832.25	0.55

Table 3 Variation of Fracture Toughness and Impact Strength with Fiber Volume Fraction of 3D C-SiC specimens

Impact Strength (kJ/m²)	6 65	7 31	7 97	8 91	9 30	9 99	10 93	11 31	11 99	12 65	13 29	13 96	14 96	15 65	15 95	16 65	17 32	17 98	18 99	19 32	19 98	20 65	21 31	22 32	22 64	23 40	24 10	24 80	25 42	26 11	26 82
Specimen No.	1	2	3	4	5	6	7	8	9	10	11	12	13	14	15	16	17	18	19	20	21	22	23	24	25	26	27	28	29	30	31
Fiber Volume Fraction (% V)	10	11	12	13	14	15	16	17	18	19	20	21	22	23	24	25	26	27	28	29	30	31	32	33	34	35	36	37	38	39	40
Fracture Toughness (J)	0 86	0 94	1 03	1 15	1 20	1 29	1 41	1 46	1 55	1 63	1 72	1 80	1 93	2 02	2 10	2 15	2 24	2 32	2 45	2 49	2 58	2 67	2 75	2 88	2 92	3 02	3 11	3 20	3 28	3 37	3 46

Table 4 Comparison of mechanical properties of 2D C–SiC composites (from literature) with experimental results of 3D C-SiC specimens

Properties	Literature Values		Experimental results of present work
	Unit	2D C – SiC (LSI)	3D C – SiC (LSI)
Fiber Volume	Vol. %	40 –42	40
Density	g/cc	2.4	2.2 – 2.4
Flexural Strength	MPa	180 – 200	210 – 230
Tensile Strength	MPa	80 – 90	70 – 90
Young's Modulus	GPa	25 – 30	32 – 35

Strain to failure	%	0.25 – 0.35	0.20 – 0.28
Impact strength	kJ / m^2	20 – 21	26 – 27

Table 5 Experimental results of impact strength of specimens with 40 % Fiber Volume Fraction

Specimen No.	Fracture toughness (J)	Impact strength (kJ/m^2) From Experiment
1	3.39	26.27
2	3.40	26.35
3	3.42	26.50
4	3.46	26.82
5	3.48	26.98

Table 6 Experimental results of flexural strengths of 3D C-SiC specimens

Specimen No.	Max. load (P_U) recorded during flexural test (N)	Flexural strength, σ_f (MPa) From Experiment
1	757	210.2
2	780	216.6
3	789	219.2
4	805	223.6
5	829	230.3

Table 7 Experimental results of tensile strengths of 3D C-SiC specimens

Specimen No.	Max. load (P_U) during tensile test (kN)	Tensile strength, σ_t (MPa) From Experiment
1	1.264	70.2
2	1.346	74.8
3	1.437	79.8
4	1.525	84.7
5	1.619	89.9

Table 8 Experimental results of Shear Strengths of 3D C-SiC specimens

Specimen No.	Fracture load (P) in shear test (kN)	Shear strength, τ (MPa)
1	3.38	28.16
2	3.64	30.33
3	3.55	29.58
4	3.66	30.50
5	3.52	29.33

The stress transfer capability of the interface between the fiber and matrix governs the mechanical properties of fiber reinforced composite materials. The interfacial compatibility is related to the interfacial shear stress, which characterizes the combination of stress necessary to de-bond the interface and the frictional forces developed at the interface. The 3D carbon preform is infiltrated by liquid silicon and the density obtained is 2.2–2.4 g cm^{-3}. The non-linear failure behavior is observed in the present composite material and it could also be observed that the failure of three dimensional C-SiC composite material occurred in a controlled manner. The average result of flexural strength is observed to be 220 MPa. The variation of failure behavior of composites is caused by alteration of the interfacial bonding between fiber and matrix. The tensile stress within the interfacial phase along the fiber radial direction is generated after the composite material is cooled down from the infiltration temperature to room temperature. It is easy for the carbon fiber to debond and be pulled out from the silicon carbide matrix. Above infiltration temperatures, the stresses at the interface become compressive which may lead to strong bond in between the constituents of the composite. Moreover, tensile stresses are developed in carbon fiber. Hence, the fiber is broken in the matrix. With the result, the composite material showed catastrophic fracture behavior as it is difficult to pull out the fiber from the matrix. Further the composite materials exhibited a non-linear fracture behavior at 1600^0C, because of creep in silicon carbide matrix. It is understood that the micro cracks contribute to the non-linear fracture mode of the composites by deflecting the crack growth. The interfacial bond in between the constituents of the composites depends on the properties of

interfacial phase and temperatures. The average value of shear strength obtained (Table 8) is 30 MPa. In the composites studied, no layer de-bonding is noticed. The average flexural strength obtained is observed to be 220 MPa. It gives an average work of fracture 26.58 kJ/m^2 for the 3D C-SiC specimens with 40% fiber volume fraction. It is observed that this value is four times that of two dimensional laminated ceramic materials. Also it is higher than that of laminated SiC composite (4.625 kJ/m^2) and much larger than monolithic ceramic material (Silicon Nitride, 80 J/m^2).

7. Conclusions

In the present work 3D C–SiC composites are prepared by LSI process using stitched preforms. The process for the fabrication of specimens is established with coal tar pitch impregnation into 3D carbon fiber preforms. The important conclusions drawn from the present work are:

1. The SEM micrographs reveal the uniformity of siliconisation and relatively less amount of un reacted silicon and carbon in the final composites.
2. It is also observed that the concentration of silicon in the composites is more at grain boundaries and at fiber bundles. This is because of slow diffusion of silicon into C-SiC in grains and relatively low availability of carbon in the fiber bundles compared to matrix bulk.
3. The mechanical properties of 3D C–SiC composites are determined experimentally. When fiber volume fraction is increased, fracture toughness and impact strength are increased correspondingly, which is proved by the experimental results obtained by conducting impact test as shown in Table 3.
4. The impact curve gives a lot of information about material properties. It also gives the information about the kind of fracture (brittle or nearly ductile) which is depicted graphically. The instrumented impact provides a better characterization of the material.
5. The experimental value of impact strength obtained for the sample Specimen No.4 with 40 % fiber volume fraction is 26.82 kJ/m^2 .
6. The maximum flexural strength obtained for the sample Specimen No.5 by conducting flexural test is 230.3 MPa.
7. The maximum shear stress from the experiment is observed to be 30.5 MPa.
8. The tensile strength obtained for the sample Specimen No.1 from the experiment is observed to be 70.2 MPa.

References

[1] R. Naslain, Ceramic Matrix Composites, Chapman & Hall, London, 1992, 199-243.

[2] T.M. Besmann, B.W. Sheldon, R.A. Lowden, Vapor-Phase Fabrication and Properties of Continuous-Filament Ceramic Composites, Science, 253, 1991, 1104-1109.

[3] T. Ishikawa, S. Kajii, K. Matsanaga, T. Hogani, Y. Kohtoku, T. Nagasawa, A Tough, Thermally Conductive Silicon Carbide Composite with High Strength up to 1600°C in Air, Science, 282,1998, 1295–1297.

[4] K.M. Prewo, Fiber-Reinforced Ceramics: New Opportunities for Composite Materials, American Ceramic Society Bulletin, 68, 1989, 395-400.

[5] M. Wang, C. Laird, Damage and fracture of a crosswoven C/SiC composite subject to compression loading, Journal of Material Science, 31, 1996, 2065-2069.

[6] J.J. Brenann, Interfacial studies of chemical-vapor-infiltrated ceramic matrix composites, Material Science & Engineering A, 126, 1990, 203-223

[7] D. Singh, J.P. Singh, M.J. Wheeler, Mechanical Behavior of SiC(f)/SiC Composites and Correlation to in situ Fiber Strength at Room and Elevated Temperatures, Journal of the American Ceramic Society, 79, 1996, 591-596.

[8] S. Prouhet, G. Camus, C. Labrugee, A. Guette, Mechanical Characterization of Si–C(O) Fiber/SiC (CVI) Matrix Composites witrTa BN–Interphase, Journal of the American Ceramic Society, 77, 1994, 649-656.

[9] F.K KO, Preform Fibre Architecture for Ceramic-Matrix Composites, American Ceramic Society Bulletin, 68, 1989, 401-414.

[10] P. Pluvinage, A.P. Majidi, T.W. Chou, Damage characterization of two-dimensional woven and three-dimensional braided SiC-SiC composites, Journal of Material Science, 31, 1996, 232–241.

[11] Y.D. Xu, L.T. Zhang, Three-Dimensional Carbon/Silicon Carbide Composites Prepared by Chemical Vapour Infiltration, Journal of the American Ceramic Society, 80, 1997, 1897-1900.

[12] Y.D. Xu, L.T. Zhang, L.F. Cheng, D.T. Yan, Microstructure and mechanical properties of three-dimensional carbon/silicon carbide composites fabricated by chemical vapor infiltration, Carbon, 36, 1998, 1051-1056.

[13] Yongdong Xu, Laifei Cheng, Litong Zhang, Hongfeng Yin, Xiaowei Yin, Mechanical Properties of 3D fiber reinforced C/SiC composites, Material science & Engineering A, 300, 2001, 196-202.

[14] Per F. Perterson, Charles W. Forsberg, Paul S. Pickard, Advanced CSiC composites for high-temperature nuclear heat transport with helium, molten salt, and sulfur-iodine thermo mechanical hydrogen process fluids, Second Information Exchange meeting on Nuclear production of Hydrogen, Argonne National Laboratory, Illinois, USA, 2-3 October, 2003.